

ELECTROANALYTICAL STUDIES OF SOME ENVIRONMENTALLY  
IMPORTANT COMPOUNDS

A thesis submitted

by

Patrick J. Hayes B.Sc., M. Appl. Sc.

Candidate for the degree of  
Doctor of Philosophy

N.I.H.E. Dublin

September 1987

## Abstract

The application of voltammetric methods to the determination of some compounds of environmental importance is described. In addition, a comparison of electrochemical (EC) detection and ultraviolet (UV) detection for the quantification of phenolic compounds in beers following separation by high performance liquid chromatography is also illustrated.

A field study is described in which differential pulse anodic stripping voltammetry (DPASV) at a mercury film electrode (MFE) was used to measure the levels of dissolved cadmium, lead and copper in the Irish Sea. Difficulties encountered with DPASV measurements in rough weather suggest that the method is not suitable for field analyses. In contrast, cold vapour atomic absorption spectroscopy is ideally suited to the quantification of mercury in field analyses.

A speciation scheme was developed to separately measure inorganic, dimethyl- and trimethyl-lead species in mixtures. Quantification was carried out using DPASV. By using a plating potential of  $-1.2V$  the three lead species are simultaneously measured. When the plating potential is

decreased to  $-0.6V$  only inorganic and dimethyl-lead are measured. On addition of a complexing agent and using the latter plating potential, dimethyllead can be measured in the presence of inorganic lead.

The HPLC method used for the separation of phenolic compounds is a modification of a previously described method. A comparison was made between a UV detector and an EC detector in series. In general, the EC detector offered lower limits of detection for most of the phenolic compounds studied. Analysis of beers indicated that EC detection was more suitable than UV detection with respect to sensitivity and selectivity.

Declaration

I declare that the research work described in this thesis is my own.

Patrick J. Hayes

Patrick J. Hayes

Malcolm R. Smyth

Malcolm R. Smyth

## Acknowledgements

I would like to thank Professor Pratt for providing the research facilities and my supervisor Dr. Malcolm Smyth for his guidance and patience throughout this work.

To my colleagues Alyn Deane B.Sc., James Fleming B.Sc., Anthony Ross B.Sc. and Don Buckley M.Sc., I wish to thank them for their continued encouragement and also for providing some diversionary moments.

The financial support provided by the National Board for Science and Technology to cover the costs of participating in the "Clione" cruise is gratefully acknowledged. In addition, I wish to thank Dr. David Harper and colleagues, Captain French and crew for their help and hospitality during this research work.

Thanks are also extended to the technical staff, especially Mick, of the Chemistry Department.

Finally, I wish to thank Anna Kinnerk and Lucy Barrett for typing this thesis.

Dedication

This thesis is dedicated to my parents, sister and brothers as well as Jim and Thomas.

"And now there came both mist and snow, and it  
grew wondrous cold:  
And ice, mast-high, came floating by,  
as green as emerald".

Samuel Taylor Coleridge  
(The Rime of the Ancient Mariner)

TABLE OF CONTENTS

Title page .....	(1)
Abstract .....	(ii)
Declaration .....	(1v)
Acknowledgements .....	( v)
Dedication .....	(vi)
Table of Contents .....	(vii)
Chapter 1	
Application of Electroanalytical Methods to	
Environmental Analysis.....	1
1.1. Introduction .....	2
1.2. General Aspects of Trace Analysis .....	4
1.3. Polarographic and Voltammetric Methods .....	6
1.4. Trace Metals .....	9
1.4.1. Environmental and Toxicological Aspects ...	9
1.4.2. Sampling and Storage of Water Samples	
for Trace Metal Analysis .....	12
1.4.2.1. Sample Collection .....	12
1.4.2.2. Storage of Water Samples .....	14
1.5. Application of Polarographic and Voltammetric	
Methods to Trace Metal Analysis .....	16
1.5.1. Determination of Trace Metals in	
Environmental Samples .....	16
1.5.1.1. Polarographic Methods .....	16

1.5.1.2. Voltammetric Methods .....	18
1.5.2. Heavy Metal Speciation in Natural Waters ..	27
1.5.2.1. Analytical Fractionation of Dissolved Metal Species .....	28
1.5.2.2. Titrimetric Methods... ..	41
1.5.2.2.1. Titration of Ligands with Metal Ions .....	41
1.5.2.2.2. Titration of Metal Ions with Ligands .....	44
1.5.2.2.3. Complexation Capacity .	45
1.5.2.3. Determination of Stability Constants and Stoichiometries of Heavy Metal Complexes .....	46
1.5.3. Problems Associated with ASV in Trace Metal Studies .....	48
1.5.3.1. Adsorption at Electrodes .....	48
1.5.3.2. Oxygen Elimination .....	49
1.5.3.3. Intermetallic Compounds .....	50
1.6. Determination of Organic Pollutants in Environ- mental Samples .....	51
1.6.1. Sulphur-Containing Compounds .....	51
1.6.2. Nitrogen-Containing Compounds .....	53
1.6.3. Oxygen-Containing Compounds .....	55
1.6.4. Organometallic Compounds .....	58
1.6.5. Miscellaneous Compounds .....	59
References .....	61



Chapter 2.

Theory .....	73
2.1. Polarographic and Voltammetric Methods .....	74
2.1.1. Introduction .....	74
2.1.2. Basic Features of Electrochemical Processes	75
2.1.2.1. Modes of Mass Transfer of Electroactive Species to an Electrode Surface .....	75
2.1.2.2. Overall Features of the Electrode Process .....	77
2.1.2.3. Faradaic and Capacitance Currents.	78
2.1.3. Direct Current Polarography .....	81
2.1.3.1. General Features of Direct Current Polarography .....	81
2.1.3.2. Types of Limiting Currents .....	85
2.1.3.2.1. Diffusion-Controlled Limiting Currents .....	85
2.1.3.2.2. Kinetic-Controlled Limiting Currents .....	89
2.1.3.2.2.1. Preceding chemical reaction	89
2.1.3.2.2.2. Following chemical reaction	91
2.1.3.2.2.3. Chemical	

	reactions	
	occurring	
	parallel	
	to the	
	electrode	
	reaction	91
	2.1.3.2.3. Adsorption-Controlled	
	Limiting Currents .....	92
	2.1.3.3. Nature of the Electrode Process ..	93
2.1.4.	Pulse Polarography .....	96
	2.1.4.1. General Principles .....	97
	2.1.4.2. Differential Pulse Polarography...	97
2.1.5.	Cyclic Voltammetry .....	103
	2.1.5.1. Fundamentals of Cyclic Voltammetry	104
2.1.6.	Stripping Voltammetry .....	109
	2.1.6.1. Introduction .....	109
	2.1.6.2. Principles of Stripping Voltammetry	109
	2.1.6.2.1. Preconcentration Step ..	109
	2.1.6.2.2. Stripping and Monitoring	
	Step .....	112
2.2.	High Performance Liquid Chromatography .....	113
	2.2.1. Chromatographic Separation .....	114
	2.2.1.1. Differential Migration .....	114
	2.2.1.2. Band Migration .....	116
	2.2.1.2.1. Eddy Diffusion .....	117
	2.2.1.2.2. Mobile-Phase Mass	

Transfer .....	117
2.2.1.2.3. Stationary-Phase Mass Transfer .....	118
2.2.1.2.4. Longitudinal Diffusion..	118
2.2.2. Retention Time and Volume .....	118
2.2.3. Efficiency of Separation .....	123
2.2.4. Resolution .....	124
References .....	125

### Chapter 3.

Determination of Dissolved Cadmium, Lead, Copper and Reactive Mercury in the Irish Sea - A Field Study .....	128
3.1. Introduction .....	129
3.2. Experimental Section .....	130
3.2.1. Reagents .....	130
3.2.2. Instrumentation .....	131
3.2.2.1. Temperature and Salinity Measurement .....	131
3.2.2.2. Anodic Stripping Voltammetry Measurements .....	132
3.2.2.3. Mercury Analyser .....	132
3.2.3. Cleaning Procedures .....	133
3.2.3.1. Cleaning of Equipment Used for Storage and Filtration of Water Samples Collected for Metal Analysis (except Mercury) .....	133

3.2.3.1.1.	Storage Bottles .....	133
3.2.3.1.2.	Filtration Apparatus and Filters .....	134
3.2.3.2.	Cleaning of Equipment Used for Storage and Filtration of Water Samples Collected for Mercury Analysis .....	135
3.2.3.2.1.	Storage Bottles .....	135
3.2.3.2.2.	Filtration Apparatus and Filters .....	135
3.2.4.	Sample Collection Techniques .....	136
3.2.4.1.	Surface Water Samples .....	136
3.2.4.2.	Deep Seawater Samples .....	137
3.2.5.	Sample Pretreatment and Storage .....	138
3.2.6.	Quantification Procedures .....	139
3.2.6.1.	Anodic Stripping Voltammetry .....	139
3.2.6.1.1.	Plating the Rotating Disk Electrode .....	139
3.2.6.1.2.	Analysis of a Seawater Sample by Differential Pulse Anodic Stripping Voltammetry .....	140
3.2.6.2.	Reactive Mercury Determination.....	140
3.3.	Results and Discussion .....	141
3.3.1.	Physical Characteristics of Sampled Stations .....	142

3.3.1.1. Historical Background to Salinity .	142
3.3.1.2. Salinity Values Measured in the Irish Sea .....	147
3.3.2. Problems Associated with On-board Metal Analysis .....	159
3.3.3. Critical Assessment of the Analytical Procedures .....	164
3.3.3.1. Sample Collection .....	164
3.3.3.2. Filtration and Preservation of Samples .....	166
3.3.3.3. Storage of Samples .....	168
3.3.3.4. Analytical Methods.....	170
3.3.3.4.1. Mercury Analysis .....	170
3.3.3.4.2. Differential Pulse Anodic Stripping Voltammetry at a Mercury Film Electrode .....	172
3.3.4. Dissolved Metal Ion Concentrations in the Irish Sea .....	173
3.3.4.1. Reactive Mercury Concentrations Measured in the Irish Sea .....	174
3.3.4.1.1. Reactive Mercury Concentrations in Liverpool Bay .....	174
3.3.4.1.2. Reactive Mercury	

	Concentrations at Stations 36 to 54 in the Irish Sea .....	180
3.3.4.2.	Dissolved Cadmium, Lead and Copper Concentrations .....	181
3.3.4.2.1.	Metal Concentrations in Cardigan Bay .....	181
3.3.4.2.2.	Metal Concentrations in Liverpool Bay .....	185
3.4.	Conclusions .....	190
	References .....	193
	Appendix .....	198
Chapter 4		207
4.1.	Introduction .....	208
4.2.	Experimental Section .....	209
4.2.1.	Reagents .....	209
4.2.2.	Preparation of Standard Solutions .....	210
4.2.3.	Preparation of Buffers .....	210
4.2.4.	Glassware Washing .....	211
4.2.5.	Instrumentation .....	212
4.3.	Results and Discussion .....	213
4.3.1.	General Polarographic and Voltammetric Behaviour of the Lead Species .....	213
4.3.1.1.	Inorganic Lead .....	214
4.3.1.1.1.	DC Polarographic	

	Studies in BR Buffers	
	pH 2.0 to 12.0 .....	214
4.3.1.1.2.	DC Polarographic	
	Studies in Acetate	
	Buffer pH 3.3 .....	218
4.3.1.1.3.	Differential Pulse	
	Polarographic Study	
	to Evaluate the	
	Effects of Methanol	
	on the Response of	
	Pb(II) .....	221
4.3.1.2.	Dimethyllead Dichloride.....	223
4.3.1.2.1.	DC Polarographic Studies	
	in Acetate Buffer pH3.3.	223
4.3.1.2.2.	DC Polarographic Studies	
	in BR Buffers pH2.0	
	to 12.0 .....	225
4.3.1.2.3.	Cyclic Voltammetric	
	Studies in Acetate	
	Buffer pH3.3 .....	228
4.3.1.2.4.	Differential Pulse	
	Polarographic	
	Studies in Acetate	
	Buffer pH3.3 .....	231
4.3.1.2.5.	Proposed Mechanism	
	for the Reduction	

	of Dimethyllead Dichloride in Aqueous Solutions.....	236
4.3.1.3.	Trimethyllead Chloride.....	240
4.3.1.3.1.	DC Polarographic Studies in Acetate Buffer pH3.3 .....	240
4.3.1.3.2.	DC Polarographic Studies in BR Buffers pH2.0 to 12.0 .....	244
4.3.1.3.3.	Cyclic Voltammetric Studies in Acetate Buffer pH3.3 .....	246
4.3.1.3.4.	Differential Pulse Polarographic Studies in Acetate Buffer pH 3.3 .	249
4.3.1.3.5.	Proposed Mechanism for the Reduction of Trimethyllead Chloride in Aqueous Solutions ...	251
4.3.2.	Development of a Voltammetric Procedure for the Determination of Inorganic, Dimethyl- and Trimethyl- lead Species in Mixtures .....	256
4.3.2.1.	Application of DP Polarography to the Determination of Inorganic and Alkyllead Species in Mixtures	256
4.3.2.1.1.	Initial Considerations	256
4.3.2.1.2.	Characteristics of the	



	Lead Species in Acetate Buffer .....	258
4.3.2.1.3.	Studies of Binary Mixtures of Lead Species .....	258
4.3.2.1.4.	Investigation of Complexation as a Method of Separating Inorganic and Dimethyllead .....	267
	4.3.2.1.4.1. Polarographic behaviour of lead species in the presence of EDTA .....	268
	4.3.2.1.4.2. Studies of binary mixture of lead species in the presence of EDTA.....	274
4.3.2.1.5.	Limitations of the Speciation Method Using DP Polarography .....	274
4.3.2.2.	Application of DPASV to the Determination of Inorganic and Alkyllead Species in Mixtures .....	276
	4.3.2.2.1. Studies in Acetate Buffer pH 3.3 .....	276
	4.3.2.2.2. Determination of the Lead Species in the Presence of EDTA .....	279
	4.3.2.2.3. Repeatability of Measurements .....	282
4.3.2.3.	Proposed Measurement Scheme Using DPASV .....	283
4.4.	Conclusions .....	285

References .....	286
Chapter 5.	
A Comparison of Electrochemical and Ultraviolet Detection Methods in High Performance Liquid Chromatography for the Determination of Phenolic Compounds in Beers	291
5.1. Introduction .....	292
5.2. Experimental Section .....	296
5.2.1. Instrumentation .....	296
5.2.2. Reagents .....	297
5.2.3. Analytical Procedures .....	298
5.2.3.1. Preparation of Standard Solutions ...	298
5.2.3.2. Extraction of Phenolic Compounds from Beers .....	298
5.2.3.3. HPLC Analysis .....	299
5.2.3.4. Voltammetric Studies .....	300
5.2.3.5. UV Studies .....	300
5.3. Results and Discussion .....	301
5.3.1. Voltammetric Studies of Phenolic Compounds ...	301
5.3.2. HPLC Separation of Phenolic Compounds .....	309
5.3.2.1. General Features of Separation of Phenolic Compounds Using Gradient Elution .....	310
5.3.2.2. Isocratic Elution as an Alternative to Gradient Elution for the Separation of Phenolic Compounds .....	321
5.3.3. Optimisation of Chromatographic Conditions ...	329
5.3.3.1. Gradient Shape and Steepness .....	329
5.3.3.2. Mobile Phase Flow-Rate .....	331
5.3.3.3. Electrochemical Detector Potential ..	339
5.3.3.4. UV Detection Wavelength .....	344
5.3.4. Comparison of UV and EC Detector Characteristics for the Determination of Phenolic Compounds .....	345
5.3.4.1. Detection Limit .....	345
5.3.4.2. Linear Dynamic Range .....	350
5.3.4.3. Precision of Measurements .....	351
5.3.5. Analysis of Beer Samples .....	352

5.3.5.1. Standardisation .....	352
5.3.5.2. Extraction of Phenolic Compounds from Standard Solutions and Beer Samples ..	354
5.3.5.3. Phenolic Content of Irish-brewed Beers .....	355
5.4. Conclusions .....	360
References .....	363
List of Publications .....	368

CHAPTER 1

APPLICATION OF ELECTROANALYTICAL METHODS  
TO ENVIRONMENTAL ANALYSIS

### 1.1. Introduction

Considerable emphasis is now placed on monitoring organic, inorganic and organometallic substances in the environment. The need for environmental monitoring stems from the large number of "chemical pollutants" that are emitted from various anthropogenic sources. A consequence of these emissions is that most people are now exposed {1} to a large number of insidious chemicals. This increased exposure to humans by "chemical pollutants" is viewed, by some, as an inevitable side effect of technological advancement. For example, city dwellers are exposed to large concentrations of insidious lead species due to the combustion of leaded petrol in cars {2}, which has given rise to an increased body burden of lead. One of the toxic manifestations associated with an increase in the body burden of lead in young children is a reduction in their learning ability {3}. Despite this knowledge, it is only in the recent past that there has been any attempt to reduce the concentration of lead in petrol.

There has been an increasing public awareness of the dangers of exposure to toxic substances. This is partially as a result of the knowledge gained in the

aftermath of large disasters. One such incident frequently cited is the Minamata Bay disaster {4} which occurred in Japan between 1953 and 1960. Untreated factory wastes containing methylmercuric chloride were disposed of in Minamata Bay; subsequently, over a hundred people died as a result of eating mercury-contaminated fish. This disaster demonstrated the ease with which a toxic substance, such as mercury, can enter the food chain when untreated waste is dumped directly into a natural system.

Obviously there is a need to control and manage the environmental burden caused by "chemical pollutants". Hence, research to ascertain the levels and pathways of these environmental pollutants has gained great significance in recent years {5-9}. When these parameters have been established, proper scientifically-based management plans may be prepared and reviewed to keep the environmental burden within tolerable levels.

Trace analytical methods play a very important role in environmental analysis. They are required for the detection and identification of "chemical pollutants" present in the environment {10,11}. It is essential that the analytical methods applied, are suitable and that they yield reliable data. Environmental management plans based on incorrect or unreliable data could lead to severe

environmental damage as a consequence.

## 1.2. General Aspects of Trace Analysis

Trace analytical determinations, subsequent to sampling and sample preparation steps, are usually carried out using instrumental methods. However, in order to be suitable for trace analysis these methods must fulfil certain basic requirements {12}. They need to have high sensitivity as many toxic chemicals are present in environmental samples at  $\mu\text{g}/\text{l}$  levels. Furthermore, the dynamic range should be large, covering a concentration range typically from several hundred  $\text{mg}/\text{l}$  down to  $\mu\text{g}/\text{l}$  levels. In situations where environmental levels of hazardous chemicals are to be established, an extension of the detection limit down to  $\text{ng}/\text{l}$  concentrations is essential. Nonetheless, it is important that the instrumental method applied is not stressed beyond its limits of reliability to avoid the risk of erroneous results {13}.

A further requirement of any instrumental method is that it has the necessary selectivity/specificity to deal with the problem in hand. This is a particularly important requirement in the context of trace metal speciation studies. Hence, instrumental methods that are

species-selective or specific have a much broader sphere of application than methods which are only element specific.

Perhaps the most important consideration in trace analysis is accuracy, that is, the closeness of agreement between the observed result and the known or true value {12}. For instrumental methods, the accuracy attained by the minimisation of systematic errors determines the reliability of the resulting data. Trace analytical procedures that involve various pretreatment stages, prior to application of the instrumental method in the measurement step, tend to have a large number of potential error sources. In order to achieve accurate and reliable results, the pretreatment stages should be kept simple and the instrumental method should have a high degree of accuracy.

There now exists a large number of instrumental methods, but not all incorporate the aforementioned requirements. Among the most suitable are the electrochemical methods of polarography and voltammetry. Voltammetry in particular has recently shown great application both in the fields of trace metal analysis {8} and in the determination of organic compounds in environmental samples {11}.



### 1.3. Polarography and Voltammetric Methods

Polarography and voltammetry belong to a class of electrochemical methods which can be used to study solution composition through current-potential relationships. Polarography is the branch of voltammetry that is used to investigate solution composition by the reduction or oxidation of ions or molecules at a dropping mercury electrode (DME) under the influence of an applied potential {14}. Direct current (DC) polarography involves measurement of the current variation at a DME as the applied potential ramp is linearly changed with time. As a result of the charging current associated with the changing potential at the DME a significant background current is observed. This effectively limits the sensitivity of DC polarography to concentrations in the low mg/l region.

Maximisation of the faradaic over the charging current has been accomplished by pulse polarography {15}. One of the most widely used pulse modes in trace analysis is differential pulse (DP) polarography. In this mode, small potential pulses are superimposed on a conventional DC voltage ramp and applied to the DME near the end of the drop lifetime. The current is sampled just before application of the pulse and again at the end of the pulse when the charging current has decayed. It is the

difference between these two current measurements that is displayed. Hence the ability of DP polarography to discriminate against the charging current increases its sensitivity over DC polarography. Because DP polarography is an extremely sensitive method, it is applicable to both inorganic and organic analysis, yielding peaks for concentrations in the  $\mu\text{g}/\text{l}$ - $\text{mg}/\text{l}$  range.

Voltammetric methods, such as anodic stripping voltammetry (ASV) or cathodic stripping voltammetry (CSV) employ stationary mercury electrodes or solid electrodes such as glassy carbon or gold. Both ASV and CSV are among the most sensitive voltammetric methods used in environmental analysis. Stripping voltammetry involves two discrete steps [16]. In the first step, the analytical species of interest are deposited either as amalgams or as mercury salts onto a stationary electrode such as a hanging mercury drop (HMDE) or mercury film electrode (MFE). The time required for the deposition step depends on the concentration of analyte present. For example, plating times of less than 1 min at 0.1 mg/l concentrations to about 10 min at 1  $\mu\text{g}/\text{l}$  concentrations have been suggested [17]. It is important that the conditions used in the deposition step, i.e., stirring rate and deposition time, are strictly controlled to ensure reproducible results. Following this first step, the deposited species are

stripped from the electrode back into solution. The most commonly used waveforms in the stripping step are the linear sweep and differential pulse modes. The DP waveform has become more popular because it is more effective at discriminating against charging currents and permits lower limits of detection. The magnitude of the stripping current is proportional to the concentration of the species of interest.

In stripping voltammetry, the type of working electrode used will determine the sensitivity of the method employed. For the analysis of trace metals down to several  $\mu\text{g}/\text{l}$  a hanging mercury drop electrode may be used, whereas a mercury film electrode is employed for even lower concentrations {18}. When mercury electrodes are used in ASV, about 20 amalgam-forming metals may be determined {17}. By contrast, metal ions such as arsenic, mercury, selenium and silver may be determined on solid electrodes such as glassy carbon or gold {17}.

For the determination of many organic and organometallic molecules of environmental importance, the trend in recent years has been to couple high performance liquid chromatography with electrochemical detectors using glassy carbon or hanging mercury drop electrodes {19}.

#### 1.4. Trace Metals

##### 1.4.1. Environmental and Toxicological Aspects

The existence of metals in the environment is not a new phenomenon. Lithogenic origins, e.g., ore deposits and volcanoes, were the predominant sources of metals before the Industrial Revolution. However, the present day levels of heavy metals in the environment are almost exclusively from anthropogenic sources {20}. These metals are released into the environment either directly by wastewater discharges and run-off or indirectly via the atmosphere absorbed to precipitates and dust. Due to the ubiquity of heavy metals in the environment, they can become incorporated in food chains and drinking water, eventually being taken up by man (Fig. 1.1).

Among the most hazardous heavy metals are Cd, Pb and Hg. These three metals are toxic at all concentrations and have no known biological function {13}. A second group of metals, containing As, Bi, In, Sb, and Tl, have no biochemical requirement by man and are only tolerated at

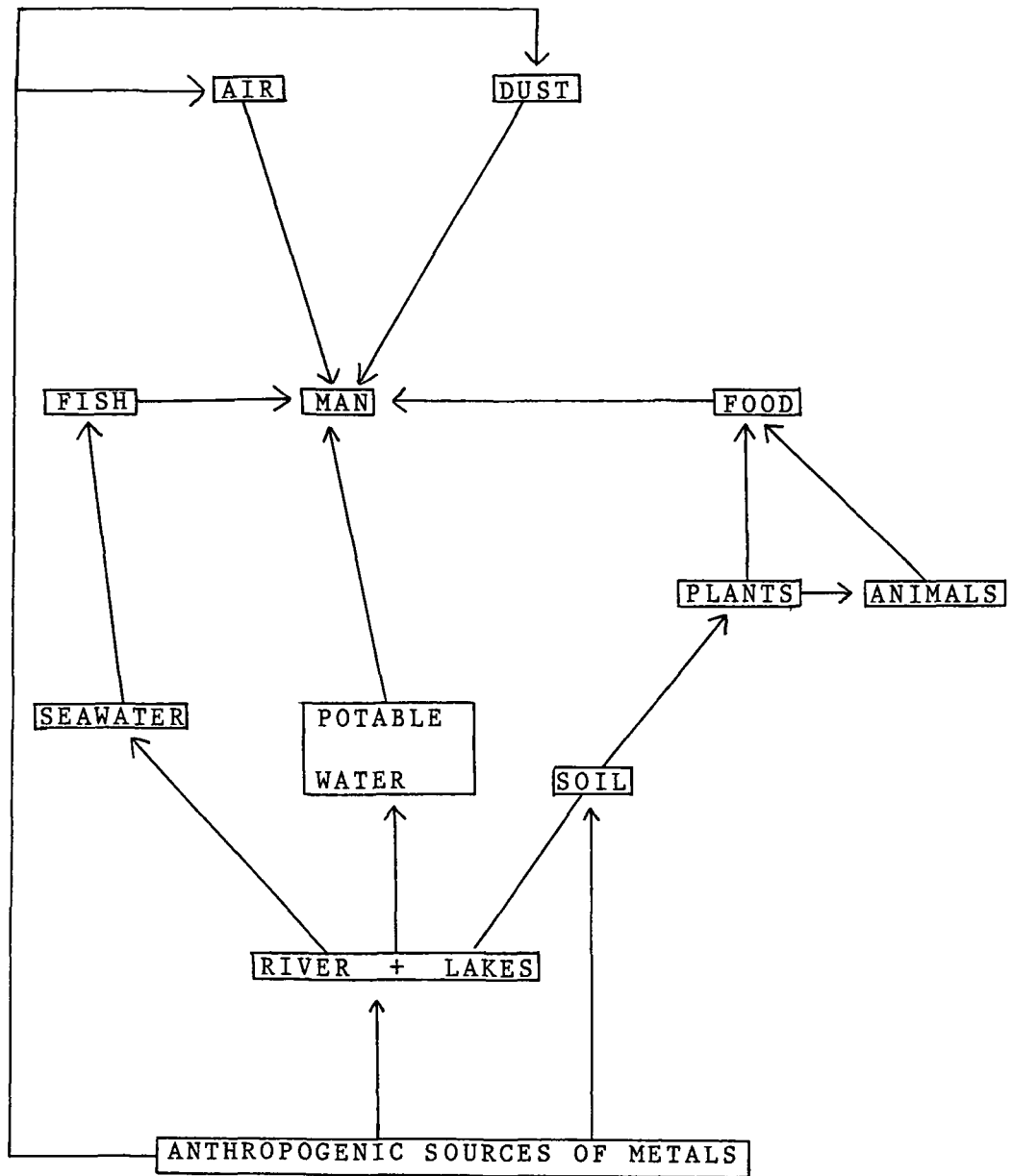


Fig. 1.1. Pathways by which heavy metals reach man.

trace levels in biochemical systems. Finally, there is a third group of metals which are known to be biochemically essential. Among these essential elements are Cu, Zn, Co, Ni, V, Se, Cr and Fe. Even this last group of metals, though essential below their respective threshold levels, become progressively toxic above certain levels. Some of these metals, e.g., Ni, Cr, Cu and Se, are known to display carcinogenic effects {21} due to their interaction with nucleic acids.

In general, the toxicity of metals stems from the fact that they are biologically non-degradable and have a tendency to accumulate in vital organs, e.g., brain, liver or bones, of man and by their accumulation become progressively more toxic {8,13}. However, the degree of toxicity exerted on a biological system depends on the chemical form or oxidation state of the particular heavy metal. For example, studies have revealed that ionic copper is far more toxic towards aquatic organisms than organically-bound copper and that the more stable the copper complex, the lower is its toxicity {22,23}. Also, it is known that As(III) is much more toxic than As(V) {24}.

Perhaps the most insidious forms of heavy metals are their alkylated derivatives. Many of these compounds, e.g., alkylleads and alkyltins, have been found in environmental samples {25}. Apart from anthropogenic sources, some of these compounds are produced naturally by chemical {26,27} or biological processes {28,29}. Consequently, many heavy metals released into the environment can become even more toxic once transformed to their alkylated forms. In particular, the alkyl compounds of mercury and lead are especially toxic because they are lipid-soluble {30}. Generally, the toxicity of alkylated species tends to increase with the degree of alkyl substitution and carbon chain length of the alkyl group {25}.

#### 1.4.2. Sampling and Storage of Water Samples for Trace Metal Analysis

In this section, only practical aspects involved in the collection and storage of water samples are considered. Theoretical aspects of sampling are to be found elsewhere in the literature {31,32}.

##### 1.4.2.1. Sample Collection

Sample collection is probably the most important

step in trace analysis. Meaningful results will only be obtained if all risks of contamination are either minimised or eliminated. This, however, is not an easy task.

The first problem that arises is trying to decide the type of sampling bottle that will be used. It is recommended that high-pressure (low density) polyethylene bottles be used {33}. Before use, these bottle should be degreased, followed by acid leaching to remove trace metals present {33}. Alternatively, Teflon bottles may be used as this is the only material that does not release zinc into a water sample {34}.

Collection of surface samples from coastal waters, estuaries, rivers and lakes is usually undertaken from small boats using a telescopic bar with an attached sample bottle {33}. Surface water samples taken in the open ocean, cannot be taken directly from a large ship because the ship is continually releasing copper, lead and zinc from its antifouling paints and cathodic protection devices {35}. In such situations, the only safe way to sample is to use a small rubber boat which is rowed to the sampling site. Sampling is undertaken at the bow of the boat whilst slowly rowing into the wind to prevent contamination of the sampled water by the boat {36}.



For the collection of samples at depths greater than 10 metres the aforementioned methods are unsuitable. The normal procedure involves clamping a sampler to a hydrowire and lowering the sampler to the required sampling depth. However, this method is prone to sample contamination by rust and grease from the hydrowire {37}. Furthermore, it has now been discovered that this method can introduce large amounts of trace metal contamination, especially lead. These contamination problems can be circumvented by using the all-Teflon Patterson C.I.T. sampler {38}. This is one of the few sampling devices that can collect deep seawater samples without metal contamination.

#### 1.4.2.2. Storage of Water Samples

Storage methods employed depend on the nature of the measurements which are to be undertaken. For speciation studies, water samples should not be acidified as this would change the nature of the speciation {24}. Likewise, freezing of water samples is not possible. As a water sample freezes, metal ions are concentrated in the unfrozen liquid in the centre of the container, where they may undergo chemical and physical alteration {35}. Thus, samples for speciation studies should be filtered through a 0.45  $\mu\text{m}$  membrane filter to remove any suspended material.

The filtrate, containing the dissolved heavy metal fraction, should subsequently be stored at 4°C, as this appears to be the safest method for both freshwater and seawater samples {39,40}. Storage of samples at higher temperatures may result in speciation changes. This has been observed for cobalt and manganese when water samples were stored at room temperature {41}. Changes induced by a pH drop due to bacterial respiration, in which oxygen was consumed and carbon dioxide was released, resulted in precipitation of cobalt and manganese carbonates.

If the dissolved heavy metal concentration of a water sample is to be determined, then the filtered sample is usually adjusted to pH 2.0 by adding a small amount (1 ml/l) of concentrated hydrochloric or perchloric acid {20}. Acidification of the sample helps prevent loss of metal by adsorption on the walls of the storage container. However, in some instances acidification may cause leaching of metals, especially lead, from the container walls {33}. The best method of sample storage is freezing to - 20°C or liquid nitrogen temperature {42}. This eliminates leaching of trace metals from the container and also losses by adsorption.

When filtered samples are stored at room temperature for less than a week, acidification is

unnecessary {43}. In the case of long term storage, filtered samples, whether acidified to pH 2.0 or unacidified, have to be deep frozen {43}.

#### 1.5. Application of Polarographic and Voltammetric Methods to Trace Metal Analysis

In the following sections the aim is to highlight the application of polarographic and voltammetric methods to the determination, both qualitative and quantitative, of metals in environmental samples, as well as illustrating their application in speciation studies.

##### 1.5.1. Determination of Trace Metals in Environmental Samples

###### 1.5.1.1. Polarographic Methods

Among the most sensitive direct methods of analysis is differential pulse polarography. This method has been successfully applied to the determination of copper, lead, cadmium, zinc and titanium in air particulates {44}. Air samples were collected on glass-fibre filters and acid-digested prior to analysis. Using an EDTA-sodium acetate electrolyte at pH 2.0, it was possible to determine all five metals in a single

polarographic scan. The results obtained with DP polarography compared favourably with those using atomic absorption spectroscopy (AAS).

DP polarography has also been used to determine the total chromium content of a river water sample {45}. Before DP polarography analysis all chromium present in the water sample was converted to Cr(VI) by oxidation with  $H_2O_2$  followed by quantification in 1M NaOH. The result was found to be in good agreement with that obtained by flame AAS. However, besides the chromium reduction peak, a second reduction peak was present. This was due to 2-methyl-1,4-naphthoquinone formed by oxidation of the corresponding hydroquinone with chromic acid in the original sample.

Direct determination of As(III) and Pb(II) in the run-off water from waste disposal grounds has been accomplished by DPP {46}. The sample pretreatment simply consisted of addition of a supporting electrolyte (2M NaCl and 2M  $H_2SO_4$ ) followed by deaeration and recording the DP polarogram at a DME. The complete analysis took twenty minutes to perform. A high sulphuric acid content was required to ensure sufficient separation of the responses of Pb(II) and As(III). If As(V) is present, it must first be reduced using hydrazine to the polarographically active

form, As(III), before it can be determined. With this method, determination limits of 40  $\mu\text{g}/\text{l}$  or less are attainable.

Generally, direct determinations are only possible when the metal concentrations are sufficiently high. For example, the detection limit for cadmium in water matrices is 10  $\mu\text{g}/\text{l}$  when DP polarography is used {47}. When surface active organic traces are present, the detection limit is restricted to higher concentrations. Recently a modified method employing fast-scan DP polarography at a slowly dropping mercury electrode was developed {48}. This had a detection limit of 5  $\mu\text{g}/\text{l}$  for cadmium. However, for the determination of ultra-trace levels of metals, e.g., 1  $\text{ng}/\text{l}$ , stripping voltammetry is required.

#### 1.5.1.2. Voltammetric Methods

The voltammetric mode most frequently used for the determination of trace metals is differential pulse anodic stripping voltammetry (DPASV). Detection levels achieved with this method depend on the choice of working electrode. When metal concentrations are below 10  $\mu\text{g}/\text{l}$  a mercury film electrode (MFE) is recommended, while a hanging mercury drop electrode (HMDE) should be used at higher concentrations to avoid overloading the thin Hg-film of the

MFE {10}. Besides these two mercury electrodes, a number of new electrodes have recently been developed for the detection of metal ions. For example, a chemically modified electrode in conjunction with DPASV has been used to measure copper at concentrations as low as 100 ng/l in laboratory prepared solutions {49}. A further example is the development of a gold-film micro-electrode, formed by plasma-sputtering gold onto carbon fibres {50}. This electrode has been applied to the detection of mercury using DPASV. A detection limit of 3.7 µg/l for mercury in laboratory test solutions was reported.

Given the ubiquity of metals in the environment, a variety of matrices is being analysed for heavy metal contents. In this context soils are especially important, as metal ions will accumulate in them via dry and wet depositions from the polluted atmosphere. A convenient and accurate analytical procedure has been developed for the simultaneous determination of Cd, Cu, Pb and Zn in soils {51}. This method is based on DPASV measurement, at a HMDE, of the analytes resulting from the digested soil. Some samples were analysed by DPASV and AAS to ascertain the applicability of the developed procedure. Good agreement was found between the results obtained with both methods.

A further application of stripping voltammetry has been in the determination of trace metals in rain water, snow and the particulate matter associated with these precipitates {52}. DPASV was used to determine Cd, Pb, Cu and Zn, while the detection of Se required differential pulse cathodic stripping voltammetry (DPCSV). A HMDE was used with both stripping methods. The only sample pretreatment required was filtration through a 0.45  $\mu\text{m}$  filter to remove the particulate matter and adjustment of the filtrate to pH 2.0 with HCl. Trace metals bound to the airborne dust particles were determined by subjecting the collected particles, together with the filter media, to low temperature ashing. In this way, the metal ions contained in the organic layer at the surface of the dust particles were digested completely and were accessible to subsequent DPASV measurement. The results suggest that the levels of trace metals in the filtered particulate matter are negligible compared with the levels dissolved in rain water or incorporated in snow. In fact, well over 90% of the trace metals brought to the ground were in the dissolved state, emphasising the efficiency of rain and snow in removing trace metals from the atmosphere to the ground.

A particularly important area of study has been the quantification of dissolved metal levels in both freshwater and seawater samples. Determination of the dissolved metal

content in these samples requires a minimum of sample pretreatment, which is an important aspect in the avoidance of error sources arising from contamination. The usual procedure involves sample filtration through a 0.45  $\mu\text{m}$  filter, to remove particulate matter present, and acidification of the filtrate to pH 2.0 with concentrated HCl. Samples are usually left to stand for several hours to allow the completion of the decomposition of most complexes present {8}. The metal ions Cu(II), Cd(II) and Pb(II) are then simultaneously determined by DPASV at a MFE, with the possibility of determining these three metals to levels as low as 1 ng/l {53}. Because of the lower hydrogen overvoltage of the MFE, less negative plating potentials of -1.0V are applied in media at pH 2.0. Hence, zinc has to be determined separately at pH 4.5 {20}.

ASV is especially suited to the analysis of seawater and other saline waters because the high salt matrix provides excellent conductivity, whereas it is a source of interference in AAS {54}. DPASV at a mercury film electrode has been employed to determine the levels of dissolved Cd, Pb and Cu in coastal and inland waters {55}. This study revealed that Cd and Pb levels were usually elevated across main shipping routes into ports, while in the immediate vicinity of these routes the levels dropped abruptly to the values of the local coastal waters. It



also found that areas where the water is rich in suspended particulate matter tended to have low dissolved metal concentrations, typically 5ng/l Cd, 18ng/l Pb and 130ng/l Cu. This is connected with the high probability of metal uptake by plankton organisms and/or metal trapping due to chemisorption at suspended inorganic and dead organic matter surfaces.

A recent survey used DPASV at a MFE to determine total and dissolved concentrations of Cd distributed in coastal and open ocean waters {56}. This survey found that coastal waters contained higher cadmium concentrations than open ocean waters. Generally, cadmium was preferentially present in the dissolved state, although in heavily polluted waters with large amounts of suspended particulate matter the total levels were higher than the dissolved contents. Because Cd was present preferentially in the dissolved state it was suggested that it can be used as a suitable tracer when studying the movement of pollution plumes in coastal waters.

Another toxic metal frequently found in the environment is mercury. A method has been developed for the determination of mercury in water samples, after acidification of the sample to pH 1.0, by DPASV at an activated gold electrode {57}. The detection limit of the method was 50 ng/l. This method was found to be suitable for the simultaneous determination of copper and mercury.

Furthermore, for high levels of copper, the gold electrode is more suitable than the mercury electrode because problems associated with the limited solubility of copper as an amalgam in mercury are eliminated. For the determination of copper in seawater, medium exchange after the plating stage was necessary. This was required because the response corresponding to chloride oxidation interferes and the chlorine formed would damage the surface of the gold electrode. For the determination of ultra-trace levels, below 30 to 50 ng/l, in seawater, a method based on DPASV in the subtractive mode at a twin gold electrode was developed {58}. The separation of the two halves of the gold disc by an insulating epoxy resin allows application of different potentials to both halves. Operation of the subtractive mode ensures a low background current. There was good correlation between results by this method and those obtained by cold vapour AAS. However, as the voltammetric response is very complicated it was suggested that for routine ultra-trace determinations of Hg the application of cold vapour AAS was more convenient.

Some heavy metals, e.g., Ni and Co, do not form stable amalgams and therefore cannot be determined by stripping techniques. For their determination, adsorption voltammetry {20} is employed. This is based on preconcentration using adsorption of a suitable heavy metal

chelate on the surface of the HMDE. It has been applied to the simultaneous determination of Ni and Co {59} using dimethylglyoxime (DMG) as chelator. Samples are adjusted to pH 9.2 with ammonia buffer followed by addition of DMG to give a concentration of about  $10^{-4}$  M. A potential of -0.7V is then applied to the working electrode while the solution is stirred for several minutes. Subsequently, the adsorbed  $\text{Ni}(\text{DMG})_2$  and  $\text{Co}(\text{DMG})_2$  are reduced by scanning the potential in the negative direction. Linear scan voltammetry can be applied to analyte concentrations above  $1 \mu\text{g}/\text{l}$ , whereas the differential pulse mode is used for concentrations down to  $1 \text{ ng}/\text{l}$ .

A new development in environmental analysis has been the construction of on-line sensors, for trace metals, based on stripping analysis{60}. An automatic voltammetric analyser for the determination of four trace metals (Cd, Pb, Cu and Zn) in water has been developed{61}. This analyser was employed for the intermittent on-line analysis of tap water supplied by water works, though it can also be applied to the analysis of wastewater samples. With this device, samples are automatically taken from the mains water supply, acidified and analysed by DPASV at a HMDE. Each sample solution is analysed twice followed by two standard additions for calibration purposes. The total time required for this procedure is 20 min. The detection

sensitivity is 0.1  $\mu\text{g}/\text{l}$ .

Another form of automated system is ASV with flow injection analysis (FIA){62}. In this type of system, small volumes of sample solution are injected into a carrier stream that transports them towards the detector. Deposition occurs while the sample is flowing through the detector and the stripping step is effected after the sample volume has passed the detector. Electrodes most commonly used are the HMDE and the MFE. For monitoring metals with oxidation potentials more anodic than that of mercury, solid gold electrodes are used{63}. The stripping mode utilized depends on the analyte concentration. For monitoring at the 5-50  $\mu\text{g}/\text{l}$  concentration range, the linear scan mode is used. At this concentration range, short deposition periods (1-3 min) are employed so that the analysis takes 2-4 min, which means that 15-30 measurements per hour are possible. At lower concentrations the differential pulse mode is used, but this considerably lengthens the time of each analysis, given the slow scan rate (2-5 mV/sec) in the stripping stage. An automated ASV flow system, based on a mercury-coated graphite tubular electrode, has been applied to the continuous monitoring of copper and zinc in marine environments{64}.

A further type of flow-through detection system for

the determination of trace metals has involved combining high performance liquid chromatography (HPLC) with electrochemical (EC) detection. A method has been developed for the specific determination of copper in tap water using reverse-phase HPLC[65]. It involves complexation of copper with dithiocarbamate(DTC) ligands. The preferred method for formation of the  $\text{Cu}(\text{DTC})_2$  complex was inclusion of a dithiocarbamate salt in the mobile phase and injection of the aqueous sample onto the column to form the complex in situ. Determination of the copper complex, using the oxidative process, was undertaken at a gold electrode. The DC response of the electrode was monitored at +0.6V. Results by this HPLC-EC detection method were compared with those obtained by AAS, and excellent agreement found between these two methods. The use of HPLC with electrochemical detection has been extended to multielement determinations. By forming diethyldithiocarbamate complexes of Cu, Ni, Cr and Co it was found possible to simultaneously determine all four metals{66}. When pyrrolidine dithiocarbamate was used as complexing ligand, Cd, Co, Cu, Pb, Hg and Ni were determinable{67}.

Other electroanalytical methods used in trace metal analysis include anodic stripping coulometry{68} and potentiometric stripping analysis (PSA){69, 70}. PSA is a

relatively new analytical method, but is very similar to voltammetric stripping analysis as it involves two discrete steps. In the first step, the analytes are deposited or dissolved in a suitable electrode by application of an appropriate potential. In the second step, the preconcentrated analyte is stripped chemically rather than electrochemically and the potential of the working electrode is measured with time. Both oxidative and reductive PSA methods have now been developed{71}. The application of PSA to the determination of Pb, Cd and Zn in seawater has been demonstrated at a MFE{72}. Other applications of PSA to the analysis of metals in environmental samples have been cited in the literature{73}.

#### 1.5.2. Heavy Metal Speciation in Natural Waters

Speciation is defined as "the determination of the individual concentrations of the various chemical forms of an element which together make up the total concentration of that element in a sample". Studies of metal speciation are important as they provide information on the toxic forms of metals present in environmental samples. It is also necessary to know the mechanisms for trace metal transport in natural waters in order to understand their chemical cycles in nature{74}. This information is

essential for evaluating the fate of trace metals that anthropogenic sources superimpose on natural systems.

In a natural aquatic environment heavy metals will be present in the following states:

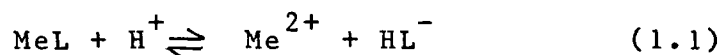
- (i) bound to suspended inorganic and organic matter;
- (ii) deposited in the surface layers of sediments; and
- (iii) present in the dissolved state.

Although sediments contain the greatest concentration of metals, only a few studies on the speciation of heavy metals in sediments have been undertaken{75}. Instead most research has focused on the dissolved state because it is effectively the nucleus for metal transfer in aquatic systems. Because of the importance of this state, a number of different approaches have been developed to determine dissolved metal species. These are illustrated in the following sections.

#### 1.5.2.1. Analytical Fractionation of Dissolved Metal Species

One of the simplest schemes based on ASV

measurement has been applied to the speciation of copper in river water{76}. In this scheme water samples were adjusted to pH 8.0 and the copper content measured by DPASV. Following this step the sample was acidified to pH 2.0 and the copper concentration was again determined. There was a ten-fold increase in the measurable copper concentration on decreasing the pH of the water sample. The decrease in the stripping current at high pH was attributed to the "non-labile" nature of the copper species present. This may be illustrated by the following equation:



At low pH, the equilibrium is shifted to the right and a significant stripping current is observed. However, at high pH, MeL is the predominant species in solution, and if the species MeL is not reducible, no stripping current is observed. Thus the term "non-labile" is applied to a species if, during the plating stage, MeL is not reduced and little of the species is converted to  $\text{Me}^{2+}$ . However, it must be emphasised that the term "non-labile" in ASV is an operational definition which depends on the duration of the plating step.

Ultrafiltration has been used as the basis of a



scheme to study metal species present in seawater{77}. Samples were first filtered through a 0.22  $\mu\text{m}$  membrane filter. This pore size was chosen to ensure the removal of microorganisms. Ultrafiltration through a membrane with nominal molecular weight limit (NMWL) of 1000 was used to distinguish between high and low molecular weight (HMW, LMW) species. This was followed by determination of "labile", acid-soluble and total Cu, Pb and Cd by DPASV at a MFE. It was found that the distribution of metals between the operational classes varied widely from one metal to another. There was a predominance of "labile" Cd in the LMW fraction suggesting that it was present as ion pairs, hydrated metal ions and/or "labile" LMW organic and inorganic complexes. Cadmium was not associated with colloidal matter nor bound in organometallic compounds. Similarly lead showed little or no association with colloids, but was found to be extensively associated with organic matter. The behaviour of samples after acidification to pH 2.8, indicated that half of the total Pb content was in LMW organometallic compounds. It was suggested that these organometallic compounds originated from adsorption of metal ions on detritus because they occurred in areas of accumulation and breakdown of organic detritus. Unlike Pb and Cd, Cu showed a more even distribution between all of the operational classes. A high proportion of the total copper was present as organic

species in all samples analysed. Much of the copper occurred in "labile" HMW species and were present as organic complexes, whereas the Cu that was "non-labile" at pH 2.8 probably occurred as organometallic compounds. In addition, the depth profile of Cu, unlike those of Cd and Pb, showed a pronounced vertical variation which indicated strong influences by biological and geochemical processes on Cu speciation.

A comprehensive scheme permitting the quantification of metal species in seven discrete groups has been developed. It is known as the Batley-Florence scheme{78}. It utilized ASV to discriminate between "labile" and bound ("non-labile") metal at pH 4.8 and has been combined with a number of separations and solution treatments to provide an extensive breakdown of metal species. Measurements were made of "labile" and total metal concentrations using ASV at a MFE. Each measurement was performed as follows:

- (i) before treatment;
- (ii) after passage through a Chelex-100 resin (the function of this step is to distinguish between metal associated with colloidal particles and metal species which are retained by the resin;

(iii) after UV-irradiation; and

(iv) after passage of the UV-irradiated sample through the Chelex-100 column.

This yielded four "labile" and four total metal concentrations for each metal. By subtraction, bound metal concentrations (bound metal concentration = total metal concentration minus "labile" metal concentration) were also obtained.

From these measurements, seven groups of species were quantified (see Table 1.1). It is now recognised that there is some overlap between the experimental classes determined in this scheme, because it is based on behavioural rather than chemical differences between metal species {79}.

Groups	Chemical forms
M + ML1 + MA1	Free metal ions + ASV-labile organic complexes dissociated by Chelex-100 + ASV-labile inorganic complexes dissociated by Chelex-100.
ML2	ASV-labile organic complexes plus labile metal adsorbed on organic colloids not dissociated by Chelex-100.
MA2	ASV-labile inorganic complexes plus labile metal adsorbed on inorganic colloids not dissociated by Chelex-100.
ML3	Non-labile organic complexes dissociable by Chelex-100.
MA3	Non-labile inorganic complexes dissociable by Chelex-100.
ML4	Non-labile organic complexes plus non-labile metal adsorbed on organic species not dissociable by Chelex-100.
MA4	Non-labile inorganic complexes plus non-labile metal adsorbed on inorganic species not dissociable by Chelex-100.

Table 1.1. Groups of species identifiable using the Batley and Florence speciation scheme.

In particular, the "non-labile" organic and inorganic complexes dissociable on the Chelex-100 column may include some metal dissociated from colloids and retained by the resin. This group may also include some of the humic and fulvic acid complexes which may be partially dissociated by the Chelex-100 resin.

The Batley-Florence scheme has been applied to the determination of the chemical forms of Cu, Pb, Cd and Zn in freshwater samples{80}. Measurements indicated that copper in river and reservoir samples was associated mainly with organic matter, probably organic colloids, whereas very little zinc was associated with organic colloids. It was found that cadmium existed almost entirely in "labile" ionic forms, and that lead was divided between "non-labile" inorganic and organic complexes. Spring water was also investigated. However, because of the anoxic nature of the sample, indicated by the distinct smell of hydrogen sulphide, it was not subjected to the complete speciation scheme. During UV irradiation, even without any peroxide present, ferrous iron was oxidised and hydrated ferric oxide precipitated. The subsequent change in the oxidation state of iron was thought to significantly alter the speciation of other trace metals present. Consequently, this problem precluded the application of the scheme to the

analysis of anoxic water samples.

The Batley-Florence scheme has also been used to study the chemical forms of Cd, Pb and Cu in seawater {81} and changes in species distribution in an estuarine system {82}. Both studies revealed that all three metals were principally associated with organic and inorganic colloidal matter. In coastal seawater, colloiddally-associated metal was shown to account for 56% of total Cu, 67% of total Pb and 33% of total Cd. The results were important as they indicated the small percentages of Cu, Pb and Cd present as simple ionic metal or weak complexes, whereas previous models of heavy metal distributions in saline waters had assumed these percentages to be higher {83}.

Arising from application of the Batley-Florence scheme to environmental samples, a number of disadvantages of the scheme were identified. The principal disadvantages are:

- (i) various metal classifications given by the scheme cannot be identified with precise chemical species in the sample;
- (ii) analytical measurements may disturb the dynamic equilibrium between metal species in the sample; and
- (iii) application of the full speciation scheme to one

sample involves almost 2 man-days of effort.

In addition, there has been criticism of some aspects of this scheme {84}. Utilization of in situ formation of the MFE has been criticised because the mercury effectively competes for free ligands in solution and may affect speciation by displacement of metal ligand equilibria. The use of acetate buffer at pH 4.8 was also criticised on the basis that acetate acts as a competing ligand, upsetting natural equilibria. A further criticism of the scheme was that changing the pH of a sample from its natural value to pH 4.8 could lead to substantial releases of complexed metals.

An alternative scheme that utilized ASV and Chelex-100 resin in successive column and batch procedures to differentiate trace metal species on the basis of relative lability has been developed. It is known as the Figura and McDuffie scheme {85}. Species were classified as "inert", "slowly labile", "moderately labile" and "very labile" depending on the characteristic time scale of the measuring technique. An important feature of this scheme is that the first three fractions can be preconcentrated thus enabling one to fractionate even ng/l metal concentrations. In addition, trace metal fractions collected on Chelex resin can be stored for an indefinite

period before being analysed. The ASV-labile measurements were carried out at pH 6.3 on fractions after filtration and resin separation as shown in Fig. 1.2. Measurements were undertaken at the optimum plating potential for each metal to avoid reduction of some complexed species at the high cathodic potentials, necessary for the simultaneous deposition of cadmium, lead and copper.

The Figura and McDuffie scheme was applied to speciation studies in aquatic environmental samples. The results showed that Cd and Zn were almost entirely in the "very labile" and "moderately labile" fractions and Cu existed primarily in "moderately labile" and "slowly labile" fractions. Between 20-70% of lead present was in the "slowly labile" fraction, though in some cases a significant but low percentage of inert Pb was found. These results were found to be consistent with those obtained using the Batley and Florence scheme {80}.

Although the Figura and McDuffie is very simple in its approach to speciation studies, it does have certain limitations {86}. The method takes 2-3 days and requires several tedious analytical steps. Also, the sample treatment that is required, introduces problems of storage without perturbing the positions of chemical equilibria.



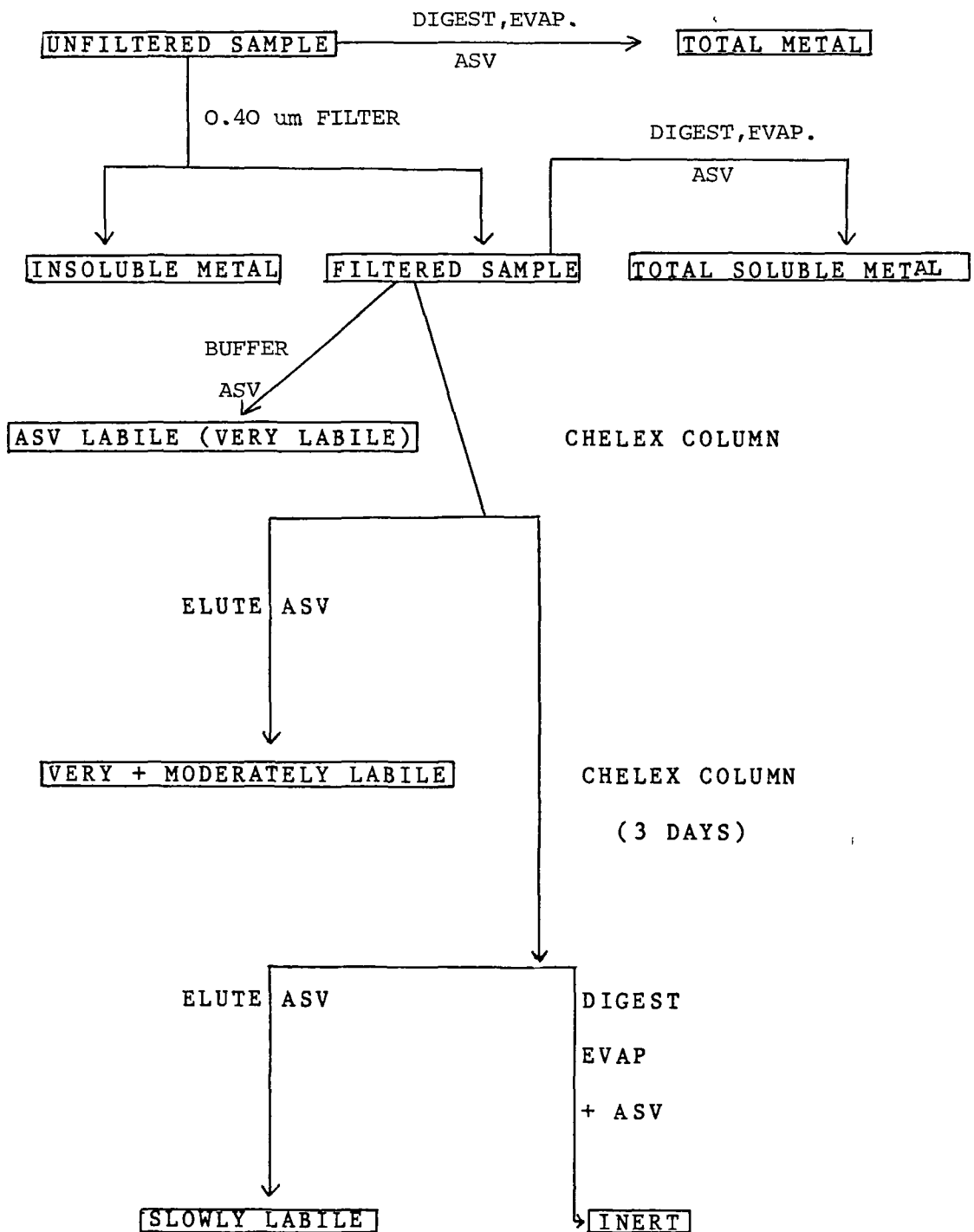


Fig. 1.2. Classification of metal speciation using the Figura and McDuffie Scheme.

Just as in the Batley and Florence scheme, the introduction of a buffer for the ASV step may shift the positions of chemical equilibria. Finally, the "very labile" fraction as determined by ASV may include colloiddally-bound metal or relatively "non-labile" metal complexes which are directly reduced at the HMDE.

A more recent development has been the Laxen and Harrison scheme which is based on aspects of other schemes, particularly that of Batley and Florence and the Figura and McDuffie scheme. Unlike other speciation schemes, this method did not involve initial sample filtration through a 0.45  $\mu\text{m}$  membrane filter. Instead, samples were filtered through filters of various pore sizes ranging from 0.015 - 12  $\mu\text{m}$ . Because this scheme utilized size - association as an indicator of speciation for trace metals, the arbitrary distinction between dissolved and particulate metal was avoided. In all, six size-fractions were defined covering the total metal in a sample. Total metal analysis was performed by ASV on each of the fractions following acidification and digestion by UV irradiation. Measurement of the ASV-labile metals at the natural pH of the sample was carried out using  $\text{CO}_2$  in a  $\text{N}_2$  purge to maintain the natural buffering capacity of the water. This avoided any possible change in speciation caused by the addition of a synthetic buffer. A HMDE was used for all ASV measurements

as this avoided any problems caused by addition of mercury to form a MFE. Chelex-labile metal was also determined.

Application of the scheme to the analysis of Cd, Pb and Cu in freshwater samples {87,88} highlighted the limitations of some components of the scheme. It was discovered that UV irradiation resulted in a considerable increase in the pH of a water sample, with simultaneous loss of ASV-labile metal. The pH rise was attributed to a loss of dissolved carbon dioxide. Loss of ASV-labile metal, particularly lead, was probably due to the destruction of organic coatings on colloidal hydrous iron oxides. Destruction of such coatings allows the iron oxides to coagulate and precipitate. Hence, metals with a strong tendency to be adsorbed by iron oxides are removed from solution by the precipitating iron oxides. Because of these difficulties, data relating to metal-organic complexation in the original sample was not obtained. However, qualitative data was derived from observing the changes in the stripping current and potential following UV irradiation. Use of ozone as an alternative to UV irradiation was unsuccessful. Again the ASV-labile metal concentration diminished in samples following ozone oxidation. In the case of lead, losses were due to formation of highly insoluble lead dioxide following oxidation of Pb(II) to Pb(IV).

Despite the problems encountered with some components of the scheme it was possible to obtain information on the species within the different size fractions. For freshwater samples with large amounts of suspended solids, cadmium, lead and copper were predominantly present in the particulate ( $>1.0\mu\text{m}$ ) fraction. In the  $0.4\text{-}1.0\mu\text{m}$  fraction, only a small proportion of these three metals were "labile" with respect to ASV and Chelex ion-exchange resin, suggesting the presence of strong complexing agents in the samples.

#### 1.5.2.2. Titrimetric Methods

In addition to the preceding direct measurement methods, ASV can provide important information on metal-ligand interactions using various titration methods.

##### 1.5.2.2.1. Titration of Ligands with Metal Ions

In this type of study, an appropriate concentration of the ligand to be studied is adjusted in a natural water sample or a model solution. The solution is then titrated with a standard metal solution and the response due to the remaining unchelated metal is measured by ASV. A titration curve is obtained by plotting the ASV response versus the total metal concentration. The shape

of the resultant titration curve depends on the particular metal-ligand interaction occurring within the solution.

Titrimetric methods have been employed in a study of the interactions of copper, thallium and cadmium with humic acid in simulated aquatic conditions {89}. By measuring both the peak currents and the shifts in peak potentials during the titration, it was possible to distinguish between "labile" and "non-labile" metal complexes. The results for the titration of humic acid with copper were indicative of "non-labile" interactions. At pH 6.2, no current response was observed until after  $4 \times 10^{-8}$  M Cu had been added to the solution because the added Cu was strongly bound in "non-labile" complexes with the available humic acid ligand sites. Above this concentration, all the "non-labile" sites were saturated and further addition of Cu resulted in the formation of "labile" complexes with other ligands, or the availability of free copper. The extent of the "non-labile" complexation was found to increase with increasing pH. Thallium exhibited interactions with both the organic ligand sites of the humic acid and the inorganic ligands found in the supporting electrolyte.

The results for cadmium illustrated the difficulties associated with the operational definition of

the terms "labile" and "non-labile". "Labile" refers to complexes whose dissociation rates are much faster than the rate of plating and "non-labile" applies to those complexes that dissociate much slower than the rate of plating. The titration of humic acid solutions with cadmium indicated a system in which the metal-ligand interactions were "labile". However, when cadmium solutions were titrated with humic acid, the results indicated the formation of "non-labile" complexes. The apparent inconsistency between results was thought to be due to the formation of complexes whose dissociation rates were similar to the rate of plating. Therefore these complexes could exhibit "labile" characteristics in some situations and "non-labile" characteristics in others. Thus the interaction of cadmium with humic acid was considered to be neither "labile" nor "non-labile" but to represent a series of interactions which produced complexes of intermediate dissociation rates.

Titrimetric methods have also been used to study the effect of calcium on the interaction of trace metals with humic acid {90}. In general, calcium did not release trace metals bound at "non-labile" sites on humic acid. However, it did compete successfully for "labile" binding sites, releasing metals, especially Cd, from their "labile" sites by forming stronger complexes with humic acid. Thus,

calcium inhibited "labile" interactions between metals and humic acid but did not affect any "non-labile" interactions.

#### 1.5.2.2.2. Titration of Metal Ions with Ligands

This is an alternative approach in the study of metal-ligand interactions. Here the concentration of the metal to be studied is adjusted in a natural water sample or a model solution. Increasing concentrations of ligand are added and the ASV response of the uncomplexed metal is measured. The response of uncomplexed metal decreases with increasing ligand concentration. By plotting the percentage uncomplexed metal versus  $\log_{10}$  of the ligand concentration, the degree of complexation of the studied metal by the titrant ligand is obtained.

Studies of this kind have been undertaken in natural and artificial seawater for Cd, Pb and Zn with nitrilotriacetic acid {91}. A larger concentration of NTA had to be added to natural seawater to achieve the same degree of complexation with Cd in both solutions. The reason for this is that alkaline earth metals strongly compete with trace metals for NTA ligands. Thus in natural waters with significant concentrations of Ca and Mg, these metals occupy a substantial number of complexation sites

and must be displaced from occupied complexation sites by the stronger complexing heavy metals present.

#### 1.5.2.2.3. Complexation Capacity

Complexing capacity is defined as "the potential of an aquatic system to bind a metal by complexation and adsorption" {79}. It is an important water quality parameter because it indicates the ability of a body of water to complex and detoxify added heavy metals. The complexing capacity of an aquatic system differs for each heavy metal added. In general, complexing capacities follow the sequence  $Cu > Pb > Cd$  {92}.

The metal-complexing capacity of natural waters is determined by voltammetric titration. Before titration, water samples are filtered to remove particulate matter. This is followed by titration of the sample with a standard heavy metal solution. After sufficient equilibration time the reversible voltammetric response of the metal is recorded. Peak current as a function of added metal concentration is plotted, yielding two lines of different slopes whose intersection corresponds to the complexing capacity. The first section of the plot represents that fraction of the added heavy metal concentration which remains as "labile" species. The second section is much



steeper as all the material able to bind the metal as "non-labile" species has been consumed. Therefore, all further additions result in totally "labile" species and consequently peak currents significantly increase.

Complexation capacity determinations on seawater samples were carried out using DPASV at a HMDE {93}. The values were found to be higher for Cu than for Pb, whereas for Cd they were zero, signifying that Cd formed only "labile" complexes. In contrast, significantly higher values were obtained for Cu and Pb in freshwaters that were well supplied with nutrients {91}.

#### 1.5.2.3. Determination of Stability Constants and Stoichiometries of Heavy Metal Complexes

Studies of this kind have been employed in the determination of stability constants for defined inorganic complexes. Generally, the metal levels used are several orders of magnitude higher than those observed in natural systems. The principal inorganic ligands studied are carbonate, fluoride and chloride, as these ligands are responsible for keeping metals in solution in natural waters {94}. These ionic ligands form "labile" mononuclear complexes with heavy metals. The heavy metal central ion in these "labile" complexes undergoes a reversible

electrode reaction. Because of complexation, the half-wave potential of the complexed metal differs from that of the uncomplexed metal. Thus, the overall stability constant and ligand number of the metal complex is determined from shifts in half-wave potential using the Lingane equation {95}.

This approach has been used to study the complexing ability of zinc and cadmium with chloride ions in seawater {96}. Zinc did not form any chloro-complexes. Instead it predominantly existed as a hydrated ion, although some zinc was present as a monohydroxy complex. However, cadmium only existed as a monochloro complex in seawater.

The stability of Cu, Pb, Cd and Zn complexes relevant to freshwater systems have been determined using DPASV and DP polarography methods {97}. Both hydroxide and carbonate ions were important in regulating the copper species present in freshwater systems. For lead, the dominant species was  $PbCO_3$ , whereas zinc existed as an insoluble hydroxide above pH 7.5. Cadmium remained almost exclusively in the hydrated form. Stability constants for copper and lead complexes with carbonate ions were determined from the shift of peak potential using the

Lingane equation.

A modified version of ASV has been developed for the determination of stability constants at natural concentrations {98}. The ASV peak heights were plotted as a function of deposition potential and a pseudo DC - polarogram was obtained. By plotting the apparent peak potentials versus ligand concentration, the stability constants of the chloro-complexes of lead and cadmium were evaluated.

### 1.5.3. Problems Associated with ASV in Trace Metal Studies

In trace metal studies using ASV, the possibility of misinterpretation of results can occur. Some of the factors that can lead to misinterpretation of results are now considered.

#### 1.5.3.1. Adsorption at Electrodes

The adsorption of organic matter, e.g., humic acids{99} and surfactants{100}, at the surface of a mercury electrode can affect ASV measurements. In particular, peak potentials may be shifted to more positive values if an adsorbed molecule forms a layer at the electrode surface and renders the metal oxidation irreversible by creating a

barrier to ion diffusion. Furthermore, adsorption can also affect the peak current, either by forming metal complexes or by adsorbing onto the electrode surface with resultant hindrance of the plating or stripping steps. These effects are a significant problem when undertaking analysis in organic-rich waters such as marshes, eutrophic lakes, sewage and rivers receiving treated wastewater{99}.

Elimination of these problems may be effected by prior destruction of the organic material{100} but because it also releases bound metals, speciation studies are not possible. An alternative approach has recently been developed using a rotating membrane-covered mercury film electrode (MCMFE){101}. The dialysis membrane provided a protective barrier and eliminated interferences caused by organic matter. This electrode has been used with DPASV to measure Cd in the presence of surfactants{102}. The MCMFE eliminated many of the adsorption problems which had previously been encountered at the HMDE as well as those seen at a bare MFE.

#### 1.5.3.2. Oxygen Elimination

In stripping voltammetry the presence of dissolved oxygen can result in partial dissolution of the metal accumulated in the plating step and thus lower analytical

results are obtained. Removal of oxygen is normally effected by purging the analytical solution with an inert gas. In natural water samples, where the pH is determined by the carbonic system, this procedure can alter the pH by removal of  $\text{CO}_2$ . Consequently, this change in pH may induce modifications in the metal speciation of a sample{84}.

A procedure has been developed which allows the removal of dissolved oxygen without any change in pH of natural water samples{103}. The evolution of  $\text{CO}_2$  was prevented by bubbling a mixture of  $\text{N}_2$  and  $\text{CO}_2$ , where the partial pressure of  $\text{CO}_2$  was adjusted to maintain constant pH of the solution.

#### 1.5.3.3. Intermetallic Compounds

The formation of intermetallic compounds at electrodes is a contributing factor to the inaccuracy of results by ASV measurement. Intermetallic interactions usually cause one of the stripping peaks to be depressed when compared with the peak height obtained in the absence of the second metal. Noted examples are the interactions of copper and zinc or copper and cadmium resulting in the depression of the zinc and cadmium stripping peaks{104}.

The problem of intermetallics can be overcome by addition of a third element to mask one of the metals {105}. For example, addition of germanium allowed zinc to be determined in the presence of copper because the Ge-Cu intermetallic compound was more stable than the Zn-Cu compound. Addition of a third element can also be useful in resolving adjacent overlapping peaks {106} in stripping analysis. However, negative effects on the accuracy of ASV determinations are possible if the third element interacts equally strongly with both metals.

#### 1.6. Determination of Organic Pollutants in Environmental Samples

Application of voltammetric methods to the analysis of selected organic pollutants is now illustrated. Reference will also be made to chromatovoltammetry, i.e., HPLC with electrochemical detection, as it is finding increasing application in organic analyses.

##### 1.6.1. Sulphur-Containing Compounds

Compounds containing an -SH moiety are particularly amenable to cathodic stripping voltammetry (CSV) due to their ability to form partially insoluble complexes with mercury. DPCSV has been applied to the

determination of some thiourea-containing agrochemicals {107}. This method was considerably more sensitive but less selective than measurement by DP polarography at a DME. The limit of detection of the DPCSV method was 1  $\mu\text{g}/\text{l}$ .

Thiourea has also been determined polarographically following complexation with  $\text{Cu(II)}$  ions {108} or by liberation of the S-atom and subsequent determination of  $\text{H}_2\text{S}$  {109}. The latter method has also been used for the determination of other S-containing pesticides, e.g., diazinon, rogor and phenkapton. It involved reduction of the pesticide by Al in HCl solutions in the presence of Ni. The  $\text{H}_2\text{S}$  evolved was then determined by monitoring the decrease of  $\text{Pb(II)}$  concentration in a  $\text{Pb(OAc)}_2$  trapping solution. The method could determine S-containing pesticides down to 0.25 mg/l in laboratory prepared solutions.

CSV has also been used to determine tetramethylthiuram disulphide (thiram) in aqueous samples {110}. Prior to CSV analysis the disulphide moiety in thiram was chemically reduced at a mercury plated platinum electrode, in a solution containing an excess of ascorbic acid. This resulted in the formation of free -SH groups which were then amenable to CSV analysis. The limit of detection of this method was considerably greater than

linear sweep or AC methods which had been previously used.

There has been little application of chromatovoltammetry to the determination of compounds containing -S-S-, =C=S or -SH moieties because their electrochemical behaviour is dependent on the use of mercury as the working electrode. In particular, problems have been encountered in coupling HPLC with a cathodic stripping voltammetric mode of detection. The use of cathodic stripping voltammetry for the determination of sulphur-containing organic species in quiescent solution is well documented but inherent problems lie in finding the correct conditions where these substances will remain plated in a flowing solution. Particular problems in this regard have been demonstrated in the case of thioamides using a thin-film mercury electrode {111}. Chromatovoltammetry has been used to quantify the potentially carcinogenic metabolite ethylene thiourea and related substances in rat urine {112}. Additionally, chromatovoltammetry has been successfully applied to the detection of the sulphur-containing pesticide dithianon in fruit down to 0.01 mg/l {113}.

#### 1.6.2. Nitrogen-Containing Compounds

Polarographic methods for the determination of



nitro compounds in effluents and wastewater have been developed. Nitrobenzene {114} was determined in industrial wastes after separating from nitrophenols by distillation. Linear sweep voltammetry was used to quantify dinitro-o-cresol {115} in water following acidification of the water sample and extraction with petroleum ether. This method was capable of detecting such compounds at levels as low as 0.004 mg/l. Nitrochlorobenzenes {116} have been determined at 0.005 mg/l concentrations in water following extraction with activated charcoal and polarographic measurement of the eluted acetone solution in a pyridinium hydrochloride supporting electrolyte. Nitrophenols, nitrocresols and nitrotoluenes were polarographically analysed in wastewater {117}. The supporting electrolyte used was 0.25M NaOH in 3:1 methanol:water; half-wave potentials in the region -0.70 to -1.20V were obtained.

Nitrogen-containing compounds that have been quantified by chromatovoltammetry are those containing an aromatic amine function. The use of carbon electrodes in the hydrodynamic chronoamperometric mode improve the detection limits of nitrogen-containing compounds, that are easily oxidised (+0.2 - +1.0V), by many orders of magnitude. This is exemplified in the case of chloroanilines where detection limits of 10-20pg have been quoted for the determination of 2-chloroaniline and

4,4'-methylenebis (2-chloroaniline) in factory atmospheres {118}. A method has also been reported for the determination of chlorinated anilines in urine {119}.

HPLC methods employing voltammetric detection offer a great improvement in sensitivity (of up to 50 times) over similar methods employing UV detection. In the analysis of benzidine, for example, a variety of different columns (both reverse-phase and ion-exchange) and detection systems (employing carbon paste, carbon black/polyethylene or reticulated vitreous carbon electrodes) have been used for its determination in wastewater {120}, in various effluents {121}, in soil {122} and in a 1000-fold excess of aniline {123}. In all cases, the methods were able to determine benzidine in the low picogram range with good precision. Other aromatic amines that have been determined by HPLC-voltammetric detection (VD) include aniline {124}, 1- and 2- naphthylamine {119, 124}, hydrazine and its monomethyl-, 1,1-dimethyl- and 1, 2-dimethyl analogues {125}, anthracene, 2-aminoanthracene and acridine {126}.

### 1.6.3. Oxygen-Containing Compounds

Although the carbonyl group is electro-reducible, the little work which has been carried out on carbonyl compounds by direct polarographic methods has been mainly

confined to aldehydes such as formaldehyde, acetaldehyde, butyraldehyde and furfural {127-131}. Detection limits in the low mg/l region in wastewaters were reported.

Derivatisation of carbonyls to semicarbazone derivatives has been exploited for their detection in natural waters and industrial effluents using twin cell potential sweep voltammetry {132}. Using a citrate buffer with EDTA added to complex interfering heavy metals, a detection limit of 0.25  $\mu\text{g}/\text{l}$  was possible without any separation or preconcentration of the sample.

Most polarographic methods for the determination of phenolic compounds have been based on prior derivatisation methods. For the analysis of phenol in water {133}, the sample was first made alkaline and concentrated by evaporation. The liquid was then acidified and the phenol extracted into diethyl ether. After evaporating to dryness, the residue was nitrated with hot concentrated nitric acid and sulphuric acid. Pulse polarography was carried out after adjustment of the nitration mixture to pH 4.9 with buffer. The limit of detection of this method was 1  $\mu\text{g}/\text{l}$ .

Application of HPLC with voltammetric detection (VD) to the determination of phenols in ground and

has been reported by several authors {134-136}. The limits of detection for compounds such as resorcinol, phenols, xylenols and chlorinated phenols were in the low picogram range. The sensitivity is much better than corresponding methods employing UV detection and should provide a complimentary means to capillary GC, which is recognised as the forerunner in this area of analysis.

Chromatovoltammetric methods have also been described for the determination of chlorophenols in urine {137} and 2-phenylphenol in orange rind {138}.

Because of the high sensitivity that voltammetric detection affords for phenolic compounds, several methods have been developed for the determination of carbamate pesticides following conversion to the corresponding phenolic derivative. This conversion is best carried out in alkaline media (pH 11-12) and is an improvement over existing gas chromatographic methods which require further derivatisation of the liberated phenol prior to analysis {139}. Several carbamate pesticides can be determined directly using chromatovoltammetry, but these compounds rely on the presence of secondary or tertiary amino moieties in their molecular structure for their electroactivity. In a theoretical study on 13 carbamate pesticides {140}, it was reported that only two compounds, aminocarb and mexacarbate, were amenable to voltammetric

detection following HPLC separation. Several workers have been able to develop working methods for the determination of aminocarb based on its oxidation behaviour {141,142}. In another study of carbamate pesticides, it was shown that voltammetric detection was more selective than UV detection, but stated that UV detection had in general the better sensitivity for this particular group of compounds {143}.

#### 1.6.4. Organometallic Compounds

Generally, there are two approaches for the polarographic and voltammetric determination of organometallic compounds in environmental samples. In tact compounds may be directly determined by an electroanalytical method<sup>1</sup>. Alternatively the compound may be degraded and subsequently either the liberated metal or the remaining organic species can be determined electrochemically.

DC polarography and linear sweep voltammetry (LSV) have been applied to the determination of three metal-containing dithiocarbamate pesticides, ziram, zineb and ferbam {144}. In 0.5M  $\text{NH}_4\text{OH}/0.5\text{M NH}_4\text{Cl}$  supporting electrolyte, ziram gave an anodic wave due to oxidation of dimethyldithiocarbamic acid, whereas in 0.2M NaOH it gave

rise to a cathodic wave due to the reduction of Zn(II) ions. The latter electrolyte was preferred as the reduction wave of Zn(II) was not affected by matrix interferences.

For the determination of organometallic species in a flowing solution a gold amalgamated mercury electrode (GAME) has been employed [145, 146]. For chromatographic purposes, the GAME has the great advantage over the DME or static mercury drop electrode (SMDE) in that it can be adopted successfully for use with oxidative voltammetric detector designs. It also gives reproducible results over a full days operation. Using HPLC in conjunction with a GAME, it has been found possible to selectively determine compounds such as methyl-, ethyl- and phenylmercury in fish material down to the 40 picogram level [146]. In addition, when the GAME is operated in the DP mode, it has been found to offer greater selectivity for the determination of both organomercury and organotin compounds [145]. Another method has been described for the determination of methylmercury in fish, but the polarographic detection method employed was found to be less sensitive than cold-vapour atomic absorption spectroscopy [146].

#### 1.6.5. Miscellaneous Compounds

A chromatovoltammetric method has been developed for the determination of aromatic and aliphatic isocyanates {147}. This method required derivatisation of the isocyanates with 1-(2-methoxyphenyl)piperazine, which formed EC and UV active derivatives. The resulting derivatives were all found to give an oxidation wave at +0.75V. A comparison was made between the chromatovoltammetric method and the corresponding method employing UV detection. The former method was found to be 20 times more sensitive than the latter method.

In some situations, derivatisation can result in more than one product. Derivatisation of 2,4-di-isocyanotoluene was carried out using p-aminophenol {148}. The separated products were detected amperometrically in the oxidative mode at a Kel-F/graphite electrode following reverse-phase HPLC. The detection limit was about 94 pg/injection. Several products were obtained because the isocyanate function can react with both the free amino and phenol functions of p-aminophenol.

HPLC-VD methods have also been described for the determination of phenoxy-acid herbicides {149}, pesticides in air {150} and nitro-substituted polynuclear hydrocarbons in diesel soot {151}.

References

1. H.A. Schroeder and D.K. Darrow, Proc. Anal. Chem., 5, 81 (1973).
2. P. Grandjean and T. Nielsen, Residue Rev., 72, 98 (1979).
3. J. Berg and M. Zapella, J. Ment. Defic. Res., 8, 44 (1964).
4. G.W. Bryan, Marine Pollution, edited by R. Johnston (Academic Press, London, 1976), p. 185.
5. C.J. Terhaar, W.S. Ewell, S.P. Dziuba, W.W. White and P.J. Murphy, Water Research, 11, 101 (1977).
6. U. Forstner and W. Salomons, Environ. Technol. Letters, 1, 494 (1980).
7. S.W. Karickhoff and K.R. Morris, Environ. Sci. Technol., 19, 51 (1985).
8. H.W. Nurnberg, Sci. Total Environment, 12, 35 (1979).
9. B.T. Hart, Chem. in Australia, 50, 13 (1983).
10. H.W. Nurnberg, P. Valenta, L. Mart, B. Raspor and L. Sipos, Fresenius Z. Anal. Chem., 282 357 (1976).
11. W.F. Smyth and M.R. Smyth, Analysis of Organic Micropollutants in Water, edited by A. Bjorseth and G. Angeletti (D. Riedel, Dordrecht, 1982), pp. 323-329.
12. G.W. Ewing, Instrumental Methods of Chemical



- Analysis, 4th Edition (McGraw-Hill, Tokyo, 1975), pp. 491-503.
13. H.W. Nurnberg, *Electrochimica Acta*, 22, 935 (1977).
  14. A.M. Bond, Modern Polarographic Methods in Analytical Chemistry (M. Dekker Inc., New York, 1980).
  15. G.C. Barker and A.W. Gardner, *Z. Anal. Chem.*, 173, 79 (1960).
  16. T.R. Copeland and R.K. Skogerboe, *Anal. Chem.*, 46 1257A (1974).
  17. J. Wang, *Environ. Sci. Technol.*, 16, 104A (1982).
  18. T.M. Florence, *J. Electroanal. Chem.*, 168, 207 (1984).
  19. M.R. Smyth, C.G.B. Frischkorn and H.W. Nurnberg, *Anal. Proc.*, 18, 215 (1981).
  20. H.W. Nurnberg, *Anal. Chim. Acta*, 164, 1 (1984).
  21. M.A. Sirover and L.A. Loeb, *Science*, 194, 1434 (1976).
  22. E. Steeman Nielsen and W. Wiium-Andersen, *Marine Biology*, 6, 93 (1970).
  23. G.W. Bryan, *Proc. Roy. Soc. London*, 177, 389 (1971).
  24. E.A. Crecelius, *Environ. Health Perspectives*, 19, 147 (1977).
  25. Y.K. Chau and P.T.S. Wong, *N.B.S. Special Publication (U.S.)*, 618, 65 (1981).
  26. J.S. Thayer, G.J. Olson and F.E. Brinkman, *Environ.*

- Sci. Technol., 18, 726 (1984).
27. I. Ahmad, Y.K. Chau, P.T.S. Wong, A.J. Carthy and L. Taylor, Nature, 287, 716 (1980).
28. W.P. Ridley, L.J. Dizikes and J.M. Wood, Science, 197, 329 (1977).
29. S. Jensen and A. Jernelov, Nature, 223, 759 (1969).
30. R.M. Sterritt and J.N. Lester, Sci. Total Environment, 14, 5 (1980).
31. B. Kratochvil and J.K. Taylor, Anal. Chem., 53, 924A (1981).
32. D.G. Walker, Effluent and Water Treatment Journal, 22, 184 (1982).
33. L. Mart, Talanta, 29, 1035 (1982).
34. K.S. Subramanian, C.L. Chakrabarti, J.E. Sueiras and I.S. Maines, Anal. Chem., 50, 444 (1978).
35. A. Zirino, Marine Electrochemistry, edited by M. Whitfield and D. Jagner (J. Wiley & Sons, Chichester, 1981), pp. 422-503.
36. L. Mart, Fresenius Z. Anal. Chem., 299, 97 (1979).
37. G.E. Batley and D. Gardner, Water Research, 11, 745 (1977).
38. B. Schaule and C.C. Patterson, Lead in the Marine Environment, edited by M. Branica and Z. Konrad (Pergamon Press, Oxford, 1980), p.31.
39. T.M. Florence, Talanta, 29, 345 (1982).
40. T.M. Florence, Anal. Chim. Acta, 141, 73 (1982).

41. P. Benes and E. Steinnes, *Water Research*, 9, 741 (1975).
42. H. Scheuermann and H. Hartkamp, *Fresenius Z. Anal. Chem.*, 315, 430 (1983).
43. L. Mart, *Fresenius Z. Anal. Chem.*, 296, 350 (1979).
44. G. Somer, G. Ozyoruk and M.E. Green, *Analyst*, 110, 151 (1985).
45. W.F. Smyth, L. Goold, D. Dadgar, M.R. Jan and M.R. Smyth, *International Laboratory*, pp. 43-50, September 1983.
46. H.N. Heckner, *Fresenius Z. Anal. Chem.*, 261, 29 (1972).
47. L. Mart, H.W. Nurnberg and P. Valenta, *Fresenius Z. Anal. Chem.*, 300, 350 (1980).
48. V. Gajda and K. Horak, *Anal. Chim. Acta*, 134, 219 (1982).
49. T. Miwa, L. Jin and A. Mizuike, *Anal. Chim. Acta*, 160, 135 (1984).
50. G.J. Svoboda, J.P. Sottery and C.W. Anderson, *Anal. Chim. Acta*, 166, 297 (1984).
51. S.J. Reddy, P. Valenta and H.W. Nurnberg, *Fresenius Z. Anal. Chem.*, 313, 390 (1982).
52. V.D. Nguyen, P. Valenta and H.W. Nurnberg, *Sci. Total Environment*, 12, 151 (1979).
53. P. Valenta, L. Mart and H. Rutzel, *J. Electroanal. Chem.*, 82, 327 (1977).

54. T.M. Florence and G.E. Batley, *Talanta*, 23, 179 (1976).
55. L. Mart, H.W. Nurnberg, P. Valenta and M. Stoeppler, *Thalassia Jugoslavica*, 14, 171 (1978).
56. L. Mart, H.W. Nurnberg and H. Rutzel, *Fresenius Z. Anal. Chem.*, 317, 201 (1984).
57. L. Sipos, J. Golimowski, P. Valenta and H.W. Nurnberg, *Fresenius Z. Anal. Chem.*, 298, 1 (1979).
58. L. Sipos, P. Valenta, H.W. Nurnberg and M. Branica, *J. Electroanal. Chem.*, 77, 263 (1977).
59. B. Pillar, P. Valenta and H.W. Nurnberg, *Fresenius Z. Anal. Chem.*, 307, 337 (1981).
60. J. Wang, *Int. Lab.*, pp. 12-25, September 1983.
61. P. Valenta, L. Sipos, I. Kramer, P. Krumpfen and H. Rutzel, *Fresenius Z. Anal. Chem.*, 312, (1982).
62. J. Wang and H.D. Dewald, *Anal. Chim. Acta*, 162, 189 (1984).
63. R.W. Andrews and D.C. Johnson, *Anal. Chem.*, 48, 1056 (1976).
64. A. Zirino, S.H. Lieberman and C. Clavell, *Environ. Sci. Technol.*, 12, 73 (1978).
65. A.M. Bond and G.G. Wallace, *Anal. Chem.*, 53, 1209 (1981).
66. A.M. Bond and G.G. Wallace, *Anal. Chem.*, 54, 1706 (1982).
67. A.M. Bond and G.G. Wallace, *J. Liq. Chromatogr.*, 6,

- 1977 (1983).
68. R. Eggli, *Anal. Chim. Acta*, 91, 129 (1977).
  69. D. Jagner and A. Graneli, *Anal. Chim. Acta*, 83, 19 (1976).
  70. A. Hussam and J.F. Coetzee, *Anal. Chem.*, 57, 581 (1985).
  71. S. Jaya and T.P. Rao, *Rev. Anal. Chem.*, 6, 343 (1982).
  72. I. Drabark, P.P. Madsen and J. Sorensen, *Intern. J. Environ. Anal. Chem.*, 15, 153 (1983).
  73. D. Jagner, *Analyst.*, 107, 593 (1982).
  74. R.J. Gibbs, *Science*, 180, 71 (1973).
  75. B. Welte, N. Bles and A. Montiel, *Environ. Technol. Letts.*, 4, 79 (1983).
  76. R.D. Guy and C.L. Chakrabarti, *Chem. Can.*, 28, 26 (1976).
  77. J.R. Hasle and M.I. Abdullah, *Mar. Chem.*, 10, 487 (1981).
  78. G.E. Batley and T.M. Florence, *Anal. Letts.*, 9, 379 (1976).
  79. T.M. Florence and G.E. Batley, *CRC Crit. Revs. Anal. Chem.*, 9, 219 (1980).
  80. T.M. Florence, *Water Research*, 11, 681 (1977).
  81. G.E. Batley and T.M. Florence, *Mar. Chem.*, 4, 347 (1976).
  82. G.E. Batley and D. Gardner, *Estuarine Coastal Mar.*

- Sci., 7, 59 (1978).
83. F.M.M. Morel and J.J. Morgan, Environ. Sci. Technol., 6, 58 (1972).
84. R.K. Skogerboe, S.A. Wilson and J.G. Osteryoung, T.M. Florence and G.E. Batley, Anal. Chem., 52, 1960 (1980).
85. P. Figura and B. Duffie, Anal. Chem., 52, 1433 (1980).
86. J.A. Cox, K. Slonawska, D.K. Gatchell and A.G. Hiebert, Anal. Chem., 56, 650 (1984).
87. D.P. Lazen and R.M. Harrison, Sci. Total Environment, 19, 59 (1981).
88. R.M. Harrison and S.J. Wilson, Analytical Techniques in Environmental Chemistry, Vol. 2 (Pergamon Press, Oxford, 1982), pp. 301-314.
89. T.A. O'Shea and K.H. Mancy, Anal. Chem., 48, 1603 (1976).
90. T.A. O'Shea and K.H. Mancy, Water Research, 12, 703 (1978).
91. H.W. Nurnberg, Trace Element Speciation in Natural Waters and its Ecological Implications, edited by G.G. Leppard (Plenum Publ. Corp., New York and London, 1983), pp. 211-230.
92. H.W. Nurnberg, Fresenius Z. Anal. Chem., 316, 557 (1983).
93. H.W. Nurnberg and P. Valenta, Trace Metals in Sea

- Water, edited by C.S. Wong, E. Boyle, K.W. Bruland, J.D. Burton and E.D. Goldberg (Plenum Press, New York and London, 1983), pp. 672-697.
94. L.R. Pittwell, *J. Hydrology*, 21, 301 (1974).
95. J.J. Lingane, *Chem. Rev.*, 29, 1 (1941).
96. A. Baric and M. Branica, *J. Polarog. Soc.*, 13, 4 (1967).
97. R. Ernst, H.E. Allen and K.H. Mancy, *Water Research*, 9, 969 (1975).
98. M. Branica, D.M. Novak and S. Bubic, *Croatica Chemica Acta*, 49, 539 (1977).
99. P.L. Brezonik, P.A. Brauner and W. Stumm, *Water Research*, 10, 605 (1976).
100. A. Beveridge and W.F. Pickering, *Water Research*, 18, 1119 (1984).
101. E.S. Stewart and R.B. Smart, *Anal. Chem.*, 56, 1131 (1984).
102. R.B. Smart and E.S. Stewart, *Environ. Sci. Technol.*, 19, 137 (1985).
103. J. Lecomte, P. Mericam, A. Astruc and M. Astruc, *Anal. Chem.*, 53, 2372 (1981).
104. F. Vydra, K. Stulik and E. Julakova, Electrochemical Stripping Analysis (Ellis Horwood, Chichester, UK, 1976), pp. 61-62.
105. E.Y. Neiman, L.G. Petrova, V.I. Ignatov and G.M. Dolgopolova, *Anal. Chim. Acta*, 113, 277 (1980).

106. J. Wang, P.A.M. Farias and D. Luo, *Anal. Chem.*, 56, 2379 (1984).
107. M.R. Smyth and J.G. Osteryoung, *Anal. Chem.*, 49, 2310 (1977).
108. H. Sohr and K. Wienhold, *Anal. Chim. Acta*, 83, 415 (1976).
109. E.S. Kosmatyi and V.N. Kavetskii, *Zav. Lab.*, 41, 286 (1975).
110. M.J.D. Brand and B. Fleet, *Analyst*, 95, 1023 (1970).
111. W. Franklin Smyth, A. Ivaska, J.S. Burmicz, I.E. Davidson and Y. Vaneesorn, *Bioelectrochem. Bioenerg.*, 8, 459 (1981).
112. J.F. Lawrence, F. Iverson, H.B. Hanekamp, P. Bos and R.W. Frei, *J. Chromatogr.*, 212, 245 (1981).
113. W. Buchberger and K. Winsauer, *Microchim. Acta*, 2, 257 (1980).
114. F.G. Dyatlovitskaya, F.I. Berezonskii and S.K. Potemkina, *Gig. I. Sanit.*, 28, 38 (1963).
115. G.S. Supin, F.F. Vaintraub and C.V. Makarova, *Gig. Sanit.*, 5, 61 (1971).
116. B. Fleszar, *Chem. Anal. (Warsaw)*, 9, 1075 (1964).
117. Z.P.M. Zaitsev and V.I. Dichenskiı, *Zavod. Lab.*, 32, 800 (1966).
118. C.J. Purnell and C.J. Warwick, *Analyst*, 105, (1980).
119. E.M. Lores, F.C. Meekins and R.F. Mozeman, *J. Chromatogr.*, 188, 412 (1980).



120. D.N. Armentrout and S.A. Cutie, J. Chromatogr., 18, 370 (1980).
121. J.R. Rice and P.T. Kissinger, J. Anal. Toxicol., 3, 64 (1979).
122. J.R. Rice and P.T. Kissinger, Environ. Sci. Technol., 16, 263 (1982).
123. V. Concialini, G. Chiavari and P. Vitali, J. Chromatogr., 258, 244 (1983).
124. R.M. Riggan and C.C. Howard, Anal. Chem., 51, 210 (1979).
125. H.R. Hunziker and A. Miserez, Mitt. Geb. Lebensmittelunters. Hyg., 72, 216 (1981).
126. W.L. Caudill, M.V. Novotny and R.M. Wightman, J. Chromatogr., 261, 415 (1983).
127. F.G. Dyatlovitskaya and F.J. Berezouskii, Gig. I. Sanit., 27, 50 (1962).
128. V.I. Bodyn and Y.S. Feldman, Gidrolizn I. Lesokhim. Prom., 16, 11 (1983).
129. I. Melcer and A. Melcerova, Drev. Vyst., 16, 59 (1971).
130. Y.P. Ponomarev, O.I. Glazyrina and T.V. Kassai, Fiz. Khim. Metody. Ochistki. Anal. Stochnykh Vod. Prom. Predpr., 91 (1974).
131. B.P. Zhantalai, A.S. Sergeeva and L.R. Kalichuk, Zn. Khim. Abst., 221, 298 (1976).
132. B.K. Afghan, A.V. Kulkarni and J.F. Ryan, Anal.

- Chem., 47, 488 (1975).
133. Y. Audouard, A. Suzanne, O. Vittori and M. Porthaut, Bull. Soc. Chim. Fr., 130 (1975).
134. D.E. Weisshaar, D.E. Tallman and J.L. Anderson, Anal. Chem., 53, 1809 (1981).
135. D.N. Armentrout, J.D. McLean and M.W. Long, Anal. Chem., 51, 1039 (1979).
136. R.E. Shoup and G.S. Mayer, Anal. Chem., 54, 1164 (1982).
137. E.M. Lores, T.R. Edgerton and R.F. Moseman, J. Chromatogr. Sci., 19, 466 (1981).
138. D.E. Ott, J.A.O.A.C., 61, 1465 (1978).
139. W.P. King, Current Separations, 2, 6 (1980).
140. G.E. Batley and B.K. Afghan, J. Electroanal. Chem., 125, 437 (1981).
141. J.L. Anderson and D.J. Chesney, Anal. Chem., 52, 2156 (1980).
142. M. Lanouette and R.K. Pike, J. Chromatogr., 190, 208 (1980).
143. W.J. Mayer and M.S. Greenberg, J. Chromatogr., 208, 295 (1981).
144. P. Nangnot, Bull. Inst. Agron. Stat. Rech. Gembloux, 28, 365 (1960).
145. W.A. MacCrehan, Anal. Chem., 53, 74 (1981).
146. W.A. MacCrehan and R.A. Durst, Anal. Chem., 50, 2108 (1978).

147. C.J. Warwick, D.A. Bagon and C.J. Purnell, *Analyst*, 106, 676 (1981).
148. S.D. Meyer and D.E. Tallman, *Anal. Chim. Acta*, 146, 227 (1983).
149. M. Akerblom and B. Lindgren, *J. Chromatogr.*, 258, 302 (1983).
150. D.A. Bagon and C.J. Warwick, *Chromatographia*, 16, 290 (1982).
151. Z. Jin and S.M. Rappaport, *Anal. Chem.*, 55, 1778 (1983).

CHAPTER 2

THEORY

## 2.1. Polarographic and Voltammetric Methods

### 2.1.1. Introduction

Any electroanalytical method in which current-voltage relationships are studied at solid, stationary or dropping mercury electrodes is termed voltammetry {1}. However, the term polarography is restricted to current-voltage measurements at a dropping mercury electrode (DME). The original discovery of polarography was due to Jaroslav Heyrovsky in the 1920's. In subsequent years voltammetric and polarographic methods were developed until by 1950, the methods appeared to be mature and completely developed. However, the decade from 1955 to 1965 saw several major modifications. Pulse methods were developed which significantly increased the sensitivity and consequently the applications of the methods. During the 1970's a resurgence of interest in voltammetry occurred, particularly in the area of environmental analysis. During the late 1970's voltammetric methods became increasingly used as detection methods in liquid chromatography. At present, the use of voltammetric methods in continuous monitoring systems is becoming increasingly important.

In the following sections the theory associated

with direct current (DC) and pulse polarographic methods as well as cyclic and anodic stripping voltammetric methods is considered. However, before discussing the theory of these methods some general features of electrolysis are illustrated.

## 2.1.2. Basic Features of Electrochemical Processes

### 2.1.2.1. Modes of Mass Transfer of Electroactive Species to an Electrode Surface

During electrolysis, three modes of mass transfer {2} are generally of importance:

- (1) migration ;
- (11) convection ; and
- (111) diffusion.

Elimination of migrational modes of mass transfer of the electroactive species in solution is accomplished by addition of an excess of supporting electrolyte. Because the ions of the supporting electrolyte are in large excess compared to the electroactive species, they carry practically the entire charge within the solution. Consequently, migration currents of the electroactive species are negligible. For example, the migration current

(expressed by the transport number,  $t$ ) of an electroactive univalent cation in the absence of a supporting electrolyte is given by

$$t = \frac{C_+ \lambda_+}{C_+ \lambda_+ + C_- \lambda_-} \quad (2.1)$$

where  $C_+$  and  $C_-$  are the concentrations of electroactive cations and anions,  $\lambda_+$  and  $\lambda_-$  are their respective ionic mobilities. If a 100-fold quantity of a univalent supporting electrolyte is added the migration current component of the electroactive cation is decreased to

$$t = \frac{C_+ \lambda_+}{C_+ \lambda_+ + C_- \lambda_- + 100 C'_+ \lambda'_+ + 100 C'_- \lambda'_-} \quad (2.2)$$

where  $C'_+$  and  $C'_-$  are the concentrations of the cationic and anionic species of the supporting electrolyte,  $\lambda'_+$  and  $\lambda'_-$  are their respective ionic mobilities. The addition of a supporting electrolyte, whose ions do not contribute to the current because they cannot be oxidised or reduced, causes the transference number of the electroactive species to decrease.

Convective mass transfer occurs under the influence of stirring or temperature gradients in solution. Although this mode of mass transfer of electroactive species to the

electrode surface is utilized in stripping voltammetry, it is undesirable in polarographic studies. Elimination of convective mass transfer is achieved by maintaining the solution in a quiescent state.

The third mass transfer mode, diffusion, is a spontaneous process. All species in solution, whether they are charged or not, undergo diffusion. In polarographic studies, electroactive species may only be transported to the electrode surface by diffusion. This is achieved by elimination of migrational and convective modes of mass transfer.

#### 2.1.2.2. Overall Features of the Electrode Process

Electrochemical reactions that involve the transfer of charge at the solution/electrode interface are classed as heterogeneous processes. The rate of the electrochemical reaction is determined by a series of steps involving transport of electroactive species to the electrode and the transfer of charge at the interface {3}. Consider a simple electrochemical reaction of the type:



Conversion of O to R involves the following steps:



- (1) diffusion of O from the bulk solution to the electrode surface;
- (11) transfer of electrons at the electrode surface to form R ; and
- (111) diffusion of R from the electrode surface into the bulk solution.

In addition to these steps the overall electrode reaction can often involve homogeneous chemical reactions which either precede or follow the heterogeneous charge transfer step. Furthermore, other heterogeneous processes such as (a) adsorption or desorption of reactants and products or (b) surface-mediated recombination of atoms or radicals, may be coupled with the electrode reaction {4}.

The kinetics of the electrochemical reaction are strongly affected by chemical reactions occurring in solution and by adsorption phenomena. Therefore, the overall rate of the electrode reaction is determined by all of the individual rates together.

#### 2.1.2.3. Faradaic and Capacitance Currents

The total observed current in an electrochemical process arises from two clearly different processes at the electrode surface. The first process gives rise to the

faradaic current which results from electron transfer across the electrode-solution interface. Faradaic currents result when either oxidation or reduction of electroactive species occurs. The magnitude of the faradaic current is determined by the mass transfer process, the method being used and whether the electrolysis is restricted by diffusion, electron transfer, chemical kinetics or adsorption {2}. In addition, the faradaic current depends on the surface area of the electrode and the applied potential.

The second process gives rise to the capacitance or charging current and results because the structure of the electrode-solution interface can change with changing potential or surface area of the mercury drop. As no electron transfer is involved, this type of current is termed a "non-faradaic" process. Capacitance currents are explained by considering the electrode-solution interface as a pseudo-capacitor because, in the absence of electroactive species, charge cannot cross the interface by electron transfer. At a given potential the charge on the electrode will be represented by an excess or deficiency of electrons. Thus the solution in the vicinity of the electrode will be made up of an excess of cations or anions. The whole structure is called the electrical double layer {5} and is electrically neutral, even if both

sides are charged.

For an electrode of area  $A$ , growing with time  $t$ , the charge  $q$  required to bring the double layer up to any potential  $E$  is

$$q = C_{F(E)} A (E_m - E) \quad (2.4)$$

where  $C_{F(E)}$  is the capacity of the double layer per unit area and  $E_m$  is the potential where  $q = 0$ .

Over the lifespan of a single mercury drop the potential remains virtually constant and the capacitance current is primarily the result of the change in electrode area. As the mercury drop grows, current must flow to bring the electrical double layer up to that potential dictated by the electrode potential. The value of the capacitance current ( $i_C$ ) is given by the expression

$$i_C = C_{F(E)} dA/dt (E_m - E) \quad (2.5)$$

From equation (2.5) it can be seen that  $i_C$  is positive when  $E$  is more negative than  $E_m$ , zero when  $E = E_m$ , and negative when  $E$  is more positive than  $E_m$ .

As stated previously, the total current ( $i_T$ )

flowing in an electrochemical cell is the sum of the following currents:

$$i_T = i_F + i_C \quad (2.6)$$

where  $i_F$  and  $i_C$  are the faradaic and capacitance currents respectively. In polarographic and voltammetric studies only faradaic currents are of interest. Many polarographic and voltammetric methods are now able to discriminate against the capacitance current, thereby increasing their sensitivity. In the following sections some of these methods are considered.

### 2.1.3. Direct Current Polarography

#### 2.1.3.1. General Features of Direct Current Polarography

Direct current (DC) polarography is an electroanalytical method in which the current flowing at a dropping mercury electrode (DME) is measured as a function of potential [1]. The potential applied between the DME and a reference electrode is linearly varied with time. The variation of current with continuously changing potential is plotted to give a current-potential curve, alternatively known as a polarogram or polarographic wave.

A typical DC polarogram for the reduction of O is illustrated in Fig. 2.1. The wave is divided into three regions. In region A, as the potential is increased, only a small residual current flows. This current is the sum of the capacitance or charging current and faradaic current due to the reduction of trace impurities in solution. In region B, the reduction potential of O is reached. At this point O ions are reduced as follows



A steep rise in current is now observed for a small increase in applied potential. However, the O ions arrive at the DME by the relatively slow process of diffusion. Since the rate of reduction increases with applied potential, a point is eventually reached at which the ions are reduced as fast as they diffuse across the concentration gradient set up at the electrode. A diagram of the concentration gradient in the immediate vicinity of the electrode surface is shown in Fig. 2.2. When the concentration of O ions at the electrode surface approaches zero, the current reaches a maximum value, shown as region C in Fig. 2.1. This arises because further increase in potential can cause no further increase in the overall electrode reaction rate which is now controlled by the rate of diffusion.

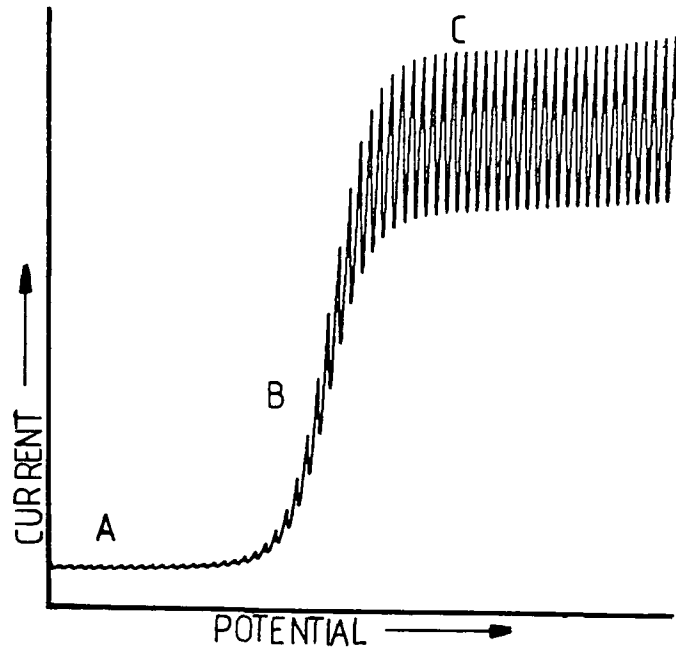


Fig. 2.1. Typical DC polarogram

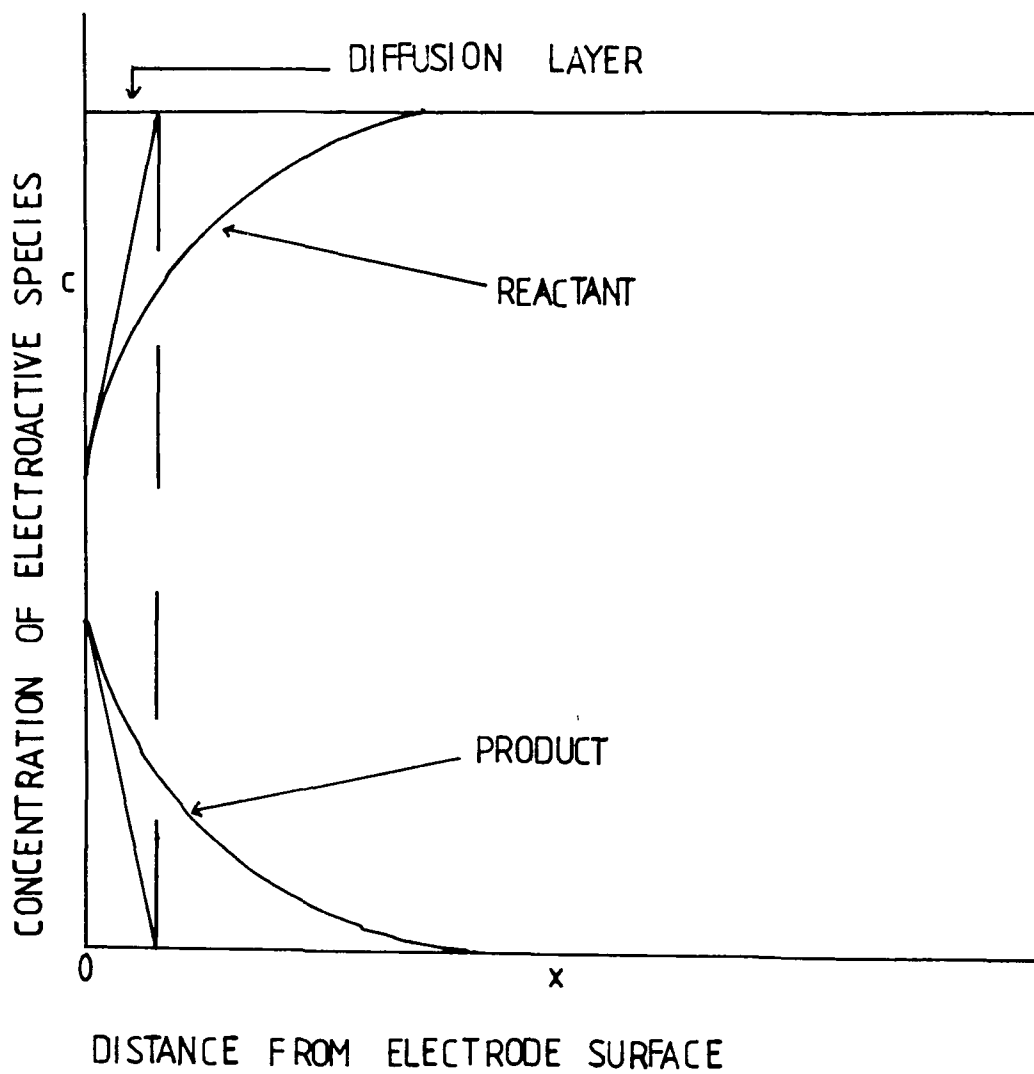


Fig. 2.2. Concentration gradient at the electrode/solution interface

Another important feature is the half-wave potential,  $E_{1/2}$ , which is defined as the potential at which the current is one-half the limiting current ( $i_{lim}$ ) value. Values of  $E_{1/2}$  are almost independent of concentration of electroactive species but are a function of parameters such as supporting electrolyte, pH, solvent system and the nature of the electroactive substance {4}. Furthermore, because the  $E_{1/2}$  value is characteristic of the substance undergoing oxidation or reduction, it may be used for qualitative characterisation purposes.

#### 2.1.3.2. Types of Limiting Currents

In this section the different types of limiting current are considered. Most limiting currents in DC polarography are diffusion-controlled; alternatively the limiting current may be controlled by kinetic, adsorption or catalytic processes.

##### 2.1.3.2.1. Diffusion-Controlled Limiting Currents

A mathematical expression for diffusion currents has been derived. Formulation of this expression is based on three laws; namely Faraday's law and Ficks first and second laws of diffusion. Faraday's law may be expressed as in equation (2.8).



$$i = nF \frac{dN}{dt} \quad (2.8)$$

where  $i$  is the electrolysis current,  $n$  is the number of electrons transferred in the electrode process,  $F$  is the Faraday constant and  $dN/dt$  is the number of moles of the electroactive substance reaching the electrode in unit time. Fick's first law of diffusion may be written as

$$dN = DA \frac{dC^0}{dx} dt \quad (2.9)$$

where  $dN$  is the number of moles of substance that diffuse across an area  $A$  at distance  $x$ ,  $dC^0/dx$  is the concentration gradient and  $D$  is the diffusion coefficient. If the mass transfer of electroactive species to the electrode is controlled only by diffusion then the diffusion current is determined by the concentration gradient at the electrode surface; thus

$$i = nFAD \left( \frac{\partial C^0}{\partial x} \right)_{x=0} \quad (2.10)$$

For unidirectional diffusion to a planar stationary electrode, Fick's second law {5} states that

$$\frac{\partial C^0}{\partial t} = D \left( \frac{\partial^2 C^0}{\partial x^2} \right) \quad (2.11)$$

If the solution of equation (2.11) is substituted into equation (2.10) then the current towards a planar stationary electrode is given by

$$i = nFAD \frac{C^0 - C^0(x=0)}{\sqrt{Dt}} \quad (2.12)$$

where  $C^0(x=0)$  is the concentration of electroactive species at the electrode surface and  $C^0$  is the concentration species in the bulk solution.

When the electrode is considered as an expanding plane or growing drop {6,7}, corrections to the above model are necessary. For unidirectional diffusion at a growing drop the diffusion equation can be written as

$$\frac{\partial C^0}{\partial t} = D \frac{\partial^2 C^0}{\partial x^2} + \frac{2}{3} \cdot \frac{x}{t} \cdot \frac{\partial C^0}{\partial x} \quad (2.13)$$

Solving equation (2.13) yields

$$\left( \frac{\partial C^0}{\partial x} \right)_{x=0} = \frac{C^0 - C^0(x=0)}{\sqrt{3/7 \pi Dt}} \quad (2.14)$$

Combining equations (2.10) and (2.14) leads to

$$i = nFAD \frac{C^0 - C^0(x=0)}{\sqrt{3/7 \pi Dt}} \quad (2.15)$$

or

$$i = 0.732 nF \left[ C^O - C^O(x=0) \right] D_m^{1/2} m^{2/3} t^{1/6} \quad (2.16)$$

where  $m$  is the rate of mercury flow and  $t$  is the drop time. Equation (2.16) is an expression for the maximum current at the end of the drop life. At the limiting current  $C^O(x=0) = 0$  and  $i = i_d$ ; so

$$i_d = 0.732 nFC^O D_m^{1/2} m^{2/3} t^{1/6} \quad (2.17)$$

Equation (2.17) is commonly referred to as the Ilkovic equation. If the mean current is considered instead of the maximum current then the numerical coefficient 0.732 in equations (2.16) and (2.17) is replaced by 0.627 {8}.

In the Ilkovic equation the parameters  $n, F, D$  and  $C$  are characteristic of the solution being studied, while  $m$  and  $t$  are characteristic of the electrode used. If the solution parameters are maintained constant then the diffusion current is expressed as

$$i_d = \text{const. } m^{2/3} t^{1/6} \quad (2.18)$$

The flow-rate of mercury through the capillary is directly

proportional to the height (h) of the mercury column. In addition, the flow-rate is directly proportional to m and inversely proportional to t. Thus,

$$i_d = \text{const. } h^{2/3} h^{-1/6} = \text{const.} h^{1/2} \quad (2.19)$$

This proportionality between  $i_d$  and h is a criterion commonly used to verify a diffusion-controlled limiting current {9}.

#### 2.1.3.2.2. Kinetic-Controlled Limiting Currents

Kinetic currents refer to situations where limiting currents are controlled by the rate of a chemical reaction occurring immediately adjacent to the mercury electrode surface. These chemical reactions may precede, follow or run parallel to the heterogeneous reaction.

##### 2.1.3.2.2.1. Preceding chemical reaction

This type of reaction may be represented by the following mechanism:



where A is the electroinactive species, O the electroactive

species, R the electrochemical reaction product and  $k_1$  and  $k_2$  are the forward and reverse rate constants respectively. The equilibrium constant for the chemical reaction may be expressed as

$$K = \frac{k_1}{k_2} \frac{[O]}{[A]} \quad (2.21)$$

If the forward rate constant  $k_1$ , is small and the equilibrium concentration of O is negligible, then the limiting current is entirely kinetic in character {4}. Therefore,

$$i_{lim} = i_k = 0.493nD_m^{1/2} t^{2/3} \sqrt{\frac{k_1}{k_2}} [A] \quad (2.22)$$

However, if the equilibrium concentration of O is appreciable in the bulk solution, then the limiting current is the sum of the diffusion and kinetic currents. Consequently,

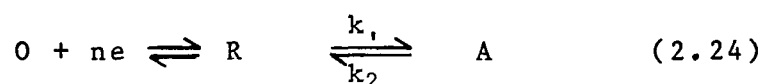
$$i_{lim} = i_d + i_k \quad (2.23)$$

To ascertain whether the limiting current is kinetically-controlled or not, a plot of  $i_{lim}$  versus  $h$  (the mercury column height) is made. If the current is entirely

kinetic in nature then  $i_{lim}$  will be independent of  $h$  {9}.

#### 2.1.3.2.2.2. Following chemical reaction

Reactions of this type are represented as follows:



In this situation the limiting current is independent of the chemical reaction and the limiting current is solely diffusion-controlled.

#### 2.1.3.2.2.3. Chemical reactions occurring parallel to the electrode reaction

In some situations the product of an electrode reaction may react with other species in solution to regenerate the original electroactive species. A general mechanism for this reaction is as follows:



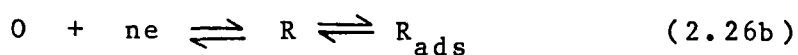
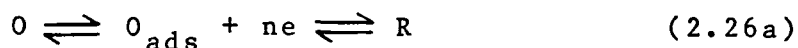
This type of reaction is known as a catalytic

process. Here the oxidised form of the redox couple is regenerated by reaction of the reduced species with a species C, which is itself not reduced at the applied potential. When  $k_1$  is very small, a negligible quantity of O is regenerated and the current will be diffusion-controlled. However, when  $k_1$  increases, more of species O is produced via the catalytic process at the electrode surface than is diffusing from the bulk solution, and the catalytic current ( $i_c$ ) is much greater than the diffusion current.

Identification of catalytic currents, via plots of limiting current versus mercury column height, is extremely difficult as they can either be independent of  $h$  or increase with  $h$ , but less rapidly than for an entirely diffusion-controlled process.

#### 2.1.3.2.3. Adsorption-Controlled Limiting Currents

Adsorption currents occur when either the electroactive species or electrode reaction products are adsorbed at the mercury drop. The electrode process may be described as



If the electroactive species is adsorbed as in equation (2.26a) then reduction of such species requires more energy than for reduction of the free species because the energy of adsorption must be overcome. Consequently, two waves appear on the polarogram; the first is due to reduction of free electroactive species and a second wave at more negative potentials due to reduction of the adsorbed species. Alternatively, if the reduced form is adsorbed as shown in equation (2.26b), less energy is required for reduction than when free species are formed, so the adsorption wave occurs as a pre-wave to the main reduction wave.

The limiting adsorption current ( $i_a$ ) is mathematically defined as

$$i_a = nFz \cdot 0.85 \cdot m^{2/3} \cdot t^{-1/3} \quad (2.27)$$

where  $z$  is the maximum number of moles adsorbed per unit electrode surface. Using equation (2.27) it can be shown that  $i_a$  is directly proportional to  $h$  but not  $h^{1/2}$ , as is the case with a diffusion process {9}.

#### 2.1.3.3. Nature of the Electrode Process

The nature of an electrode process at an electrode



surface is described in terms of its electrochemical reversibility or irreversibility. A reversible process, as in equation (2.28), represents a situation in which the rate of electron transfer is fast enough to conform to thermodynamic predictions.



For the forward reaction, the current flowing is expressed as

$$i = nFAk_f C^0(x=0) \quad (2.29)$$

where  $k_f$  is the heterogeneous rate constant of the forward reaction. The rate of the forward and reverse reactions {10} may be expressed as

$$k_f = k^0 \exp \left[ -\frac{\alpha nF}{RT} (E-E^0) \right] \quad (2.30)$$

and

$$k_b = k^0 \exp \left[ \frac{(1-\alpha)nF}{RT} (E-E^0) \right] \quad (2.31)$$

where  $k^0$  is the heterogeneous rate constant of the electrode process at the standard potential ( $E^0$ ),  $\alpha$  is the transfer coefficient (fraction of the applied potential influencing the rate of reduction) and  $n, F, E, R$  and  $T$  have their usual significance. Substituting equations (2.30)

and (2.31) into (2.29) give

$$i_f = nFAC^O(x=0)k^O \exp\left[\frac{-\alpha nF(E - E^O)}{RT}\right] \quad (2.32)$$

and

$$i_b = nFAC^R(x=0)k^O \exp\left[\frac{(1-\alpha)nF(E - E^O)}{RT}\right] \quad (2.33)$$

The convention has been adopted of regarding the forward current ( $i_f$ ) as positive and the backward current ( $i_b$ ) as negative. Under equilibrium conditions,  $E=E^O$  and since  $i_f$  equals  $i_b$ , equations (2.32) and (2.33) can be equated to obtain

$$E = E^O + \frac{RT}{nF} \ln \frac{C^O(x=0)}{C^R(x=0)} \quad (2.34)$$

which is the well-known form of the Nernst equation. Hence a reversible electrode process is defined as one in which the concentration of the oxidised and reduced species at the electrode surface may be predicted by the Nernst equation. Departures from Nernstian (or reversible) behaviour are allowed provided that the rate of the electron exchange process remains high; typically  $\geq 2 \times 10^{-2}$  cm/sec in DC polarography. In these situations, a small net current flow in one direction can be maintained without excessive departure from equilibrium concentrations so that the Nernst equation is still applicable. Electrode processes in which kinetic rather than thermodynamic laws

determine the electrode surface concentrations of species O and R are said to be non-Nernstian or irreversible.

Combining the Nernst and Ilkovic equations the following expression is obtained

$$E = E_{1/2} + \frac{RT}{nF} \log\left(\frac{1}{i_d} - 1\right) \quad (2.35)$$

which describes the shape of a polarographic wave for a reversible process with a diffusion-controlled limiting current. To determine the reversibility of a DC electrode process, a plot of  $\log(i/i_d - 1)$  versus E should be linear with a slope  $2.303 RT/nF$  and intercept on the x-axis of  $E_{1/2}$ .

#### 2.1.4. Pulse Polarography

The discovery of pulse polarography in the 1950's is attributed to Barker {11}, arising from his work on square wave polarography. Since then it has become one of the most powerful electroanalytical methods for both chemical analysis and the study of electrode processes {12,13}. In the following sections the general principles of pulse polarography are outlined, followed by consideration of the theory of differential pulse (DP) polarography.

#### 2.1.4.1. General Principles

Unlike DC polarography where charging currents limit sensitivity, pulse polarography minimises the measurement of such currents thereby achieving greater sensitivity. To illustrate these principles a situation in which no faradaic process occurs is first considered. Prior to application of a polarising pulse at a mercury drop, the only current flowing is a DC capacitance current associated with the charging of the double layer as the drop grows {14}. If the potential is stepped (pulsed) instantaneously to a new value, then a large capacitance current flows to charge the double layer to the new potential. However, this current decreases exponentially with time. The capacitance current will contain both DC and pulse components. In the presence of a faradaic process occurring at the electrode surface, application of a polarising pulse results in both charging and faradaic currents. Because the charging current decreases more rapidly than the faradaic current, the current measured near the end of the pulse duration is primarily faradaic.

#### 2.1.4.2. Differential Pulse Polarography

In DP polarography, a normal DC voltage ramp is applied to the dropping electrode. At a fixed time during

the life cycle of each drop the current flowing,  $i_{ft1}$ , is sampled and a small-amplitude pulse, ( $\Delta E \leq 100\text{mV}$ ), is superimposed on the voltage ramp as shown in Fig. 2.3. The current flowing,  $i_{ft2}$ , at the end of the pulse is again sampled at a fixed time after application of the pulse. The difference between the two currents,  $\Delta i$ , is the parameter measured. To derive an expression for  $\Delta i$ , the following assumptions are made.

- (i) the growth (in terms of area) of the mercury drop during the difference measurement is zero; and
- (ii) the ratio of  $t_m$  (time interval between pulse application and current measurement) to  $t_p$  (time during which the mercury drop has grown prior to pulse application) is small.

Thus for a reversible electrode process the differential pulse current is given by the expression

$$\Delta i = nFAC \sqrt{\frac{D}{\pi t_m}} \frac{P_A \sigma^2 - P_A}{\sigma + P_A \sigma^2 + P_A + P_A^2 \sigma} \quad (2.36)$$

where

$$P_A = \exp \frac{nF}{RT} \left[ \frac{E_1 + E_2}{2} - E_{1/2}^r \right]$$

$$\sigma = \exp \frac{nF}{RT} \left[ \frac{E_2 - E_1}{2} \right]$$

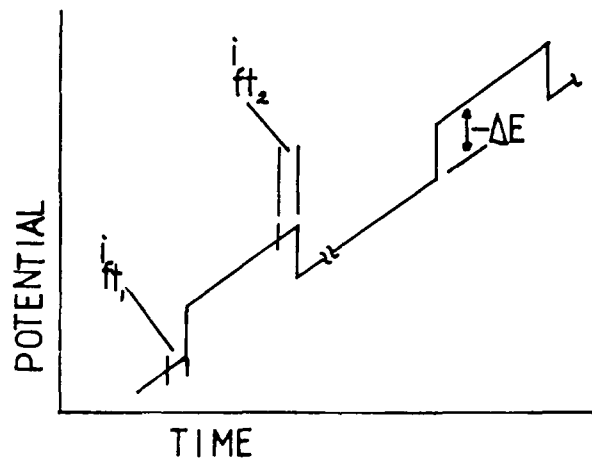


Fig. 2.3. Waveform used in DP polarography

$E_2 - E_1 = E = \text{pulse amplitude}$

$E_1 = \text{potential at which the current } i_{ft1}, \text{ is measured prior to the application of the pulse.}$

$E_2 = \text{potential at which the current } i_{ft2} \text{ is measured after the pulse has been applied.}$

Equation (2.36) is valid for all values of  $\Delta E$ . At the maximum or peak current  $P_A = 1$  so that equation (2.36) simplifies to

$$(\Delta i)_{\max} = nFAC \sqrt{\frac{D}{\pi t_m}} \left( \frac{\sigma - 1}{\sigma + 1} \right) \quad (2.37)$$

In the situation where  $\Delta E/2$  is smaller than  $RT/nF$  then the equation for the maximum current is simplified to the small amplitude case.

$$(\Delta i)_{\max} = \frac{(n^2 f^2)}{4 RT} AC (\Delta E) \sqrt{\frac{D}{\pi t_m}} \quad (2.38)$$

Alternatively when  $\Delta E/2$  is larger than  $RT/nF$ ,  $(\sigma - 1)/(\sigma + 1)$  approaches unity and  $(\Delta i)_{\max}$  becomes

$$(\Delta i)_{\max} = nFAC \sqrt{\frac{D}{\pi t_m}} \quad (2.39)$$

The above equations are only applicable for simplified treatments of electrode processes. However,

when considering rigorous treatments of electrode processes, the DC contributions to the pulse current must be included because they are not compensated by measuring the difference in the currents  $i_{ft1}$  and  $i_{ft2}$  {15}. The first of these contributions contains a faradaic DC component. When the potential ( $E$ ) is in the region in which a faradaic current flows, then before application of the pulse a DC current  $i_{DC}(t_p)$  must be present. The current  $i_{DC}(t_p + t_m)$  included in  $i_{ft2}$  must be different since the time of measurement in the drop life is different. Therefore, the output current will contain a faradaic DC contribution  $\Delta i_{DC}$ . In addition, there is a charging current contribution. The current  $i_{ft1}$  contains a double layer charging current,  $i_C(E, t_p)$  necessary to maintain the constant charge density on the growing drop and  $i_{ft2}$  will contain a similar current  $i_C(E + E, t_p + t_m)$ . Since neither the potential nor the time is the same for these two charging currents, the output will contain a further DC component,  $\Delta i_C$ , due to the difference in the charging currents.

For a reversible electrode process at a DME the faradaic current measured in the differential pulse experiment is

$$\Delta i_f = i_{\text{pulse}} + \Delta i_{DC} \quad (2.40)$$



where  $i_{\text{pulse}}$  is the pulse current. As shown in equation (2.40), the faradaic current measured is the desired pulse current plus a DC contribution due to the growth of the mercury drop. The manifestation of the DC faradaic effect is a shift in baseline. For reduction processes the baseline following the peak is shifted upward, becoming quite pronounced at short drop times {16}. For analytical purposes the peak current should be measured from the baseline extrapolated from before the peak.

The DC charging current contribution is

$$\Delta i_C = - \frac{2}{3} k m^{2/3} \left[ \frac{q(E_2)}{(t_p + t_m)^{3/2}} - \frac{q(E_1)}{(t_p)^{3/2}} \right] \quad (2.41)$$

where  $k$  is a constant and  $q$  is the charge density. In equation (2.41) even if the ratio of  $t_m$  to  $t_p$  tends to zero a term due to the difference of the potentials results.

As the concentration of the electroactive species is decreased the faradaic response decreases proportionally so that eventually the charging current masks the faradaic current. To overcome this limitation associated with the charging current, a static mercury drop electrode (SMDE) was introduced instead of the DME {17}. At the SMDE the mercury drop grows quickly and remains

constant until the drop is dislodged. This significantly reduces the charging current and increases the sensitivity of DP polarography. However, the baseline offset due to  $\Delta_{DC}$  still exists {18}.

The potential at which the current reaches its maximum value is given by

$$E_p = E_{1/2}^r - \frac{\Delta E}{2} \quad (2.42)$$

The values of  $E_p$  are shifted in a positive direction as the pulse amplitude increases. Furthermore, the larger the value of  $\Delta E$  the larger is the value of  $(\Delta i)_{max}$ . Increases in  $\Delta E$ , however, increase the peak width which decreases the overall resolution. In practice, values of  $\Delta E$  between 10 and 100 mV are used as these offer the best compromise between adequate resolution and sensitivity.

#### 2.1.5. Cyclic Voltammetry

Since the development of cyclic voltammetry (CV) in 1938 by Matheson and Nichols{19} the method has become widely used for the study of electrode reactions. The

effectiveness of CV results from its capability for rapidly observing the redox behaviour of electroactive species over a wide potential range. In addition, CV is useful for studying homogeneous chemical reactions that are coupled to the electron transfer process.

In the following section the theory of cyclic voltammetry is illustrated.

#### 2.1.5.1. Fundamentals of Cyclic Voltammetry

Cyclic voltammetry consists of cycling the potential of a working electrode and measuring the resulting current. The potential of the working electrode is controlled versus a reference electrode such as a saturated calomel electrode (SCE) or a silver/silver chloride (Ag/AgCl) electrode. The voltage applied to the working electrode is scanned linearly from an initial value,  $E_1$ , to a predetermined switching potential,  $E_{\lambda}$ , where the direction of the scan is reversed. Single or multiple cycles may be used. Often there is very little change between the first and successive scans; however, the changes that do result are important as they can reveal information about reaction mechanisms {20}.

A cyclic voltammogram is obtained by measuring the current at the working electrode during the potential scan. Cyclic voltammograms are characterised by several important parameters

- (i) the cathodic ( $E_{pc}$ ) and anodic ( $E_{pa}$ ) peak potentials;
- (ii) the cathodic ( $i_{pc}$ ) and anodic ( $i_{pa}$ ) peak currents; and
- (iii) the cathodic peak potential ( $E_p$ ) and half-peak potential ( $E_p/2$ ).

In Fig. 2.4 a typical cyclic voltammogram is shown, illustrating the aforementioned parameters. As the potential is scanned in the negative direction, indicated by the arrow, the current rises to a peak and then decays in a regular manner. The current depends on two steps

- (a) movement of the electroactive material to the working electrode surface; and
- (b) the rate of the electron transfer reaction.

The rate of electron transfer for a reduction process is a function of potential and is theoretically described as:

$$k_f = k^0 \exp\left(\frac{-\alpha nF}{RT} (E - E^{\circ'})\right) \quad (2.43)$$

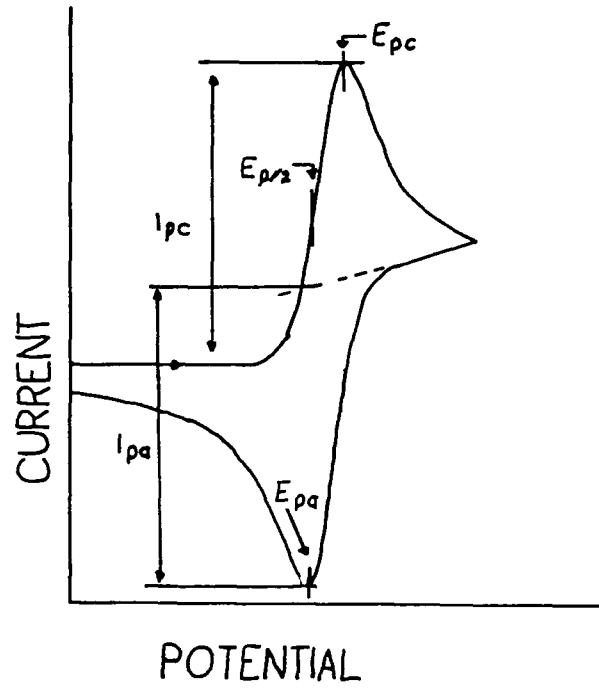


Fig. 2.4. Typical cyclic voltammogram

where  $k^0$  is the standard heterogeneous electron-transfer rate constant,  $\alpha$  is the transfer coefficient,  $E^{0'}$  is the formal reduction potential and  $n, F, R, T$  and  $E$  have their usual significance. Similarly for the reverse (or oxidation) process, the electron-transfer rate constant is controlled by potential as shown in equation (2.44).

$$k_b = k^0 \exp \left( \frac{(1-\alpha)nF}{RT} (E-E^{0'}) \right) \quad (2.44)$$

When the electron transfer process is reversible, the difference between anodic and cathodic peak potentials is  $59/n$  mV. This relationship may be used to evaluate  $n$ . Under reversible conditions the electron transfer reaction at the electrode surface is fast enough to maintain the concentrations of the oxidised and reduced forms in equilibrium with each other. The equilibrium ratio for a given potential at the electrode surface is determined by the Nernst Equation:

$$E = E^{0'} + \frac{RT}{nF} \ln \left( \frac{[R]}{[O]} \right)_{x=0} \quad (2.45)$$

where  $O$  and  $R$  are the oxidised and reduced forms respectively. It should be noted that the reversibility of a system depends on the voltage scan rate [21]. At high scan rates the electron transfer reaction may not be fast enough to maintain equilibrium conditions as the potential

changes. Departures from reversibility are manifested by increased separation of anodic and cathodic peak potentials so that

$$\Delta E_p = E_{pa} - E_{pc} \left( > \frac{59}{n} \text{ mV} \right) \quad (2.46)$$

These systems are known as irreversible processes.

The peak current,  $i_p$ , is given by the following equation {20}:

$$i_p = k n^{3/2} A D^{1/2} C^o v^{1/2} \quad (2.47)$$

where  $k$  is the Randles-Sevcik constant,  $v$  is the scan rate and the other symbols have their usual meaning. The dependence of  $i_{pc}$  and  $i_{pa}$  on  $v^{1/2}$  is a further characteristic identifying a reversible system.

Some electrode reactions involve electron transfer at the electrode surface and are not complicated by coupled chemical reactions. However, many electrode reactions include chemical steps which take place in solution near the electrode surface and may occur prior to electron transfer, following electron transfer or interposed between electron transfer steps. Cyclic voltammetry is a powerful method for the detection and characterisation of such

coupled chemical reactions. Diagnosis of coupled chemical reactions is often based on the relative heights of the anodic and cathodic peaks {22}.

#### 2.1.6. Stripping Voltammetry

##### 2.1.6.1. Introduction

The chief limitation to the sensitivity of the polarographic methods described in the previous sections is the unfavourable ratio of faradaic to charging current. Using stripping voltammetry, the faradaic current is increased by accumulating the element to be analysed at the electrode surface while maintaining the charging current at values associated with the electroanalytical method used for monitoring the stripping process. Because of the large faradaic response per unit concentration associated with stripping voltammetry, extremely low detection limits are attainable. Hence this method is increasingly used for measuring heavy metals at concentration levels ranging down to the fractional parts per billion range {23}.

##### 2.1.6.2. Principles of stripping Voltammetry

###### 2.1.6.2.1. Preconcentration Step

This is the first step in stripping analysis. In this step the analytical species are electrodeposited



onto or into a working electrode held at a constant potential, usually within the limiting current potential region of the deposited substance. The species reach the electrode surface by diffusion and forced convection due either to rotating the working electrode or stirring the solution. These species are then deposited either in the form of

- (i) an amalgam or film on the surface of the mercury (drop or film); or
- (ii) a film on a solid electrode.

After a predetermined time the stirring is stopped and the solution is left to become quiescent. During this period the quantity of species transported to the working electrode decreases and consequently the magnitude of the electrolytic current also drops very fast.

The current flowing at any time,  $i_t$ , during the electrolysis step is given by equation (2.48){24}:

$$i_t = 0.62nFAD^{2/3} \omega^{1/2} \nu^{1/6} C^0 \quad (2.48)$$

where  $\omega$  is the rate of electrode rotation or solution stirring,  $\nu$  is the kinematic viscosity of the solution and  $C^0$  is the bulk concentration of analyte at time,  $t$ , during

deposition. In equation (2.48) the parameters which may be controlled are  $\omega$ ,  $\nu$ ,  $A$  and  $T$ . The viscosity of aqueous solutions does not vary greatly. In addition, given its sixth root dependency, it is unlikely to be important in determining the efficiency of the preconcentration step, unless comparisons in different solvents are being considered. However, the rate of electrode rotation or stirring rate can be increased to improve electrolysis efficiency. The value of  $\omega$  can be increased to the point where the ability to maintain a hanging mercury drop becomes critical, while vortex formation and frothing of the solution occurs with other types of electrode systems {25}. Increasing the electrode area may be used to increase the amount of substance deposited per unit time.

During the preconcentration step only a fraction of a given substance is deposited on the working electrode, under reproducible conditions. If a constant current is maintained during the deposition step then the concentration of substance deposited is given by Faraday's Law. For a hanging mercury drop electrode (HMDE) the concentration in the drop,  $C_{am}$ , may be calculated by the following equation {26}.

$$C_{am} = \frac{3it}{4\pi nFr^3} \quad (2.49)$$

where  $i$  is the cathodic or anodic current during deposition and  $r$  is the radius of the mercury drop. For a mercury film electrode (MFE) of thickness  $L$  and area  $A$  the concentration in the film is:

$$C_{am} = \frac{it}{ALnF} \quad (2.50)$$

Equations (2.49) and (2.50) are applicable at the end of the rest period following the preconcentration step as a uniform concentration of deposited species in the mercury electrode is established rapidly after the electrolytic current has ceased.

#### 2.1.6.2.2. Stripping and Monitoring Step

Voltammetric stripping methods are termed either cathodic or anodic, depending on the character of the stripping process (reduction or oxidation respectively). The stripping step is the second stage and is undertaken at the end of the rest period. During the stripping step, the potential is changed with time and the stripping current is measured as a function of potential. Peaks are formed on the resultant current-potential voltammogram, their position being characteristic of the given substance and height is proportional to the concentration of analyte in the analytical solution.

When a DC linear potential is used with a HMDE the situation is analogous to that of cyclic voltammetry. The stripping peak current ( $i_p$ ) is given by {27}:

$$i_p = kn^{3/2} D^{2/3} r v^{1/2} C^0 t m \quad (2.51)$$

where  $k$  is a numerical constant,  $v$  is the voltage scan rate and  $m$  is the mass-transport coefficient. The potential at which this peak occurs is given by

$$E_p = E_{1/2} - 1.1 \frac{RT}{nF} \quad (2.52)$$

The chief limitation of the DC linear scan method at a HMDE is the high charging current as a direct result of using fast scan rates, typically 50 mV/sec or greater are employed. Other waveforms, such as the differential pulse waveform, have been found to be sufficiently more sensitive {28}.

## 2.2. High Performance Liquid Chromatography

Since the development of high performance liquid chromatography (HPLC) in the 1960's it has become a very successful analytical method {29}. The real forte of HPLC is the ability to separate and analyse complex mixtures quickly. In the following sections the essential features

governing separation by this method are described.

### 2.2.1. Chromatographic Separation

Two features characterise the process of chromatographic separation; (i) differential migration of the various components of a sample and (ii) band migration of the molecules of a single compound through the analytical column {30}.

#### 2.2.1.1. Differential Migration

Differential migration refers to the different rates of movement of compounds through a column {30}. During separation there is an equilibrium distribution of the various compounds between the stationary and mobile phase. In Fig. 2.5 the differential migration of compounds A and B is illustrated. The molecules of compound A are preferentially distributed in the stationary phase with only a small fraction present in the mobile phase. For compound B, the opposite is the situation, as most molecules of compound B are present in the mobile phase.

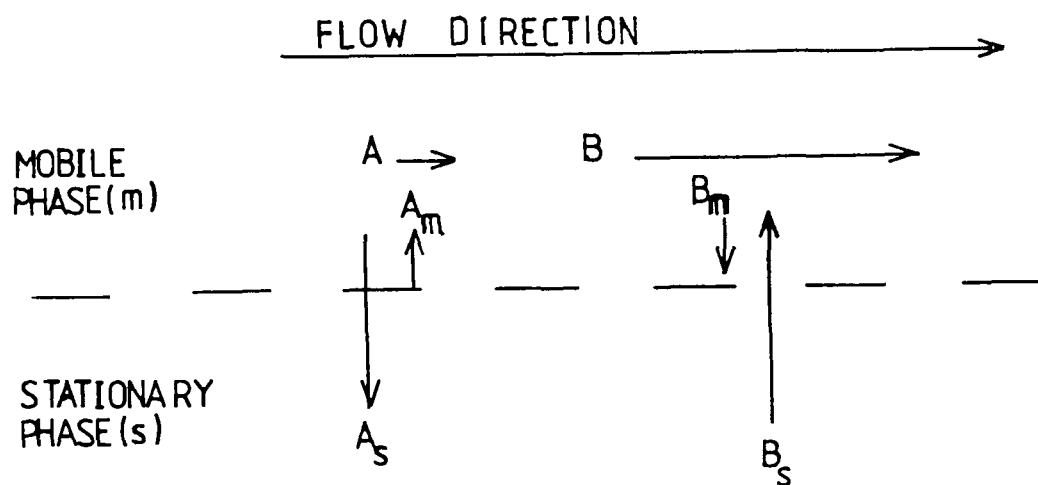


Fig. 2.5. Differential migration of compounds A and B through a HPLC column.

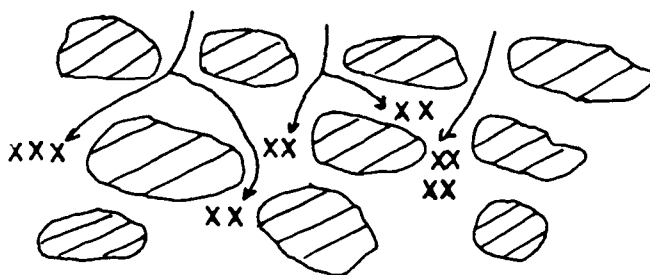


Fig. 2.6. Different flowstreams between the packing particles of a HPLC column particles

Because sample molecules do not move through the column when present in the stationary phase, the speed at which a compound moves through the column is determined by the number of molecules of the compound in the mobile phase at any time. Therefore compound A moves through the column slowly, because most of the molecules are in the stationary phase, while compound B moves through the column more rapidly as these molecules are distributed mainly in the mobile phase. If a change in differential migration is sought to improve separation, then one of the following variables may be altered:

- (a) composition of the mobile phase;
- (b) composition of the stationary phase; or
- (c) temperature.

#### 2.2.1.2. Band Migration

As the molecules of a single compound move through a column they become increasingly spread over a wider portion of the column. This spreading is due to differences in the rates of migration of the individual molecules {29}. These differences are caused by the following physical processes.

#### 2.2.1.2.1. Eddy Diffusion

Eddy diffusion results from the different flowstreams that the mobile phase follows between particles in a column (Fig. 2.6) {31}. Hence, sample molecules may take different paths of varying length through the column packing. Furthermore, the mobile phase velocity depends on the path width; mobile phase molecules move faster in wide rather than in narrow paths. Therefore, molecules that travel in wide paths will have moved a greater distance along the column than those in narrow paths.

#### 2.2.1.2.2. Mobile Phase Mass Transfer

In a single flowstream the flow-rate is not uniform. Mobile phase close to the surface of column-packing particles moves very slowly or not at all, whereas mobile phase in the centre of the flowstream moves fastest. As a result, sample molecules near the surfaces of column-packing particles move a short distance and sample molecules in the middle of the flowstream move a greater distance. This also results in a spreading of sample molecules along the column.



#### 2.2.1.2.3. Stationary Phase Mass Transfer

When the packing particles of a column are porous, sample molecules may diffuse into these pores and either become attached to the stationary phase or penetrate it. Molecules that penetrate deep into the stationary phase spend long periods in the packing particle and travel shorter distances down the column. Molecules that spend only a little time moving into and out of the stationary phase return to the mobile phase sooner and move further down the column.

#### 2.2.1.2.4. Longitudinal Diffusion

Whether the mobile phase within the column is moving or at rest, sample molecules tend to diffuse randomly in all directions. This causes a further spreading of sample molecules along the column. In general, longitudinal diffusion is not an important effect, but is significant at low mobile-phase flow-rates for small-particle columns.

#### 2.2.2. Retention Time and Volume

It is possible to mathematically define differential and band migration. If the situation for

compound A in Fig. 2.5 is considered, then the velocity at which it moves through the column ( $u_A$ ) is defined as follows:

$$u_A = uR \quad (2.53)$$

where  $u$  is the average velocity of mobile phase molecules and  $R$  is the fraction of molecules A in the mobile phase. If the value of  $R$  is zero, then no migration can occur and so  $u_A$  is zero. However, if  $R$  were equal to unity then all the molecules of A are in the mobile phase and  $u_a = u$ .

The quantity  $R$  may be expressed in a different manner. To do this the capacity factor ( $k'$ )<sup>{32}</sup> is defined as follows:

$$k' = \frac{n_s}{n_m} \quad (2.54)$$

where  $n_s$  is the total moles of A in the stationary phase and  $n_m$  is the total moles of A in the mobile phase.

Re-writing equation (2.54) yields

$$\begin{aligned} k' + 1 &= \frac{n_s}{n_m} + \frac{n_m}{n_m} \\ &= \frac{n_s + n_m}{n_m} \end{aligned} \quad (2.55)$$

Since  $R$  describes the mole fraction of compound A present in the mobile phase and is given by:

$$R = \frac{n_m}{n_s + n_m} \quad (2.56)$$

Then

$$R = \frac{1}{1 + k'} \quad (2.57)$$

and from equation (2.53)

$$u_A = \frac{u}{1 + k'} \quad (2.58)$$

It is possible to relate  $u_A$  to the retention time ( $t_R$ ) and column length ( $L$ ). Thus the time taken for compound A to move through a column of length  $L$  and velocity  $u_A$  is

$$t_R = \frac{L}{u_A} \quad (2.59)$$

The time taken for unretained molecules to move through the column is

$$t_o = \frac{L}{u} \quad (2.60)$$

Combining equations (2.59) and (2.60) yields

$$t_R = \frac{ut_o}{u_A} \quad (2.61)$$

Substitution of equation (2.61) into equation (2.58) yields:

$$k' = \frac{t_R - t_0}{t_0} \quad (2.62)$$

Equation (2.62) provides a method of calculating  $k'$  in terms of retention time;  $k'$  tells where a compound elutes relative to unretained mobile phase molecules and is frequently used to identify a peak. However, sometimes  $k'$  is calculated in terms of retention volume ( $V_R$ ) rather than retention time ( $t_R$ ), because  $t_R$  varies with flow-rate, whereas  $V_R$  is independent of flow-rate. Therefore, equation (2.62) may be expressed in terms of retention volume as follows:

$$k' = \frac{V_R - V_0}{V_0} \quad (2.63)$$

where  $V_R$ , the retention volume, is the total volume of mobile phase required to elute to the centre of a peak and  $V_0$  is the void volume which is a measure of the internal volume of a HPLC system from injector to detector. In practice it is measured on a chromatogram from the injection point to the first peak, since any compounds not retained will elute at the void volume (see Fig. 2.7).

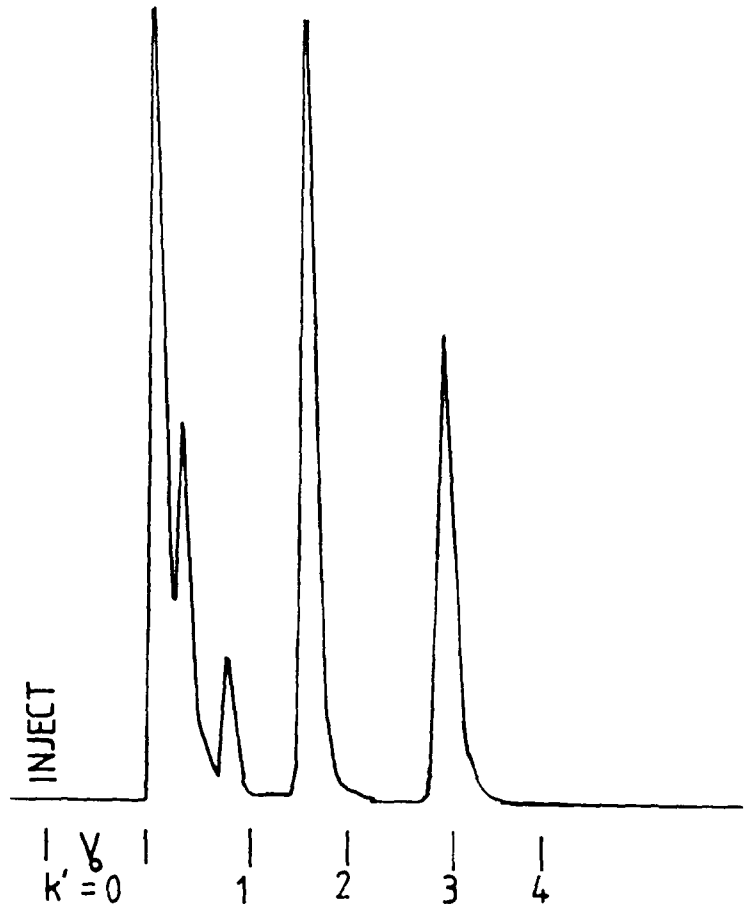


Fig. 2.7. Chromatogram showing the void volume ( $V_0$ ) measured from injection point to the solvent front and  $k'$  in void volume increments.

### 2.2.3. Efficiency of Separation

The efficiency of column separation may be considered in terms of the height equivalent to a theoretical plate (HETP) approach. A theoretical plate is a purely imaginary concept; yet it is a convenient parameter for evaluating efficiency. The height of plate is defined as:

$$H = \frac{L}{N} \quad (2.64)$$

where L is column length and N is the number of theoretical plates. For high efficiency a large number of plates and small values of H are required. The number of plates in a column length L is shown from statistical considerations to be

$$N = 16 \left( \frac{t_R}{W} \right)^2 \quad (2.65)$$

where  $W$  is the extrapolated peak width measured at the baseline. In chromatography it is desirable for  $W$  and  $H$  to be as small as possible so that peaks will be narrow and sharp. The physical processes that govern band migration can adversely affect the width of a peak. In these situations peak widths are increased because these processes cause spreading of molecules in the analytical column.

#### 2.2.4. Resolution

The objective in chromatography is adequate separation between the components of a sample mixture. Resolution is a measure of the magnitude of this separation. It is defined as follows {33}:

$$R = \frac{t_B - t_A}{0.5 (W_A + W_B)} \quad (2.66)$$

where  $t_A$  and  $t_B$  are the retention times of components A and B respectively and  $W_A$  and  $W_B$  are their corresponding baseline peak widths. It is possible to define  $R$  in terms of  $k'$  and  $N$  as follows

$$R = 0.25 \left( \frac{\alpha - 1}{\alpha} \right) \sqrt{N} \left( \frac{k'}{k' + 1} \right) \quad (2.67)$$

where  $\alpha$  is the separation factor between adjacent peaks and is equal to the ratio of their  $k'$  values. Using equation (2.67) resolution may be controlled by varying  $\alpha$ ,  $N$  or  $k'$ .

References

1. D.R. Turner and M. Whitfield, Marine Electrochemistry, edited by M. Whitfield and D. Jagner (J. Wiley & Sons, Chichester, 1981), pp. 79-81.
2. J.T. Maloy, J. Chem. Educ., 60, 285 (1983).
3. D.R. Crow and J.V. Westwood, Q. Rev., 19, 57 (1965).
4. A.M. Bond, Modern Polarographic Methods in Analytical Chemistry, (Marcel Dekker Inc., New York, 1980).
5. W.J. Moore, Physical Chemistry (Longman, London, 1972), pp. 510-513.
6. D. Ilkovic, J. Chim. Phys., 35, 129 (1938).
7. D. Ilkovic, Collect. Czech. Chem. Commun., 6, 498 (1934).
8. J. Heyrovsky and J. Kuta, Principles of Polarography (Academic Press, New York, 1966).
9. J. Heyrovsky and P. Zuman, Practical Polarography (Academic Press, New York, 1967), pp. 30-42.
10. D.R. Crow, Polarography of Metal Complexes (Academic Press, New York, 1969), pp. 19-40.
11. G.C. Barker and A.W. Gardner, U.K., At. Energy Res. Establ. Harwell, C/R 2297, 1958.
12. J. Osteryoung and K. Hasebe, Rev. Polarogr., 22, 1 (1976).
13. J. Osteryoung, J.H. Christie and R.A. Osteryoung,



- Bull. Soc. Chim. Belg., 84, 647 (1975).
14. G.C. Barker and A.W. Gardner, Z. Anal. Chem., 173, 79 (1960).
  15. J.H. Christie and R.A. Osteryoung, J. Electroanal. Chem., 49, 301 (1974).
  16. A.M. Bond and B.S. Grabaric, Anal. Chim. Acta, 88, 227 (1977).
  17. W.M. Peterson, Am. Lab., 11, 69 (1979).
  18. J.E. Anderson, A.M. Bond and R.D. Jones, Anal. Chem., 53, 1016 (1981).
  19. L.A. Matheson and N. Nichols, Trans. Electrochem. Soc., 73, 193 (1938).
  20. G. Cauquis and V.D. Parker, Organic Electrochemistry, edited by M.M. Baizer (M. Dekker Inc., New York, 1973), pp. 115-127.
  21. D.D. MacDonald, Transient Techniques in Electrochemistry (Plenum Press, New York, 1973), Chap. 6, p. 193.
  22. R.S. Nicholson and I. Shain, Anal. Chem., 36, 706 (1964).
  23. P. Valenta, L. Mart and H. Rutzel, J. Electroanal. Chem., 82, 327 (1977).
  24. T.R. Copeland and R.K. Skogerboe, Anal. Chem., 46, 1257A (1974).
  25. J. Wang, Talanta, 29, 125 (1982).
  26. F. Vydra, K. Stulik and E. Julakova, Electrochemical

- Stripping Analysis (Ellis Horwood, England, 1976), p. 46.
27. J. Wang, *Environ. Sci. Technol.*, 16, 104A (1982).
28. G.E. Batley and T.M. Florence, *J. Electroanal. Chem.*, 55, 23 (1974).
29. L.R. Snyder and J.J. Kirkland, Introduction to Modern Liquid Chromatography (J. Wiley & Sons, Chichester, 1979).
30. J.H. Knox (editor), High Performance Liquid Chromatography (Edinburgh University Press, Edinburgh, 1978), pp. 5-19.
31. R.J. Hamilton and P.A. Sewell, Introduction to High Performance Liquid Chromatography (Chapman and Hall, London, 1977), pp. 12-36.
32. G.W. Ewing, Instrumental Methods of Chemical Analysis (McGraw-Hill, Tokyo, 1975), p. 361.
33. A. Braithwaite and F.J. Smith, Chromatographic Methods, 4th Edition (Chapman and Hall, London and New York, 1985), pp. 11-23.

CHAPTER 3

DETERMINATION OF DISSOLVED CADMIUM,  
LEAD, COPPER AND REACTIVE MERCURY IN  
THE IRISH SEA - A FIELD STUDY

### 3.1. Introduction

The sea is an important stage in the natural cycle of heavy metals. It constitutes a pseudo-sink for metals transferred from terrestrial environments {1}. Sources of marine heavy metals include direct inputs by freshwaters, run-off and coastal discharges. Indirect inputs, via the atmosphere, include metals dissolved in precipitates, as well as those adsorbed to dust particles. Once these metals enter the marine environment they are rapidly distributed between the dissolved and particulate phases. In a water column, the total metal concentration is distributed between the dissolved state and the surface zones of suspended inorganic and organic matter. The dissolved state is especially important because it is the state in which metals are transferred to and from the other phases of an aquatic system. More importantly, marine biota such as fish and plankton can ingest metals directly from the dissolved state. Subsequently, these metals are concentrated in living organisms through the foodchain, eventually reaching man {2,3}. Therefore, monitoring programmes to establish the concentrations of heavy metals present in the marine environment are very necessary. There is also a need to determine the fate and distribution of metals introduced into this environment by coastal discharges and freshwater inputs.

This chapter illustrates the suitability of DPASV at a MFE as a means of quantifying dissolved concentrations of cadmium, lead and copper in seawater. Reactive mercury, i.e., mercury which is reducible by stannous chloride, was measured using cold-vapour AAS. Samples were taken from various coastal locations around the Irish Sea using the British research vessel "Clione" during the period December 8-18th, 1984. This cruise was carried out in association with the Ministry of Agriculture, Fisheries and Food (MAFF), Norwich. One objective of this study was to ascertain the concentrations of the aforementioned metals by sampling and field analysis of the collected samples. Additionally, the feasibility of field analysis was also examined. However, because this was just a pilot study, it was not particularly comprehensive in terms of the number of stations sampled or the number of samples taken at each station. Results were required merely to indicate areas with above average metal levels rather than trying to elucidate trace metal pathways or distribution in the Irish Sea.

### 3.2. Experimental Section

#### 3.2.1. Reagents

All acids used were either analytical or ultrapure

grade, unless otherwise stated. Reagents used in the preparation of standard solutions for calibration purposes were all ultrapure grade.

Standard solutions of the individual metals were prepared prior to the commencement of the research cruise. Each of the standard solutions containing 1.0 mg/l of the respective metal was prepared in 0.1% (V/V) ultrapure nitric acid. All standard solutions containing 1.0 mg/l mercury were prepared in 0.1% (V/V) ultrapure hydrochloric acid.

Distilled, deionised water (D.D.W.) was used in the preparation of all solutions.

### 3.2.2. Instrumentation

#### 3.2.2.1. Temperature and Salinity Measurement

Temperature and salinity values were recorded at each station using a Model 8770 portable conductivity, salinity, temperature and depth (CSTD) system. The probe consisted of a stainless steel pressure case which contained the electronic circuitry whilst the physical sensors were mounted in a cage enclosure and fastened to the pressure case. This sensory unit, housed in a large

wooden box on the ship's deck, received a continuous pumped supply of surface seawater. Values of temperature and salinity were displayed on a digital recorder situated in the main laboratory. These values were measured at each station as the samples were being taken. On completion of the sampling programme for each day the digital recorder and probe were switched off.

#### 3.2.2.2. Anodic Stripping Voltammetry Measurements

All stripping voltammograms were recorded using a PAR Polarographic Analyser Model 264A, a rotating disk electrode coupled with an EG+G Speed Controller Unit and a Rikadenki X-Y recorder. Also used was an Aplab Solid State Sine Wave Inverter to ensure a constant power supply to the polarographic analyser. The cell assembly was located in an Hepaire Laminar flow to ensure that contamination of the sample by dust particles was avoided. The cell comprised of a working electrode, mercury film on glassy carbon support, a platinum wire counter electrode and a saturated calomel reference electrode.

#### 3.2.2.3. Mercury Analyser

Reactive mercury concentrations were quantified using the cold vapour atomic absorption spectroscopy (AAS)

method. Because reactive mercury concentrations were low, a pre-concentration step was necessary before applying the cold vapour AAS method. The pre-concentration step employed the amalgamation of mercury on elemental gold, which was then subsequently heated electrically to vapourise the mercury.

The mercury analyser comprised of a 500 ml pyrex reduction vessel equipped with a dreschel head and fritted glass distribution tube. The mercury collector, housing the gold foil, was made of silica. A resistance wire wound round the collector was used to electrically heat the gold foil in order to vapourise any amalgamated mercury. Detection of the mercury was performed using a Perkin-Elmer Mercury Analyser. This was linked to a Rikadenki X-Y recorder.

Teflon tubing was used for connecting the various components. All teflon-glass joinings were secured with sleeves of silicone rubber.

### 3.2.3. Cleaning Procedures

#### 3.2.3.1. Cleaning of Equipment Used for Storage and Filtration of Water Samples Collected for Metal Analysis (except Mercury)

##### 3.2.3.1.1. Storage Bottles

Leaching and adsorption are the major factors in altering the concentration of dissolved metals in stored water samples. In order to overcome these problems, storage bottles must be rigorously cleaned to prevent contamination, and treated to prevent adsorption.

Low-density polyethylene bottles (2 litre capacity)



were used for storage purposes, as they are acknowledged to be the most appropriate type for samples of this nature {4}. These bottles were first washed out with D.D.W. to remove dust and swarf from the manufacturing process. A five day soak in 40% (V/V) reagent grade nitric acid/D.D.W. followed by 5 days in 10% (V/V) ultrapure nitric acid/D.D.W. cleans and pretreats the plastic surfaces. Prior to use, the bottles were kept filled with 0.1% (V/V) ultrapure nitric acid/D.D.W.. Before taking a sample the bottles were very thoroughly washed out with D.D.W. and the sample itself.

#### 3.2.3.1.2. Filtration Apparatus and Filters

Filtration was carried out using the "top pressure" filtration method. This method represents the cheapest, quickest and cleanest method of separation.

The plastic (polycarbonate) unit was cleaned with detergent and then soaked in 10% (V/V) analytical grade hydrochloric acid/D.D.W. Subsequently, it was stored in 10(V/V) ultrapure hydrochloric acid/D.D.W for 5 days before use.

Nucleopore polycarbonate filters (0.45  $\mu\text{m}$ ) were soaked in 50% (V/V) analytical grade hydrochloric acid/D.D.W. and rinsed with D.D.W. five times before being

dried at approximately 50°C and weighed. Before use, the filters were washed through with 1% (V/V) analytical grade hydrochloric acid/D.D.W. followed by 3 water rinses. The filters were always handled with plastic forceps.

### 3.2.3.2. Cleaning of Equipment Used for Storage and Filtration of Water Samples Collected for Mercury Analysis

#### 3.2.3.2.1. Storage Bottles

Glass equipment is used for mercury sampling and storage as plastic often contains mercury. Furthermore, plastic is also porous to mercury in the vapour phase, allowing an equilibrium to be set up between the sample and the surrounding atmosphere.

Pyrex bottles were cleaned by soaking for 5 days in 50% (V/V) analytical grade hydrochloric acid/D.D.W. The bottles were then filled with 0.1% (V/V) ultrapure hydrochloric acid/D.D.W. and stored until required. Before taking a sample the bottles were rinsed with copious amounts of D.D.W.

#### 3.2.3.2.2. Filtration Apparatus and Filters

Samples for mercury analysis were 'vacuum' filtered because this type of filtration is normally carried out using glass apparatus.

All glass vacuum filter units were first washed with detergent and then repeatedly rinsed with D.D.W. The glassware was then soaked in 50% (V/V) analytical grade

hydrochloric acid/D.D.W. for 5 days before use.

Glass fibre filters were cleaned by ashing them at 450°C in a muffle oven overnight. The filters were stored, wrapped in aluminium foil. Just before use, the filters were washed with 50% (V/V) ultrapure hydrochloric acid/D.D.W. followed by 4 or 5 washings with D.D.W.

#### 3.2.4. Sample Collection Techniques

##### 3.2.4.1. Surface Water Samples

An 'Azlon' water sampler was used to collect surface water samples, i.e., samples taken from a depth of four metres. In practice the sampling depth varied between 3 and 4 metres due to the yawing of the ship and the distortion of curvature of the sampling cord by the ships drift and currents.

The 'Azlon' sampler consists of a two litre plastic bottle, at the top of which are two separate inlets, which are stoppered before and after sampling. A spring is attached to the handle of the sample while a calibrated cord is connected to the other end of the spring. The stoppers are also directly attached to the cord.

Prior to sample collection, the sampler was twice washed out with seawater from the sampling station. Before collecting a sample, the two openings at the top of the sampler were stoppered. Subsequently, the sampler was manually lowered over the side of the ship, using the calibrated cord, to the required sampling depth. Tugging the cord released the stoppers and allowed the sampler to fill. On removal of the sampler from the water these openings were again stoppered to eliminate any possibility of sample contamination.

For overnight storage the sampler was conditioned with seawater. Prior to commencing this study it had been conditioned with a 0.5% (V/V) hydrochloric acid/seawater solution.

#### 3.2.4.2. Deep Seawater Samples

A "Go-Flo" sampler was employed to collect samples from depths greater than 10 metres. It consists of a cylindrical PVC body, ball valves with Delrin stopcocks and push rod, and stainless steel nuts for the wire clamps.

To operate this sampler, the valves at both ends were closed before lowering it into the water. This avoids contaminating the interior of the sampler with metals

released from the ship. The sampler was attached to a hydrowire and lowered to the sampling depth. Once the sampler had been lowered 10 metres a pressure-activated release mechanism opens the valves. When the sampler was positioned at the required depth, a messenger was attached to the hydrowire. This travels along the hydrowire and triggers the closing mechanism.

At the end of each day the sampler was washed out with seawater but was not conditioned overnight.

#### 3.2.5. Sample Pretreatment and Storage

Samples for ASV analysis were treated as follows. Using a plastic graduated cylinder one litre of seawater was transferred from the sampler to the "top pressure" filtration unit. Under nitrogen pressure, the sample was filtered through a 0.45  $\mu\text{m}$  membrane filter into a one litre low-density polyethylene bottle. The filtrate was acidified with 1 ml of concentrated ultrapure hydrochloric acid. The bottle was then tightly sealed and wrapped in a plastic bag. Once filtration had been completed, the filter was removed and stored in a covered petri dish. Analysis of the particulate matter was to be undertaken at a later stage.

In the case of mercury analysis, samples were filtered through an ashed 5F/F glass fibre filter using a vacuum filtration system. Samples for reactive mercury determination were analysed immediately after filtration. Those for total mercury analysis were stored in glass bottles and preserved with 1ml of concentrated ultrapure hydrochloric acid. These samples were wrapped in plastic bags as a further precaution against contamination. Again all filters were stored in petri dishes for quantification of particulate mercury at a later stage.

### 3.2.6. Quantification Procedures

#### 3.2.6.1. Anodic Stripping Voltammetry

##### 3.2.6.1.1. Plating the Rotating Disk Electrode

The 50 ml of seawater (collected at station 9) in the cell was added 0.5 ml of a standard (1000 mg/l) mercury solution. The solution was degassed for five minutes with "zero grade" argon. Two depositions, each of ten minutes duration, were carried out. Each deposition was followed by a scan. This procedure was undertaken at the beginning of each day.

#### Instrument Settings

Deposition Time: 600 seconds;  
Electrode Speed: 600 r.p.m;  
Deposition/Initial Potential: - 0.9V;  
Modulation Amplitude: 50 mV;

Final Potential: - 0.06V;  
Scan Rate: 10 mV/sec;  
Mode: Differential Pulse.

3.2.6.1.2. Analysis of a Seawater Sample by Differential Pulse Anodic Stripping Voltammetry (DPASV)

Exactly 50 ml of sample, previously acidified and filtered, was added to the cell and degassed for five minutes with "zero grade" argon. Metals in the sample were then deposited in the mercury film for 15 minutes and the electrode equilibrated for 30 seconds before being scanned anodically.

Calibrations were performed using the method of standard additions. A composite standard of 10 µg/l Cd(II), 10 µg/l Pb(II) and 40 µg/l Cu(II) was prepared in distilled water. Subsequently, 50 µl of this composite standard was added to the seawater sample in the cell and the analysis repeated as already described. Following this, a second standard addition was carried out.

Instrument settings were the same as those used in the electrode plating step, except that the deposition time was extended to 900 seconds.

3.2.6.2. Reactive Mercury Determination

Reactive mercury is that which is reducible by

stannous chloride. The procedure used for quantifying this type of mercury is as follows. To 500 ml of filtered seawater in a reduction vessel was added to 0.26 M  $\text{SnCl}_2$  in 3M HCl. Subsequently, argon was bubbled through the sample to the mercury collector for 30 min. During this period all reactive mercury in the sample was concentrated on the gold foil in the mercury collector. On completion of the concentration step, the argon was diverted to the absorption cell. When the spectrophotometer had been blanked and the chart recorder gave a steady baseline, the gold foil sample collector was heated to  $600^\circ\text{C}$ . the absorbance of the peak at 253.7nm was then recorded.

Calibrations were preformed using standard solutions whose mercury concentrations varied from 2 to 50 ng/l. The method applied was as for the samples. Calibration plots were obtained by plotting peak height against concentration and unknown samples quantified from these plots.

### 3.3. Results and Discussion

A complete log of events during this research cruise is shown in appendix A. In all, 54 stations were selected along the west coast of England and the east coast of Ireland. Although it was possible to sample very close to the English coastline, the same was not possible



along the Irish coast due to the 3 mile exclusion zone around Ireland. The stations sampled around the Irish Sea are shown in Figs. 3.1 and 3.2. The chief area of interest was Liverpool Bay (see Fig 3.2); hence, the large number of sampling points in this area compared with the remaining sampling locations. The reasons for the interest in Liverpool Bay will be discussed in later sections.

Before discussing the metal levels in parts of the Irish Sea, the physical properties of the various sampling locations are considered.

### 3.3.1. Physical Characteristics of Sampled Stations

#### 3.3.1.1. Historical Background to Salinity

The most commonly used parameter to discriminate between the various types of natural waters, e.g., freshwater, brackish water and seawater, is salinity. However, the definition of salinity has changed considerably since its inception in 1865 {5}.

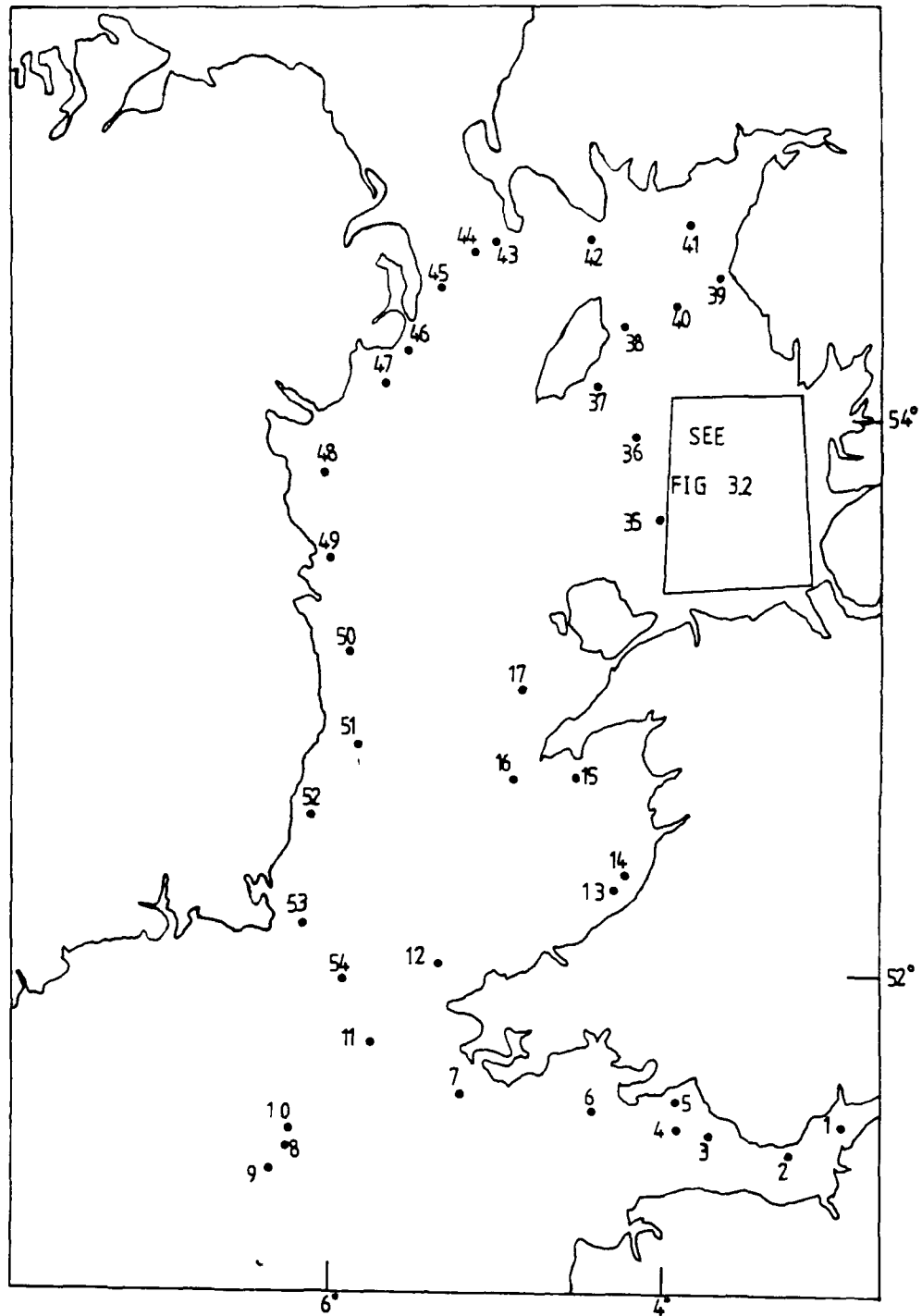


Fig. 3.1. Sampling stations in the Irish Sea.

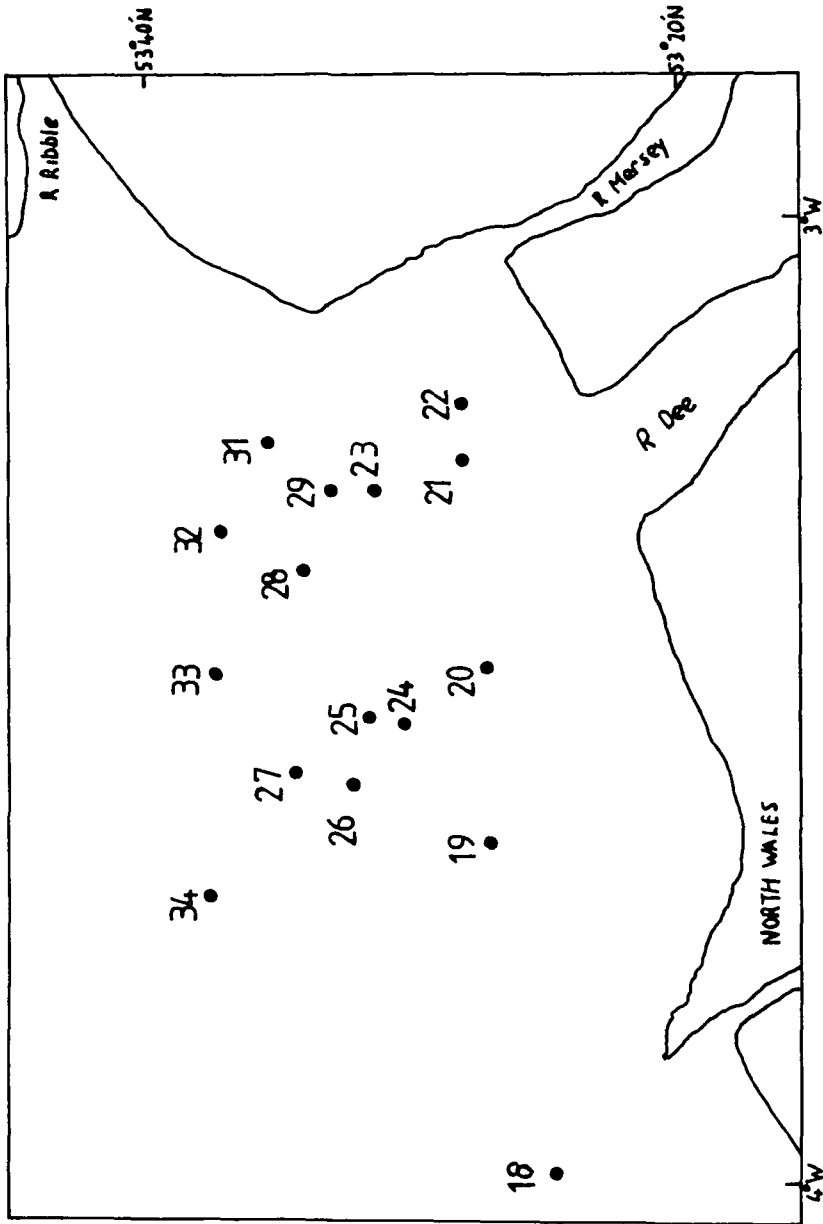


Fig. 3.2. Sampling stations in Liverpool Bay.

The term was originally used to describe the amount of sea salt per unit volume of seawater. Unfortunately, this definition was too naive as it is impossible to evaporate seawater and weight the remaining salt because of the non-uniform temperature at which the salt hydrates disintegrate {6}. By 1900, an investigation was initiated to determine hydrographic constants in order to relate the chlorinity to the salinity and the density of seawater. An equation was developed to show the relation between chlorinity and salinity {6}.

$$S \times 10^3 = 1.805 Cl \times 10^3 + 0.030 \quad (3.1)$$

where S and Cl represent salinity and chlorinity respectively. Because this definition of salinity was in terms of chlorinity, the accuracy of chlorinity determination became the factor limiting the precision with which salinity was known. For this reason conductivity measurement was adopted in 1969 as the recommended method of comparing a sample salinity with that of a standard. This replaced the chlorinity method which had been used up to that time. As absolute conductivity is difficult to measure, a ratio technique was used in which the conductivity of a sample was compared with a "standard seawater". An empirical relationship between conductivity ratio at 15°C and salinity was developed as shown in

equation (3.2) {6}.

$$S \times 10^3 = -0.08996 + 28.29720 R_{15} + 12.80823 R_{15}^2 - 10.67869 R_{15}^3 + 5.98624 R_{15}^4 - 1.32311 R_{15}^5 \quad (3.2)$$

where  $R_{15}$  is the conductivity ratio at  $15^\circ\text{C}$  relative to the conductivity of "standard seawater" having a salinity of  $35.00 \times 10^{-3}$  and a chlorinity of  $19.374 \times 10^{-3}$ .

In 1981, a new definition of salinity was proposed. This new salinity concept enabled all researchers using conductivity-temperature-depth (CTD) instruments to report their data in a consistent manner, compatible with sample measurements obtained from bench salinometers. Furthermore, the existing tables giving salinity as a function of conductivity ratio do not go below  $10^\circ\text{C}$ , which makes them unsuitable for use in the majority of CTD applications. Under the new definition, absolute salinity ( $S_A$ ) is defined "as the ratio of the mass of the dissolved material in seawater to the mass of solution". In practice this quantity cannot be measured directly and practical salinity ( $S$ ) will be used for reporting oceanographic observations. The practical salinity scale is based on a standard seawater having a conductivity ratio ( $K_{15}$ ) of unity at  $15^\circ\text{C}$  to a potassium chloride solution containing 32.4356g KCl in a mass of 1kg

of solution. The practical salinity scale is defined in terms of the ratio  $K_{15}$  by the following equation:

$$S \times 10^3 = 0.0080 - 0.1692K_{15}^{1/2} + 25.3851 K_{15} + 14.0941 K_{15}^{3/2} - 7.0261K_{15}^2 + 2.7081 K_{15}^{5/2} \quad (3.3)$$

Using equation (3.3) salinity may now be determined from conductivity ratio over a wide range of salinity, temperature and pressure values.

#### 3.3.1.2. Salinity Values Measured in the Irish Sea

In this particular study, salinity values were measured in situ using a conductometric measurement method. The usefulness of the salinity parameter is in being able to distinguish the different types of waters. This is largely based on assigning open oceanic seawater a salinity value of 35‰ (parts per thousand). All other types of seawater, e.g., "near coastal" seawater and estuarine water, have lower salinity values. In addition, the salinity value of freshwater is very low. Because of the variations in salinity with water type, vertical and horizontal profile studies of salinity are used to study the mixing process of waters of differing salinities.

Recorded salinity, temperature and depth values are presented in Table 3.1. Temperature and salinity values were not recorded at stations 8-10, although depth values were measured at these stations.

Stations 1-7 are located in the Bristol Channel/Severn Estuary system (Fig. 3.1). This system is characterised {7} by:

- (i) the largest tidal range around the English coast;
- (ii) large freshwater input; and
- (iii) semi-enclosed nature.

Consequently, these features produce a water body that is well mixed as a result of the high energy of tidal movements. However, this water body has a restricted exchange with waters outside the Channel, resulting in a pronounced variation in salinity values along the length of the Severn Estuary and Bristol Channel. Values of salinity recorded during this study along the Bristol Channel/Severn Estuary system are illustrated in Fig. 3.3. The pronounced variation in salinity is clearly shown from the values recorded during this research work.

Table 3.1a Physical Properties of Stations 1-27 sampled during RV Clione Cruise (14b/84), Dec. 1984

Station No.	Depth (m)	Time	Temp. ( $^{\circ}$ C)	Salinity (‰)
1	20	10.02	9.55	21.39
2	34	11.01	10.07	26.20
3	22	12.51	10.78	30.41
4	30	13.50	11.06	31.57
5	25	14.23	10.70	31.38
6	44	16.55	11.59	33.01
7	63	20.03	12.22	34.07
8	118	8.30	-	-
9	110	11.02	-	-
10	107	14.31	-	-
11	120	17.45	12.44	34.41
12	67	19.47	12.20	34.33
13	28	8.30	10.32	33.37
14	17	11.29	10.02	33.07
15	42	16.41	9.82	32.23
16	108	18.53	11.57	33.83
17	57	20.46	11.61	33.90
18	26	7.46	10.17	32.86
19	28	9.41	10.35	32.93
20	21	11.00	9.64	32.54
21	19	12.35	9.14	31.67
22	16	14.00	8.91	32.10
23	14	15.25	9.17	31.55
24	28	16.16	10.17	32.71
25	30	16.56	10.10	32.65
26	30	18.00	10.19	32.75
27	34	18.31	10.41	32.93



Table 3.1b Physical Properties of Stations 28-54 sampled during RV Clione Cruise (14b/84), Dec. 1984

Station No.	Depth (m)	Time	Temp. ( $^{\circ}$ C)	Salinity ( $^{\circ}$ / $\infty$ )
28	19	7.57	8.88	31.29
29	14	8.40	8.52	30.79
30	15	8.59	8.66	31.02
31	12	9.38	8.56	31.01
32	20	10.40	8.94	31.36
33	30	11.39	10.33	32.77
34	30	12.33	10.84	32.20
35	49	14.28	11.19	33.38
36	44	15.52	11.21	33.39
37	33	17.08	10.88	33.40
38	28	18.33	10.61	33.37
39	22	7.48	8.57	30.61
40	38	9.15	10.04	32.25
41	32	10.59	9.57	31.70
42	32	13.29	10.34	32.66
43	252	15.38	10.97	32.81
44	132	7.00	11.17	33.23
45	56	10.44	11.09	33.36
46	29	12.50	10.31	33.24
47	30	13.54	9.74	33.14
48	36	15.54	9.95	33.33
49	27	17.59	9.63	33.43
50	37	7.57	10.56	33.92
51	28	10.00	10.05	33.69
52	28	12.37	9.84	33.57
53	71	15.28	11.04	34.08
54	100	17.39	-	-

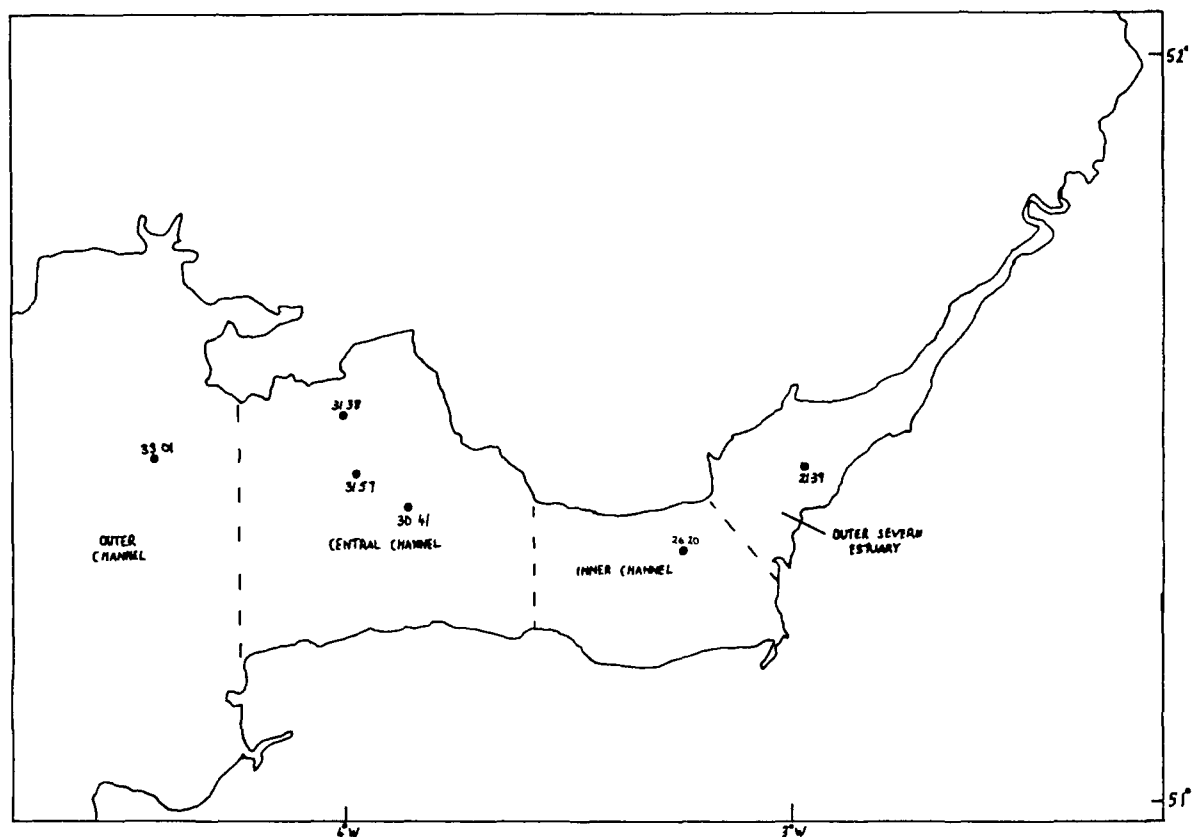


Fig. 3.3 Salinity values recorded in Bristol Channel/  
Severn Estuary in December 1984.

At station 1, which is located in the Outer Severn Estuary, the salinity was 21.39‰. (see Fig. 3.3) It is not surprising that the salinity in this region is low given that the freshwater input into the Severn Estuary/Bristol Channel is of the order of  $300-400\text{m}^3/\text{sec}$  {7}. During the summer months the salinity in this area increases as a direct result of reduced freshwater input from the river Severn. Despite the seasonal variance in surface salinity in the region around station 1, the difference between surface and benthic salinity rarely exceeds  $0.1\text{‰}$ {8}. This is a consequence of the thorough mixing of the freshwater and seawater in this area. On moving seaward from station 1, a gradual increase in salinity occurs, as is to be expected as one approaches the open sea. The decrease in salinity from station 4 to 5 (see Fig. 3.3) results from a large anti-clockwise gyre in this region. This causes water escaping downstream of the inner channel to be confined to the area close to the Welsh coast as it moves through the central channel. This anti-clockwise gyre is known {7} to extend into the outer channel, although there is no evidence from this particular study to corroborate this fact. However, the lack of stations in the outer channel would negate identification of such a gyre.

Finally, the salinity value recorded at station 7 is typical of a coastal seawater.

The water temperatures recorded in the Bristol Channel/Severn Estuary are typical of values for mid-latitudes (between 30-60<sup>o</sup>N) during the winter period. The decrease in water temperature on moving inland from station 7 to station 1 reflects the increasing freshwater influence. Freshwaters are, without exception, cooler than seawaters in mid-latitudes. Therefore, the decreasing temperature on moving inland reflects the increasing presence of freshwater.

Salinity and temperature values were not recorded at stations 8-10 located in the Celtic Deep region. One can surmise that salinities at these stations would be slightly higher than those recorded at stations 7 and 11. This is highly probable given that any freshwater inputs likely to decrease salinity values by dilution would not occur in this region.

Very little significant change is observed in salinities from stations 11-17, which are located along the Welsh coastline. The values are typical of coastal waters. The marine environment along the Welsh coast is directly influenced by the northerly flowing currents which carry seawater from the Celtic Deep. However, unlike the Bristol

Channel/Severn Estuary system, where the massive freshwater input is of sufficient magnitude to dilute the near coastal seawater, no similar system of such magnitude occurs along the Welsh coast from stations 12-17. This accounts for the relatively high salinity values.

Stations 19-34 are located in Liverpool Bay (see Fig. 3.2). However, for the purpose of simplicity, stations 18 and 35 are included in comments on this area of the Irish Sea, even though they would not be encompassed by the following definition of Liverpool Bay. Liverpool Bay is usually defined as "that part of the Irish Sea delimited by the North Wales coast east of Great Ormes Head and by the Lancashire coast as far north as the Ribble Estuary" {9}. It is a semi-enclosed water body. Although the pattern of water circulation within the Bristol Channel/Severn Estuary system is thoroughly understood, the same is not true for Liverpool Bay. In fact there are two opposing schools of thought as to the general surface water circulation pattern in the Bay. Division exists as to whether the water circulation is clockwise or anticlockwise. To date, evidence for a clockwise circulation has come chiefly from studies of plankton distribution {10,11}. Evidence for an anticlockwise circulation has been demonstrated by current meter studies {12,13}. However, more recent studies have

demonstrated that both circulation patterns occur in the Bay, though the circulation type is seasonally dependent {14,15}. A clockwise circulation results from density-driven advection currents. These currents are generated in areas, such as estuaries or coastal waters, where large density gradients occur [16]. Density-driven advection currents develop off an open coast where there is an influx of freshwater. In an advective process, freshwater enters the bay from the east and moves westward at the surface while dense saline water moves eastward at depth. By contrast, the anticlockwise circulation is caused by south-easterly directional winds. Which of the two circulation patterns dominates is dependent on the relative effectiveness of wind and density forcing agents. Generally, wind becomes a significant factor at speeds greater than 5 m/s and the dominant factor at speeds greater than 10 m/s {14}.

A simple approach to try and elucidate water circulation patterns in Liverpool Bay has been proposed using salinity, temperature and chemical characteristics (such as silicate, phosphate, nitrate, nitrite, ammonia){17}. None of the aforementioned chemical characteristics were measured in this study. However, temperature and salinity values were recorded. Temperature and salinity values are presented in Tables 3.1a and 3.1b.

Freshwater inputs into Liverpool Bay arise from the rivers Dee, Mersey and Ribble. The pattern of movement of freshwater from these rivers should be detectable in the bay. As the freshwater moves into the saline environment, dilution occurs as a result of various mixing processes. Consequently, areas where such mixing occurs are recognised by lower salinities compared with areas further seaward. In fact, low salinity surface waters are known to extend at least 12 miles from the mouth of the Mersey river into Liverpool Bay {18}. This is a result of partial mixing of saline water and freshwater. The movement of this partially mixed water should be detected by areas of lower salinity. Low salinity values were recorded at those stations nearest the coast (stations 21, 23, 28, 29, 30, 31, 32 as shown in Fig. 3.2). Curiously, the salinity at station 22 is higher than that recorded at neighbouring stations. This may be a consequence of locally produced currents. Alternatively, it may reflect lateral variation of salinity, which can occur under certain circumstances {16}. In such situations, the lower salinity water occurs on the right-hand side (in the northern hemisphere) looking towards the sea. Lateral variation occurs when there is a net seaward flow of freshwater on the right and a compensating flow of higher salinity water on the left.

The present situation of attempting to determine a water circulation pattern using only salinity values is extremely difficult. Salinity values recorded along the North Welsh coast increase as one moves from station 21 to 18. This may indicate a seaward movement of freshwater, suggesting a clockwise circulation pattern. However, salinity values at stations 29, 30 and 31 are the lowest values recorded in Liverpool Bay. These values may reflect a net seaward movement of low salinity water from the Mersey river. Alternatively, they may be located in the path of freshwater emanating from the river Ribble. More stations would need to be located at the mouth of the Ribble to determine the salinities of water in this region. Overall, the salinities appear to increase seaward, suggesting a clockwise circulation pattern as shown in Fig. 3.4.



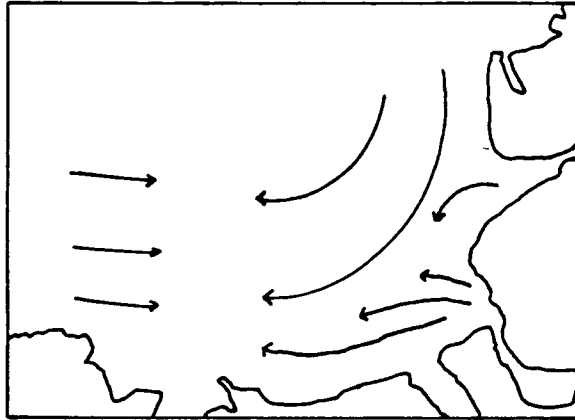


Fig. 3.4. Clockwise circulation pattern for surface waters in Liverpool Bay.

For the remainder of stations along the English coast, salinities tend to decrease landward while they increase seaward from station 41 to 43 along the southern coast of Scotland. Very little variation in salinity occurs along the Irish coast.

### 3.3.2. Problems Associated with On-board Metal Analysis

The notion of on-board analysis of seawater samples is advantageous for a number of reasons. Such a situation means that once water samples have been taken from a station they can be analysed almost immediately. Therefore, the possibility of chemical or biological mediated changes occurring are eliminated, or at the very least minimised. One of the problems associated with the storage of water samples for long periods is that speciation changes can occur, thereby leading to erroneous results and interpretation. A further advantage of on-board analysis is that once the research cruise is completed, results are immediately available for interpretation and statistical examination.

Amongst the chief analytical prerequisites for on-board analysis are

- (1) access to a clean laboratory with full laboratory facilities (chemicals, glassware);
- (2) elimination of all potential sources of contamination;
- (3) utilisation of maintenance-free equipment; and
- (4) all analytical methods employed should be portable for easy transfer from the laboratory to the research vessel.

Additionally, sample numbers would need to be minimised if all analyses are to be completed during the cruise. However, such a constraint could cause the overall data gathered to be of limited value. In some situations, for example, monitoring a dumping ground at sea, an intensive sampling programme may be necessary. Furthermore, it is unlikely that all samples collected in such a situation could be completely analysed on-board ship because in addition to the large number of samples collected, a large and varied number of parameters may have to be measured.

One of the objectives of this particular study was to ascertain the feasibility of on-board analysis. Unfortunately, several problems were encountered which could negate the likelihood of such work. These problems are now outlined.

For the quantitation of Cd(II), Pb(II) and Cu(II), DPASV at a mercury film electrode was employed. Unlike other methods, such as AAS, voltammetric methods are portable, and thus ideally suited to on-board analysis. Despite this advantage, difficulties were encountered with this method during this study. In particular, measurements were impossible during rough weather conditions. The tilting of the research vessel was quite severe under such conditions. This caused severe turbulence of the sample in the electrochemical cell. The problem was confined to periods of stormy weather. Nevertheless, in exposed areas such as the Irish Sea, periods of stormy weather are not restricted to the winter months. Consequently, it is questionable as to whether this type of analytical method is suitable for on-board analysis in such waters. One solution to the problem is the use of a larger research vessel as it would have greater stability in stormy conditions. Whilst it is a very expensive solution to the problem, it may well be that DPASV at a MFE can only be successfully employed on large research vessels. A further possibility is to employ rapid staircase anodic stripping voltammetry (RSASV) [19]. This method is insensitive to electrode rotation in the stripping stage as demonstrated by the fact that similar results were obtained from stationary and stirred stripping. Consequently, RSASV has been considered as an ideally suited method to field

studies {19}.

A further problem associated with DPASV is the slowness of the method. It should be stressed that this difficulty is not solely confined to on-board analysis, it is a particular characteristic of the method employed. A single analysis, including two standard additions, required approximately 90 min. Thus, over a typical 8 hour period, a maximum of 5 samples could be satisfactorily analysed. During this study, 65 samples were taken; yet only 17 were analysed by DPASV on-board ship. Although delays due to rough weather form part of the explanation for not completing all analyses, it does not conceal the fact that DPASV is slow. Circumvention of this problem could be achieved by employing RSASV as an alternative voltammetric technique. Equally, square-wave stripping voltammetry could be used as it has the advantage of speed over DPASV {20}. The only problem with square-wave stripping voltammetry is that it cannot successfully measure trace levels of Pb(II) {20}. Perhaps RSASV is the more suited of the two alternative methods for on-board analysis.

Avoiding sample contamination is extremely difficult under ideal laboratory conditions. On a research vessel which does not have a purpose built analytical laboratory, it is almost impossible. When determining

trace metals concentrations, typically  $\mu\text{g}/\text{l}$  levels, it is desirable that a dust-free clean room be used. Typical metal concentrations for a dust-free clean room are 1 ng Fe, 2ng Cu and 0.2ng Pb per  $\text{m}^3$ , whereas a conventional laboratory will usually contain 200ng Fe, 20ng Cu and 400ng Pb per  $\text{m}^3$  {21}. However, laboratory air on research vessels can be severely polluted with trace metals such as Pb, Ni and Zn {4}. Contributory factors to this problem include frequent paint-scrubbing and maintenance with lead-based anti-corrosion paints during the course of a research cruise. This type of work causes contamination of the air with lead.

In this particular study, the laboratory where all metal analysis was carried out, had on previous cruises been used as an oceanographic laboratory. Thus, it was not an ideal arrangement for the type of work being carried out. Dust particles were ubiquitous in this laboratory. In addition, the problem of contamination was exacerbated by allowing the door into the laboratory to be continuously left ajar. This was necessary due to the absence of adequate ventilation. However, some effort was made to minimise sample contamination by undertaking some sample preparatory work as well as stripping voltammetry in a laminar-airflow unit. The small size of this unit meant that the step of transferring the sample from the sampler

to the filtration unit was carried out in the laboratory atmosphere. Consequently, avoidance of sample contamination was not completely achieved.

### 3.3.3. Critical Assessment of the Analytical Procedures

Aspects of the analytical procedures employed during the course of this study are now examined.

#### 3.3.3.1. Sample Collection

Before any analysis can be carried out, it is common practice for a sample of the matrix to be analysed to be taken. It is essential that this step be devoid of error. For example, contamination of the sample either in the sampling or subsequent subsampling steps will tend to produce results that are consistently either too high or too low {22}.

With regard to the sampling of seawaters, considerable time and effort has been devoted to the sampling methodology {23,24}. In view of these developments, consideration is now given to the sampling procedures used in this particular study.

Surface seawater samples, that is, samples taken at

4 metre depths, were taken by manually lowering the sampler over the side of the vessel. This is a far from ideal sampling procedure, particularly as the potential of a ship to contaminate the water in its vicinity, especially when stationary, has been realised {25}. The water around any vessel is constantly being contaminated by heavy metals from antifouling paints {26} as well as exhaust emissions, dirt and dust particles. Ideally, samples should have been collected at least 500 m from the research vessel using a small rubber boat {23}. When collecting a sample, the small boat is steered against the wind while sampling is carried out in front of the bow of the rubber boat as it is continuously moves into uncontaminated water. Even this small boat will cause the water around it to become polluted by heavy metals as soon as it becomes stationary. Although the aforementioned sampling procedure is the ideal way to circumvent sample contamination, such a system would not be possible during the encountered weather conditions. It is certain that this type of sampling procedure would have, if used, jeopardized the lives of those taking the samples.

A novel sampling and filtration device has recently been developed by one of the researchers on this cruise {27}. This system is suitable for the collection and filtration of surface water samples. Water is brought onto



the research vessel via an all-teflon pump and teflon tubing from a buoy deployed away from the vessel. The sample is delivered directly into a polycarbonate pressure reservoir and is subsequently filtered through a polycarbonate filter and in-line holder. Deployment of the buoy is possible in all but the very worst weather conditions, that is, when it is too rough to go on deck. A further advantage of this system is that the will move away from the ship due to wind drift. Thus, contaminated water immediately around the vessel is avoided.

#### 3.3.3.2. Filtration and Preservation of Samples

Filtration to remove particulate matter ( $> 0.45 \mu\text{m}$ ) is necessary when analysing coastal waters. These waters contain large quantities of suspended matter, originating principally from outflowing rivers but also arising from re-suspension of deposited sediments in the turbulent estuarine zone. If samples were stored unfiltered, then losses of metals would ensue either by adsorption on suspended matter or precipitation caused by microbiological mediated pH changes due to bacteriological respiration and photosynthesis {28}. The only time that filtration is unnecessary is when open oceanic regions are sampled, as there is a negligible quantity of suspended matter in such areas {29}.

Because all sampling stations in this study were located in coastal or near-coastal waters all samples were filtered. Subsequently, all samples were acidified with either nitric or hydrochloric acid. A number of reasons have been forwarded to justify sample acidification. First, adsorption of trace metals, such as lead, on the walls of the storage container is prevented {4}. Adsorption of lead chiefly occurs in samples stored at natural pH; however, acidification to pH 2.0 redissolves any adsorbed lead. In general, seawater samples are less affected by adsorption losses because the large concentrations of alkali and alkaline earth metals compete for adsorption sites {4}. A further reason for sample acidification is that biological activity is severely inhibited. Consequently, biologically-induced pH changes causing precipitation of metals are prevented. Finally, acidification causes decomposition of moderately stable metal complexes, provided the samples are allowed to stand for several hours to permit complete decomposition of such complexes {30}. The principal limitation of acidification is that it precludes speciation studies of metals at natural pH values.

Because all samples were acidified, speciation studies at natural pH values were not possible. It would have been useful to have performed such measurements if a

fuller understanding of trace metal distribution in the Irish Sea is to be developed. Measurements of metal concentrations at natural pH values would give a realistic assessment of the bio-available metals present at the various sampling positions. It is questionable as to whether metal concentrations measured at pH 1.0 accurately reflect the bioavailable metal fraction. It is possible that all metal concentrations measured at pH 1.0 over-estimate the bioavailable portion, particularly as such low pH values never occur in marine environments. Maintaining the natural pH of a sample is easily achieved during stripping voltammetry. Samples are simply degassed with a mixture of CO<sub>2</sub> and N<sub>2</sub> while the partial pressure of CO<sub>2</sub> is adjusted to maintain the natural pH of the sample {31}.

#### 3.3.3.3. Storage of Samples

Any precautions taken to avoid contamination or loss of metals in the aforementioned procedures will be negated by incorrect storage methods. In the course of this work, samples were stored at room temperature after filtration and acidification. All samples for Pb(II), Cu(II), and Cd(II) analysis were stored in polyethylene bottles and those for reactive Hg analysis were stored in glass bottles. It is now universally accepted that

polyethylene bottles are suitable for storing water samples when determinations other than mercury are to be carried out {4,32}. Mercury losses due to volatilisation occur when samples are stored in polyethylene containers. However, these losses can be eliminated by preserving samples with a mixture of nitric acid and potassium dichromate, if polyethylene storage containers must be used {33}.

Storage of water samples at room temperature for periods longer than one week is very undesirable. There is a tendency for the lead concentration to increase in samples stored at room temperature due to leaching from the walls of polyethylene bottles {23}. In contrast, cadmium concentrations usually decrease in the same sample due to adsorption losses. Even storage at + 5°C does not fully eliminate the aforementioned problems. Storage at - 20°C is necessary before these problems are finally prevented. The only problem regarding sample storage at - 20°C is that speciation changes will occur once the sample has been thawed after storage. Therefore, storage at - 20°C is only suitable when total metal concentrations are to be determined.

Because all samples were stored at room temperature, some of the lead and cadmium results may be

unreliable. All samples collected from stations 1-27 were stored at room temperature for over a week before they were finally refrigerated at + 4°C.

#### 3.3.3.4. Analytical Methods

##### 3.3.3.4.1. Mercury Analysis

A number of analytical methods have been developed for the quantification of mercury in freshwater and seawater samples. The determination of mercury at low concentrations, typically  $\mu\text{g}/\text{l}$  concentrations, is usually performed using a cold-vapour method in conjunction with either atomic absorption spectrometry {34} or atomic fluorescence spectrometry {35}. Flame atomic absorption methods lack the sensitivity necessary for trace mercury determinations. However, even cold-vapour methods lack sufficient sensitivity when ultra-trace concentration, i.e., less than 100 ng/l, have to be measured. A preliminary concentration step is needed in such situations. The most widely used concentration step is amalgamation of mercury vapour on finely dispersed gold {36,37}. An advantage of this method is in the separation of mercury from interfering substances, particularly those present in seawater {36}. Pre-concentration in a liquid trap {37} has also been developed, though the method is not

as extensively used as the amalgamation procedure.

Cold-vapour atomic absorption spectrometry with a gold amalgamation pre-concentration step was the analytical method employed in this study. A magnesium perchlorate trap was not included prior to the gold-trap. The usefulness of a magnesium perchlorate trap is in the prevention of adsorption of water-mist on the adsorption cell as well as reducing the possibility of 'poisoning' of the gold-trap by volatile materials {39}.

The mercury form measured was that reducible by stannous chloride. Samples were retained for total mercury measurement, following UV irradiation. Although UV irradiation is a virtually contamination free method of destroying organomercury compounds, it is quite slow. Each sample must be irradiated for several hours before complete degradation of organomercury compounds is effected. Furthermore, this method can only be applied in a laboratory, thus allowing the possibility of loss of organomercury compounds if samples must be stored prior to analysis. An alternative method in which bromination is used to degrade organically bound mercury in aqueous samples has been developed {40}. Bromination successfully cleaved both aryl- and alkyl-mercury bonds, thereby generating inorganic mercury. The advantage of this method

is the rapidity at which this reaction occurs; complete reaction occurs in five minutes. Furthermore, it can easily be carried out in field work. This type of degradation method should be employed in further studies of this nature. The simplicity of the method and the rapidity of the degradation step lends itself to field analysis.

Mercury concentrations in seawater have been measured by DPASV at twin gold electrode {41}. However, in view of the difficulties outlined in Section 3.3.2. (DPASV analysis at a MFE), the aforementioned voltammetric method cannot be recommended as an alternative to cold-vapour AAS for field analysis.

#### 3.3.3.4.2. Differential Pulse Anodic Stripping Voltammetry at a Mercury Film Electrode

Despite the difficulties associated with DPASV analysis (Section 3.3.2) the method is very amenable to seawater analysis. Seawater is a particularly favourable medium as its salt content fulfils the function of a supporting electrolyte {42}. This eliminates the need to add further electrolyte, thus reducing the possibility of contamination.

Some reservations must be expressed regarding the

evenness of the mercury film on the MFE. The mercury film was formed on a polished glassy carbon surface. However, only in the plating solution is the film on such a surface of even distribution. Once the electrode is removed from the plating solution coalescence of the mercury droplets causes patchiness of the film texture {43}. This leads to an increase in the residual current. One possible means of overcoming the aforementioned problem is to "roughen" the electrode surface {43} prior to coating with mercury. In this way a more even film is produced which withstands repeated removal of solutions and repeated washing with a stream of water. A further way of avoiding the problem of film patchiness involves formation of the mercury film in-situ {43}. However, use of in-situ mercury film formation has been questioned, particularly when used in conjunction with speciation studies {44}.

#### 3.3.4. Dissolved Metal Ion Concentrations in the Irish Sea

The only results available are those generated during the field work since the analyses carried out subsequent to the cruise have not been published. For this reason the discussion in the subsequent section is somewhat limited. For example, no results were available for Cd(II), Pb(II) and Cu(II) in Irish coastal waters. Thus,



comparisons between metal levels in eastern and western regions of the Irish Sea were not possible.

#### 3.3.4.1. Reactive Mercury Concentrations Measured in the Irish Sea

As previously mentioned (see Section 3.2.6.2) only reactive mercury concentrations were measured. Results are presented in Tables 3.2 and 3.3; station locations are illustrated in Figs. 3.1 and 3.2. It is clearly observable from the results that the mercury concentrations are very low. Moreover, the results illustrate the sensitivity of the gold amalgamation pre-concentration step when determining ultra-trace reactive mercury concentrations.

##### 3.3.4.1.1. Reactive Mercury Concentrations in Liverpool Bay

Liverpool Bay has many different sources of Hg inputs. The rivers Dee, Mersey and Ribble accounted for a total discharge of 0.35 tons/annum of Hg during the period 1976/1977 {9}. In addition, 2.9 tons/annum of Hg was also dumped into the bay via direct sewage and industrial discharges during the same period. Other sources of Hg arise from the dumping of sewage sludge, industrial wastes and dredged spoil at various dumping sites in Liverpool Bay (Fig. 3.5). Between 1976-1980 an average of 1.5 tons/annum

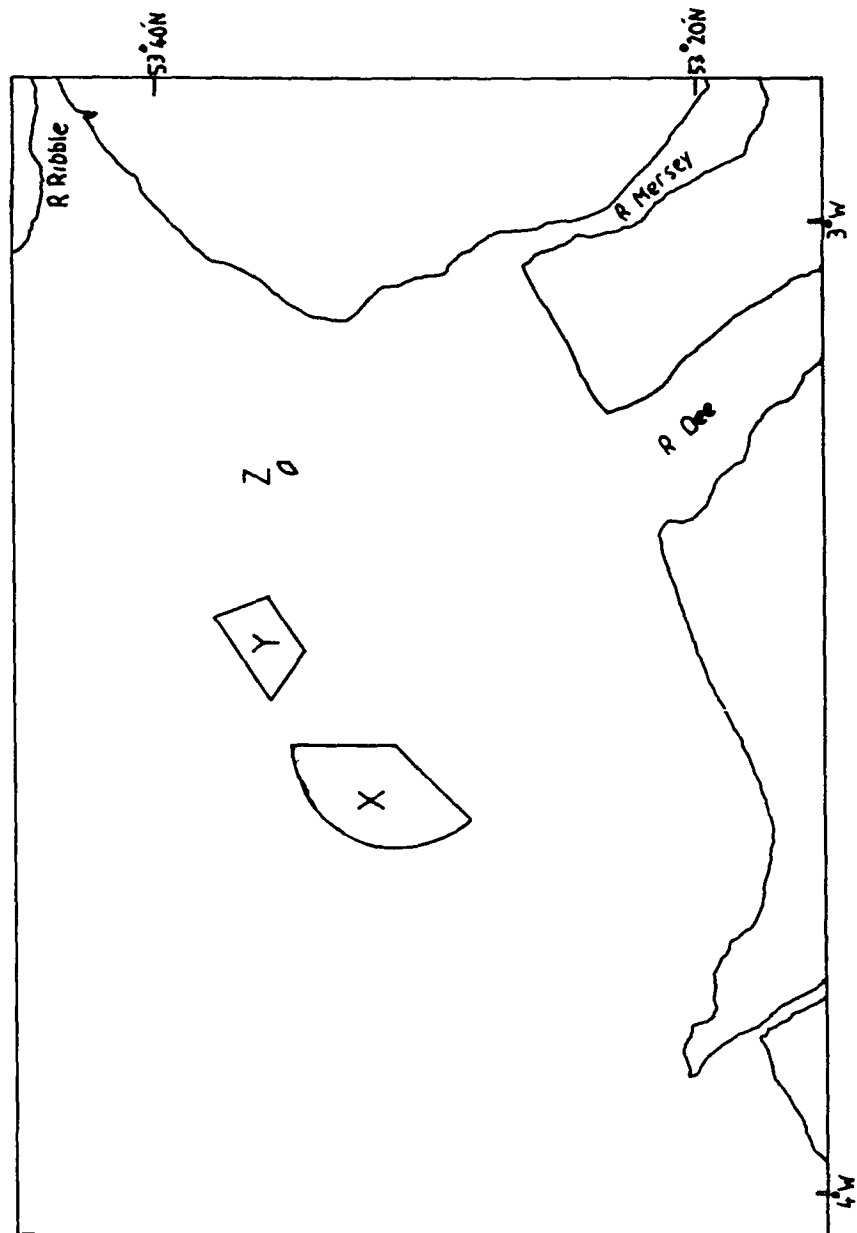


Fig. 3.5. Dumping areas for sewage sludge (X), industrial wastes (X) and dredged spoil (Y and Z) in Liverpool Bay.

of Hg associated with sewage sludge was dumped in the bay {9}. A further 4.02 tons/annum of Hg associated with dredged spoil was also dumped.

Although the present study was undertaken approximately 4 years after the study which generated the aforementioned numerical data it is unlikely that any significant alteration in the quantities of Hg discharged into the bay has occurred in the intervening period. Levels of reactive mercury present at various sampling stations in Liverpool Bay are shown in Table 3.2. Considering the numerous inputs of Hg to the bay, the concentrations are quite low. The average concentration of reactive Hg in Liverpool Bay is 1.84 ng/l, compared with average value of 6.6 ng/l for reactive Hg in the North Sea {45}. Surprisingly, stations 24, 25, 26, 27, 31, 32 and 33, which are located very close to the dumping sites, do not show elevated reactive Hg concentrations compared with the remaining stations. Consequently, despite the considerable quantity of Hg dumped in Liverpool Bay each year, extremely little is in the form of reactive Hg. This possibly reflects the ease with which Hg becomes adsorbed onto particulate matter and sediments {46}. Any reactive Hg present is probably in the form of chloro-complexes{47}.

Station Number	Depth (m)	Reactive Mercury Concentration (ng/l)
18	4	3.5
19	4	2.0
20	4	2.0
21	4	1.7
22	4	1.8
23	4	1.1
24	4	1.7
25	4	1.5
26	4	1.2
27	4	1.5
28	4	2.1
29	4	1.6
31	4	1.9
32	4	1.7
33	4	2.0
34	4	2.1
35	4	1.2
35	20	1.6
35	40	2.6

Table 3.2. Concentrations of reactive mercury (ng/l) at various stations in Liverpool Bay. These results were obtained during the period December 12th - 18th 1984.

More stable organomercury complexes, e.g., mercury-humate complexes {48} or methylmercury compounds, will not have been measured. These organo-complexes are not accessible to stannous chloride reduction {45} and require prior degradation before Hg in these forms can be measured. Thus, the total dissolved Hg concentrations will be considerably higher.

Only at station 18 was the reactive mercury concentration considerably higher than that measured at the remaining stations in Liverpool Bay. There is no immediate explanation to account for this apparently inconsistent result. Unlike the vast majority of sampling sites, station 18 is not adjacent to any of the dumping sites. Moreover, it is not located in the vicinity of any major river outlet. Without further sampling points in the area around station 18 it is not possible to identify the source of mercury in this region.

A vertical profile of reactive Hg was determined at station 35 (Table 3.3). The reactive Hg concentration was found to increase with depth. Such a vertical distribution could result from mercury released from sediments under oxidising conditions {49}. Alternatively, the distribution may represent increased complexation of Hg by organic matter in the surface waters compared with that at greater

Station Number	Depth (m)	Reactive Mercury Concentration (ng/l)	Station Number	Depth (m)	Reactive Mercury Concentration (ng/l)
36	4	1.9	45	4	2.2
37	4	2.0		25	1.4
38	4	1.7		47	2.0
39	4	1.4	47	4	4.4
40	4	1.9	48	4	3.2
41	4	2.6	49	4	3.0
42	4	1.6	50	4	3.0
43	4	1.3	51	4	2.6
	50	1.9	52	4	2.2
	100	1.0	53	4	2.5
	250	1.1	54	4	3.9
44	4	2.3		20	3.3
	40	1.9		50	3.1
	80	1.8		100	2.6
	128	2.1			

TABLE 3.3. Concentrations of reactive mercury (ng/l) at various sampling locations and depths in the Irish Sea. These results were obtained during the period December 12 - 18 1984.

depths.

3.3.4.1.2. Reactive Mercury Concentrations at Station 36 to 54 in the Irish Sea

Little variation in reactive mercury levels occurs between stations 36 and 42 (Table 3.3). The reactive mercury concentrations at these stations are within the range of values measured in Liverpool Bay.

Vertical profiles were determined at stations 43-45 situated across the Northern Channel. Surface concentrations (4m depth), although similar at stations 44 and 45, are higher than the value at station 43. It was also noted that the pattern of reactive Hg distribution which occurred at station 35 was not evidenced here. In fact, the trend was a reversal of that at station 35 as the reactive Hg concentrations decreased slightly between surface and benthic locations at stations 43-45. At intermediate depths, various anomalies exist. For example, at station 43 the reactive Hg level increased down to 50m followed by a decrease from 50m to 250m. At stations 44 and 45, reactive Hg concentrations decreased between surface and intermediate depths, but increased again towards the benthic sampling point. These variations are possibly due to local circulation currents.

Mercury concentrations along the Irish coastline (stations 47-54) are higher than the values measured in Liverpool Bay. The unavailability of organic material compared with Liverpool Bay may explain the higher levels of reactive Hg along the Irish coastline. Unlike Liverpool Bay, there are no known direct discharges of Hg into the waters along the Irish coastline. Consequently, the

results may reflect the background levels of reactive Hg in the Irish Sea.

#### 3.3.4.2. Dissolved Cadmium, Copper and Lead Concentrations

Levels of cadmium, lead and copper were quantified, following sampling and on field analyses, for Cardigan Bay and Liverpool Bay. Zinc levels were not measured because of the restriction caused by the lower hydrogen overvoltage of the the MFE at pH 2.0 {50}. Furthermore, without the intervention of a third element {51}, e.g. Ga or Ge, the Zn-Cu intermetallic compound is formed on the surface of the MFE.

##### 3.3.4.2.1. Metal Concentrations in Cardigan Bay

Levels of dissolved Cd(II), Pb(II) and Cu(II) measured at three stations in Cardigan Bay (see Fig. 3.1) are presented in Table 3.4.



Station Number	Depth (m)	Metal Ion Concentration (ng/l)		
		Cd (11)	Cu(11)	Pb(11)
13	4	24	1200	15
14	4	27	1000	51
15	4	21	-	69

TABLE 3.4. Concentrations of dissolved metal ions in Cardigan Bay measured by DPASV at a MFE. Sampling and analyses were performed between December 10-18th, 1984.

Inadequate sampling locations in this area limit the usefulness of the data in Table 3.4. Very few inferences are possible based on results from three stations within an area as large as Cardigan Bay. Realistically, a denser network of stations is required if accurate and adequate metal distributions are to be established.

Very little information exists on metal levels in Cardigan Bay. One particular study between 1967-1971 measured the metal fraction removed on passage of a water sample through a chelating resin {52}. The mean concentrations were as follows: Cd(II), 1.11  $\mu\text{g/l}$ ; Cu(II), 1.72  $\mu\text{g/l}$ ; Pb(II), 2.24  $\mu\text{g/l}$ . Direct comparison between these results and those of this study to ascertain the trend of metal levels is not entirely possible. The metal concentrations in Table 3.4, measured at pH 2.0, will include:

- (a) free metal species;
- (b) labile inorganic and organic species; and
- (c) metals released from dissolved organic matter and colloids by exchange processes with  $\text{H}^+$  ions.

Some of the aforementioned fractions, (a) and (b),

will be included in the results from the 1967-1971 survey. Differences arise where metal complexes are dissociable by chelating resins but are ASV "non-labile". Additionally, the present day awareness of sample contamination did not fully exist at the time the 1967-1971 survey was carried out. Therefore, some errors are expected in the results of this 1967-1971 survey. Consequently, extrapolations for the various metals from these two sets of data are not possible.

A relatively recent study has indicated that average metal concentrations (at pH 2.0) in surface coastal seawaters {53} are Cd(II), 10-20 ng/l; Pb(II), 100-200 ng/l; Cu(II), 200-500 ng/l. Comparing these values with those in Cardigan Bay shows the Pb(II) concentrations to be lower than average, whereas the Cd(II) levels are above average. However, the Cd(II) concentrations in the bay are not significantly higher than the average value. By contrast, the Cu(II) concentrations are several times higher. In fact, the Cu(II) concentrations measured in December 1984 are comparable with those measured in the 1967-1971 survey, whereas the Cd(II) and Pb(II) concentrations are very much lower in the 1984 survey. Inter-comparison of stations indicates little variation for Cd(II) between the three stations. Most, if not all, of this cadmium will be as chloro-complexes, as these are the

predominant Cd(II) species in seawater {54,55}. The Pb(II) concentrations increase from station 13 to 15, though the greatest increase is between stations 13 and 14. For lead, the dominant species are  $\text{PbCO}_3$  and  $\text{PbOH}^+$ . The Pb-chloro complexes only account for approximately 20% of lead speciation in seawater {55}. The difference between Pb(II) concentrations at stations 13 and 14 may represent some local regulating system at station 13. A high concentration of suspended particulate matter will scavenge lead species. This is possibly the situation at station 13. However, analysis of the suspended particulate matter is the only way of knowing whether or not this is the case. As previously mentioned, the Cu(II) concentrations are higher than the typical values in coastal seawater. These elevated concentrations are partially the result of anthropogenic activities. In addition, significant concentrations of metal ions arising from processes such as leaching and weathering, are transported into the bay by the many freshwater inputs {52}.

#### 3.3.4.2.2. Metal Concentrations in Liverpool Bay

Many diverse sources contribute to the metal levels in Liverpool Bay. The data in Table 3.5 represent inputs from material dumped and discharges into the bay {9}. Dredged spoil contains the largest quantities of Cu

Input Source	Metal Quantity / Input (tons/annum)		
	Cd	Cu	Pb
Sewage sludge	1.84	95	58.8
Industrial wastes	ND	1.18	0.46
Dredged spoil	1.26	247.2	114.8
Rivers (Mersey)			
(Dee )	34	75	NQ
(Ribble)			
Sewage and Industrial discharges	16	53	47

TABLE 3.5. Quantities of metals contained in wastes discharged or dumped in Liverpool Bay.

ND = Not detected

NQ = Not quantified.

and Pb. This material arises from maintenance dredging of the channel approaches to the River Mersey, the Mersey itself, the docks and harbours along its length and the Manchester Ship Canal. The rivers Mersey, Dee and Ribble represent the largest single source of Cd discharged into the bay. The reason for this is that Cd is less scavenged by particulate matter than Pb or Cu {56}. Much of the Cu and Pb contained in the dredged spoil is due to their removal in the estuarine zone of the River Mersey. In the freshwater-seawater mixing zone, humic substances and hydrated iron oxides are precipitated. Many dissolved metals, e.g., Cu, Pb, Zn, are readily absorbed by hydrated iron oxides or chelate with humic acids {57} and are subsequently transferred to the sediments by the precipitating substances. This controlling mechanism relieves a river of its metal load before it enters the sea.

The concentrations of Cd(II), Pb(II) and Cu(II) in Liverpool Bay are presented in Table 3.6. Stations 26 and 27 are located directly over a sewage sludge and industrial waste dumping ground (Fig. 3.5). Because the sewage sludge contains a significant amount of copper and lead, elevated concentrations of these two metals are expected at stations 26 and 27. Stations 24, 25 and 33 located near the

Station No.	Sample Depth(m)	Dissolved Metal Ion Concentration (mg/l)		
		Cd(11)	Pb(11)	Cu(11)
18	4	37	58	950
19	4	56	54	--
20	4	42	59	1100
21	4	35	42	440
22	4	72	66	1200
23	4	60	56	1100
24	4	30	49	890
25	4	51	44	1300
26	4	31	18	1700
27	4	17	57	1400
29	4	130	120	2100
31	4	57	130	490
32	4	44	49	1500
33	4	69	45	1800

TABLE 3.6. Concentrations of Cd, Cu and Pb (ng/l) determined by DPASV at a MFE for stations in Liverpool Bay. Sampling and analyses were carried out between December 11-18th, 1984.

sewage sludge and industrial waste dumping ground would also be expected to contain elevated metal concentrations. From Table 3.6, it is clear that this is not the situation. The highest concentrations of Cd(II) and Cu(II) were measured at station 29. It must therefore be assumed that this station is situated close to or directly over a dumping ground.

Coastal stations show considerable variations in metal concentrations. Cd(II), Pb(II) and Cu(II) concentrations at stations 18 are amongst the lowest values recorded in Liverpool Bay. At station 22 which is located near the mouth of the River Mersey increased Cd(II) and Pb(II) levels were found. It is not surprising that the Cd(II) levels should be high because, as seen from Table 3.5, the rivers are the single largest source of Cd discharged into the bay. The elevated concentrations at station 29 are most probably due to dumping in this area.

No clear picture emerges of the impact that the dumping sites have on dissolved metal levels in Liverpool Bay. Migration of metals from sediments may possibly contribute to the concentrations in the overlying water. Under oxidising conditions, metal ions such as Cd(II), Pb(II) and Cu(II) associated with organic or sulphide solids in sediment are transformed into carbonate or hydroxo complexes [49]. The increased solubility of the metal carbonate and hydroxo species mobilises these metals. Conversely, the existence of reducing



conditions reduces mobilisation of metal ions. It is possible that the latter conditions predominate in Liverpool Bay. This would explain the relatively low concentrations at stations 26 and 27 despite being located directly over a dumping ground.

Shipping traffic in the Liverpool Bay region will also contribute to metal ion concentrations {53}. None of the stations in this study were purposely located along shipping routes. Consequently, these contributions cannot be ascertained.

In Section 3.3.2. difficulties were encountered when attempting to elucidate the water circulation pattern in the bay utilizing only physical parameters. The usefulness of Cd as a method of studying water movement has been successfully demonstrated {56}. Unfortunately, such an application is not possible in Liverpool Bay. Given that parts of the bay are used as dumping grounds, the Cd contributions from such sources will be superimposed on those emanating from the various freshwater inputs.

#### 3.4. Conclusions

Application of DPASV to the measurement of dissolved metal fractions at ng/l concentrations demonstrates the sensitivity of this method when applied to marine trace metal analysis. The difficulties encountered with the method during

rough weather conditions suggests that it is not entirely suited to field analysis. Certainly the method is of limited use in areas where rough conditions prevail for a large period of the year.

The cold vapour AAS method employed to measure reactive mercury concentrations is suitable for field analysis. Unlike DPASV, this method may be operated in even the roughest weather conditions. Had a bromination step been included to degrade organomercury complexes, it is possible that total mercury concentrations could also have been determined.

Reactive mercury concentrations in the Irish Sea are low. However, without data for total mercury concentrations it is impossible to obtain an overall view of mercury distributions.

Regarding Cd(II), Pb(II) and Cu(II) concentrations in Cardigan Bay, it appears that Cd(II) and Pb(II) levels are within the normal range for coastal seawater. Copper concentrations are higher than the typical coastal values. The concentrations may be related to leaching and weathering processes, in the nearby mountains, in which released metals are transported to the bay by the numerous freshwater inputs.

Dissolved metal levels in Liverpool Bay probably arose from dumping activities and direct coastal discharges. Without

knowledge of the bound metal fractions (released by UV irradiation) it is not possible to ascertain the impact the dumping activities are having on Liverpool Bay. Future studies should include vertical profile examinations of the waters over the various dumping grounds. This would allow a fuller evaluation of the impact, if any, that these dumping grounds have on metal ion levels in Liverpool Bay.

Subsequent studies should choose the same stations as those in this study to enable the development of a data bank on metal distributions in the Irish Sea. In addition, some stations should also be located in the central Irish Sea as no data is available on metal ion concentrations in this area.

References

1. H.W. Nurnberg, *Fresenius Z. Anal. Chem.*, 316, 557 (1983).
2. E.S. Nielsen and S. Wium-Andersen, *Mar. Biology*, 6, 93 (1970).
3. C.A.M. King, Introduction to Physical and Biological Oceanography (E. Arnold, London, 1975), p. 304.
4. L. Mart, *Talanta*, 29, 1035 (1982).
5. T.R.S. Wilson, Marine Electrochemistry, edited by M. Whitfield and D. Jagner (J. Wiley, Chichester, 1981), p. 151.
6. K. Grasshoff, Methods of Seawater Analysis, 2<sup>nd</sup> edition, edited by K. Grasshoff, M. Ehrhardt and K. Kremling (Verlag Chemie, Weinheim, 1983), Chap. 3.
7. L.A. Murray, M.G. Norton, R.S. Nunny and M.S. Rolfe, The field assessment of effects of dumping wastes at sea: 7 Sewage sludge and industrial waste disposal in the Bristol Channel, *Fish. Res. Tech. Rep.*, No. 59, MAFF Direct. Fish. Res., Lowestoft, 1980.
8. P. Hamilton, *Geophys. J.R. Astr. Soc.*, 32, 409 (1973).
9. M.G. Norton, A. Franklin, S.M. Rowlatt, R.S. Nunny and M.S. Rolfe, The field assessment of effects of dumping wastes at sea: 12 The disposal of sewage

- sludge, industrial wastes and dredged spoils in Liverpool Bay, Fish. Res. Tech. Rep., No. 76, MAFF Direct. Fish. Res., Lowestoft, 1984.
10. D.I. Williamson, Bull. Mar. Ecol., 4, 87 (1956).
  11. M.A. Khan and D.I. Williamson, J. Exp. Mar. Biol. Ecol., 5, 285 (1970).
  12. J.W. Ramster and H.W. Hill, Nature, 224, 59 (1969).
  13. J.W. Ramster, Out of Sight, Out of Mind, Appendix 6, Volume 2 (Her Majesty's Stationary Office, London, 1972), pp. 55-79.
  14. N.S. Heaps and J.E. Jones, J.R. Astr. Soc., 51, 393 (1977).
  15. P. Foster, K.B. Pugh and D.T.E. Hunt, Estuar. and Coastal Mar. Sci., 7, 71 (1978).
  16. K.F. Bowden, Chemical Oceanography, 2<sup>nd</sup> Edition, edited by J.P. Riley and G. Skirrow (Academic Press, London, 1975), Chap. 1.
  17. P. Foster and D.T.E. Hunt, Nature, 265, 129 (1977).
  18. K.R. Dyer, Estuaries : A Physical Introduction (J. Wiley, London, 1973), pp. 51-54.
  19. D.R. Turner, S.G. Robinson and M. Whitfield, Anal. Chem., 56, 2387 (1984).
  20. L. Tipping, Proc. Conf., Recent Applications of Analytical Voltammetry in Industrial and Environmental Chemistry, (N.I.H.E., Dublin, 1984), p. 5.

21. A. Mizuike, Enrichment Techniques for Inorganic Trace Analysis (Springer-Verlag Berlin, Heidelberg, 1983), Chap. 3.
22. K. Grasshoff, Methods of Seawater Analysis, 2<sup>nd</sup> Edition, edited by K. Grasshoff, M. Ehrhardt and K. Kremling (Verlag Chemie, Weinheim, 1983), Chap. 1.
23. L. Mart, *Fresenius Z. Anal. Chem.*, 296, 350 (1979).
24. B. Schaule and C.C. Patterson, Lead in the Marine Environment, edited by M. Branica and Z. Konrad (Pergamon Press, Oxford, 1980), pp. 31-43.
25. L. Mart, *Fresenius Z. Anal. Chem.*, 299, 97 (1979).
26. M.H. Gitlitz, *J. Coatings Technol.*, 53, 46 (1981).
27. D. Harper, private communication.
28. G.E. Batley and D. Gardner, *Water Research*, 11, 745 (1977).
29. H.W. Nurnberg, *Anal. Chem. Acta*, 164, 1 (1984).
30. H.W. Nurnberg, *Sci. Total Environment*, 12, 35 (1979).
31. J. Lecomte, P. Mericam, A. Astruc and M. Astruc, *Anal. Chem.*, 53, 2372 (1981).
32. D.E. Robertson, *Anal. Chem.*, 40, 1067 (1968).
33. J.M. Lo, C.M. Wai, *Anal. Chem.*, 47, 1869 (1975).
34. W.R. Hatch and W.L. Ott, *Anal. Chem.*, 40, 2085 (1968).
35. R.C. Hutton and B. Preston, *Analyst*, 105, 981 (1980).

36. P. Freimann and D. Schmidt, *Fresenius Z. Anal. Chem.*, 313, 200 (1982).
37. B. Welz, M. Melcher, H.W. Sinemus and D. Maier, *At. Spectrosc.*, 5, 37 (1984).
38. M.P. Bertenshaw and K. Wagstaff, *Analyst*, 107, 664 (1982).
39. S. Blake, Method for the determination of low concentrations of mercury in fresh and saline waters. Technical Report TR 229, Water Research Centre, August, 1985, 28pp.
40. B.J. Farey, L.A. Nelson and M.G. Rolph, *Analyst*, 103, 656 (1978).
41. L. Sipos, P. Valenta, H.W. Nurnberg and M. Branica, *J. Electroanal. Chem.*, 77, 263 (1977).
42. T.M. Florence, *J. Electroanal. Chem.*, 168, 207 (1984).
43. M.I. Abdullah, B. Reusch Berg and R. Klimek, *Anal. Chim. Acta*, 84, 307, (1976).
44. R.K. Skogerboe, S.A. Wilson and J.G. Osteryoung, *Anal. Chem.*, 52, 1960 (1980).
45. M. Stoeppler, P. Valenta and H.W. Nurnberg, *Fresenius Z. Anal. Chem.*, 297, 22 (1979).
46. P.G. Brewer, *Chemical Oceanography*, 2<sup>nd</sup> Edition, edited by J.P. Riley and G. Skirrow (Academic Press, London, 1975), pp. 415-496.
47. T.M. Florence and G.E. Batley, *Crit. Rev. Anal.*

- Chem., 9, 219 (1980).
48. R.F.C. Mantoura, A. Dickson and J.P. Riley, *Estuar. Coast. Mar. Sci.*, 6, 387 (1978).
49. J.C.S. Lu and K.Y. Chen, *Environ. Sci. Technol.*, 11, 174 (1977).
50. H.W. Nurnberg, *Anal. Chim. Acta*, 164, 1 (1984).
51. E.Y. Nieman, L.G. Petrova, V.I. Ignatov and G.M. Dolgoplova, *Anal. Chim. Acta*, 113, 277 (1980).
52. M.I. Abdullah, L.G. Royle and A.W. Morris, *Nature*, 235, 158 (1972).
53. L. Mart, H.W. Nurnberg, P. Valenta and M. Stoepler, *Thalassia Jugoslavica*, 14, 171 (1978).
54. A. Baric and M. Branica, *J. Polarog. Soc.*, 13, 4 (1967).
55. H.W. Nurnberg, Trace Element Speciation in Surface Waters and its Ecological Implications, edited by G.G. Leppard (Plenum Publishing Corporation, New York, 1983), pp. 211-230.
56. L. Mart, H.W. Nurnberg and H. Rutzel, *Fresenius Z. Anal. Chem.*, 317, 201 (1984).
57. L. Musani, P. Valenta, H.W. Nurnberg, Z. Konrad and M. Branica, *Estuar. Coast. Mar. Sci.*, 11, 639 (1980).



Appendix A

Log of events of Clione cruise from  
December 7 - 18<sup>th</sup>, 1984

7<sup>th</sup> December 1984

Load Equipment

8<sup>th</sup> December

Depart from Barry at 7.30 hours  
Arrive at Station 1 at 10.02 hours  
Locality: 51° 27.2'N 2° 59.7'W  
Gear: Azlon Water Sampler

Arrive at Station 2 at 11.01 hours  
Locality: 51° 21.3'N 3° 15.2'W  
Gear: Azlon Water Sampler

Arrive at Station 3 at 12.51 hours  
Locality: 51° 24.2'N 3° 44.9'W  
Gear: Azlon Water Sampler

Arrive at Station 4 at 13.50 hours  
Locality: 51° 26.6'N 3° 57.1'W  
Gear: Azlon Water Sampler

Arrive at Station 5 at 14.23 hours  
Locality: 51° 31.4'N 3° 56.0'W  
Gear: Azlon Water Sampler

Arrive at Station 6 at 16.55 hours  
Locality: 51° 28.0'N 4° 25.5'W  
Gear: Azlon Water Sampler

Arrive at Station 7 at 20.03 hours  
Locality: 51° 33.0'N 5° 13.5'W  
Gear: Azlon Water Sampler

9<sup>th</sup> December

Arrive at Station 8 at 8.30 hours  
Locality: 51° 20.2'N 6° 15.0'N  
Gear: Granton Trawl

Arrive at Station 9 at 11.02 hours  
 Locality: 51° 15.1'N 6° 19.8'W  
 Gear: Granton Trawl

Arrive at Station 10 at 14.31 hours  
 Locality: 51° 24.3'N 6° 13.7'W  
 Gear: Azlon Water Sampler  
 Granton Trawl

Arrive at Station 11 at 17.45 hours  
 Locality: 51° 45.6'N 5° 48.4'W  
 Gear: Azlon Water Sampler

Arrive at Station 12 at 19.47 hours  
 Locality: 52° 01.9'N 5° 23.0'W  
 Gear: Azlon Water Sampler

10<sup>th</sup> December

Arrive at Station 13 at 8.30 hours  
 Locality: 52° 18.6'N 4° 17.1'W  
 Gear: Azlon Water Sampler  
 Granton Trawl

Arrive at Station 14 at 11.29 hours  
 Locality: 52° 21.7'N 4° 15.2'W  
 Gear: Azlon Water Sampler  
 Granton Trawl

Arrive at Station 15 at 16.41 hours  
 Locality: 52° 42.0'N 4° 35.2'W  
 Gear: Azlon Water Sampler  
 Granton Trawl

Arrive at Station 16 at 18.53 hours

Locality:  $52^{\circ} 43.1'N 4^{\circ} 55.1'W$

Gear: Azlon Water Sampler

Arrive at Station 17 at 20.46 hours

Locality:  $53^{\circ} 03.9'N 4^{\circ} 51.6'W$

Gear: Azlon Water Sampler

11<sup>th</sup> December

Arrive at Station 18 at 7.46 hours

Locality:  $53^{\circ} 25.0'N 3^{\circ} 59.9'W$

Gear: Azlon Water Sampler

Arrive at Station 19 at 9.41 hours

Locality:  $53^{\circ} 27.1'N 3^{\circ} 39.5'W$

Gear: Azlon Water Sampler

Arrive at Station 20 at 11.00 hours

Locality:  $53^{\circ} 27.1'N 3^{\circ} 28.9'W$

Gear: Azlon Water Sampler

Arrive at Station 21 at 12.35 hours

Locality:  $53^{\circ} 28.4'N 3^{\circ} 15.1'W$

Gear: Azlon Water Sampler

Arrive at Station 22 at 14.00 hours

Locality:  $53^{\circ} 28.6'N 3^{\circ} 12.5'W$

Gear: Azlon Water Sampler

Arrive at Station 23 at 15.25 hours

Locality:  $53^{\circ} 31.0'N 3^{\circ} 17.4'W$

Gear: Azlon Water Sampler

Arrive at Station 24 at 16.16 hours  
Locality: 53° 30.1'N 3° 31.6'W  
Gear: Azlon Water Sampler

Arrive at Station 25 at 16.56 hours  
Locality: 53° 31.3'N 3° 31.3'W  
Gear: Azlon Water Sampler

Arrive at Station 26 at 18.00 hours  
Locality: 53° 31.9'N 3° 35.7'W  
Gear: Azlon Water Sampler

Arrive at Station 27 at 18.31 hours  
Locality: 53° 34.2'N 3° 35.4'W  
Gear: Azlon Water Sampler

12<sup>th</sup> December

Arrive at Station 28 at 7.57 hours  
Locality: 53° 33.8'N 3° 22.0'W  
Gear: Azlon Water Sampler

Arrive at Station 29 at 8.40 hours  
Locality: 53° 33.1'N 3° 17.3'W  
Gear: Azlon Water Sampler

Arrive at Station 30 at 8.59 hours  
Locality: 53° 34.2'N 3° 17.1'W  
Gear: Azlon Water Sampler

Arrive at Station 31 at 9.38 hours

Locality: 53° 35.1'N 3° 13.9'W

Gear: Azlon Water Sampler

Arrive at Station 32 at 10.40 hours

Locality: 53° 36.8'N 3° 19.2'W

Gear: Azlon Water Sampler

Arrive at Station 33 at 11.39 hours

Locality: 53° 36.9'N 3° 28.8'W

Gear: Azlon Water Sampler

Arrive at Station 34 at 12.33 hours

Locality: 53° 37.6'N 3° 42.2'W

Gear: Azlon Water Sampler

Arrive at Station 35 at 14.28 hours

Locality: 53° 50.6'N 4° 00.4'W

Gear: Azlon Water Sampler

Go-Flo Sampler

Arrive at Station 36 at 15.52 hours

Locality: 53° 58.2'N 4° 10.6'W

Gear: Azlon Water Sampler

Arrive at Station 37 at 17.08 hours

Locality: 54° 07.9'N 4° 23.6'W

Gear: Azlon Water Sampler

Arrive at Station 38 at 18.33 hours  
 Locality: 54° 18.4'N 4° 14.2'W  
 Gear: Azlon Water Sampler

13<sup>th</sup> December

Arrive at Station 39 at 7.48 hours  
 Locality: 54° 29.3'N 3° 42.3'W  
 Gear: Azlon Water Sampler

Arrive at Station 40 at 9.15 hours  
 Locality: 54° 23.8'N 3° 58.0'W  
 Gear: Azlon Water Sampler

Arrive at Station 41 at 10.59 hours  
 Locality: 54° 39.1'N 3° 53.4'W  
 Gear: Azlon Water Sampler

Arrive at Station 42 at 13.29 hours  
 Locality: 54° 36.4'N 4° 26.8'W  
 Gear: Azlon Water Sampler

Arrive at Station 43 at 15.38 hours  
 Locality: 54° 35.9'N 5° 04.0'W  
 Gear: Azlon Water Sampler  
 Go-Flo Sampler

14<sup>th</sup> December

Arrive at Station 44 at 6.59 hours  
 Locality: 54° 31.6'N 5° 09.3'W  
 Gear: Azlon Water Sampler  
 Go-Flo Sampler

Arrive at Station 45 at 10.41 hours

Locality:  $54^{\circ} 26.6'N$   $5^{\circ} 21.5'W$

Gear: Azlon Water Sampler

Go-Flo Sampler

Arrive at Station 46 at 12.50 hours

Locality:  $54^{\circ} 14.2'N$   $5^{\circ} 32.5'W$

Gear: Azlon Water Sampler

Arrive at Station 47 at 13.54 hours

Locality:  $54^{\circ} 07.6'N$   $5^{\circ} 42.1'W$

Gear: Azlon Water Sampler

Arrive at Station 48 at 15.54 hours

Locality:  $53^{\circ} 52.6'N$   $6^{\circ} 02.8'W$

Gear: Azlon Water Sampler

Arrive at Station 49 at 17.59 hours

Locality:  $53^{\circ} 33.2'N$   $6^{\circ} 00.0'W$

Gear: Azlon Water Sampler

15<sup>th</sup> December

Arrive at Station 50 at 7.57 hours

Locality:  $53^{\circ} 12.0'N$   $5^{\circ} 56.5'W$

Gear: Azlon Water Sampler

Arrive at Station 51 at 10.00 hours

Locality:  $52^{\circ} 56.6'N$   $5^{\circ} 53.1'W$

Gear: Azlon Water Sampler



Arrive at Station 52 at 12.37 hours  
Locality: 52° 35.9'N 6° 06.8'W  
Gear: Azlon Water Sampler

Arrive at Station 53 at 15.28 hours  
Locality: 52° 11.3'N 6° 08.6'W  
Gear: Azlon Water Sampler

Arrive at Station 54 at 17.39 hours  
Locality: 51° 58.0'N 5° 57.0'W  
Gear: Azlon Water Sampler  
Go-Flo Sampler

18<sup>th</sup> December

Arrive at Lowestoft at 5.20 hours

CHAPTER 4

VOLTAMMETRIC DETERMINATION OF INORGANIC  
LEAD AND DIMETHYL- AND TRIMETHYL-LEAD  
SPECIES IN MIXTURES

#### 4.1. Introduction

The presence of lead and its alkyl derivatives in the environment is well documented {1-3}. One of the principal sources of lead is exhaust emissions from cars. A large proportion of the lead emitted into the atmosphere from this source is in the form of inorganic salts. In addition, a small fraction escapes unchanged, existing either as tetramethyllead or tetraethyllead. Once released into the environment these tetraalkyllead compounds may undergo photolytic dissociation {3} to intermediary alkyl species and also inorganic lead {4}. A serious consequence of this dissociation process is the possible dissolution of dialkyl and trialkyl-lead species, as well as inorganic lead, in aquatic ecosystems. On entry into such systems these alkyl species can cause deleterious effects in both freshwater and marine biota {5}. The toxic effects of the alkyllead compounds have been attributed to the trialkyl species{6}. In general, alkyllead species are more toxic than inorganic lead.

Obviously, analytical procedures are required to quantify these various lead species. Methods for the determination of tetraalkylleads are well established {7-9}, but fewer methods exist for the determination of dialkyl-and trialkyl-lead species. Some of the existing

methods are based on complexation and spectrophotometric determination {10-12}, but are not applicable to trace metal studies owing to their lack of sensitivity. More sensitive methods involving gas chromatography with flame ionization detection {13} and electron capture detection {14} are capable of determining alkyllead compounds at low  $\mu\text{g}/\text{l}$  levels. Gas chromatography has also been interfaced with atomic absorption spectrometry and used for the detection of alkylleads in water samples {15,16}. One of the problems with some of these gas chromatographic procedures is that prior derivatisation, e.g., butylation or phenylation, is necessary.

Electroanalytical methods have been used extensively in speciation studies of metals {17,18}. In the case of lead there have been some publications on the speciation of organic and inorganic species {19,20}. The possibility of using polarographic and voltammetric techniques to separate mixtures of inorganic, dialkyl- and trialkyl-lead was explored.

#### 4.2. Experimental Section

##### 4.2.1. Reagents

Dimethyllead dichloride and trimethyllead chloride were supplied by Associated Octel Co. Ltd., England. These reagents were of analytical grade and were used without further purification. All other reagents used were of analytical grade. Millipore-grade water was used in the preparation of stock solutions of the various lead species.

#### 4.2.2. Preparation of Standard Solutions

Individual standard solutions (each  $10^{-2}$  M concentration) of the lead species were prepared using Millipore-grade water. These solutions were stored in glass containers because organolead compounds strongly adsorb on the walls of plastic containers.

Standard solutions in the range  $10^{-4}$  to  $10^{-7}$  M were prepared by taking aliquots of the  $10^{-2}$  M solution and making them up to final volume in either 100% buffer or buffer/methanol(50/50). These standard solutions were freshly prepared each day.

All standard solutions were stored in the dark in a refrigerator. This inhibited degradation of the organolead species.

#### 4.2.3. Preparation of Buffers

A stock Britton-Robinson (BR) buffer solution (pH 1.9) was prepared from a mixture of 0.04M boric acid, 0.04M glacial acetic acid and 0.04M orthophosphoric acid. From this solution, buffer solutions of varying pH were prepared by the addition of 0.2M sodium hydroxide.

An acetate buffer, composed of 0.2M glacial acetic acid and 0.2M sodium acetate, was also used. Buffer solutions over the range pH 3.3 to 5.0 were prepared by adjusting the pH of the aqueous acetic acid solution with sodium acetate.

#### 4.2.4. Glassware Washing

All glassware used in the preparation and storage of standard solutions of lead species was initially washed with a detergent solution. Subsequently, it was soaked for twelve hours in 2M nitric acid. Finally, all glassware was washed with copious amounts of Millipore-grade water.

Periodically, the glassware was soaked in chromic acid. Such a procedure was necessary to remove the "greasy" film which built up on the inner surface over a period of several months. Chromic acid was prepared by adding 800ml concentrated sulphuric acid to 92g sodium dichromate in 458ml water. Glassware was soaked for twelve

hours in freshly prepared chromic acid. After the acid wash, glassware was twice soaked in  $3.6 \times 10^{-2} \text{M}$  ethylenediaminetetraacetic acid (EDTA) solution for several hours and finally rinsed at least ten times with Millipore-grade water.

#### 4.2.5. Instrumentation

DC polarographic studies were carried out using a Metrohm E505 polarographic analyser and a Metrohm 626 chart recorder. The polarographic cell contained a dropping mercury working electrode, a platinum wire counter electrode and a saturated calomel electrode (SCE) as the reference electrode. Solutions were degassed for 15 min with oxygen-free nitrogen prior to recording DC polarograms.

Both differential pulse polarographic and differential pulse anodic stripping voltammetric studies were performed using an EG+G Princeton Applied Corp. (PARC) Model 174A polarographic analyser. This was used in conjunction with a EG+G PARC Model 303 static mercury drop electrode (SMDE). The cell comprised of a dropping mercury working electrode, a platinum wire counter electrode and a Ag/AgCl (3M KCl) reference electrode. All DPASV studies were performed at a hanging mercury drop electrode (HMDE)

using an EG+G Model 305 stirrer. Solutions were purged with oxygen-free nitrogen for 4 min prior to polarographic and voltammetric investigation.

Cyclic voltammograms were obtained using an EG+G PARC Model 174A polarographic analyser and an EG+G PARC Model 175 universal analyser. All voltammograms were recorded at a HMDE using a Houston X-Y chart recorder. Because of the slow response of the recorder, measurements at scan rates above 100 mV/sec were not possible.

All pH measurements were made using a Philips PW 9410 digital pH meter with an Orion combination pH electrode.

#### 4.3. Results and Discussion

##### 4.3.1. General Polarographic and Voltammetric Behaviour of at the Lead Species

A study of the polarographic and voltammetric behaviour of the three lead species was undertaken to ascertain the factors which affect their reduction in aqueous media.



#### 4.3.1.1. Inorganic Lead

##### 4.3.1.1.1. DC Polarographic Studies in BR Buffers

##### pH 2.0 to 12.0

Given the solubility difficulties associated with many lead salts in aqueous media, lead nitrate was chosen in this study as it is completely soluble in aqueous solutions, and does not require the addition of acid for dissolution. Initial DC polarographic studies of inorganic lead (subsequently referred to as Pb(II)) in BR buffer/methanol (50/50) were undertaken to ascertain the pH dependence of parameters such as half-wave potential and wave height.

Between pH 2.0 and 7.0 the half-wave potential of Pb(II) is pH dependent. It moves towards more negative potentials with increasing pH (Fig. 4.1), whereas the limiting current is unchanged. The reversibility of the reduction was determined at pH 3.0, 5.0 and 7.0 from graphs of  $\log(1/i_d - 1)$  versus potential (E). All graphs were linear with slopes of 39, 41 and 42 mV, respectively. From these slopes the respective transfer coefficients were calculated as 0.75, 0.71 and 0.70 for an irreversible {2e} two-electron transfer.

Examination of the limiting current at three pH values between 2.0 and 7.0 showed that the current varied

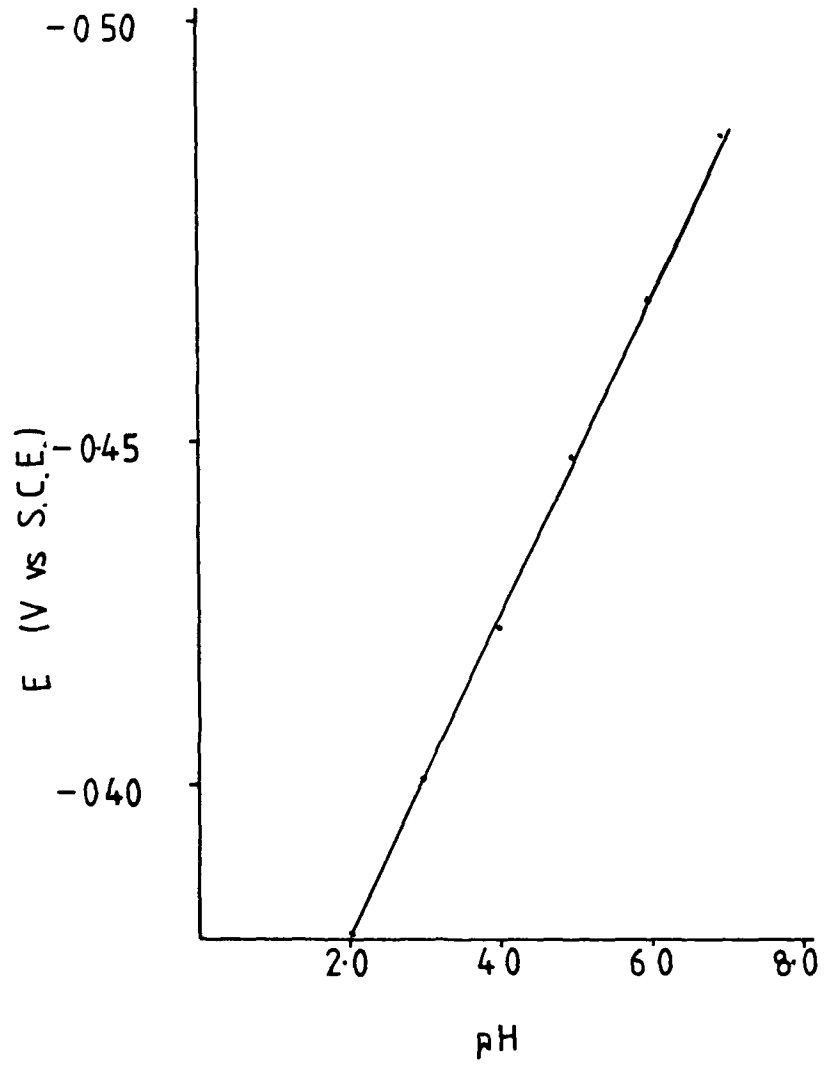
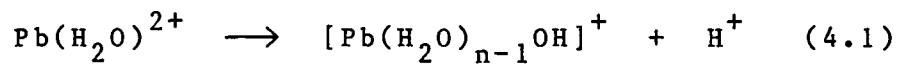


Fig. 4.1. Half-wave potential as a function of pH for  $0.98 \times 10^{-4}$  M Pb(II) in BR buffer/methanol (50/50).

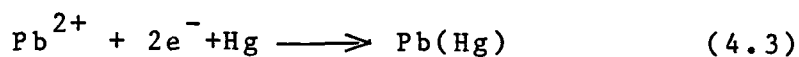
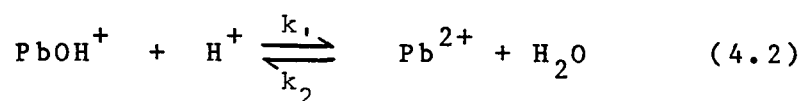
linearly with the square root of the mercury column height, indicating that it was diffusion-controlled {22}.

The shift of the half-wave potential to more negative values increasing pH is indicative of a change in the state of Pb(II) in solution. Hydrolysis of Pb(II) leading to the formation of a monohydroxy Pb(II) species occurs in mildly acidic solutions {23,24}.

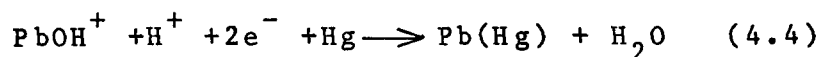


Therefore, the polarographic wave observed is due to reduction of the monohydroxy Pb(II) species.

Based on these observations, the following mechanisms are postulated to explain the reduction of Pb(II) between pH 2.0 and 7.0. Reduction of the monohydroxy species has been shown to involve a single proton {25}. In the first of the postulated mechanisms, proton transfer precedes electron transfer. (For the purposes of simplicity  $[\text{Pb}(\text{H}_2\text{O})_{n-1}\text{OH}]^+$  is written as  $\text{PbOH}^+$ ).



Alternatively, proton transfer may be considered to occur during the electron transfer step.



Any possibility of proton transfer subsequent to electron transfer can be dismissed, because in such situations the half-wave potential is pH independent, however, this was not observed.

If the mechanism involving antecedent proton transfer is considered, then the total process is described as a chemical electrochemical (CE) process. In such processes, the limiting current is usually kinetically-controlled by the preceding chemical reaction. Kinetic currents involving proton transfer usually decrease with increasing pH because the rate of the preceding chemical reaction is pH-dependent. However, in this study the limiting current remained pH-independent and was diffusion rather than kinetically-controlled. This would suggest that the first postulated mechanism (shown in equations 4.2 and 4.3) is not applicable. On the other-hand, if the rate of the forward reaction ( $k_1$ ) in equation 4.2 is so fast that the rate of transformation of  $\text{PbOH}^+$  to  $\text{Pb}^{2+}$  occurs at a diffusion-controlled rate, then the limiting current is purely diffusion-controlled. This

could indeed be the situation. Confirmation of this possible mechanism would necessitate further investigations by cyclic voltammetry to establish the possibility of a CE mechanism {26}.

If, as suggested by some workers {25} that  $\text{Pb(OH)}^+$  is electroactive, then the mechanism postulated in equation 4.4 may indeed describe the electrode process at the DME.

Polarographic studies between pH 7.5 and 11.5 were impossible due to the formation of insoluble  $\text{Pb(OH)}_2$ . No reduction wave was detected for Pb(II) at concentrations down to  $10^{-5}\text{M}$ , indicating that  $\text{Pb(OH)}_2$  is electroinactive under the present experimental conditions.

A single reduction wave was recorded for Pb(II) at pH 12.0, which represents an irreversible two-electron process. The limiting current was found to be diffusion-controlled. The formation of  $\text{Pb(OH)}_3$  in alkaline solution (pH > 11.5) {24} suggests that the electrode process represents reduction of this anionic hydroxy complex.

#### 4.3.1.1.2. DC Polarographic Studies in Acetate

##### Buffer pH 3.3

Although determination of Pb(II) in BR buffer is possible between pH 2.0 and 7.0, it was decided to use a single anion buffer system such as acetate buffer to decrease the possibility of interactions between Pb(II) and other anions in the buffer.

DC polarographic studies were undertaken in acetate buffer pH 3.3/methanol (50/50). A single reduction wave was found for Pb(II). The slope of a graph of  $\log (1/i_d - i)$  versus  $E$  was found to be 38mV, which corresponds to an irreversible two-electron transfer. From the linear dependence of the limiting current on the square root of the mercury column height, a diffusion-controlled current was inferred.

Comparison of the limiting current for Pb(II) in BR buffer pH 3.3 and acetate buffer pH 3.3 revealed an increased current response in the latter buffer (Table 4.1). The reduced response of Pb(II) in BR buffer is possibly due to complexation by either the borate or phosphate anions in the buffer. Changes in the diffusion coefficient ( $D$ ) can occur on complexation;  $D$  is different when the hydrated sheath is removed.

The increased response in acetate buffer, indicates that it is more suitable than BR buffer for

Concentration  M X 10 <sup>-4</sup>	Limiting Current (μA)	
	Acetate Buffer pH 3.3	BR Buffer pH 3.3
0.5	0.44	0.35
1.0	0.91	0.73
2.0	1.80	1.41
4.0	3.80	2.86
7.0	6.50	4.96
9.0	8.20	6.65
10.0	9.00	7.10

Table 4.1. A comparison of DC polarographic limiting currents for various concentrations of  $\text{Pb}(\text{NO}_3)_2$  measured in two different buffers at pH 3.3 containing 50% methanol.

quantitative determinations of Pb(II).

4.3.1.1.3. Differential Pulse Polarographic Study to Evaluate the Effects of Methanol on the Response of Pb(II)

Reduction of Pb(II) in acetate buffer pH 3.3/methanol (50/50) was characterised by a single reduction peak, which was linearly dependent on concentration between  $10^{-5}$  and  $10^{-3}$  M.

The effect of methanol concentration on peak currents and peak potentials was examined. A reduction in the methanol concentration in solution caused minimal changes in peak potential values; however, peak current values increased as the methanol concentration was reduced (Table 4.2). This behaviour is unlikely to result from changes in the solution viscosity. Methanol has a lower viscosity than water; therefore, increasing the methanol concentration in solution would lower the overall viscosity. This decrease in viscosity should cause an increase in peak current because diffusion is more easily facilitated {27}. However, the opposite effect was observed in this study. Alternatively, the decrease of peak current may be attributed to a reduction of the dielectric constant of the electrolyte as the methanol concentration is increased.



Methanol Concentration % (V/V)	$E_p$ (V vs. Ag/AgCl)	$i_p$ ( $\mu$ A)
0	- 0.380	8.70
10	- 0.380	8.18
20	- 0.382	7.40
30	- 0.382	7.07
40	- 0.382	6.50
50	- 0.382	6.06
60	- 0.385	5.59
70	- 0.395	5.19
80	- 0.400	4.64

Table 4.2. Effects of solvent composition on the peak potential ( $E_p$ ) and peak current ( $i_p$ ) of  $1 \times 10^{-4}$  M  $Pb(NO_3)_2$  in acetate buffer pH 3.3.

#### 4.3.1.2. Dimethyllead Dichloride

##### 4.3.1.2.1. DC Polarographic Studies in Acetate

##### Buffer pH 3.3

Dimethyllead dichloride (subsequently referred to as  $\text{Me}_2\text{Pb}^{2+}$ ) gives rise to four waves in acetate buffer pH 3.3/methanol (50/50). A typical DC polarogram showing the four waves is illustrated in Fig. 4.2.

Characterisation of wave 1 proved impossible. In particular, the dependence of the limiting current on the height of the mercury column could not be properly established. A similar problem was encountered with wave 3. Therefore, only some qualitative features of these two waves are discussed.

Examination of the nature of the limiting current revealed that both waves 2 and 4 varied linearly with the square root of the mercury column height, indicating that both processes are diffusion-controlled. Further evidence for the diffusion-controlled behaviour of wave 2 comes from the dependence of its limiting current with concentration. The height of wave 2 was found to linearly increase with concentration over the concentration range studied. In contrast, the height of wave 4 increased slowly with

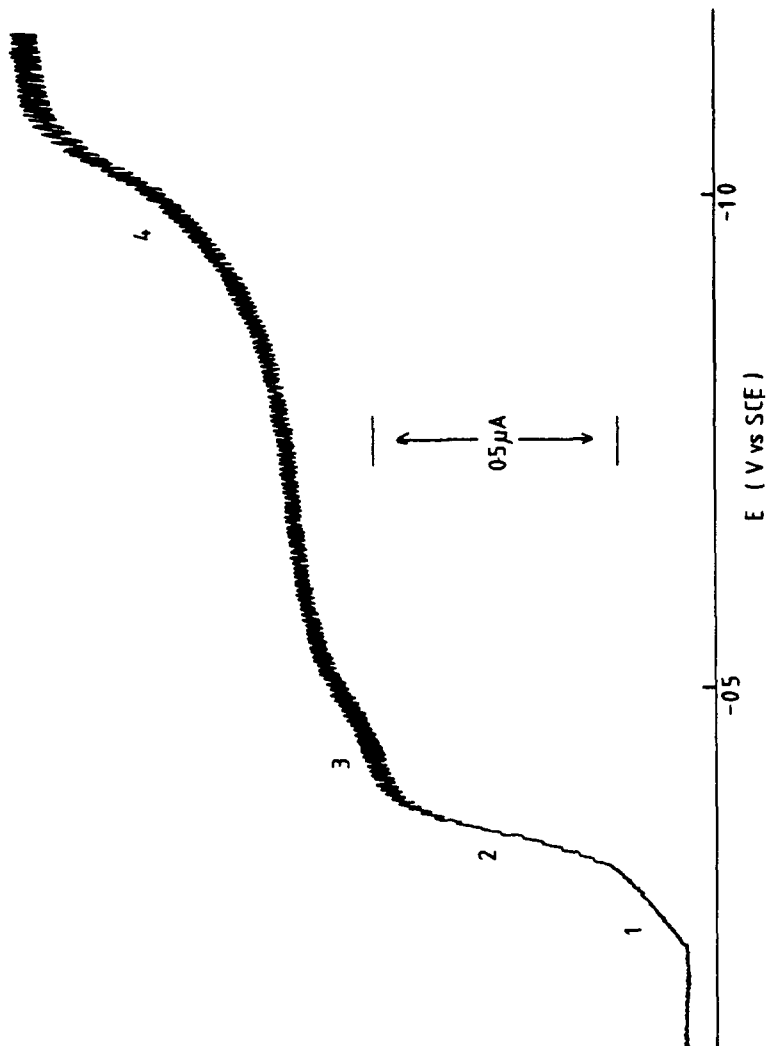


Fig. 4.2. DC polarogram of  $0.97 \times 10^{-4} \text{ M}$   
 $\text{Me}_2\text{PbCl}_2$  in acetate buffer pH 3.3/  
methanol (50/50),

increasing concentration of  $\text{Me}_2\text{Pb}^{2+}$  (Fig. 4.3). Because of the linear dependence of wave 2 on concentration, it can therefore be used for DC analytical determinations. However, wave 4 appears to be unsuitable for analytical purposes as it is relatively independent of concentration.

A graph of  $\log (i/i_d - 1)$  versus  $E$  for wave 2 was found to be linear with a slope of 46 mV indicating that the process giving rise to this wave is irreversible. From the slope of this graph the transfer coefficient was calculated to be 0.65 for a two-electron process. Wave 4 was also found to be irreversible in nature and probably represents a two-electron reduction step. Ideally, controlled potential electrolysis experiments would need to be undertaken to confirm the number of electrons involved with waves 2 and 4. However, in the present study this was not possible. Further evidence to verify the irreversible nature of waves 2 and 4 comes from the dependence of their half-wave potentials on the height of the mercury column (Table 4.3). Such dependence is indicative of an irreversible electrode process, unlike a reversible process where the half-wave potential is independent of drop time, flow-rate of mercury and mercury column height {28}.

#### 4.3.1.2.2. DC Polarographic Studies in BR Buffers

pH 2.0 to 12.0

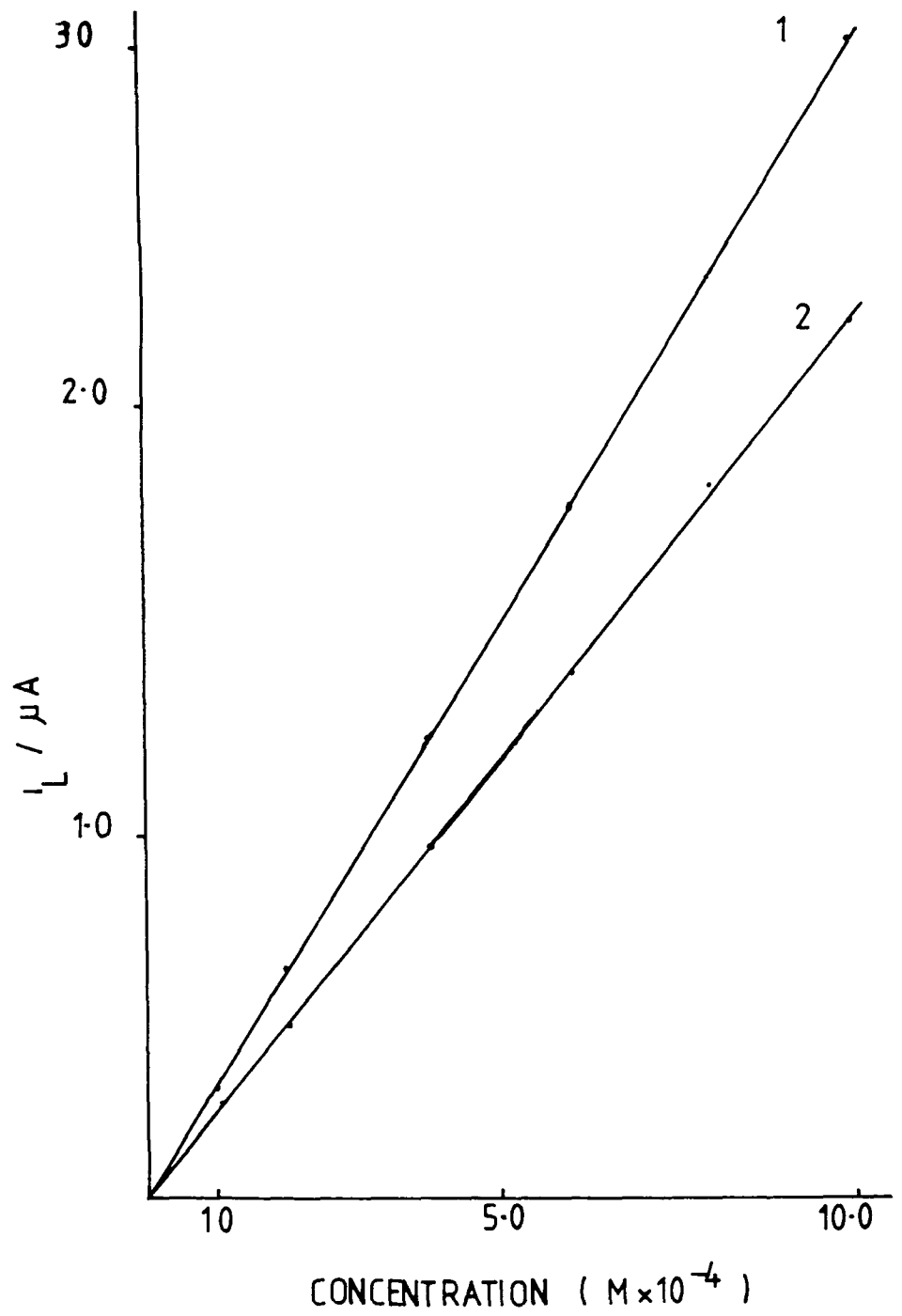


Fig. 4.3. Dependence of the DC limiting current ( $i_L$ ) on the concentration of  $\text{Me}_2\text{PbCl}_2$ .  
(1) Wave 2; (2) Wave 4

Mercury Column Height (cm)	Half-Wave Potential(V vs. Ag/AgCl)	
	Wave 2	Wave 4
40	- 0.38	- 1.09
44	- 0.385	- 1.095
48	- 0.39	- 1.095
56	- 0.395	- 1.10
64	- 0.40	- 1.15
72	- 0.41	- 1.15
80	- 0.42	- 1.20

Table 4.3. Dependence of the half-wave potentials of waves 2 and 4 for  $10^{-4} \text{M Me}_2\text{Pb}^{2+}$  on mercury column height.

The pH dependence of the reduction waves for  $\text{Me}_2\text{Pb}^{2+}$  were studied in BR buffer/methanol (50/50) from pH 2.0 to 12.0. Between pH 2.0 and 6.5,  $\text{Me}_2\text{Pb}^{2+}$  gave rise to four waves; polarograms were similar to those observed in acetate buffer pH 3.3. However, in solutions with pH values in the range  $6.5 > \text{pH} \leq 9.0$  only three waves were observed. Wave 3 as labelled in Fig. 4.2, was absent. In solutions with  $\text{pH} > 9.5$ , wave 3 was again present.

The relationship between half-wave potential and pH for these waves was also examined. At  $\text{pH} < 4.0$ , only wave 4 displayed any pH-dependence; however, at higher pH values all waves become more negative with increasing pH. Furthermore, the limiting current of wave 4 decreased with increasing pH, although the limiting current for wave 2 remained independent of pH. The pH dependence of wave 4 over the entire pH range is indicative of a proton transfer step coupled to the electron transfer reaction. As the pH increases, the rate of protonation decreases; consequently, the wave height decreases and the half-wave potential moves to more negative values.

#### 4.3.1.2.3. Cyclic Voltammetric Studies in Acetate

##### Buffer pH 3.3

Cyclic voltammetry permits the study of electrode reactions at scan rates far in excess of those possible in DC polarography {29}. In addition, it affords the opportunity of being able to study the anodic as well as the cathodic electrode steps.

A typical cyclic voltammogram of a  $1 \times 10^{-4}$  solution of  $\text{Me}_2\text{Pb}^{2+}$  in acetate buffer pH 3.3/methanol (50/50) is shown in Fig. 4.4. It is seen that there are three cathodic peaks (1c, 2c and 4c) and a single anodic peak (2a). No peak corresponding to wave 3 was seen. At concentrations greater than  $5 \times 10^{-4}$  M, the cyclic voltammogram becomes very complicated, therefore, further examinations were confined to  $10^{-4}$  M.

As seen in Fig. 4.4, the first cathodic peak (1c) is rather broad and ill-defined. Peak 2c shifted to more negative potentials with increasing scan rate; furthermore, the peak current was linearly dependent on the square root of the scan rate. Both observations indicate that peak 2c represents an irreversible electrode process. Similar behaviour was noted for peak 4c, indicating that it is also an irreversible process.

A single peak (2a) observed in the anodic sector. This corresponds to the re-oxidation of peak 2c. No



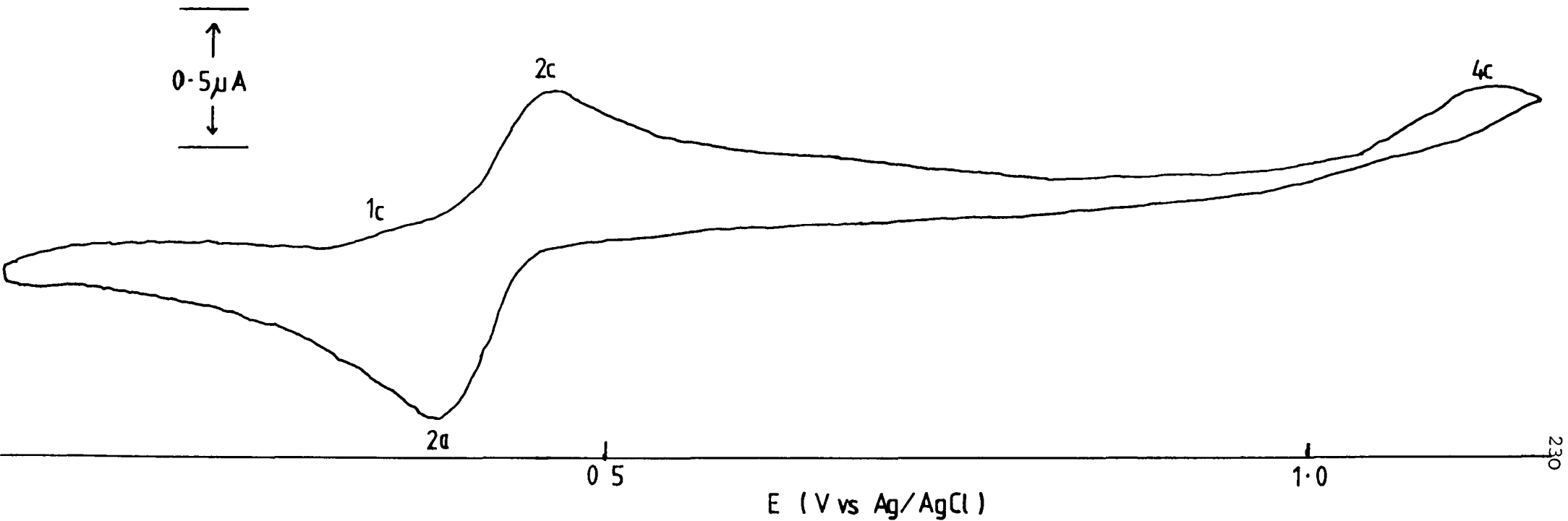


Fig. 4.4. Cyclic voltammogram of  $1 \times 10^{-4}$  M  $\text{Me}_2\text{PbCl}_2$  in acetate buffer pH 3.30/methanol (50/50). Scan rate 10 mV/sec

re-oxidation peak was observed for peak 4c at scan rates up to 100 mV/sec. Higher scan rates could not be used under the present experimental conditions (see Section 4.2.5.). When the cathodic scan was switched prior to the commencement of the electrode process represented by peak 4c, no change in the anodic sector was observed. Anodic peak 2a has the same peak potential value as the anodic peak corresponding to the oxidation of elemental lead. This suggests that elemental lead is a principal product in the reduction of dimethyllead. If other products are generated they must either be electroinactive or undergo subsequent chemical reaction to form elemental lead.

#### 4.3.1.2.4. Differential Pulse Polarographic Studies in Acetate Buffer pH 3.3

Dimethyllead dichloride shows four differential pulse polarographic peaks in acetate buffer pH 3.3/methanol (50/50) (Fig. 4.5). Peak 1 overlapped with peak 2, consequently, measurement of the height of peak 1 was a particularly difficult task. Peak 2 has a similar potential to Pb(II) under the same experimental conditions. Peaks 2 and 4 were found to be linearly dependent on concentration. However, because peak 4 was relatively independent of concentration, it could not be used for analytical determinations. Similar behaviour was observed

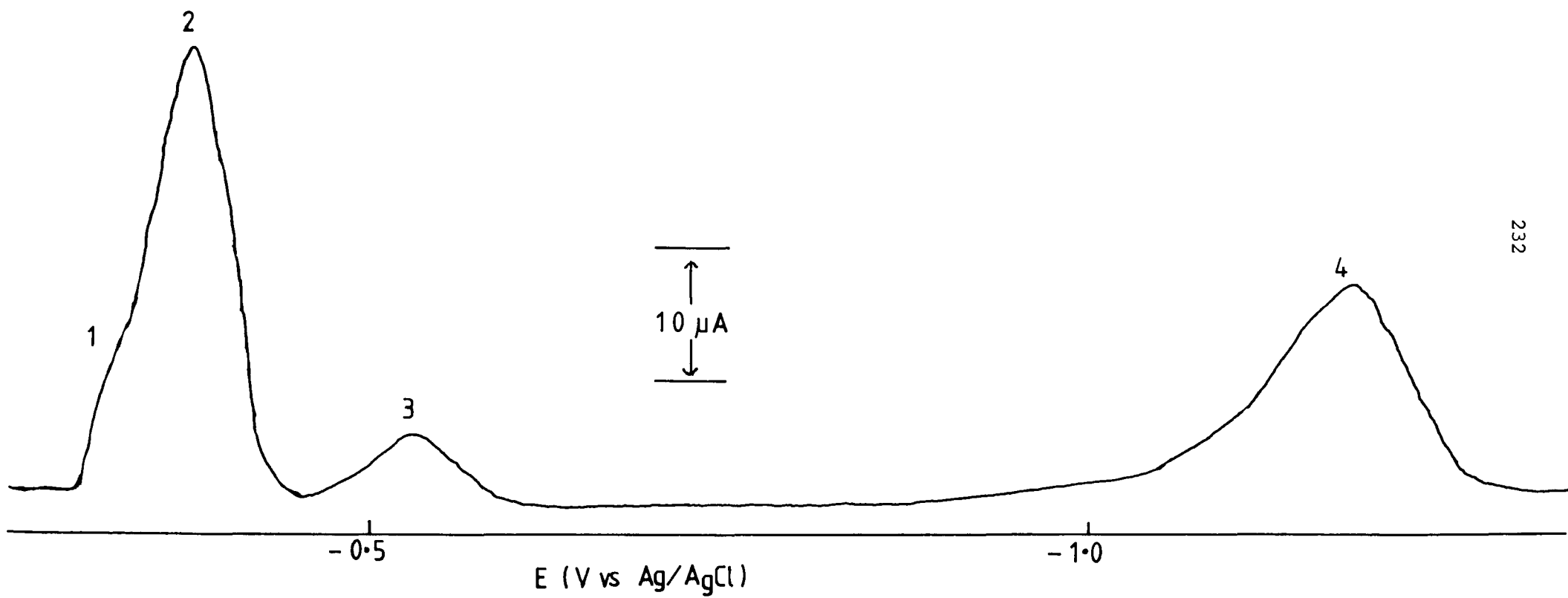


Fig. 4.5. DP polarogram of  $1 \times 10^{-4}$  M  $\text{Me}_2\text{Pb}^{2+}$  in acetate buffer pH 3.3 containing 50% (V/V) methanol

for wave 4 in DC polarographic studies (see Fig. 4.3). Consequently, only peak 2 may be used for quantification purposes. The concentration dependence of peaks 1 and 3 could not be accurately assessed.

The dependence of peak currents and peak potentials on the methanol concentration was then established; results are illustrated in Tables 4.4 and 4.5, respectively. Accurate measurement of the peak current and peak potential for peak 1 in solutions containing more than 40% (V/V) methanol was not possible. When the methanol concentration exceeded 40% (V/V), peak 1 increasingly overlapped with peak 2. At 80% (V/V) methanol, peaks 1 and 2 had almost completely overlapped, appearing as a single broad peak.

The relationship between peak current and methanol concentration is not the same for all four peaks (Table 4.4). Peak 2 decreased on increasing the methanol concentration; similar behaviour was observed for Pb(II). By contrast, the peak current for peak 3 appears to be almost independent of the methanol concentration. However, the peak current values for peaks 1 and 4 increased as the methanol concentration was increased.

Except for peak 4, the peak potentials of the remaining peaks became slightly more negative as the

Methanol Concentration % (V/V)	Peak Current ( $\mu\text{A}$ )			
	Peak 1	Peak 2	Peak 3	Peak 4
0	1.18	5.51	0.71	0.83
10	1.30	4.53	0.71	0.83
20	1.46	3.94	0.71	1.10
30	1.61	3.62	0.71	1.10
40	1.73	3.43	0.71	1.22
50	N.D.	3.35	0.71	1.38
60	N.D.	3.35	0.75	1.54
70	N.D.	3.20	0.91	1.57
80	N.D.	3.10	0.98	1.57

Table 4.4. Dependence of peak current on methanol concentration for  $1 \times 10^{-4} \text{ M Me}_2\text{Pb}^{2+}$ .

N.D. - Not Determined.

Methanol Concentration % (V/V)	Peak Potential (V vs. Ag/AgCl)			
	Peak 1	Peak 2	Peak 3	Peak 4
0	- 0.290	- 0.370	- 0.515	- 1.060
10	- 0.290	- 0.370	- 0.515	- 1.080
20	- 0.300	- 0.370	- 0.520	- 1.100
30	- 0.300	- 0.375	- 0.525	- 1.125
40	- 0.305	- 0.375	- 0.530	- 1.145
50	N.D.	- 0.375	- 0.535	- 1.165
60	N.D.	- 0.375	- 0.540	- 1.200
70	N.D.	- 0.380	- 0.550	- 1.245
80	N.D.	- 0.385	- 0.570	- 1.295

Table 4.5. Dependence of peak potential on methanol concentration for  $1 \times 10^{-4} \text{ M Me}_2\text{Pb}^{2+}$ .

N.D. - Not Determined.

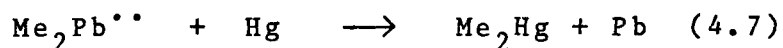
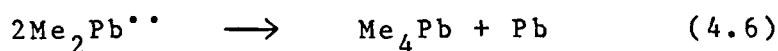
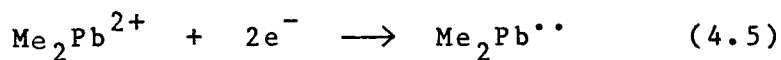
methanol concentration was increased (Table 4.5). A large shift in peak potential was noted for peak 4.

For analytical purposes, maximum sensitivity of peak II (which has already been established to be useful for quantitative determinations of  $\text{Me}_2\text{Pb}^{2+}$ ) is achieved in the absence of methanol in solution.

#### 4.3.1.2.5. Proposed Mechanism for the Reduction of Dimethyllead Dichloride in Aqueous Solutions

From DC polarographic studies it appears that waves 2 and 4 are associated with electroreduction of dimethyllead dichloride. The limiting currents of both waves are diffusion controlled as shown by the linearity of graphs of current against concentration and also by the linear dependence on the square root of the mercury column height. Inspection of the heights of waves 2 and 4 shows that they are almost equal, indicating that both processes involve the same number of electrons. This was confirmed from graphs of  $\log(1/i_d - 1)$  versus E. Both waves represent irreversible two-electron reduction steps.

The following mechanism can therefore be suggested as representative of the reduction process for wave 2 at a DME.



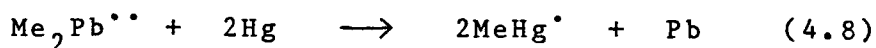
In the first step, the dimethyllead dication takes up two electrons to form the diradical species, which is known to be very unstable {30}. It is unlikely that the diradical species decays by polymerisation, although this is known to occur for dialkyltin compounds {31, 32}. Unlike polymeric tin compounds in which the tin-tin bonds are strong, the lead-lead bonds are considerably weaker and very unstable. Polymeric lead species which do exist are only observed at liquid nitrogen temperatures {33}. Therefore, the diradical must decay by a different pathway.

An alternative pathway invokes either some type of disproportionation as represented by equation 4.6, or a transmethylation reaction between the diradical and the mercury electrode (equation 4.7). If the disproportionation reaction is assumed to be the predominant pathway, then a tetramethyllead species and elemental lead would be the products. Tetraalkyllead would be electroinactive {34} under the present experimental conditions and therefore would not display any



polarographic waves. However, it should be possible to verify the presence of tetraalkyllead, by studying the reduction behaviour of  $\text{Me}_2\text{Pb}^{2+}$  in non-aqueous solvents such as dichloromethane. Subsequently, the oxidation behaviour of the electrode products could be studied by DP polarography under the same conditions. It has now been established that tetramethyllead gives an oxidation peak when studied in non-aqueous solution by DP polarography at a DME {34}. This would be a relatively easy means of establishing whether or not tetramethyllead is generated as one of the products in the reduction of  $\text{Me}_2\text{Pb}^{2+}$  at a DME.

This possibility that transmethylation represents the subsequent reaction of the diradical species must also be entertained. The bond energy of the lead-carbon bond {35} in the tetramethyl form is 32.9 kcal/mole and the bond energy of a mercury-carbon bond {36} is 27 kcal/mole. Therefore, the possibility of transmethylation is equally probable, given the similarity of the bond energies. It has been postulated that the transmethylation reaction may proceed via the following intermediate step {37}.

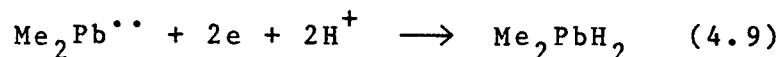


In this intermediate step an alkylmercury radical is formed. This radical can then decompose to

dimethylmercury. Wave 1 may in fact represent adsorption of this dimethylmercury species as a similar type of wave was observed in the reduction of diethyllead {30}. The likelihood of wave 1 arising from adsorption of the alkylmercury radical can be dismissed because such species only have a life-time of a few hundredths of a second {37}.

It is obvious from cyclic voltammetric studies that elemental lead is produced in the first two-electron reduction step. This elemental lead is then oxidised during the anodic scan, giving rise to the single anodic peak 2a. However, because elemental lead can be produced by both transmethylation and disproportionation, it is possible for the electrode reaction to proceed by either pathway. Alternatively, both pathways may occur concurrently in parallel.

Wave 4 also represents an irreversible two-electron reduction step. This wave displayed a pH-dependence in BR buffer from pH 2.0 to 12.0, indicating that proton transfer either precedes or occurs during electron transfer. The following mechanism is proposed to explain the reduction step represented by wave 4.



Wave 3 observed in acidic and alkaline solutions is possibly due to the reduction of some dialkyllead complexes. Alternatively, it may be due to reduction of unionised dialkyllead compounds. A similar type of behaviour was seen for the reduction of dibutyllead diacetate in aqueous-ethanolic solutions {38}.

During this study many similarities were noted between wave 2 for  $\text{Me}_2\text{Pb}^{2+}$  and the reduction wave for  $\text{Pb(II)}$ . In particular, the dependence on methanol concentration was the same for both waves. Both have very similar half-wave and peak potentials. Indeed, it has been suggested that wave 2 does not represent reduction of  $\text{Me}_2\text{Pb}^{2+}$  but  $\text{Pb(II)}$  {39}. Further evidence from the complexation behaviour of the two lead species, reveals that this hypothesis is unfounded (see Section 4.3.2.1.4.1.).

#### 4.3.1.3. Trimethyllead Chloride

##### 4.3.1.3.1. DC Polarographic Studies in Acetate

###### Buffer pH 3.3

A typical DC polarogram of trimethyllead chloride (subsequently referred to as  $\text{Me}_3\text{Pb}^+$ ) in acetate buffer pH3.3/methanol(50/50) is illustrated in Fig. 4.6.

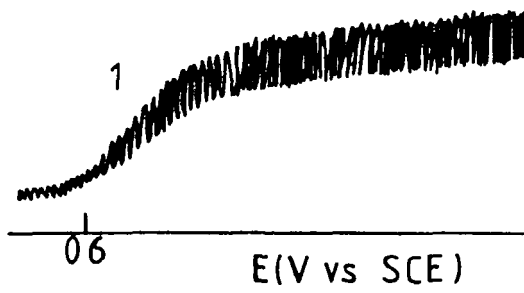
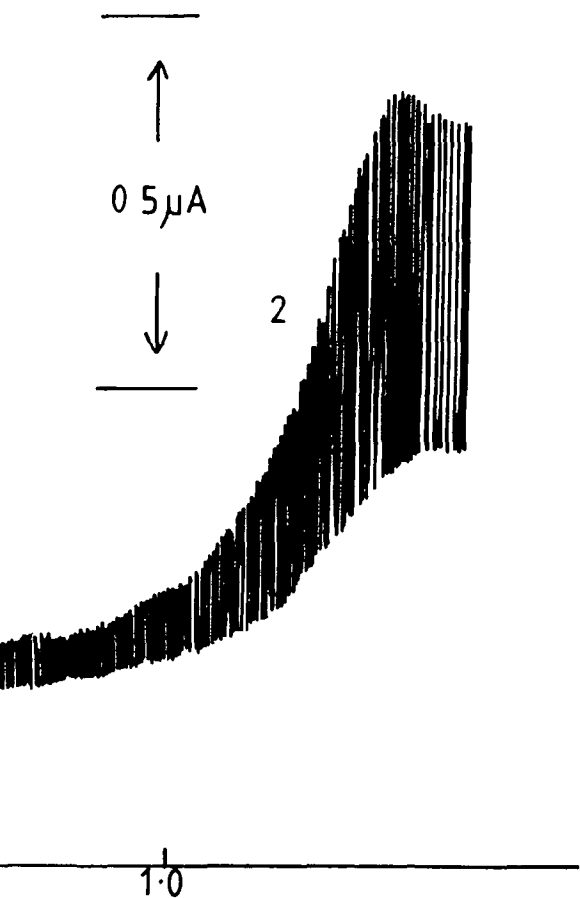


Fig. 4.6.



DC polarogram of  $1 \times 10^{-4} \text{M}$   $\text{Me}_3\text{PbCl}$  in acetate buffer pH 3.3 containing 50% (V/V) methanol.

Two waves (1 and 2) were found to be present at concentrations up to  $1 \times 10^{-3} \text{ M}$ ; the behaviour at higher concentrations was not determined. The appearance of a small symmetrical maximum at the top of wave 2 was noted. This maximum was present over the entire concentration range studied ( $5 \times 10^{-5}$  to  $10^{-3} \text{ M}$ ). Furthermore, it also showed a dependence on the height of the mercury column. The maximum increased with increasing mercury flow-rate as the height of the mercury column increased. Such behaviour is typical of a "maximum of the second kind" {40}. Maxima of this type have a hydrodynamic origin. At mercury flow-rates greater than 2cm/sec, mercury flows directly to the bottom of the mercury drop. The difference in surface tension between the bottom and neck of the mercury drop causes an upward motion of mercury at the surface of the mercury drop. This motion produces a stirring action in solution, thereby transporting larger amounts of analyte to the electrode surface; consequently, the current increases. Suppression of maxima of the second kind is achieved by addition of a surface-active substance to the solution. The motion of the mercury carries the surface-active substance to the neck of the mercury drop; where it accumulates. Consequently, the surface tension at the neck of the drop decreases compared with that of the bottom of the drop.

Addition of Triton X-100 to solution of  $\text{Me}_3\text{Pb}^+$ , suppressed the maximum. Therefore, all data relating to waves 1 and 2 was obtained in the presence of 0.001% (V/V) Triton X-100.

The limiting current of wave 1 showed a linear dependence on concentration indicating that it was diffusion-controlled. Further evidence for the diffusion-controlled nature of wave 1 was ascertained from the linear dependence of the limiting current on the square root of the mercury column height.

The limiting current of wave 2 was seen to linearly increase with concentration. Therefore, it might be assumed that wave 2 is also diffusion-controlled. However, this could not be verified from the dependence of the limiting current on the square root of the mercury column height. Even in the presence of Triton X-100, a maximum was present on the rising part of wave 2. This maximum was only observed at high mercury flow-rate, the drop-time is not long enough to allow the accumulation of sufficient suppressing agent at the neck of the drop.

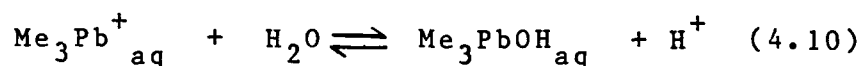
A graph of  $\log(i/i_d - i)$  versus  $E$  for wave 1 proved to be linear with a slope of 92mV. Therefore, wave 1 probably represents an irreversible one-electron reduction

step. A similar procedure was undertaken for wave 2 using a drop-time for 5sec. The slope of the graph was found to be 35mV which probably corresponds to an irreversible three-electron transfer. The irreversibility of wave 1 was substantiated by the dependence of the half-wave potential on mercury column height (Table 4.6). However, the maximum associated with wave 2 at high mercury flow-rates prohibited any accurate measurement of the half-wave potential. Therefore, further evidence for the irreversibility of wave 2 was not possible using DC polarography.

#### 4.3.1.3.2. DC Polarographic Studies in BR Buffers pH2.0 to 12.0

At pH values between 2.0 and 10.0, wave 1 did not exhibit any change in half-wave potential. With further increase in pH up to 12.0, the half-wave potential was shifted to more negative values.

The trimethyllead cation exists in solutions as the hydrated cationic species (denoted by the aq subscript) at neutral pH values {41}. Increasing the pH results in hydrolysis of the hydrated species.





---

Mercury Column Height (cm)	Half-Wave Potential (Vvs.Ag/AgCl)
40	-0.630
44	-0.630
48	-0.635
56	-0.640
64	-0.650
72	-0.655
80	-0.660

---

Table 4.6. Dependence of the half-wave potential of wave 1 for  $1 \times 10^{-4}$  M  $\text{Me}_3\text{PbCl}$  on mercury column height.

The change in the form of  $\text{Me}_3\text{Pb}^+$  is represented in the polarograms as a shift of half-wave potential to more negative values. This shift of potential arises because the hydroxy trimethyllead species ( $\text{Me}_3\text{PbOH}_{\text{aq}}$ ) requires more energy in order to undergo reduction at the DME than the hydrated cationic form {42}.

Subsequent condensation of the hydroxy lead complex with hydrated cationic form is also possible.



However, this condensation reaction only occurs in concentrated solutions ( $> 1 \times 10^{-3} \text{ M Me}_3\text{Pb}^+$ ) and is very unlikely to occur in this study, given that the concentration of  $\text{Me}_3\text{Pb}^+$  is  $1 \times 10^{-4} \text{ M}$ .

The half-wave potential of wave 2 showed a pH-dependence over the entire pH range studied. In addition, the limiting current decreased with increasing pH. Taken together, this behaviour is exhibited by an electrode reaction involving proton transfer. Increasing the pH causes the rate of protonation to decrease, which is manifested as a reduction of the limiting current.

#### 4.3.1.3.3. Cyclic Voltammetric Studies in Acetate Buffer pH3.3

A typical cyclic voltammogram of a  $1 \times 10^{-4} \text{ M}$  solution of  $\text{Me}_3\text{Pb}^+$  in acetate buffer pH3.3/methanol (50/50) is shown in Fig.4.7.

In the cathodic sector, two well-defined peaks (1c and 2c) are present at concentrations lower than

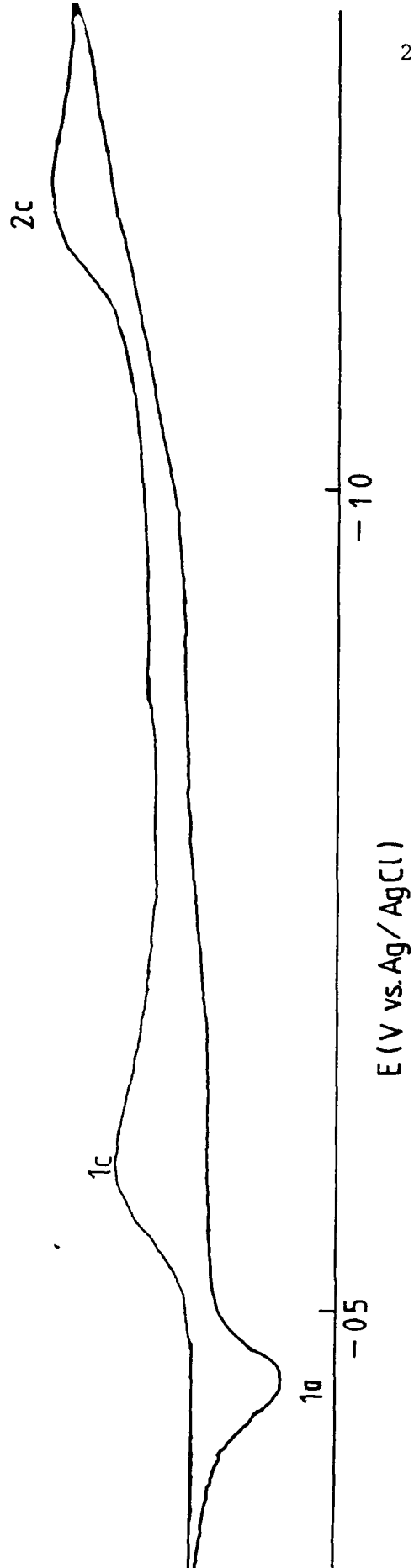


Fig. 4.7. Cyclic voltammogram of  $1 \times 10^{-4} \text{ M}$   $\text{Me}_3\text{PbCl}$  in acetate buffer pH 3.3/ Methanol (50/50).

Scan rate 50 mV/sec

$1 \times 10^{-3}$  M. The potential of peak 1c becomes more positive on increasing the scan rate from 10 to 100 mV/sec. This is typical of a process in which the product is adsorbed at the electrode surface {43}. The potential of peak 2c was shifted in a negative direction as the scan rate was increased from 10 and 100 mV/sec. The peak current for peak 1c was linearly dependent on the square root of the scan rate. The characteristics are indicative of the irreversibility of the electrode processes represented by both peaks {43}.

A single anodic peak(1a) was present at concentrations below  $1 \times 10^{-3}$  M. The single anodic peak corresponds to oxidation of elemental lead. Switching the cathodic scan prior to the commencement of peak 2 did not produce any change in the anodic sector of the voltammogram. It appears that elemental lead is a product of the electrode reactions represented by peak 1c. Confirmation that the anodic peak was due to the oxidation of elemental lead was achieved by addition of inorganic lead nitrate to the solution containing trimethyllead chloride, where upon a large increase in the peak current of the single anodic peak was noticed. The potential of the anodic peak obtained for the mixture was exactly the same as the value of each species measured in the absence of the other.

This cyclic voltammetric study was undertaken in the absence of Triton X-100. However, considering that different results can be obtained for  $\text{Me}_3\text{Pb}^+$  in the presence of Triton X-100 {44}, this oversight makes interpretation of the electrode process more difficult.

#### 4.3.1.3.4. Differential Pulse Polarographic Studies in Acetate Buffer pH3.3

DP polarographic studies of  $\text{Me}_3\text{Pb}^+$  were carried out in acetate buffer pH3.3/methanol(50/50) (Fig. 4.8). It is seen from Fig. 4.8 that there are two well-defined DP polarographic peaks (1 and 2). The height of peak 1 was found to linearly increase with concentration up to  $1 \times 10^{-3} \text{ M}$ .

The height of peak 2 was proportional to concentration up to  $1 \times 10^{-3} \text{ M}$ . As the concentration of  $\text{Me}_3\text{Pb}^+$  was increased, a minimum appeared after peak 2. Furthermore, the peak potential became more negative as the concentration of  $\text{Me}_3\text{Pb}^+$  increased in solution.

The dependence of peak current and peak potential values for peaks 1 and 2 on the methanol concentration was also ascertained. The peak potentials of both peaks shifted negatively on increasing the methanol

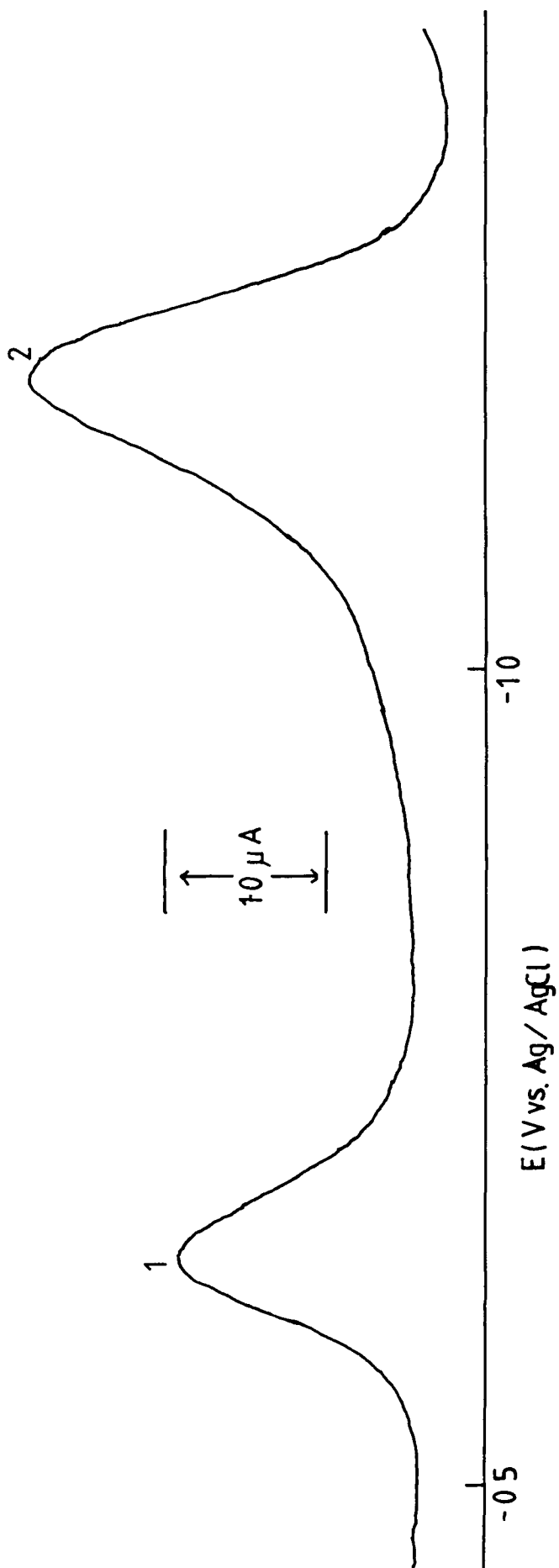


Fig. 4.8. DP polarogram of  $1 \times 10^{-4}$  M  $\text{Me}_3\text{PbCl}$   
in acetate buffer pH 3.3/Methanol (50/50)

concentration, though the shift for peak 2 is considerably larger than for peak 1 (Table 4.7). The peak current of peak 1 decreased as the methanol concentration was increased (Table 4.8). Because of the minimum associated with peak 2, accurate measurement of peak current was not possible. The minimum increased on decreasing the methanol concentration.

#### 4.3.1.3.5. Proposed Mechanism for the Reduction of Trimethyllead Chloride in Aqueous Solutions

The data obtained from DC polarograms, in acetate buffer pH3.3, suggest that a single electron is involved in the first reduction step of  $\text{Me}_3\text{Pb}^+$ . The irreversibility of this step was determined from a graph of  $\log(i/i_d - i)$  versus E. Confirmation of the irreversibility of the first reduction step was gained from cyclic voltammetric studies. In addition, product adsorption was indicated for the first reduction step. At first, this appeared to be an anomalous result because this was not indicated from DC polarography. Product adsorption is recognised in DC polarograms by a prewave at a more positive potential than the main reduction wave. The absence of a prewave is explained by the inhibitory effect of Triton X-100 which was added to solutions during DC polarographic studies. Addition of Triton X-100 was

Methanol Concentration % (V/V)	Peak Potential (V vs . Ag/AgCl)	
	Peak 1	Peak 2
0	-0.60	-1.09
10	-0.61	-1.10
20	-0.62	-1.12
30	-0.63	-1.13
40	-0.64	-1.15
50	-0.65	-1.17
60	-0.66	-1.21
70	-0.67	-1.24
80	-0.68	-1.28

Table 4.7. Dependence of the peak potentials of  $1 \times 10^{-4} \text{M}$   $\text{Me}_3\text{Pb}^+$  on methanol concentration in acetate buffer pH3.3.

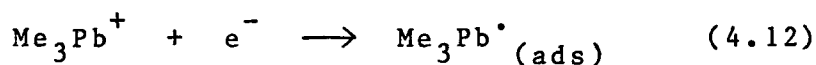


Methanol Concentration % (V/V)	Peak Current ( $\mu\text{A}$ )
	Peak 1
0	1.97
10	1.86
20	1.79
30	1.69
40	1.61
50	1.57
60	1.52
70	1.46
80	1.42

Table 4.8. Dependence of peak current on methanol concentration for  $1 \times 10^{-4} \text{ M Me}_3\text{Pb}^+$ .

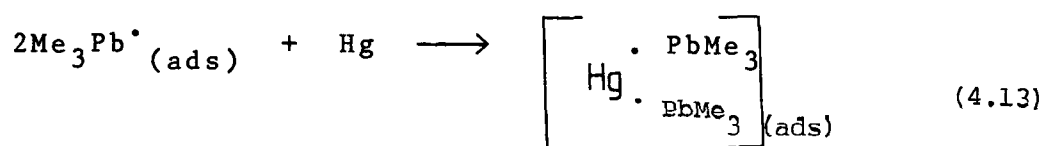
necessary to suppress the maximum associated with wave 2; however, adsorption waves are also suppressed{45}.

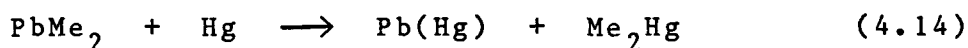
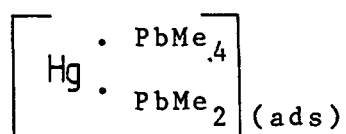
The first reduction step of  $\text{Me}_3\text{Pb}^+$  at a DME probably corresponds to the following process



Because elemental lead is indicated as the final product of the first reduction step, decomposition of the radical must subsequently occur. Dimerisation is one possible route for the decomposition step leading to the formation of tetraalkyllead and inorganic lead. A similar mechanism has been used to explain the decomposition of triphenyllead radicals in aqueous-ethanolic solutions{46}.

An alternative mechanism for the decomposition of  $\text{Me}_3\text{Pb}^\bullet$  has been proposed by other workers {44}. The radical adsorbed on the surface of the mercury decomposes by dismutation rather than dimerisation. The dimethyllead formed is highly reactive and decomposes by transmethylation with mercury; yielding elemental lead and dimethylmercury as final products. The pathway for this decomposition is represented as follows



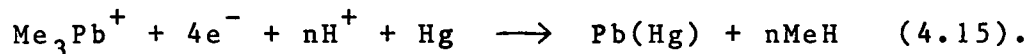


Similar products have been proposed for the reduction of triphenyllead species in 20% (V/V) aqueous methanolic solutions at pH3.5 {47}.

The stability exhibited by the trimethyllead dimer in aqueous solutions {48} suggests that dimerisation may not be the decomposition pathway of the radical species.

Because of the difficulties encountered with the second wave, it is only possible to describe some features of this reduction step. The irreversibility was established from semi-logarithmic analysis of DC polarograms. Corroboration of the irreversibility comes from CV experiments. A pH-dependence of the half-wave potential and limiting current was displayed from pH2.0 to 12.0.

The overall reaction mechanism for the reduction of  $\text{Me}_3\text{Pb}^+$  can therefore be described as follows:



This is in good agreement with other mechanisms used to describe the reduction of trialkyl-[{44}](#) and triphenyl-lead [{47}](#).

#### 4.3.2. Development of a Voltammetric Procedure for the Determination of Inorganic, Dimethyl- and Trimethyl-lead Species in Mixtures

In the first section the possibility of using DP polarography to individually quantify the lead species when simultaneously present in solution is described.

##### 4.3.2.1. Application of DP Polarography to the Determination of Inorganic and Alkyllead Species in Mixtures

###### 4.3.2.1.1. Initial Considerations

On the basis of the polarographic behaviour of inorganic and alkyllead species in aqueous-methanolic solutions, it is evident that sensitivities are increased

in the absence of methanol in the electrolytic solution. In all cases the peak of analytical importance of each lead species increased as the methanol concentration was reduced. Consequently, further studies were carried out in the absence of methanol.

The problems encountered with Pb(II), due to the formation of insoluble  $Pb(OH)_2$  in BR buffer between pH 7.5 and 11.5, indicated the unsuitability of this buffer as a supporting electrolyte. Further evidence of the unsuitability of BR buffer comes from a comparison of limiting current values of inorganic lead measured in BR buffer pH3.3 and acetate buffer pH3.3 (Table 4.1). Limiting current values were larger in the latter buffer.

Ideally, measurements performed on "real" samples should be carried out at the natural pH of the sample. In this way alterations to existing chemical equilibria are avoided. It has been demonstrated that speciation measurements at the natural pH of samples are possible by purging samples with a mixture of nitrogen and carbon dioxide, where the partial pressure of carbon dioxide is adjusted to maintain constant sample pH {49}. Purging with nitrogen causes pH increases in samples {50}.

In this study, measurement at the natural pH of

synthetic samples was not attempted. the main objective was to ascertain whether or not lead species could be individually measured in the presence of each other.

#### 4.3.2.1.2. Characteristics of the Lead Species in Acetate Buffer

Preliminary studies of the three lead species were carried out in acetate buffer pH3.3 using DP polarography. It was assumed that the electrode process for each species was the same as that ascertained by DC polarography in acetate buffer pH3.3/methanol (50/50).

Typical DP polarograms of all three species are shown in Fig. 4.9-4.11. Inorganic lead is characterised by a single reduction peak at  $-0.40\text{V}$ , which represents a single two-electron reduction step (Fig. 4.9). The DP polarogram for dimethyllead contains four peaks (Fig. 4.10). Peaks 2 and 4 both represent two-electron reductions. Trimethyllead exhibited two peaks; the first at  $-0.65\text{V}$  which represents a single electron reduction step and the second peak at  $-1.12\text{V}$  which represents a three-electron reduction (Fig.4.11).

#### 4.3.2.1.3. Studies of Binary Mixtures of Lead Species

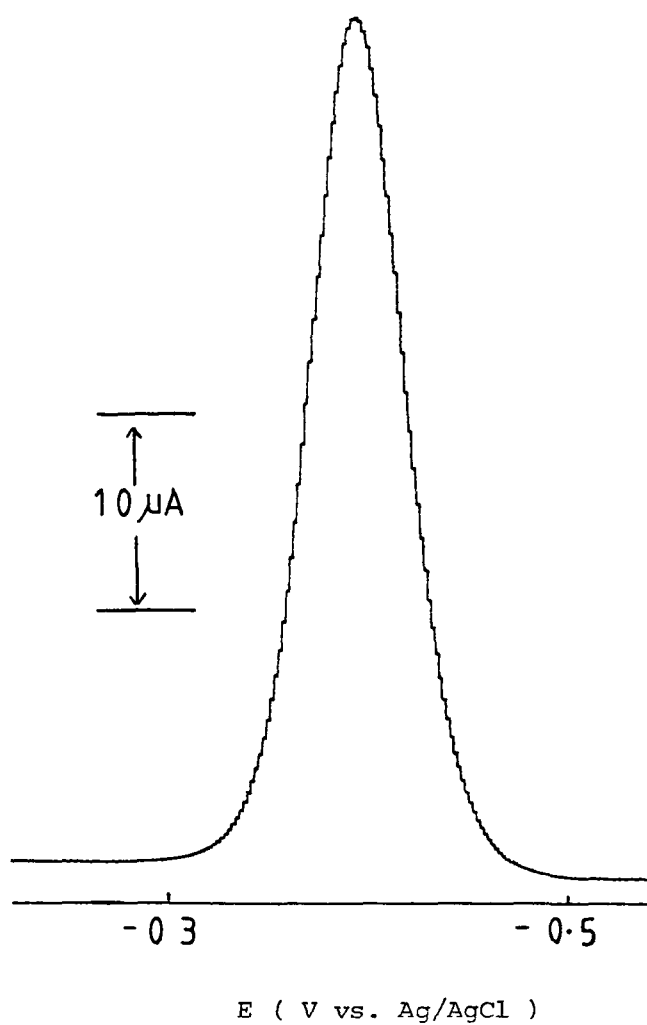


Fig. 4.9. DP polarogram of  $1 \times 10^{-4} \text{ M Pb}(\text{NO}_3)_2$   
in acetate buffer pH 3.30

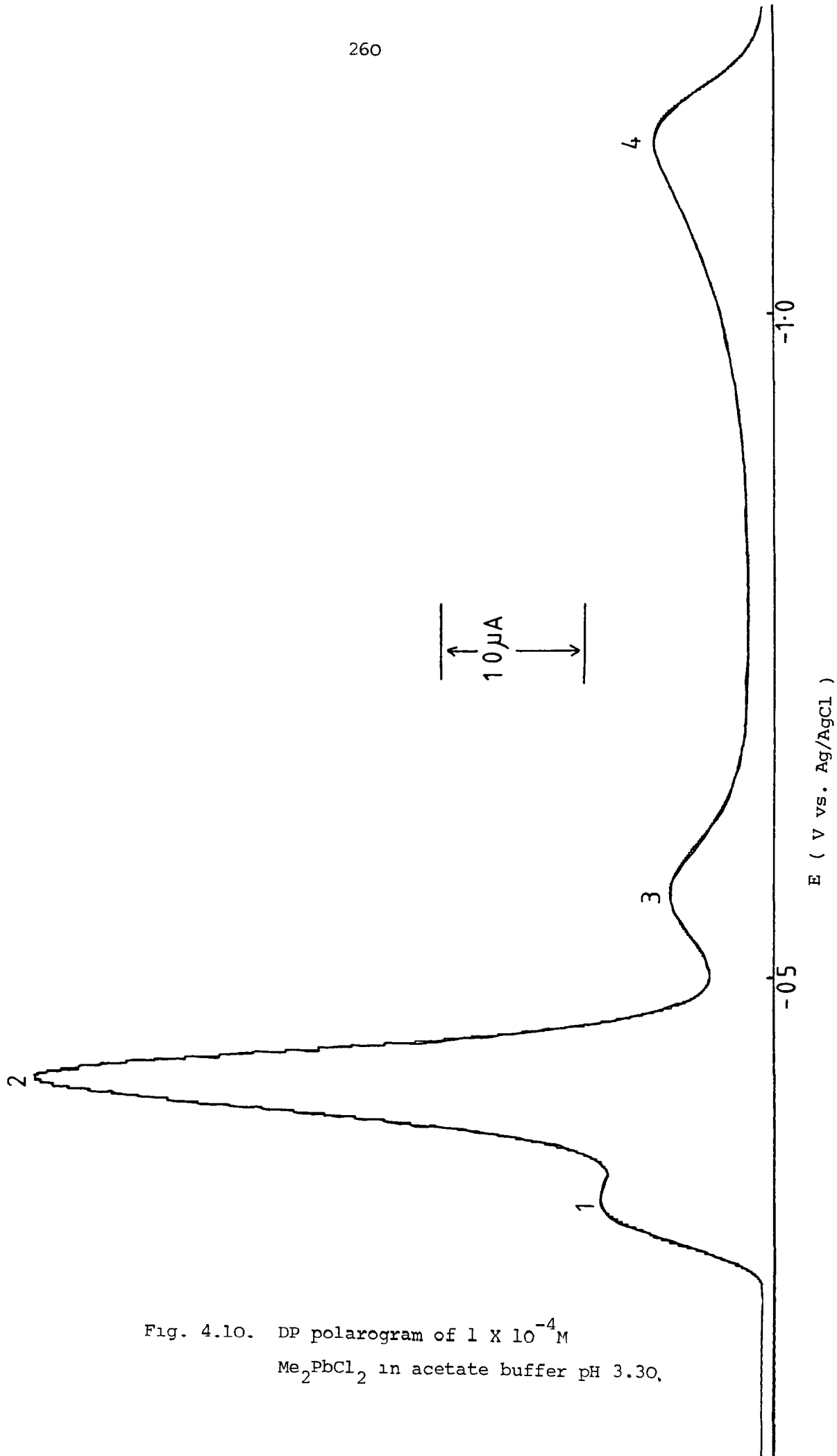


Fig. 4.10. DP polarogram of  $1 \times 10^{-4} \text{ M}$   
 $\text{Me}_2\text{PbCl}_2$  in acetate buffer pH 3.30.



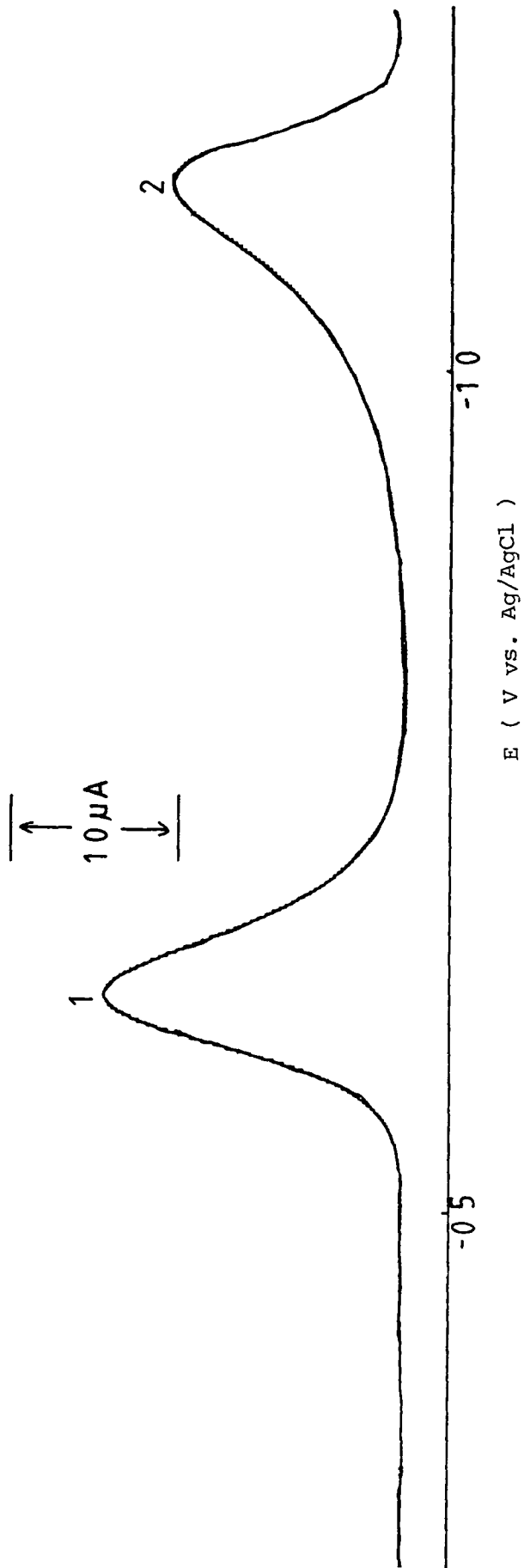


Fig. 4.11. DP polarogram of  $1 \times 10^{-4}$  M  $\text{Me}_3\text{PbCl}$  in acetate buffer pH 3.30

Initial studies were confined to binary mixtures of lead species, although in "real" samples it is probable that all three species would be present simultaneously in solution.

Examination of equimolar ratios of Pb(II) and  $\text{Me}_2\text{Pb}^{2+}$  (Fig. 4.10) overlapped with the single reduction peak for Pb(II). It may therefore be concluded that Pb(II) and  $\text{Me}_2\text{Pb}^{2+}$  cannot be independently measured by DP polarography when simultaneously present in solution.

Mixtures of  $\text{Me}_2\text{Pb}^{2+}$  and  $\text{Me}_3\text{Pb}^+$  also resulted in peak overlap (Fig. 4.12). Peaks 1 and 2 for  $\text{Me}_3\text{Pb}^+$  (Fig. 4.11) overlapped with peaks 3 and 4 respectively for  $\text{Me}_2\text{Pb}^{2+}$  (Fig. 4.10). Overlap occurred for equimolar ratios between  $10^{-6}$  and  $10^{-4}$  M. However, because peak 2 (which is linearly dependent on concentration) does not overlap, it is possible to quantify  $\text{Me}_2\text{Pb}^{2+}$  in the presence of  $\text{Me}_3\text{Pb}^+$ . Unfortunately, the converse is not possible. Some further studies were undertaken to establish whether or not interferences between the two lead species occurred. Initially, a calibration graph was prepared for  $\text{Me}_2\text{Pb}^{2+}$  between  $10^{-5}$  and  $10^{-4}$  M. This graph was based on measurements obtained using peak 2. Subsequently, mixtures of  $\text{Me}_2\text{Pb}^{2+}$  and  $\text{Me}_3\text{Pb}^+$  were prepared and DP polarograms of these mixtures recorded. The concentrations of  $\text{Me}_2\text{Pb}^{2+}$  in

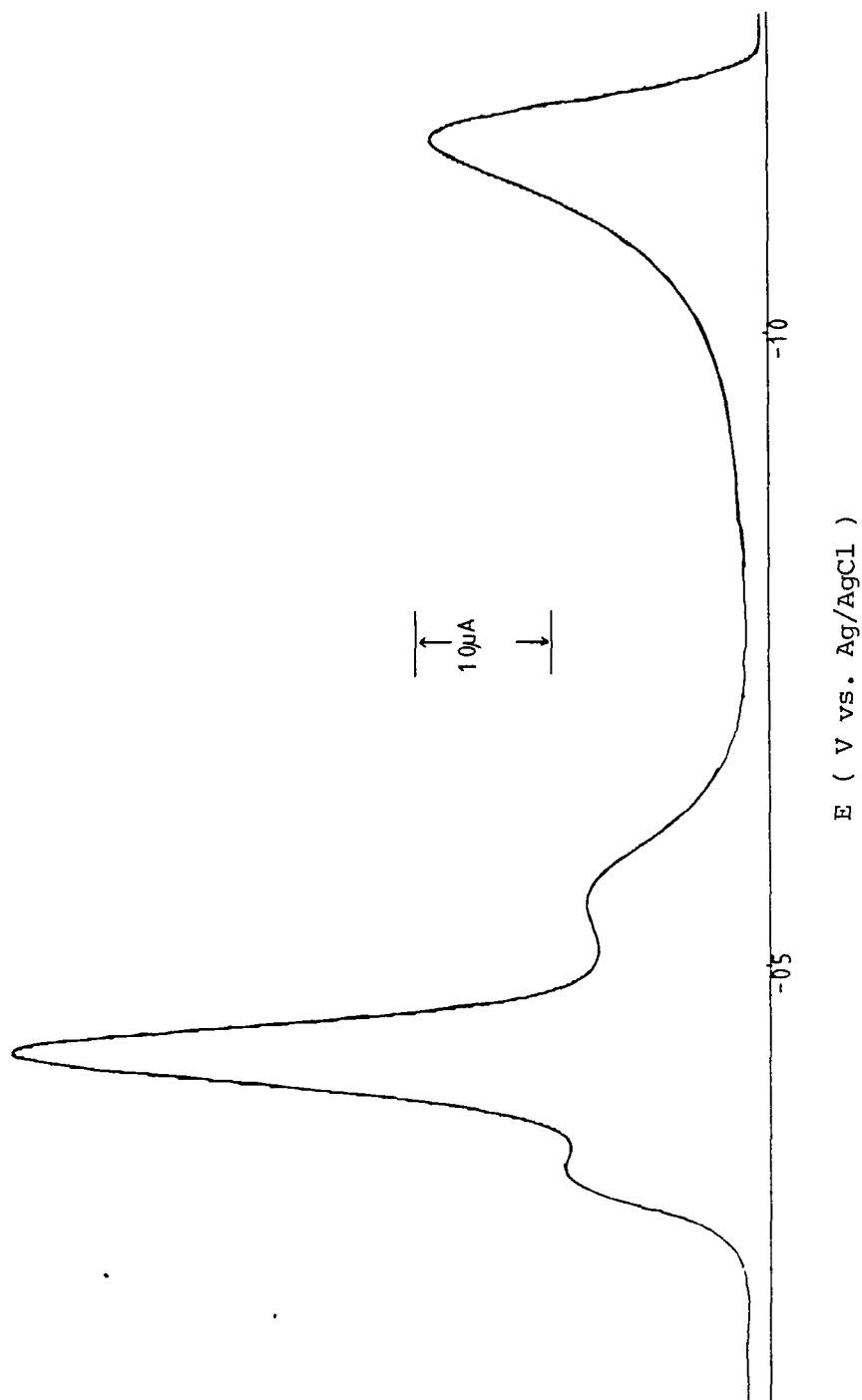


Fig. 4.12. DP polarogram of a binary mixture of  $1 \times 10^{-4} \text{ M}$   $\text{Me}_2\text{PbCl}_2$  and  $1 \times 10^{-4} \text{ M}$   $\text{Me}_3\text{PbCl}$  in acetate buffer pH 3.3

these mixtures were determined from the previously prepared calibration graph. Results are illustrated in Table 4.9. In all cases, the results determined from the calibration graph were practically the same as the actual concentrations of  $\text{Me}_2\text{Pb}^{2+}$  in the solutions, indicating that no interference occurred.

Overlapping peaks were not observed in DP polarograms for binary mixtures of  $\text{Pb(II)}$  and  $\text{Me}_3\text{Pb}^+$  (Fig. 4.13). Using concentrations ranging from  $10^{-6}$  to  $10^{-4}\text{M}$ , and mole ratios from 1:1 to 1:10; always resulted in separate peaks for the two species. Again the possibility of interferences occurring between the two lead species was investigated. The procedure was the same as that utilized in the  $\text{Me}_2\text{Pb}^{2+}$  -  $\text{Pb(II)}$  study; the only difference being that calibration graphs were prepared for  $\text{Me}_3\text{Pb}^+$  and  $\text{Pb(II)}$ .

For both species, results determined from the calibration graphs were very similar (approx  $\pm 5\%$ ) to the actual concentration of the individual species in the mixture. These results indicate that no obvious interferences occur when both species are simultaneously determined by DP polarography.

In conclusion, it appears that  $\text{Pb(II)}$  and  $\text{Me}_3\text{Pb}^+$

Lead Species	Concentrations of individual species ( $\times 10^{-5}$ M)	Concentration determined from calibration graph ( $\times 10^{-5}$ M)	Difference between concentration (%)
$\text{Me}_2\text{Pb}^{2+}$	8.65	8.35	3.5
$\text{Me}_3\text{Pb}^+$	1.00		
$\text{Me}_2\text{Pb}^{2+}$	7.00	7.15	2.1
$\text{Me}_3\text{Pb}^+$	4.66		
$\text{Me}_2\text{Pb}^{2+}$	5.43	5.28	2.8
$\text{Me}_3\text{Pb}^+$	5.65		
$\text{Me}_2\text{Pb}^{2+}$	3.12	3.28	4.9
$\text{Me}_3\text{Pb}^+$	7.26		
$\text{Me}_2\text{Pb}^{2+}$	1.12	1.05	6.3
$\text{Me}_3\text{Pb}^+$	9.15		

Table 4.9. Simultaneous determination of  $\text{Me}_3\text{Pb}^+$  and  $\text{Me}_2\text{Pb}^{2+}$  in acetate buffer pH3.3 using DP polarography.

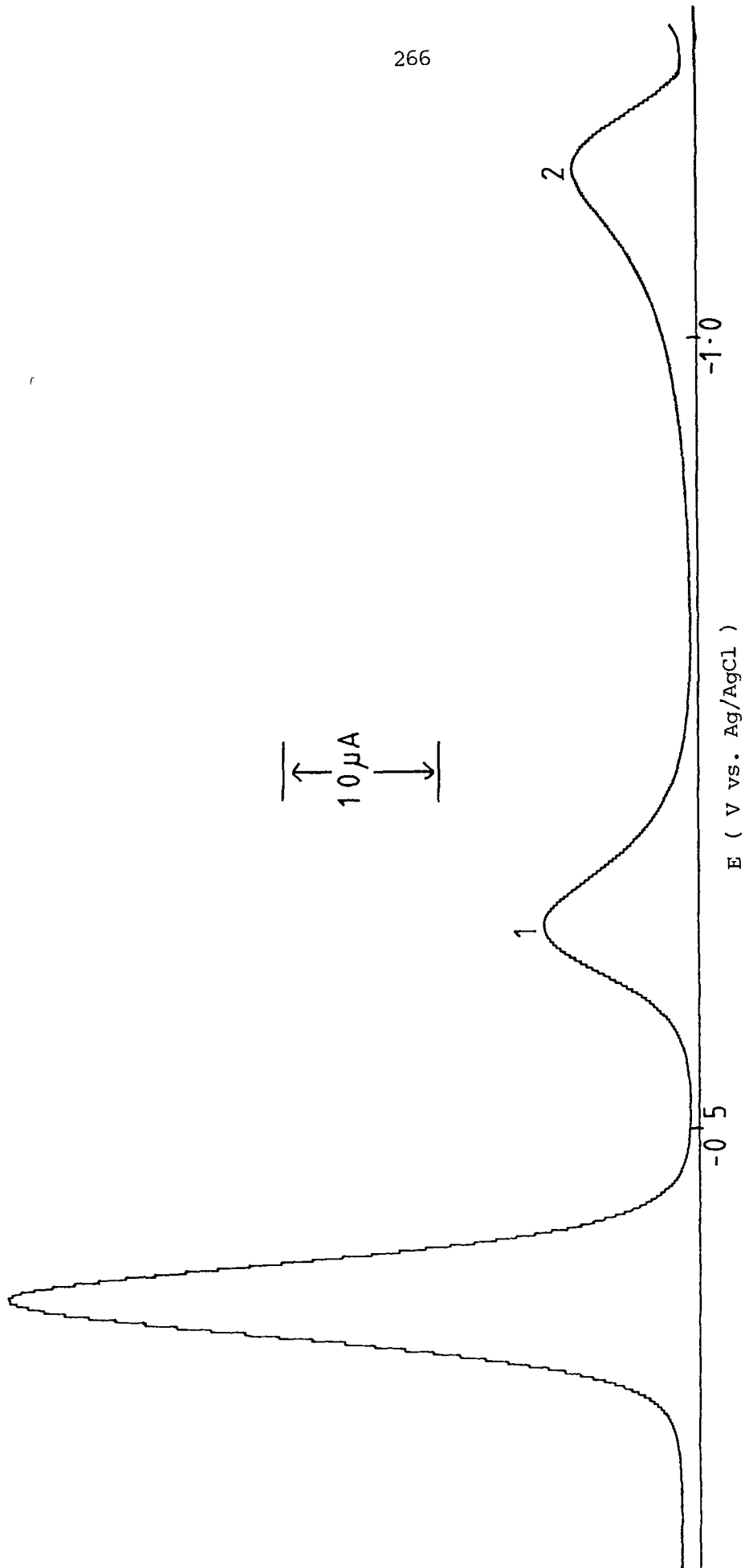


Fig. 4.13. DP polarogram for a mixture of  $1 \times 10^{-4}$  M  $\text{Pb}(\text{NO}_3)_2$  and  $5 \times 10^{-6}$  M  $\text{Me}_3\text{PbCl}$  in acetate buffer pH 3.30

can both be quantified when present as binary mixtures in solution. Furthermore,  $\text{Me}_2\text{Pb}^{2+}$  can be determined in the presence of  $\text{Me}_3\text{Pb}^+$ . However, all three species cannot be individually quantified when simultaneously present in solution due to restrictions imposed by overlap of the reduction peak for  $\text{Pb(II)}$  with peak 2 for  $\text{Me}_2\text{Pb}^{2+}$ . Hence, further studies were necessary to determine whether or not these two species could be separated.

#### 4.3.2.1.4. Investigation of Complexation as a Method of Separating Inorganic and Dimethyllead

The difficulties encountered with binary mixtures of lead species arise because of the similarities in peak potential for all three species. However, selective changes in peak potentials are possible using complexing agents.

A number of complexing agents were examined to see whether or not they form complexes with any of the lead species. The complexing agents examined include 1,10-phenanthroline, sodium diethyldithiocarbamate (NaDEDTC), 2-mercaptobenzothiazole, 2,2-bipyridine, 8-hydroxyquinoline, acetylacetonate and ethylenediaminetetraacetic acid (EDTA). Only NaDEDTC and EDTA were found to complex with inorganic lead. However,

at concentrations above  $1 \times 10^{-4}$  Pb(II), precipitation of the Pb(II)-DEDTC complex occurred. Increased solubility of the metal complex may be achieved in the presence of chloroform {51}. In view of the reduced sensitivities of the lead species when determined in aqueous-methanolic solutions, it was decided to confine studies to EDTA.

#### 4.3.2.1.4.1. Polarographic behaviour of lead species in the presence of EDTA

Addition of EDTA to a  $1 \times 10^{-4}$  Pb(II) solution resulted in a second peak at -0.88 V. A typical DP polarogram for a mixture of EDTA and Pb(II) is shown in Fig. 4.14. The first peak at -0.4V is due to the two-electron reduction of uncomplexed Pb(II). The second peak at -0.88V is due to reduction of the Pb(II)-EDTA complex. At equimolar concentrations Pb(II) is predominantly complexed with EDTA; this was indicated in DP polarograms by the absence of peak 1. It was also inferred that dissociation of Pb(II) from the Pb(II)-EDTA complex does not occur to any great extent, which is in contrast to the Cd(II)-EDTA complex {52}.

Characteristics of the peak representing reduction of the Pb(II)-EDTA complex include increased peak width and decreased current when compared with that of



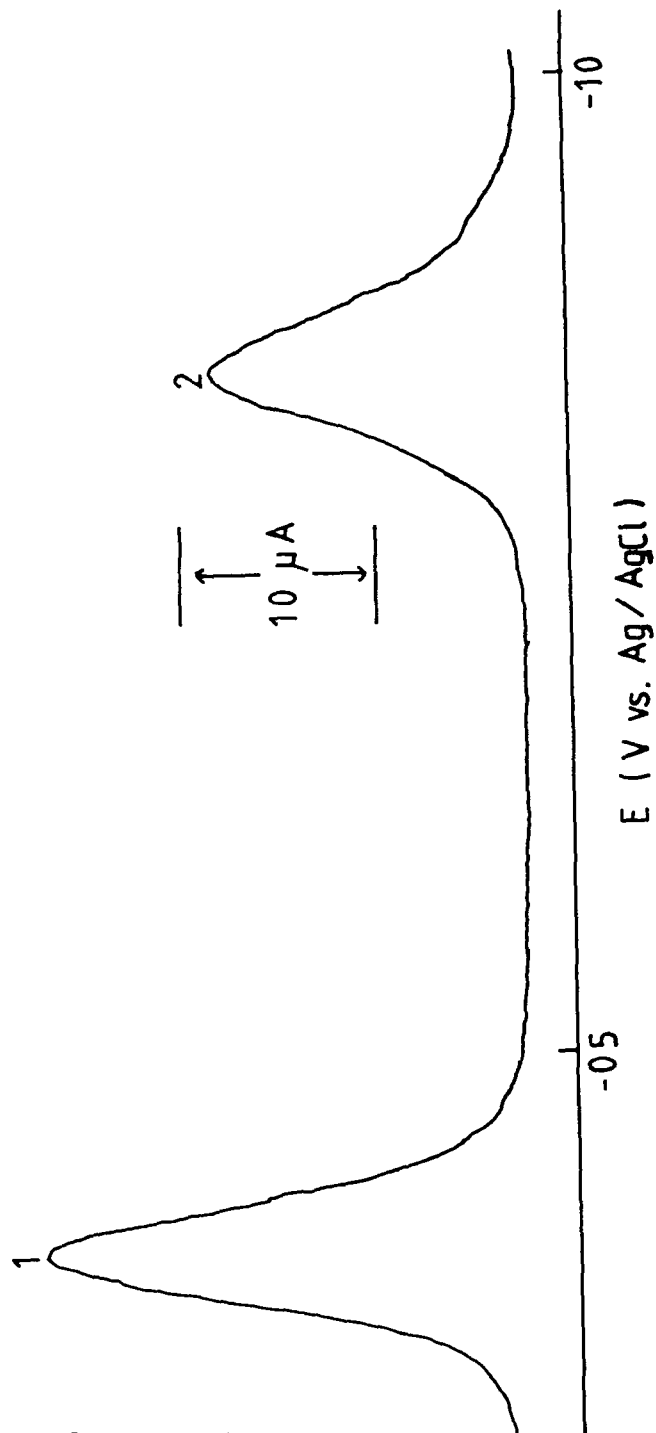


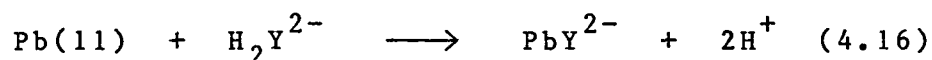
Fig. 4.14. Simultaneous determination of Pb(II) 1 and Pb (II) - EDTA 2 in acetate buffer pH 3.3 by DP polarography  
Scan rate 2 mV/sec

Pb(II) measured in the absence of EDTA. The broadened peak shape is due to increased irreversibility of the electrode reaction {53}. This was verified by cyclic voltammetric studies where the peak potential for reduction of the Pb(II)-EDTA complex becomes more negative on increasing the scan rate. The 62% decrease in peak current of Pb(II) on complexation with EDTA possibly reflects a change in the diffusion coefficient of the complex relative to the uncomplexed Pb(II). Such reductions in peak current have on occasions been attributed to a dissociation rate step prior to the reduction {54}. In the present study this is not possible. DC polarographic studies showed that the limiting current of the Pb(II)-EDTA complex was diffusion-controlled. This was established from the dependence of the limiting current on both the height and the square root of the height of the mercury column. If a dissociation step was rate-limiting, then the limiting current would be expected to adopt the characteristics associated with kinetically-controlled currents.

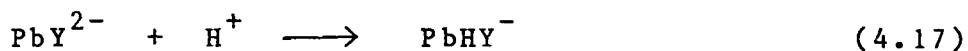
The pH-dependence of both the peak potential and peak current of the Pb(II)-EDTA complex were examined between pH 3.3 and 5.0 in acetate buffer. Increasing the pH resulted in a shift of peak potential to more negative values and a corresponding decrease in peak current. For the purpose of analytical determinations, pH 3.30 represents

the optimum condition for quantification of the Pb(II)-EDTA complex. Interpretation of these results is as follows.

The reaction between Pb(II) and EDTA (represented as  $H_2Y^{2-}$ ) can be represented by

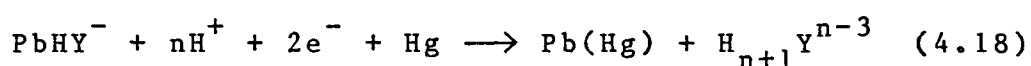


However, it has been established that  $PbY^{2-}$  is non-labile {55}. In view of the non-labile nature of  $PbY^{2-}$ , it must be concluded that if  $PbY^{2-}$  was the species being reduced at the DME, then the limiting current would be kinetically-controlled. In fact, the limiting current is diffusion-controlled. Therefore, it is necessary to consider that a protonated complex is formed, if the presence of a reduction peak for Pb(II)-EDTA is to be explained. Protonated metal-EDTA complexes are known to exist in acidic media {56}. The following reaction is postulated in which a monoprotonated complex is formed.



It is not unreasonable to assume that both  $PbY^{2-}$  and  $PbHY^-$  are simultaneously present in solution. Indeed, the formation of the non-labile  $PbY^{2-}$  could explain why such a large reduction in peak current was observed for Pb(II) on

complexation. The reaction represented by equation 4.17 would also explain the diminution of peak current with increasing pH. Increasing the pH favours formation of the non-labile complex, which results in peak current decrease. The cathodic shift of peak potential is indicative of an electrode reaction in which proton availability becomes limiting with increasing pH. The electrode reaction may be represented as follows

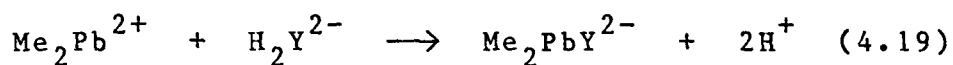


Dimethyllead was also found to complex with EDTA. The reduction potential of the  $\text{Me}_2\text{Pb-EDTA}$  complex is  $-0.54\text{V}$  in acetate buffer pH 3.3. This further indicates that peak 2, shown in Fig. 4.10 represents the reduction of  $\text{Me}_2\text{Pb}^{2+}$  and not  $\text{Pb(II)}$ . The shift in potential of peak 2 for  $\text{Me}_2\text{Pb}^{2+}$  on complexation with EDTA is only 160 mV compared with 480 mV for  $\text{Pb(II)}$  (for a concentration of  $1 \times 10^{-5}\text{M}$ ). In the case of  $\text{Pb(II)}$ , EDTA is able to coordinate to all six coordination sites. However, because  $\text{Me}_2\text{Pb}^{2+}$  exists in solution as a linear carbon-lead-carbon skeleton {57}, all six coordination sites are not available for coordination. Consequently, EDTA can only coordinate to four sites, resulting in a weaker complex than that formed with  $\text{Pb(II)}$ .

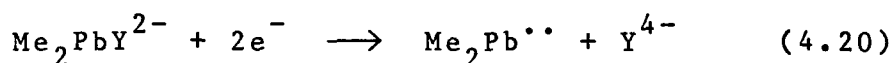
Complexation of  $\text{Me}_2\text{Pb}^{2+}$  with EDTA resulted in a 20% reduction in peak current.

DC polarographic studies established the diffusion-controlled nature of the  $\text{Me}_2\text{Pb-EDTA}$  complex. Both the peak current and peak potential of the  $\text{Me}_2\text{Pb-EDTA}$  complex were found to be independent of pH in acetate buffer between pH3.3 and 5.0.

Formation of the  $\text{Me}_2\text{Pb-EDTA}$  complex can be considered as follows



The electrode reaction may be represented as



Trimethyllead does not complex with EDTA. No changes in peak current and peak potential values for  $\text{Me}_3\text{Pb}_+$  were observed in DP polarograms on addition of EDTA. In aqueous solution,  $\text{Me}_3\text{Pb}^+$  has a planar structure {57}. This coordination geometry, in association with only three available coordination sites around the central lead atom eliminates the possibility of complexation with EDTA.

#### 4.3.2.1.4.2. Studies of binary mixtures of lead species in the presence of EDTA

DP polarograms obtained for equimolar mixtures of  $\text{Me}_2\text{Pb}^{2+}$  and  $\text{Me}_3\text{Pb}^+$  in the presence and absence of  $1 \times 10^{-4} \text{M}$  EDTA did not reveal any major differences. The only noticeable change was the negative shift of peak 2 after formation of the  $\text{Me}_2\text{Pb-EDTA}$  complex. Therefore, although  $\text{Me}_2\text{Pb}^{2+}$  can be quantified in the presence of  $\text{Me}_3\text{Pb}^+$ , the converse is not possible because peak 1 for  $\text{Me}_3\text{Pb}^+$  still overlaps with peak 3 for  $\text{Me}_2\text{Pb}^{2+}$ .

Separation of  $\text{Pb(II)}$  and  $\text{Me}_2\text{Pb}^{2+}$ , when simultaneously present in solution, was possible in the presence of EDTA. The reduction of the  $\text{Pb(II)-EDTA}$  complex occurs at  $-0.88\text{V}$ , whereas, reduction of the  $\text{Me}_2\text{Pb-EDTA}$  complex occurs at  $-0.88\text{V}$ . Thus, separation of previously overlapping peaks can now be achieved. Comparison of peak currents for  $\text{Pb(II)-EDTA}$  and  $\text{Me}_2\text{Pb-EDTA}$  (peak 2) measured in the absence and presence of each other did not yield any significant differences.

Finally,  $\text{Pb(II)-EDTA}$  did not overlap with the two reduction peaks of  $\text{Me}_3\text{Pb}^+$ .

#### 4.3.2.1.5. Limitations of the Speciation Method Using DP Polarography

In the absence of EDTA, quantification of the individual lead species in a ternary mixture is impossible. Nonetheless, if the species are only present as binary combinations, some determinations are possible. The following measurements are possible using DP polarography.

- (i)  $\text{Pb(II)}$  and  $\text{Me}_3\text{Pb}^+$  can be individually quantified when simultaneously present in solution; and
- (ii)  $\text{Me}_2\text{Pb}^{2+}$  may be determined in the presence of  $\text{Me}_3\text{Pb}^+$ .

Limitations arise from not being able to quantify  $\text{Me}_3\text{Pb}^+$  in the presence of  $\text{Me}_2\text{Pb}^{2+}$ . Furthermore, neither  $\text{Pb(II)}$  or  $\text{Me}_2\text{Pb}^{2+}$  can be determined when simultaneously present in solution.

Some of the aforementioned limitations are overcome by using EDTA as a complexing agent. In addition to measurements (i) and (ii),  $\text{Pb(II)}$  can now be determined in the presence of  $\text{Me}_2\text{Pb}^{2+}$ . Yet the problem of not being able to determine  $\text{Me}_3\text{Pb}^+$  in the presence of  $\text{Me}_2\text{Pb}^{2+}$  still exists.

For ternary mixtures, the presence of EDTA enables both  $\text{Pb(II)}$  and  $\text{Me}_2\text{Pb}^{2+}$  to be quantified. Unfortunately,  $\text{Me}_3\text{Pb}^+$  could not be determined in this ternary mixture.

Despite the impossibility of being able to determine all three species simultaneously by DP polarography, the results do suggest that it may be

possible using anodic stripping voltammetry.

Realistically, if the method is to be capable of quantifying the lead species in "real" samples, lower detection limits than those possible with DP polarography are required. Consequently, further investigations were pursued using DPASV at a HMDE.

#### 4.3.2.2. Application of DPASV to the Determination of Inorganic and Alkyllead Species in Mixtures

##### 4.3.2.2.1. Studies in Acetate Buffer pH 3.3

The influence of the plating potential on the peak current of the individual lead species was determined. From Fig. 4.15 it is evident that both  $\text{Me}_2\text{Pb}^{2+}$  and  $\text{Pb(II)}$  can be detected using plating potentials between  $-0.6$  and  $-1.5\text{V}$ . In contrast,  $\text{Me}_3\text{Pb}^+$  is not detected at potential more positive than  $-0.65\text{V}$ . Consequently, by choosing a plating potential of  $-0.6\text{V}$  only  $\text{Me}_2\text{Pb}^{2+}$  and  $\text{Pb(II)}$  are detected in the presence of  $\text{Me}_3\text{Pb}^+$ . Choosing a value more negative than  $-0.65\text{V}$ , all three species are simultaneously measured. The optimum plating potential for measuring all three lead species simultaneously is  $-1.2\text{V}$ . Some increase in sensitivity is achieved at more negative plating potentials, but the electrode process becomes more complicated due to evolution of hydrogen. Hydrogen evolution at the DME can hamper the plating step, and thus



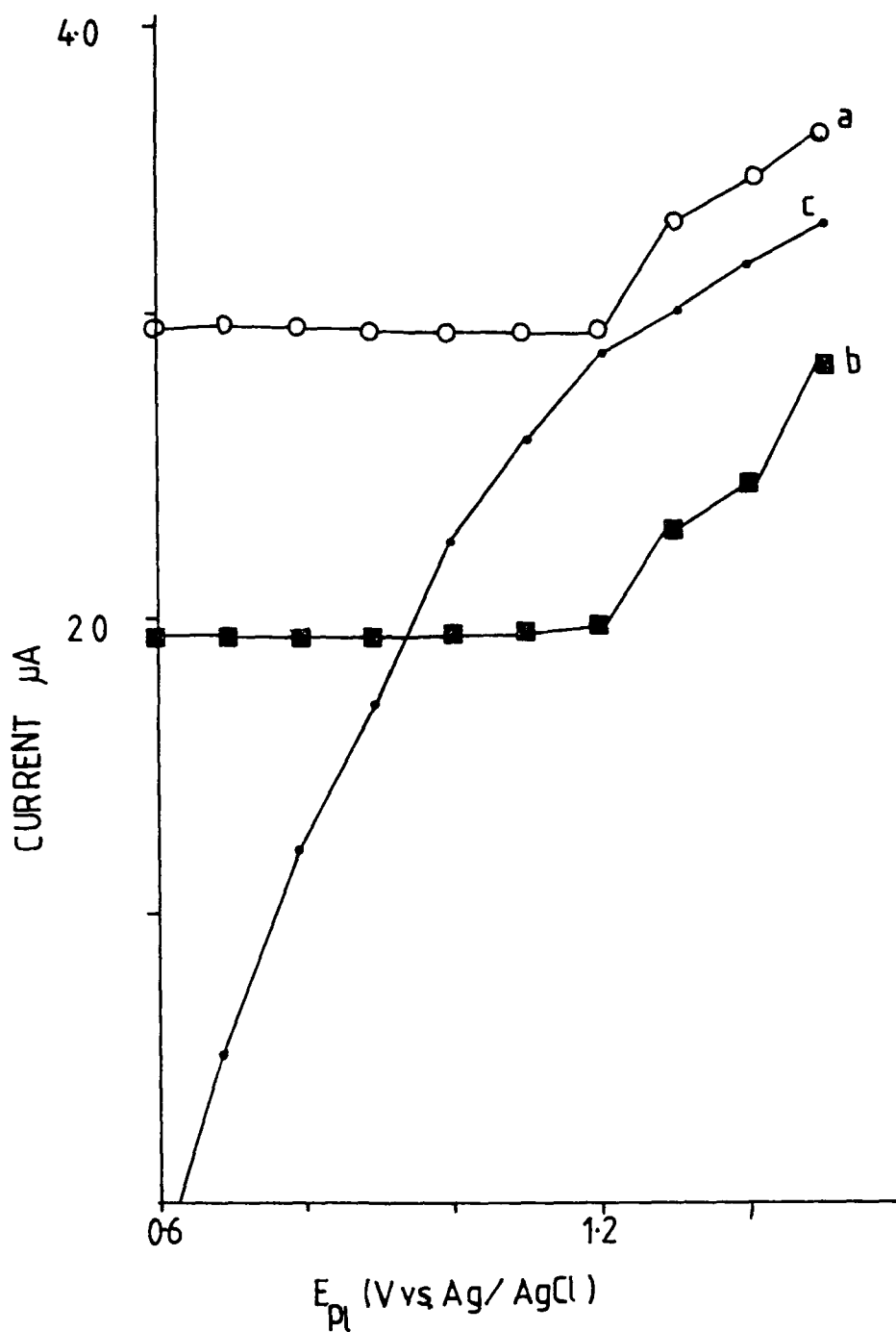
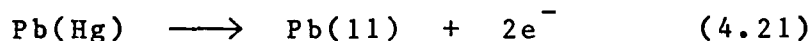


Fig. 4.15. Effect of plating potential on peak current for (a)  $1 \times 10^{-7} M Pb(NO_3)_2$  (b)  $1 \times 10^{-7} M Me_2PbCl_2$  and (c)  $1 \times 10^{-7} M Me_3PbCl$  in acetate buffer pH 3.3.

affect the reproducibility of results. A further reason for choosing a plating potential of  $-1.2\text{V}$  is the independence of the peak currents of  $\text{Me}_2\text{Pb}^{2+}$  and  $\text{Pb(11)}$  between  $-0.6$  and  $-1.2\text{V}$ . Thus any increase in peak current on changing the plating potential from  $-0.6$  to  $-1.2\text{V}$  is attributable to  $\text{Me}_3\text{Pb}^+$ .

The peak potential for the oxidation step is the same for all three lead species. The electrode process is



Because lead amalgam is the product of the reduction step for all three lead species, the oxidation steps are indistinguishable for all three species.

Examination of the dependence of the peak currents on scan rate was undertaken. Peak currents increased with scan rates up to  $10\text{mV/sec}$ ; at higher scan rates the current decreased. Associated with increasing scan rate was an increase in peak width at half-height and a shift of the peak potential to more positive values. A scan rate of  $5\text{mV/sec}$  was chosen as a suitable compromise between the peak characteristics altered on increasing the scan rate.

Finally, the relationship between peak current and deposition time was ascertained. In general, the peak currents increased with deposition times up to 20 min. Longer deposition times did not result in increased peak currents. This behaviour may be due to interferences between the lead species at deposition times greater than 20 min, or may possibly indicate complete coverage of the electrode surface.

Although a deposition time of 20 min represents maximum response in terms of peak current, it was decided to use a deposition time of 4 min. It has been found that deposition times of less than 5 min ensure that the overall chemical equilibrium of a sample is not disturbed {58}. If very long deposition times are used, then removal of electroactive components can cause changes in the overall solution composition. For this reason the deposition time was minimised to ensure that chemical equilibrium between the lead species are not seriously altered.

#### 4.3.2.2.2. Determination of the Lead Species in the Presence of EDTA

In the previous section it was seen that by choosing a plating potential of  $-0.6V$  only  $Me_2Pb^{2+}$  and  $Pb(11)$  are measured. The problem now lies in the

resolution of these two species. It has already been found that  $\text{Me}_2\text{Pb}^{2+}$  and  $\text{Pb(II)}$  are reduced at different potentials in the presence of EDTA. The  $\text{Me}_2\text{Pb-EDTA}$  complex is reduced at  $-0.54\text{V}$  whilst the  $\text{Pb(II)-EDTA}$  complex is reduced at  $-0.88\text{V}$ . From Fig. 4.16 it is seen that by using plating potentials of less than  $-0.80\text{V}$  only  $\text{Me}_2\text{Pb}^{2+}$  is measured. It might therefore be inferred that any reduction in peak current which occurs when EDTA is added to a sample and using a plating potential of  $-0.6\text{V}$ , is solely due to  $\text{Pb(II)}$ . Such a conclusion would be erroneous. Addition of EDTA not only eliminates the response of  $\text{Pb(II)}$  at  $-0.6\text{V}$  but reduces the response of  $\text{Me}_2\text{Pb}^{2+}$ . From DP polarographic studies the reduction in peak current for  $\text{Me}_2\text{Pb}^{2+}$  after complexation with EDTA was approximately 20%. Consequently, further studies were carried out to evaluate the exact percentage reduction of the peak current. Freshly prepared solutions of  $\text{Me}_2\text{Pb}^{2+}$  were used. The procedure involved measurement of the peak current in the absence of EDTA using a plating potential of  $-0.6\text{V}$ . This was followed by addition of EDTA and subsequent measurement of the reduced peak current. The average reduction in peak current was 22%. Therefore, in the presence of EDTA only 78% of the total  $\text{Me}_2\text{Pb}^{2+}$  concentration is measured. This concentration must be multiplied by a factor of 1.28 to enable the exact concentration of  $\text{Me}_2\text{Pb}^{2+}$  to be known.

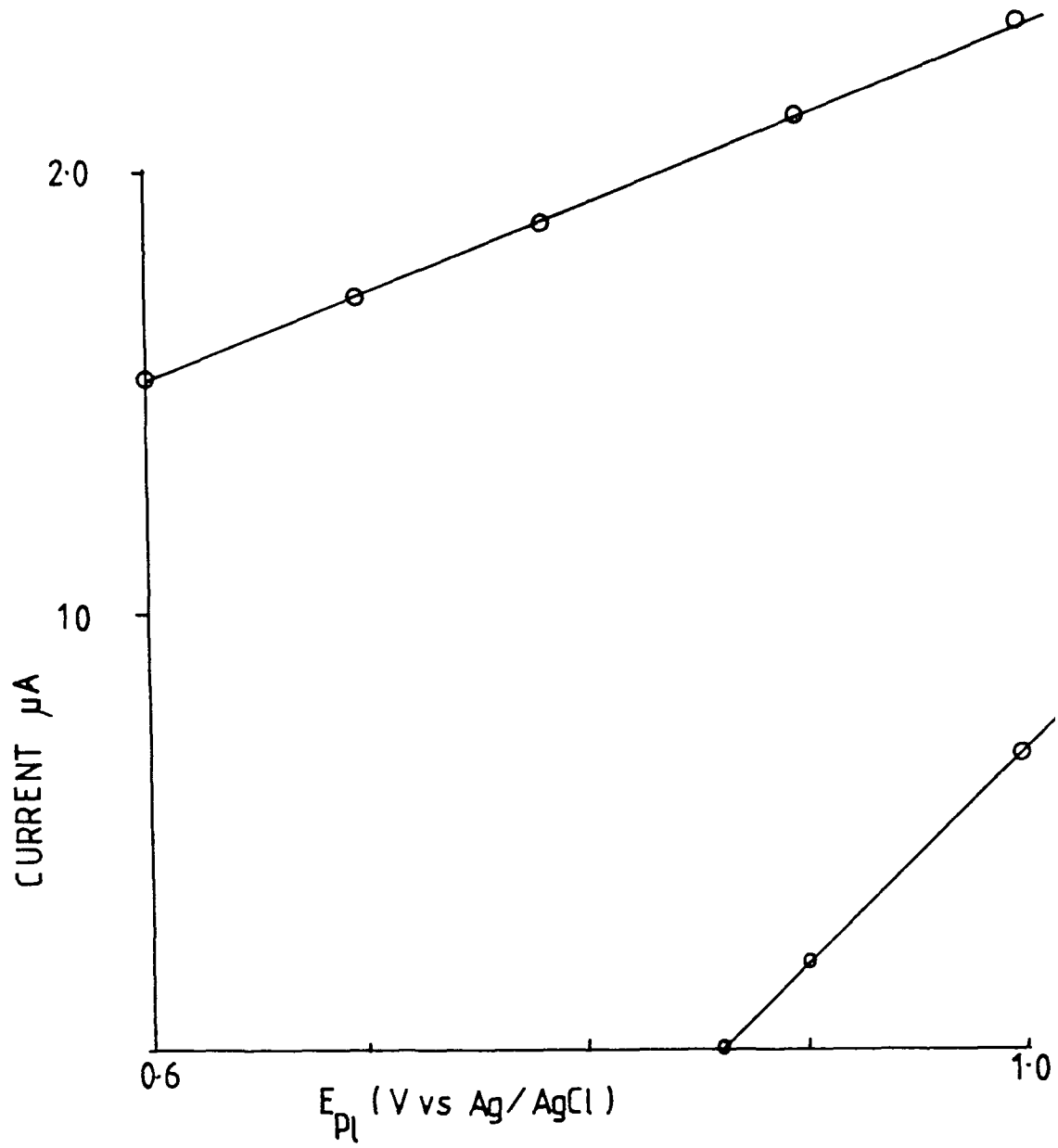


Fig. 4.16. Dependence of current on plating potential ( $E_{pl}$ ) for A,  $1 \times 10^{-7} M Pb(NO_3)_2$  and B,  $1 \times 10^{-7} M Me_2PbCl_2$  in acetate buffer pH 3.3 containing  $1 \times 10^{-6} M EDTA$

#### 4.3.2.2.3. Repeatability of Measurements

In quantitative analysis, it is important to know the repeatability of measurements. If the results vary significantly then the suitability of the analytical method employed in the quantification step must be questioned.

For all three lead species, the repeatability of the peak current measurements were very good. The percentage difference between the lowest and highest values, following ten measurements, was only 7%. This is surprisingly good, particularly as the use of a stirrer bar in ASV measurements is considered to be such an ill-defined hydrodynamic system {59}.

Unfortunately, the capillary of the DME was broken in a subsequent study and was replaced by a new electrode. It was decided to examine the repeatability of the peak current measurements using this replacement electrode. The repeatability of the measurements had deteriorated significantly. Measurements differed by as much as 30%. The irregularity of the results was attributed to varying drop size, arising from a damaged capillary. In view of the irreproducibility of the results further quantitative measurements were not possible. The difficulties encountered with the replacement electrode

illustrate that constancy of results cannot always be presumed, even with a new electrode.

#### 4.3.2.3. Proposed Measurements Scheme Using DPASV

An analytical scheme for the speciation of inorganic and alkyllead compounds is illustrated in Fig. 4.17.

In the first step, all three lead species are simultaneously measured using a plating potential of  $-1.2\text{V}$ . the concentration measured in this first step does not represent the total lead concentration. Many non-labile lead complexes exist in natural water samples which require decomposition by acid digestion or UV irradiation before the lead associated with these complexes can be measured. In the next step a plating potential of  $-0.6\text{V}$  is used, in which the combined concentration of  $\text{Pb(II)}$  and  $\text{Me}_2\text{Pb}^{2+}$  is measured. The difference between the concentrations measured in steps 1 and 2 respectively, represents the concentration of  $\text{Me}_3\text{Pb}^+$  in the sample. Finally, a third measurement is undertaken in the presence of EDTA, again using a plating potential of  $-0.6\text{V}$ . Only  $\text{Me}_2\text{Pb}^{2+}$  is measured in this third step. At this plating potential only 78% of the total  $\text{Me}_2\text{Pb}^{2+}$  concentration is measured.

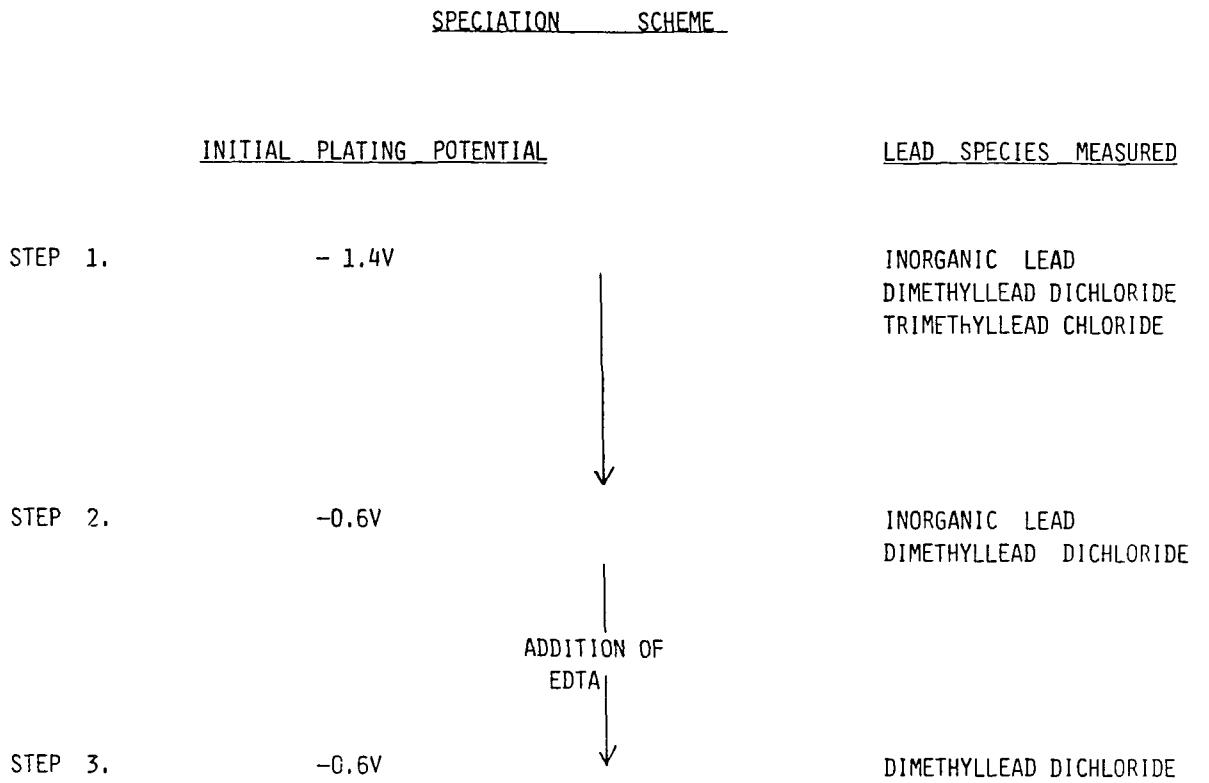


Fig. 4.17. Proposed scheme for simultaneous determination of inorganic lead, dimethyllead and trimethyllead species.



Therefore, to obtain the total  $\text{Me}_2\text{Pb}^{2+}$  concentration, the value obtained in step 3 must be multiplied by 1.28.

The concentration of  $\text{Pb(II)}$  is obtained by subtraction of the total  $\text{Me}_2\text{Pb}^+$  concentration from the combined concentration of  $\text{Me}_2\text{Pb}^{2+}$  and  $\text{Pb(II)}$  measured in Step 2.

#### 4.4. Conclusion

Using DP polarography, individual measurement of the three lead species is not possible, even in the presence of EDTA; however, such measurements are possible using DPASV.

Many aspects of the proposed scheme (Fig. 4.17) still need investigation. In particular, the possibility of measuring the lead species in a sample at its natural pH needs investigation. There is also a need to determine the metals and organics that are likely to interfere with measurement of the lead species. Finally, the possibility of using a MFE as an alternative to a HMDE needs to be established. A MFE would allow much lower detection limits than is possible using a HMDE.

References

1. D. Bryce-Smith, Trends in Anal. Chem., 1, 199 (1982).
2. Y.K. Chau and P.T.S. Wong, N.B.S. Special Publication (U.S.), 618, 65 (1981).
3. R.M. Harrison and D.P.H. Laxen, Environ. Sci. Technol., 12, 1384 (1978).
4. A.W.P. Jarvie, R.N. Markall and H.R. Potter, Environ. Research, 25, 241 (1981).
5. Y.K. Chau, P.T.S. Wong, O. Kramar, G.A. Bengert, R.B. Crue, J.O. Kinrade, J. Lye and J.C. Van Loon, Bull. Environ. Contam. Toxicol., 24, 265 (1980).
6. P. Grandjean and T. Nielsen, Residue Rev., 72, 98 (1979).
7. G.R. Sirota and J.F. Uthe, Anal. Chem., 49, 823 (1977).
8. Y.K. Chau, P.T.S. Wong and P.D. Goulden, Anal. Chim. Acta, 85, 421 (1976).
9. Y.K. Chau, P.T.S. Wong, G.A. Bengert and O. Kramar, Anal. Chem., 51, 186 (1976).
10. G. Pilloni and G. Plazzogna, Anal. Chim. Acta, 35, 325 (1966).
11. U. Schmidt and F. Huber, Anal. Chim. Acta, 98, 147 (1978).

12. W.N. Aldridge and B. Street, *Analyst*, 106, 60 (1981).
13. W. De Jonghe and F. Adams, *Fresenius Z. Anal. Chem.*, 314, 552 (1983).
14. D.S. Forsyth and W.D. Marshall, *Anal. Chem.*, 55, 2132 (1983).
15. Y.K. Chan, P.T.S. Wong, and O. Kramar, *Anal. Chim. Acta*, 146, 211 (1983).
16. D. Chakraborti, W.R.A. De Jonghe, W.E. Van Mol, R.J.A. Van Cleuvenbergen and F.C. Adams, *Anal. Chem.*, 56, 2692 (1984).
17. G.E. Batley and D. Gardner, *Estuarine Coastal Mar. Sci.*, 7, 59 (1978).
18. D.P.H. Laxen and R.M. Harrison, *Sci. Total Environ.*, 19, 59 (1981).
19. D.J. Hodges and F.G. Noden, *Proc. Int. Conference Management and Control of Heavy Metals in the Environment*, London, Sept, 1979, pp. 408-411.
20. M.P. Colombini, G. Corbini, R. Fuoco and P. Papoff, *Ann. Chim.*, 71, 609 (1981).
21. A.M. Bond, Modern Polarographic Methods in Analytical Chemistry (Marcel Dekker Inc, New York, 1980), p. 21.
22. D.R. Crow, Polarography of Metal Complexes (Academic Press, New York, 1969), p. 28.
23. F.A. Cotton and G. Wilkinson, Advanced Inorganic

- Chemistry, Third Edition (J. Wiley & Sons, New York, 1972), p. 331.
24. P. Benes, Z. Kristofikova and M. Obdrzalek, J. Radioanal. Chem., 54, 15 (1979).
25. M.G. Pjescic and D. Minic-Guozdic, Glas. Hem. Drus. Beograd., 43, 429 (1978).
26. R.S. Nicholson and I. Shain, Anal. Chem., 36, 706 (1964).
27. H. Lund and P. Iversen, Organic Electrochemistry, edited by M.M. Baizer (Marcel Dekker Inc., New York, 1973), pp. 208-218.
28. D.R. Crow, Polarography of Metal Complexes (Academic Press, New York, 1969), p. 38.
29. C.E. Freidline and R.S. Tobias, Inorg. Chem., 5, 354 (1966).
30. M.D. Morris, J. Electroanal. Chem. 20, 263 (1969).
31. M.D. Morris, Anal. Chem., 39, 476 (1967).
32. I. Zezula and K. Markusova, Coll. Czech. Chem. Commun., 37, 1081 (1972).
33. L.C. Willemsens, Organolead Chemistry (International Lead Zinc Research Organization, New York, 1964), p. 45.
34. A.M. Bond and N.M. McLachlan, J. Electroanal. Chem., 182, 367 (1985).
35. M.F. Lappert, J.B. Pedley, J. Simpson and T.R. Spadling, J. Organometal. Chem., 29, 195 (1971).

36. J.J. Eisch, The Chemistry of Organometallic Compounds (MacMillan, New York, 1967), p. 63.
37. D. Chantal and L. Etienne, Bull. Soc. Chim. France, 2228 (1968).
38. B. Fleet and N.B. Fouzder, J. Electroanal. Chem., 99, 227 (1979).
39. P. Papoff, private communication.
40. J. Heyrovsky and J. Kuta, Principles of Polarography (Academic Press, New York, 1966), pp. 450-456.
41. R.S. Tobias, Organometals and Organometalloids - Occurrence and Fate in the Environment, edited by F.E. Brinkman and J.M. Bellama (American Chemical Society, Washington D.C., 1978), pp. 130-148.
42. D.R. Crow, Polarography of Metal Complexes (Academic Press, London, 1969), pp. 56-57.
43. A.M. Bond, Modern Polarographic Methods in Analytical Chemistry (Marcel Dekker Inc., New York, 1980), p. 195.
44. M.P. Colombini, R. Fuoco and P. Papoff, Ann. Chim. (Rome), 72, 547 (1982).
45. J. Heyrovsky and J. Kuta, Principles of Polarography (Academic Press, New York, 1966), pp. 287-337.
46. B. Fleet and N.B. Fouzder, J. Electroanal. Chem., 99, 215 (1979).
47. J.P. Colliard and M. Devand, Bull. Soc. Chim. France, 4068 (1972).

48. D.P. Arnold and P.R. Wells, *J. Organomet. Chem.*, 111, 285 (1976).
49. J. Lecomte, P. Mericam. A. Astruc and M. Astruc, *Anal. Chem.*, 53, 2372 (1981).
50. C.J.M. Kramer, Y.G. Hui and J.C. Duinker, *Fresenius Z. Anal. Chem.*, 317, 383 (1984).
51. O. Liska, J. Lehotay, E. Brandsteterova, G. Guiochon and H. Colin, *J. Chromatogr.*, 172, 384 (1979).
52. M.H. Kim and R.L. Birke, *Anal. Chem.*, 55, 1735 (1983).
53. R. Ernst, H.E. Allen and K.H. Mancy, *Water Res.*, 9, 969 (1975).
54. J. Buffle, F.L. Greter, G. Nembrini, J. Paul and W. Haerdi, *Fresenius Z. Anal. Chem.*, 282, 339 (1976).
55. D.R. Turner and M. Whitfield, *J. Electroanal. Chem.*, 103, 61 (1979).
56. T.J. Janjic, L.B. Pfendt and V. Popov, *J. Inorg. Nucl. Chem.*, 41, 63 (1979).
57. R.S. Tobias, *Organometal. Chem. Rev.*, 1, 93 (1966).
58. K.H. Mancy, *Prog. Water Technol.*, 3, 63 (1973).
59. W. Davison, *J. Electroanal. Chem.*, 87, 395 (1978).

CHAPTER 5

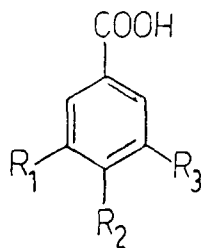
A COMPARISON OF ELECTROCHEMICAL AND ULTRAVIOLET DETECTION  
METHODS IN HIGH PERFORMANCE LIQUID CHROMATOGRAPHY FOR THE  
DETERMINATION OF PHENOLIC COMPOUNDS IN BEERS.

### 5.1. Introduction

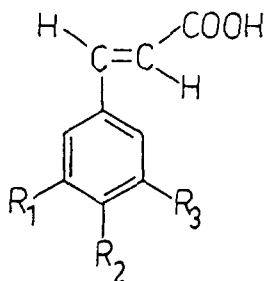
Phenolic compounds constitute an important group of naturally occurring compounds in plants{1,2}. Their presence in alcoholic beverages such as beers and wines stems from the raw materials used. The phenolic compounds present in beers show considerable diversity in their structures and may be divided into several different classes of compounds (Fig. 5.1). Amongst the classes of simple monocyclic acids are the hydroxybenzoic and hydroxycinnamic acids. The importance of the monocyclic acids arises from their ability to undergo decarboxylation either by thermal fragmentation or through the activities of micro-organisms {3,4}. Consequently, highly flavour-active phenols are produced {5}. Although these flavour-active phenols may be appreciated in certain beers{4}, in others they may be regarded as distasteful{6}.

Another important class of phenolic compounds found in beers are the flavanols. These polyphenols form a diverse range of compounds and have been classified into three sub-classes, based on their chromatographic behaviour {7}. The first of the sub-classes, the simple flavanols, exist as monomers (e.g., (+)-catechin and (-)-epicatechin), dimers or trimers. Oxidation and polymerisation of simple flavanols results in the formation of polymeric flavanols. These polymeric flavanols constitute the second sub-class. Finally, there are the complexed flavanols, which are formed on complexation of polyphenols with proteins{8}.

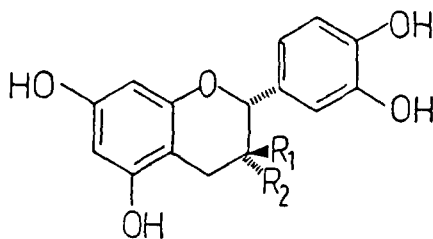


Benzoic acid derivatives

Gallic acid,  $R_1 = R_2 = R_3 = \text{OH}$   
 Protocatechuic acid,  $R_1 = R_2 = \text{OH}, R_3 = \text{H}$   
 p-Hydroxybenzoic acid,  $R_1 = R_3 = \text{H}, R_2 = \text{OH}$   
 Vanillic acid,  $R_1 = \text{OMe}, R_2 = \text{OH}, R_3 = \text{H}$   
 Syringic acid,  $R_1 = R_3 = \text{OMe}, R_2 = \text{OH}$

Cinnamic acid derivatives

Caffeic acid,  $R_1 = R_2 = \text{OH}, R_3 = \text{H}$   
 p-Coumaric acid,  $R_1 = R_3 = \text{H}, R_2 = \text{OH}$   
 Ferulic acid,  $R_1 = \text{OMe}, R_2 = \text{OH}, R_3 = \text{H}$   
 Sinapic acid,  $R_1 = R_2 = \text{OMe}, R_3 = \text{OH}$

Flavanols

(+) - Catechin,  $R_1 = \text{H}, R_2 = \text{OH}$   
 (-) - Epicatechin,  $R_1 = \text{OH}, R_2 = \text{H}$

Fig. 5.1. Structure of phenolic compounds studied

The overall significance of flavanols stems from their influence on the quality of beers. Flavanols are assumed to be the precursors of haze formation in unstabilised beers{9}. In particular, simple and complexed flavanols have been implicated because their presence in beers seems to be associated with the tendency towards instability{7}. Furthermore, the attainment of stability is only possible by reducing the content of simple flavanols below a currently unspecified, but presumably very low, threshold.

Considering the importance of phenolic compounds in ascribing flavour and quality to beers, monitoring of these compounds during brewing is necessary. The analytical methods most commonly used for qualitative and quantitative purposes are those based on modern chromatographic separation methods. In the past, paper chromatography {10} and thin-layer chromatography {11} were employed using non-specific detection reagents, rendering the methods inaccurate. Gas-liquid chromatography (GLC) has been used for the detection of phenols{12}. One of the problems associated with GLC analysis is that non-volatile phenolic compounds require derivatisation{13} prior to the quantification step, thereby adding to the preliminary preparation of samples. However, the problem of derivatisation does not arise when using high performance

liquid chromatography (HPLC). Furthermore, many different detection methods are available in HPLC analysis {14}. In general, ultraviolet (UV) detectors are most popular and have been extensively used in the detection of phenols {15,16}. However, electrochemical (EC) detectors are being used increasingly in HPLC analysis as they exhibit high sensitivity and selectivity {17}. One of the limitations of EC detectors is that the analyte must be electroactive, otherwise it will not be detected. Phenols are electro-oxidisable compounds and therefore are amenable to EC detection. Several analytical methods based on HPLC with EC detection for phenolic compounds have been developed using isocratic conditions {18,19}.

Although both EC and UV detection methods have been separately applied to the determination of phenolic compounds in beer, a comparison of both detectors, under identical experimental conditions, has not been undertaken. The purpose of this study was to undertake such a comparison by placing the detectors in series. Furthermore, gradient rather than isocratic conditions were used in conjunction with reverse-phase HPLC, thereby reducing the analysis time.

## 5.2. Experimental Section

### 5.2.1. Instrumentation

The liquid chromatograph used was an ACS Model 353 ternary solvent system equipped with an ACS Model 750-11 fixed wavelength (254 nm) UV detector. An electrochemical detector, based on the wall-jet principle, was connected in series with the UV detector. The EC detector comprised of a Metrohm 656 electrochemical detector (detector cell) and a Metrohm 641 VA detector (electronic controller). The detector cell consisted of a glassy carbon working electrode, a silver/silver chloride reference electrode and a glassy carbon counter electrode. Outputs from both detectors were coupled to a Houston Instrument Omniscribe dual channel chart recorder, thereby allowing easy comparison of the chromatograms. Chromatographic separations were carried out on a 25cm x 4.6mm i.d. reverse phase Nucleosil 10 C<sub>18</sub> stainless steel column (Macherey-Nagel, Duren, F.R.G.) with a short guard column packed with Nucleosil 10 C<sub>18</sub>. Samples were injected onto the column through a Rheodyne Model 7125 injection valve with a 20- $\mu$ l sample loop.

Voltammetric studies of the phenolic compounds were performed using an EG+G Princeton Applied Research

Corp. (PARC) Model 174A polarographic analyzer. This was used in conjunction with an EG+G PARC Model 303 SMDE. The cell consisted of a glassy carbon working electrode, a platinum wire counter electrode and a silver/silver chloride reference electrode.

Spectroscopic studies were carried out with a Shimadzu UV-240 visible recording spectrophotometer connected, via a Shimadzu OPI-1 option program interface, to a Shimadzu PR-1 graphic printer.

All pH measurements were made using a Philips PW 9140 digital pH meter with an Orion combination pH electrode.

#### 5.2.2. Reagents

All phenolic standards were kindly donated by Arthur Guinness Son and Co. Ltd., Dublin. These standards were of analytical-reagent grade except for the following which were of technical grade: protocatechuic acid, p-hydroxybenzoic acid, syringic acid and (-)-epicatechin. These four standards were not purified owing to the small initial amounts available. With the exception of ethanol, which was doubly distilled prior to use, all organic solvents used were of HPLC grade and did not require further

purification. Both glacial acetic and hydrochloric acids were of analytical-reagent grade and were diluted, where necessary, with Millipore-grade water.

### 5.2.3. Analytical Procedures

#### 5.2.3.1. Preparation of Standard Solutions

Individual standard solutions containing 1000 mg/l of the phenolic compounds were prepared in methanol. A standard mixture containing 1.0 mg/l of each phenolic compound in methanol was then prepared and used in the optimisation of the HPLC method.

Standard solutions of phenolic compounds for calibration purposes were also prepared. Stock solutions containing 1000 mg/l of the phenolic standards were prepared in 5% (V/V) aqueous ethanol. From these stock solutions mixtures of phenolic compounds were prepared over the concentration range 0.1 - 5 mg/l.

#### 5.2.3.2. Extraction of Phenolic Compounds from Beers

The following procedure was used for extracting phenolic compounds from bottled beer samples and standard solutions prepared in 5% (V/V) aqueous ethanol. Duplicate

extractions were carried out on all samples.

Step 1. Beer samples were degassed by simply transferring the sample from one container to another and removing the "fob" (frothy head) on each transfer. This was carried out for 25 transfers and was found to be more effective than subjecting the samples to sonication for 20 min.

Step 2. Degassed ("flat") samples (100 ml) were then acidified to pH 2.0 with 2M HCL.

Step 3. Acidified samples were extracted with two 100-ml portions of iso-octane.

Step 4. The remaining aqueous phase was extracted with four 100-ml portions of ethyl acetate and the organic layers were removed following centrifugation at 3000 rev/min for 5 min.

Step 5. Ethyl acetate extracts were evaporated to 1-2 ml under reduced pressure at 25°C and diluted to 10 ml with methanol.

#### 5.2.3.3. HPLC Analysis

Prior to use, mobile phase solvents were filtered through a 0.45 µm filter (Millipore, USA) and degassed for fifty minutes using an ultrasonic bath. During HPLC analysis, the mobile phase solvents were constantly degassed with helium, thereby reducing the possibility of gas bubbles forming in the HPLC pump.

The experimental parameters used for analysing beer extracts were as follows: electrochemical detector potential, + 1.0V; ultraviolet detector wavelength, 254 nm; flow-rate, 2 ml/min; mobile phase composition, A = 3.5% (V/V) aqueous acetic acid, B = 100% methanol; linear gradient, 0% B to 50% B (V/V) over thirty minutes.

#### 5.2.3.4. Voltammetric Studies

Cyclic voltammograms of  $1 \times 10^{-4}$  M solutions of the individual phenolic compounds in 50/50 methanol/2.5% (V/V) aqueous acetic acid were obtained using a scan rate of 50 mV/sec. All solutions were purged with oxygen-free nitrogen for 4 min prior to recording a voltammogram and a continuous stream of nitrogen was passed over the solutions while measurements were being undertaken.

#### 5.2.3.5. UV Studies

UV spectra of  $5 \times 10^{-5}$  M solutions of phenolic compounds in 50/50 methanol/2.5% (V/V) aqueous acetic acid were recorded in the range 400-220 nm.



### 5.3. Results and Discussion

#### 5.3.1. Voltammetric Studies of Phenolic Compounds

In order to establish a suitable amperometric detection potential for the phenolic compounds, preliminary studies were undertaken using cyclic voltammetry. These studies were performed at a glassy carbon working electrode with a scan rate of 50 mV/sec.

The results obtained in this preliminary examination are tabulated in Table 5.1. Only the flavanols gave two anodic peaks, but only the first of these peaks represents a reversible couple. The second anodic peak at more positive potentials represents an irreversible electron transfer step.

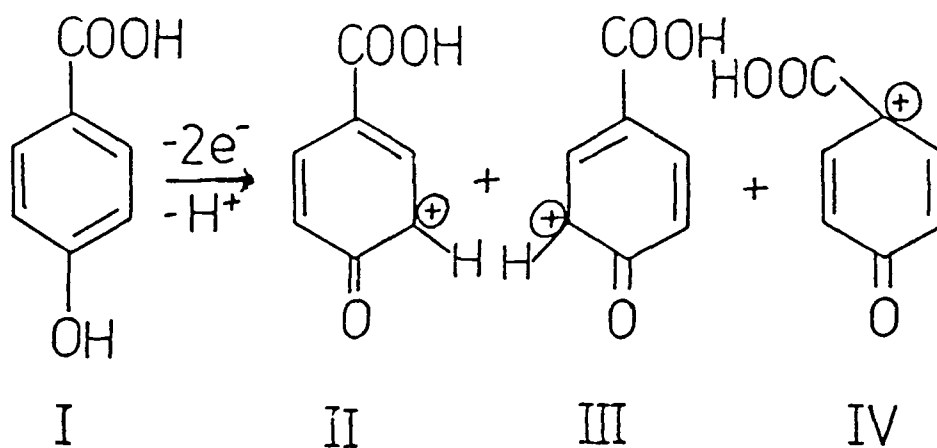
Single anodic and cathodic peaks were obtained for the benzoic and cinnamic acid derivatives. The difference between the anodic and cathodic peak potential values is considerable, indicating an irreversible electrode process. The variations in oxidation potential between the individual constituents of the benzoic and cinnamic acid groups reflect their structural differences (see Fig. 5.1).

Phenolic Compound	Peak Potential (V vs. Ag/Ag Cl)	
	Anodic Peak	Cathodic Peak
<u>Benzoic acid derivatives</u>		
Gallic acid	0.67	0.44
Protocatechuic acid	0.75	0.57
Syringic acid	0.77	0.42
Vanillic acid	0.90	0.77
p-Hydroxybenzoic acid	1.20	1.00
<u>Cinnamic acid derivatives</u>		
Caffeic acid	0.60	0.35
Sinapic acid	0.67	0.54
Ferulic acid	0.83	0.72
p-Coumaric acid	0.95	0.63
<u>Flavanols</u>		
(-) - Epicatechin	(1) 0.49	0.46
	(2) 0.85	-
(+) - Catechin	(1) 0.51	0.48
	(2) 0.89	-

TABLE 5.1. Electrochemical parameters measured by cyclic voltammetry for  $1 \times 10^{-4}$  M solutions of phenolic compounds in 50/50 methanol/2.5% (V/V) aqueous acetic acid. Scan rate, 50 mV/sec.

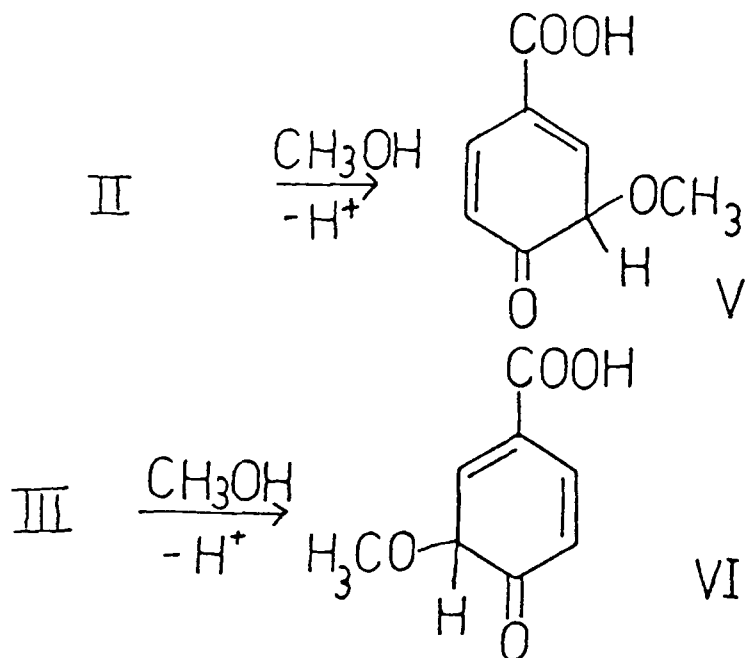
Although the number of electrons transferred in the various oxidation steps was not experimentally determined, it can be inferred from other studies that it involves two electrons {20,21}. In acidic media non-ionised phenols undergo a two-electron irreversible oxidation step to give the phenoxonium ion, which may then undergo further chemical reactions. However, in basic media, phenol ionises to the phenoxide anion, which subsequently undergoes a reversible one-electron oxidation yielding a phenoxy radical. Therefore, given the irreversibility of the electrode process indicated by the cyclic voltammetric results plus the acidic nature of the supporting electrolyte (pH 3.5), the inference of a two-electron step seems reasonable.

If the oxidation of p-hydroxybenzoic acid (I) is considered in terms of a two-electron step, then the following mechanism is possible:



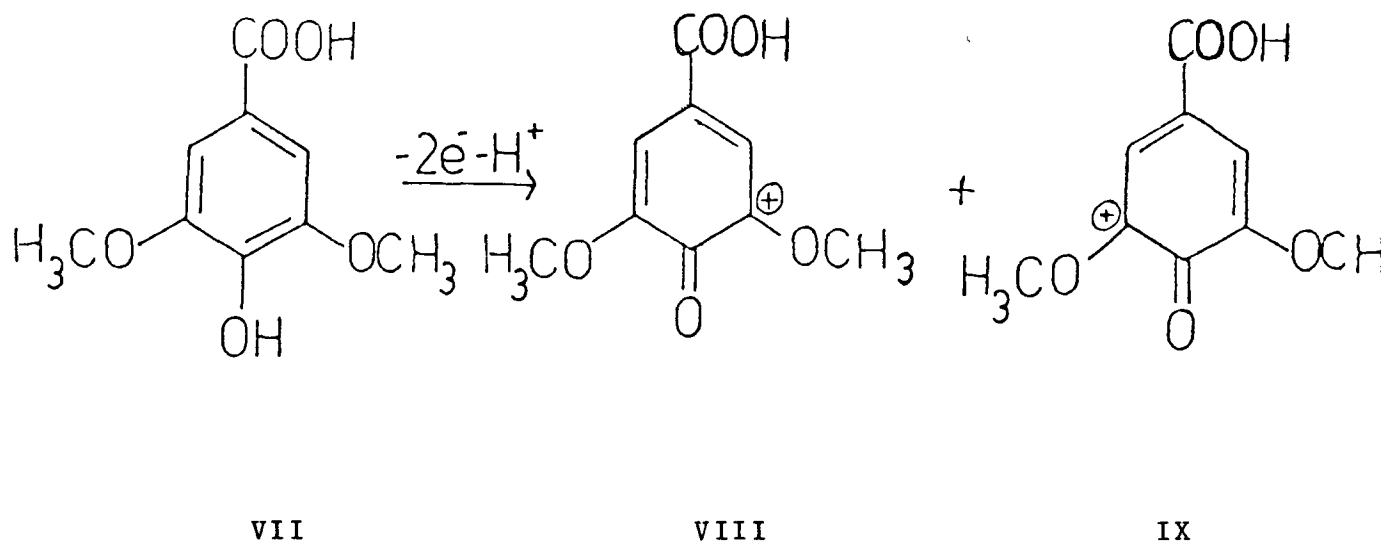
A number of possible phenoxonium ion intermediates may be formed on oxidation of (I). Closer examination of these intermediary products reveals the improbability of (IV) ever existing. The COOH group attached to the benzene ring has an overall electron-withdrawing effect. Hence, any charge on the carbon attached to this COOH substituent is especially unstable {22}. Although the COOH group withdraws electrons from all positions of the benzene ring, it especially withdraws them from the carbon to which it is attached. Therefore, this carbon atom, which already suffers an electron deficit, is unable to accommodate this extra positive charge. Consequently, it is highly unlikely that (IV) is formed.

Further chemical reaction of (II) and (III) follows the initial electrochemical step. In the presence of methanol, the phenoxonium ion is known to undergo nucleophilic attack resulting in the formation of a single major product {23}. Under the present experimental conditions a similar reaction is predicted for phenoxonium ions (II) and (III):



Comparison of the anodic peak potential value for p-hydroxybenzoic acid with those for the remaining benzoic acid derivatives reveals that p-hydroxybenzoic acid is the most difficult phenolic compound to oxidise. This is related to structural differences between the individual benzoic acid derivatives (Fig. 5.1). All the benzoic acid derivatives except p-hydroxybenzoic acid have substituents meta to the  $\text{COOH}$  group. These meta substituents, e.g.,  $\text{OH}$  and  $\text{OCH}_3$ , are electron-releasing, thereby facilitating easy oxidation of the para  $\text{OH}$  group. In addition, these electron-releasing substituents are also able to stabilise

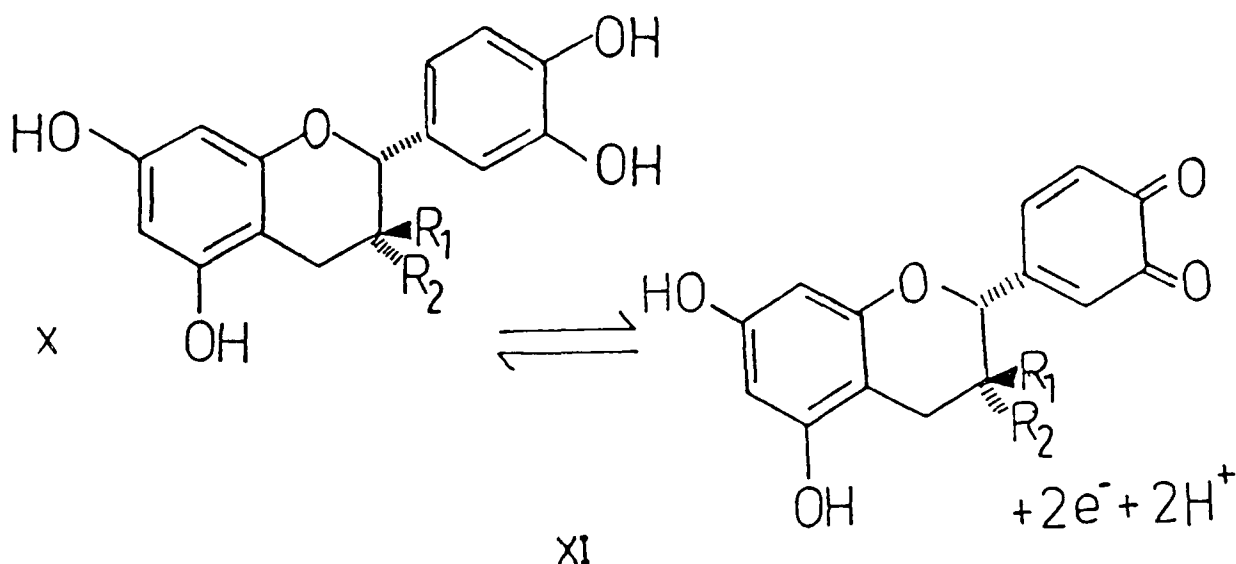
any intermediary cationic species produced during electrochemical oxidation. For example, if the oxidation of syringic acid (VII) is considered, then the following initial products are possible:



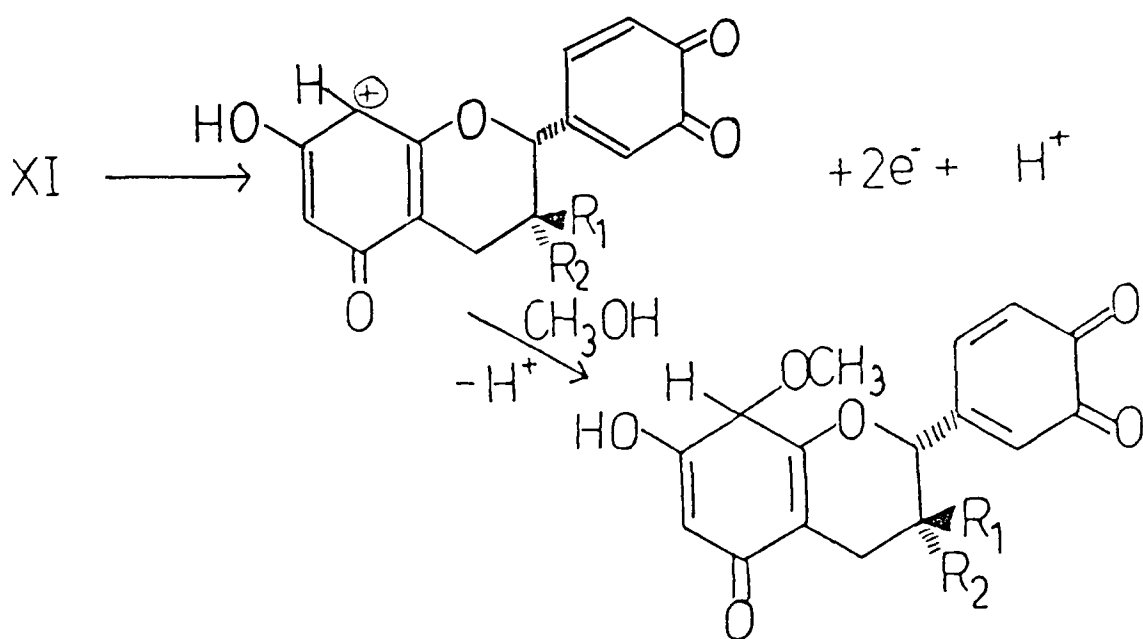
Products (VIII) and (IX) are the most probable because the electron-donating properties of the meta - methoxy group stabilise the positive charge on the carbon to which it is attached. Because (VIII) and (IX) are only transient products, further chemical reactions, probably involving nucleophilic attack by methanol, will occur, resulting in final products similar to those postulated for p-hydroxybenzoic acid.

Cinnamic acid derivatives also undergo an irreversible two-electron oxidation step. A number of possible oxidation sites exist for cinnamic acid derivatives. Chemical oxidation of the vinylic side-chain can occur under mild oxidation conditions {24}. However, the likelihood of electrochemical oxidation at the same position when the side-chain contains the COOH electron-withdrawing group is remote. The other possibility is oxidation of the hydroxy group attached to the aromatic ring. Such a mechanism would be similar to that already postulated for the benzoic acid derivatives.

The anodic peak potentials of the two flavanols are very similar, which is hardly surprising as both are isomeric forms of one another. The 30 mV difference between the first anodic and cathodic peaks indicates that the first step is a reversible two-electron transfer. This may be represented as follows:



The presence of the second more positive anodic peak indicates further irreversible oxidation of (XI). The similarity of peak heights of the two anodic peaks suggests a further two-electron process, yielding (XII) as a possible product. This may then undergo a subsequent chemical reaction:



The appearance of a single cathodic wave indicates that sufficient product (XI) is present in the vicinity of



the electrode to be reduced back to (X).

In summary, the cyclic voltammetric results indicate an irreversible two-electron oxidation step for benzoic and cinnamic acid derivatives. The intermediary cationic species most likely undergo subsequent nucleophilic attack to give stable products. By contrast, flavanols undergo a reversible two-electron step followed by a further irreversible electrochemical step.

Based on the cyclic voltammetric results, a detection potential of + 0.9V would appear suitable for the detection of all phenolic compounds studied except p-hydroxybenzoic acid. This value was subsequently used in the initial HPLC studies. However, because hydrodynamic rather than quiescent conditions prevail in the electrochemical detector, further optimisation of this detection potential was necessary (see Section 5.3.3.3).

### 5.3.2. HPLC Separation of Phenolic Compounds

The original analytical scheme on which this work is based was developed at A. Guinness & Co. Ltd., Dublin, and was applied to the determination of phenolic compounds in beers and worts {25}. This method comprised of reverse-phase HPLC and incorporated a linearly increasing

methanol gradient from 0 to 50% (V/V) in 2.5% (V/V) aqueous acetic acid over thirty minutes.

5.3.2.1. General Features of Separation of Phenolic Compounds Using Gradient Elution

When the original gradient conditions described above were used in this study the same degree of resolution was not achieved. A further increase in acid concentration from 2.5 to 3.5% (V/V) was necessary before a comparable separation was achieved.

In Table 5.2 the retention times for a mixture of phenolic compounds are listed. The elution order is typical of reverse-phase chromatography; that is, polar compounds elute first, followed by

Peak No.	Phenolic Compound	Retention Time (min)	
		UV Detector	EC Detector
1	Gallic acid	5.90	6.00
2	Protocatechuic acid	8.50	8.60
3	p-Hydroxybenzoic acid	13.24	nd
4	(+)-Catechin	13.24	13.34
5	Vanillic acid	16.50	16.60
6	Caffeic acid	17.60	17.70
7	Syringic acid	18.20	18.30
8	(-)-Epicatechin	18.60	18.70
9	p-Coumaric acid	22.80	22.90
10	Ferulic acid	24.30	24.40
11	Sinapic acid	25.00	25.10

TABLE 5.2. Retention times for a mixture of phenolic compounds determined by reverse-phase gradient elution HPLC using UV and EC detectors. The concentration of each phenolic compound in this mixture was 1 mg/l.

nd - not detected.

those of decreasing polarity. Typical chromatograms for the eleven-component mixture of phenolic compounds using UV and EC detectors are shown in Fig. 5.2. The chromatogram corresponding to the EC detector (Fig. 5.2b) does not contain any peak due to p-hydroxybenzoic acid because the applied detector potential is not sufficiently positive to oxidise it. Voltammetric studies indicate that a detector potential of approximately + 1.20V is necessary to detect p-hydroxybenzoic acid. Nonetheless, this illustrates how varying the electrochemical detector potential achieves the selective determination of compounds. However, such selectivity is only possible if the anodic peak potentials are separated by a 100mV difference. In such instances if the least positive potential is chosen for detection purposes, only those compounds whose oxidation potentials are less than or equal to this value are detected. Those species with more positive oxidation potentials remain undetected. However, in situations where two compounds whose peak potentials differ by less than 100 mV then both will be detected even if the peak potential of the least positive compound is used. In such circumstances, differential pulse detection mode offers greater selectivity over amperometric detection {26,27}.

In general, the response of the EC detector was remarkably good. Furthermore, the mobile phase acted as a

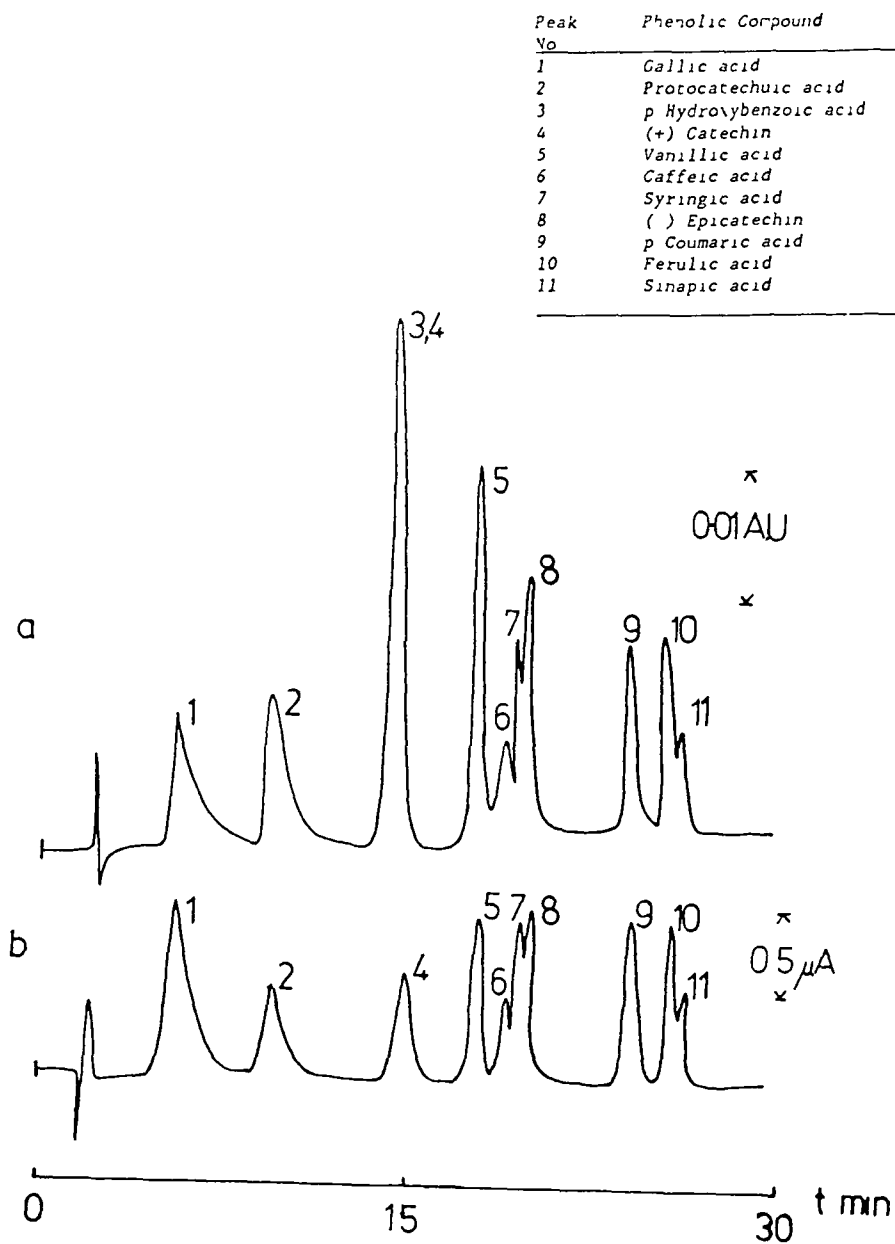


Fig. 5.2. Comparison of HPLC separation of phenolic compounds using (a) an ultraviolet and (b) an electrochemical detector connected in series.

sufficiently good electrolyte and did not require the presence of additional electrolyte. Poor conductivity of solutions is manifested by increased noise problems even when detectors are operated at low sensitivities. In such situations, baseline fluctuations are the most common indication of noise. However, this type of behaviour was not evidenced, even at high sensitivity settings.

Chromatograms obtained with the UV detector (Fig. 5.2a) contain ten instead of the expected eleven peaks. This arises because p-hydroxybenzoic acid and (+)-catechin co-elute and appear as a single peak in the chromatogram. This fact was established by analysing binary mixtures of phenolic compounds and also by injecting each compound separately onto the column to ensure that each compound was being detected by the UV detector. When separately injected, p-hydroxybenzoic acid and (+)-catechin each resulted in a single peak but their retention times were very similar (Table 5.3).

---

Phenolic Compound	Retention Time (min)
p-Hydroxybenzoic acid	13.23
(+)- Catechin	13.26

---

TABLE 5.3. Retention times for 1 mg/l p-Hydroxybenzoic acid and 1 mg/l (+)- Catechin measured from their UV chromatograms.

The similarity in the retention times of these compounds explains why these two compounds co-elute.

Occasionally, additional peaks were noticed in the later sections of the UV and EC chromatograms. At first it was thought that these peaks were caused by solvent impurities because gradient elutions are particularly prone to such problems {28,29}. Solvent impurities are manifested in chromatograms as extraneous peaks and severe baseline drift. By carrying out gradient elutions in the absence of injected sample solutions a straight baseline without any peaks was obtained. This was followed by

injections of methanol at the commencement of the gradient elution. Again the same results as before was obtained. Therefore, these additional peaks were not due to impurities present in the mobile phase solvents or the solvent in which the phenolic compounds were prepared. Further examination of this problem revealed that these additional peaks were only present in the chromatograms of phenolic compounds. Consequently, it appeared that some "new products" were being formed in these mixtures. Fresh mixture of the phenolic compounds were prepared and injected onto the column. Chromatograms similar to those in Fig. 5.2 were obtained. However, after one week, additional peaks began to appear. These additional peaks eluted with the same retention times as those observed in previous chromatograms. Furthermore, these peaks always eluted before the peaks corresponding to the cinnamic acid derivatives, suggesting that these 'new products' are similar in polarity to these compounds. It has been demonstrated that these additional peaks are due to the presence of cis-isomers of the cinnamic acid derivatives {30,31}. The possibility of cis- and trans-isomer forms of cinnamic acid derivatives arises because of a vinyl side-chain (see Fig. 5.1). On exposure of the trans-isomer to UV radiation or daylight, an equilibrium cis-trans mixture forms in methanolic solutions. However, equilibrium mixtures are formed more rapidly in solutions



exposed to UV radiation than those exposed to daylight. This explains why it took approximately a week before the cis-isomer peaks appeared in UV and EC chromatograms. In all further studies samples were constantly stored in darkness, consequently, isomerisation was prevented.

Under the experimental conditions used in this study the cis- and trans-isomers were sufficiently resolved to allow quantification of the two forms. This illustrates the suitability of the column packing and mobile phase composition to separate geometrical isomers of some cinnamic acid derivatives.

Another feature of the separation was peak tailing associated with gallic and protocatechnic acids (peaks 1 and 2 in Fig. 5.2). This tailing was very pronounced, rendering these peaks unsuitable for analytical purposes. Isolation and elimination of this phenomenon is difficult because tailing is caused by any of a variety of factors {32}, e.g., column overloading, poor resolution, solute ionisation or poorly packed columns. Given that both compounds contain a COOH group, the possibility of the tailing arising from solute ionisation was checked. Solute ionisation occurs chiefly when the pH of the mobile phase either equals or is slightly greater than the  $pK_a$  of the solute. The severity of the tailing is greatest when the

$pK_a$  of the solute equals the pH of the mobile phase because approximately half the compound is ionised. However, the ionisation, and consequently the peak tailing, is suppressed by lowering the pH or alternatively buffering the mobile phase {32}. In the present study, the pH of the mobile phase was lowered by increasing the acetic acid concentration from 3.5 to 10.0% (V/V). Unfortunately, this did not eliminate the peak tailing; in fact, it tended to exacerbate the problem. Furthermore, there was a considerable loss of resolution in the middle section of chromatograms from both detectors. The increase in acid concentration caused vanillic, caffeic and syringic acids to co-elute. In general, increasing the acetic acid concentration caused a reduction in the retention times of the phenolic compounds because the solvent strength was effectively decreased. The reduction in retention times was greater for the benzoic acid derivatives than it was for the cinnamic acid derivatives, Hence, in the middle section of the UV and EC chromatograms where both benzoic and cinnamic acid derivatives elute, the relative separation between the two groups changes because their retention times are changing at different rates.

As the tailing did not seem to result from solute ionisation, the possibility of it arising from poor resolution was examined. On decreasing the mobile phase

flow-rate the appearance of a shoulder on both peaks became apparent. This type of behaviour is associated with a poor resolution between two components so that they appear as a single tailing peak and is referred to as "pseudo-tailing" {32}. These pseudo-tails associated with gallic and protocatechuic acids are probably degradation products of the former phenolic compounds. This was suggested by the increased severity of the tailing with increasing age of the standards.

A problem usually encountered in reverse-phase HPLC, especially when using bonded-phase packing with low concentrations (typically less than 10% (V/V)) of organic solvent, is peak broadening {33}. It happens because bonded-phase packings such as C<sub>18</sub> are very hydrophobic; therefore, "wetting" or contact between it and the mobile phase is poor as both phases are very dissimilar. Improvements in "wetting" can be made by adding organic solvent to the mobile phase. In some instances, as much as 40-50% (V/V) of organic solvent may be required to satisfactorily accomplish high efficiency operating conditions {34}. In order to check the "wetting" efficiency of the column by the mobile phase, methanol was added to the aqueous acetic acid. At the beginning of the gradient elution the concentration of organic solvent is minimal; therefore, the greatest improvement was expected

in the early sections of the chromatograms. Unfortunately, because of the pseudo-tailing of gallic and protocatechuic acids, no improvement in the parent peaks was observed. For the remaining peaks the increase in methanol concentration did not cause any noticeable decrease in peak broadening. The only effect that the change in methanol concentration has was a reduction in resolution and retention times. Even with only a 1% (V/V) increase in methanol concentration a considerable loss of resolution in the middle section of the chromatograms occurred. A further increase in methanol concentration only further disimproved the resolution in this middle section. In general, a decrease in the retention times of the phenolic compounds was observed as the methanol concentration increased. Furthermore, the retention times of the cinnamic acid derivatives decreased faster than those for the benzoic acid derivatives. Consequently, the separation between these two groups decreased. In order to explain this behaviour, the structures of these two groups must be considered. The presence of a vinyl side-chain in the cinnamic acids is the principal difference between these two groups. This non-polar side-chain will increase solubility of the cinnamic acid derivatives in methanol. Consequently, increasing the methanol content of the mobile phase will favour the solubility of the cinnamic acid derivatives and correspondingly decrease their retention

times more than those of the benzoic acid derivatives. This accounts for the loss of resolution in the middle section of the chromatograms because the retention time of caffeic acid is decreasing faster than that for vanillic acid, so the peaks begin to overlap. Eventually these two acids co-elute and resolution between the two acids is lost.

In summary, it appears that the middle section of the UV and EC chromatograms, where benzoic and cinnamic acid derivatives elute, is very sensitive to any change in mobile phase composition. The most suitable mobile phase composition appears to be a linearly increasing methanol gradient from 0-50% (V/V) in 3.5% aqueous acetic acid over thirty minutes. However, under these conditions p-hydroxybenzoic acid and (+)-catechin co-elute. Any increase in either the acetic acid or methanol content of the mobile phase does not resolve these two compounds.

#### 5.3.2.2. Isocratic Elution as an Alternative to Gradient Elution for the Separation of Phenolic Compounds

In general, isocratic separations are preferred to gradient elution in HPLC analysis as it is possible to obtain greater precision of quantitative data. One of the chief disadvantages encountered in gradient elutions is

baseline drift, which is especially evident in chromatograms when high detector sensitivities are used. The nuisance value of baseline drift is that it makes the measurement of peak heights extremely difficult because of the uncertainty in trying to establish the true baseline. Because of this uncertainty in baseline, accurate measurements of peak heights are often almost impossible or at the very least, extremely error prone. Hence, the validity of results obtained under such circumstances is questionable. A further problem associated with gradient elution is the appearance of a spurious peaks, interspersed with the normal chromatographic peaks of eluting compounds. These spurious peaks arise from impurities present in the mobile phase solvents {29}.

Given the advantages of isocratic elution, the possibility of its application to the separation of the phenolic compounds was explored. On the basis of the gradient elution studies a mobile phase composition of 25% methanol - 75% water (containing 3.5% (V/V) acetic acid) was used in isocratic elutions. The remaining experimental conditions are the same as those used in the gradient elution previously described.

One of the most noticeable aspects of changing from gradient to isocratic elution was the change in

retention times ( $t_R$ ). As shown in Table 5.4, the retention times of the phenolic compounds increased considerably compared with the  $t_R$  values obtained using gradient elution (see Table 5.2). The largest increases in  $t_R$  values were observed for the cinnamic acid derivatives. In particular, sinapic acid which is the most strongly retained phenolic had a retention time of 114 min. compared with 25 min. using gradient elution. This represents an approximate five-fold increase in its  $t_R$  value on switching to isocratic elution. Although the increase in  $t_R$  values for the remaining phenolic compounds are not as large as that for sinapic acid, nevertheless, the increases are significant.

Associated with the large  $t_R$  values was severe band broadening of p-coumaric, ferulic and sinapic acids. To illustrate the severity of this band broadening, the peak widths at half-height ( $W_h$ ) of the aforementioned phenolic compounds are shown in Table 5.5. These values are compared with the corresponding  $W_h$  values using the previously gradient elution system.

Phenolic Compound	Retention Time (min )	
	UV Detector	EC Detector
Gallic acid	7.80	7.90
Protocatechuic acid	8.30	8.40
p-Hydroxybenzoic acid	18.60	nd
(+)- Catechin	18.60	18.70
Vanillic acid	24.80	24.90
Caffeic acid	25.10	25.20
Syringic acid	30.00	30.10
(-)-Epicatechin	39.00	39.10
p-Coumaric acid	56.50	56.60
Ferulic acid	81.00	81.10
Sinapic acid	114.00	114.10

TABLE 5.4. Retention times for a mixture of phenolic compounds determined by reverse-phase isocratic elution HPLC using UV and EC detectors. The concentration of each phenolic compound was 1mg/l. Flow-rate, 2.0 ml./min. nd - not detected.



Phenolic Compound	$W_h$ (mm)	
	Isocratic Elution	Gradient Elution
p-Coumaric acid	17.0	2.5
Ferulic acid	23.5	2.0
Sinapic acid	28.0	2.0

TABLE 5.5. Comparison of peak widths at half-height ( $W_h$ ) of three cinnamic acid derivatives using isocratic and gradient elutions. Values of  $W_h$  were determined from chromatograms corresponding to the UV detector.

Whilst the  $W_h$  values shown in Table 5.5. were measured from chromatograms obtained with the UV detector, the same severity in band broadening occurred in chromatograms corresponding to the EC detector.

As a result of band broadening, the peaks corresponding to these three cinnamic acid derivatives are totally unsuitable for analytical purposes. In particular, there is the danger of peak overlap being undetected given

the large size of these phenolic peaks. Such a situation could lead to erroneous results if the peak area were used for quantitative purposes. In order to be suitable for analytical measurement, the  $W_h$  values would need to be similar in size to those values measured from gradient elution chromatograms.

A further feature of the separation was that the co-elution of p-hydroxybenzoic acid and (+)-catechin remained despite the change from gradient to isocratic conditions. Also, the pseudo-tailing associated with gallic and protocatechuic acids still existed. The peaks giving rise to these pseudo-tails were not sufficiently resolved from the parent peaks to allow the parent peaks to be used for quantitative purposes.

The problems of band broadening and loss of resolution arise because the phenolic compounds have a wide range of retention times or capacity factor ( $k'$ ) values. Numerical calculation of  $k'$  values were made using the following equation {35}:

$$k' = \frac{t_R - t_0}{t_0} \quad (5.1)$$

where  $t_R$  is the retention time of any retained compound and

$t_0$  the time for unretained solvent molecules to move from one end of the column to the other. The calculated values are shown in Table 5.6. A considerable diversity of  $k'$  values were found. The optimum range for  $k'$  is  $1 < k' < 10$ . However, the  $k'$  values of some phenolics are outside this range. In order to reduce the  $k'$  and  $t_R$  values, the solvent strength would have to be increased, i.e., the polarity of the mobile phase would be reduced. This could be achieved by increasing the percentage methanol in the mobile phase. This would reduce retention times and also  $k'$  values, and consequently diminish, if not eliminate, the problem of band broadening. However, the increased solvent strength would cause further loss of resolution between gallic and protocatechuic acids and also between vanillic and caffeic acids because of decreased  $k'$  values. These early-eluting compounds would require that their  $k'$  values be increased, which would necessitate a reduction in solvent strength. It is not possible to simultaneously suit both conditions using isocratic conditions.

As shown in Section 5.3.2.1. gradient elution overcomes the problems encountered in isocratic elution. This is largely due to the fact that in gradient elutions the mobile phase composition is continuously changing. Thus, it allows separate optimisation of  $k'$  values of the individual phenolic compounds as they move through the

Phenolic Compound	Capacity Factor	
	UV Detector	EC Detector
Gallic acid	2.19	2.23
Protocatechuic acid	2.40	2.44
p-Hydroxybenzoic acid	6.62	nd
(+)-Catechin	6.62	6.66
Vanillic acid	9.16	9.20
Caffeic acid	9.28	9.32
Syringic acid	11.29	11.33
(-)-Epicatechin	14.98	15.02
p-Coumaric acid	22.15	22.19
Ferulic acid	32.19	32.23
Sinapic acid	45.72	45.76

TABLE 5.6. Capacity factor values of phenolic compounds calculated from retention times corresponding to their UV and EC chromatograms. Isocratic elution was used to separate the phenolic compounds.  
nd - not detected.

column. Therefore, the problems of band broadening, poor resolution of early-eluting compounds and long separation time encountered in isocratic elution, are overcome.

### 5.3.3. Optimisation of Chromatographic Conditions

In this section the various experimental parameters pertaining to the separation and resolution of the phenolic compounds are optimised in terms of the response from the UV and EC detectors. The principal objective of this optimisation was to increase the sensitivity of the analytical method, however, it also serves to illustrate some differences in the operating principles of the two detectors.

#### 5.3.3.1. Gradient Shape and Steepness

These are important parameters which must be considered when designing any gradient elution separation. Improper selection of these parameters will simultaneously cause over-separation of some compounds and inadequate resolution of others in a single chromatogram.

A number of options exist for gradient shape. It may be linear or alternatively it can be varying grades of concave or convex.

A linear gradient was employed for the separation of the phenolic compounds (Fig. 5.2). This resulted in an even distribution of peaks over an entire chromatogram, indicating the suitability of the gradient shape used. Furthermore, peak widths are similar for all components except gallic and protocatechuic acids. If the gradient shape had been incorrectly chosen then the peak widths of the later-eluting peaks would be different from those eluting in the early section of a chromatogram.

Gradient steepness, or rate of change with time, is determined by the time scale required for gradient elution from solvent A to solvent B and is normally expressed as  $\Delta\%v\ B/\text{min}$ . The linear gradient employed for the separation of the phenolic compounds shown in Fig. 5.2 has a gradient steepness equal to  $1.67\%v\ B/\text{min}$ . In order to ascertain the suitability of this gradient steepness, the steepness was changed. It was first reduced to  $1.25\%v\ B/\text{min}$ , i.e., the time taken to carry out the gradient elution was increased. This decrease in steepness caused a considerable increase in the resolution of the phenolic compounds but this benefit was negated by a loss of sensitivity and an increase in separation time. Reduced sensitivity was manifested by a decrease in peak heights in the UV and EC chromatograms. In addition, the reduction in gradient steepness also caused a broadening of the peaks;

the peaks became rounded and were not as sharply defined as those at the steeper gradient (1.67%v B.min).

On increasing the gradient steepness to 2%v B/min the opposite effect was observed. Sensitivity increased as the peaks became sharper and narrower but the resolution between peaks decreased as they became more tightly bunched together. This was due to the decrease in separation time on increasing the gradient steepness.

Based on the preceding results a gradient steepness of 1.67%v B/min, or 3.2%v B/t<sub>0</sub>, was chosen as the optimum condition for adequate resolution of the phenolic compounds. This gradient steepness is the best compromise in terms of sensitivity and resolution.

#### 5.3.3.2. Mobile Phase Flow-Rate

Another possible option for improving resolution in gradient elution is to change the mobile phase flow-rate through the column. Altering the flow-rate changes the number of theoretical plates (N) in the column, thereby changing the column efficiency.

In the present study the flow-rates examined were limited to values between 1.5 and 2.2 ml/min. An upper

limit of 2.2 ml/min was imposed because higher flow-rates caused the column pressure to exceed its operating limit of 3000 p.s.i. Flow-rates of less than 1.5 ml/min require separation times in excess of forty minutes, which is too long if this analytical method is to be useful in industrial applications. In the previous section an optimum gradient steepness equal to  $3.2\% v B/t_0$  was chosen. However, to maintain this optimum steepness as the flow-rate is changed, the rate of change of mobile phase composition must also be proportionally changed. If the rate of change of mobile phase composition remained unaltered, as the flow-rate was decreased, then the gradient steepness would effectively increase. This arises because of the dependence of the gradient steepness ( $\% v B/\text{min}$ ) on  $t_0$  (retention time of unretained mobile phase molecules) as shown by the following equation {36}:

$$\Delta\% v B/\text{min} = \text{constant}/t_0 \quad (5.2)$$

Values were calculated from equation 5.2 for the rate of change of mobile phase composition corresponding to each flow-rate. These calculated values and the elapsed time for each gradient elution at the particular flow-rate employed are shown in Table 5.7. As the flow-rate is increased the rate of change of solvent B increased and the elapsed time for the gradients decreased. Consequently, the gradient steepness is maintained equal to the optimum value of  $3.2\% v B/t_0$ .



Flow-Rate (ml/min)	$t_0^+$ (min)	Rate of Change of Solvent B* per minute ( $\Delta\%v$ B/min)	Elapsed Time for Gradient (min)
1.5	2.56	1.25	40.00
1.6	2.41	1.33	37.59
1.7	2.21	1.45	34.48
1.8	2.15	1.49	33.56
1.9	2.04	1.57	31.85
2.0	1.92	1.67	30.00
2.1	1.84	1.74	28.73
2.2	1.76	1.82	27.47

Table 5.7. Values calculated for  $\Delta\%v$  B/min at each flow-rate to maintain the gradient steepness equal to  $3.2\% v B/t_0$ . Also shown are the elapsed time for each gradient elution at the corresponding flow-rate.

$t_0^+$  refers to the retention time of unretained solvent molecules.

\* B corresponds to 100% methanol.

The dependence of detector response, measured in terms of peak heights, on mobile phase flow-rate was markedly different for the UV and EC detectors. First the results for the UV detector are considered. UV detector chromatograms for mixtures of phenolic compounds displayed an overall average decrease of 2.5% in peak height as the mobile phase flow-rate was increased from 1.5 to 2.0 ml/min. However, further increase in flow-rate from 2.0 to 2.2 ml/min caused an average 4.5% decrease in peak height. Additional examination revealed the consistency of these results. In all cases there was a larger reduction in peak height using flow-rates greater than 2.0 ml/min. Whilst these decreases in peak heights are quite small, the results do indicate some dependence on mobile phase flow-rate.

Resolution between peaks was also affected by changing the flow-rate. On increasing the flow-rate from 1.5 to 2.2 ml/min a decrease in peak resolution resulted. However, despite this decrease, the peaks were sufficiently resolved even at 2.2 ml/min to be separately measured without any difficulty. Although the peaks were well resolved at 1.5 ml/min, p-hydroxybenzoic acid and (+)-catechin still co-eluted.

Because the response of UV detectors is independent

of flow-rate, the decrease in peak height on increasing mobile phase flow-rate cannot be attributed to the operating characteristics of the detector. Instead, it may be interpreted in terms of a reduction in the theoretical plate number (N) of the column on increasing the flow-rate. Increasing the flow-rate reduces the value of N, which causes the column efficiency and the resolution between peaks to decrease. At flow-rate above 2.0 ml/min the decrease in effective plate number occurring means that the optimum flow-rate is in the range of 1.5 to 2.0 ml/min when the UV detector is used.

Contrasted with the results for the UV detector are those obtained with the EC detector. The dependence of peak height or peak current of (+)-catechin, vanillic acid and sinapic acid on mobile phase flow-rate is illustrated in Fig. 5.3. These results are representative of the trend for the other phenolic compounds not shown.

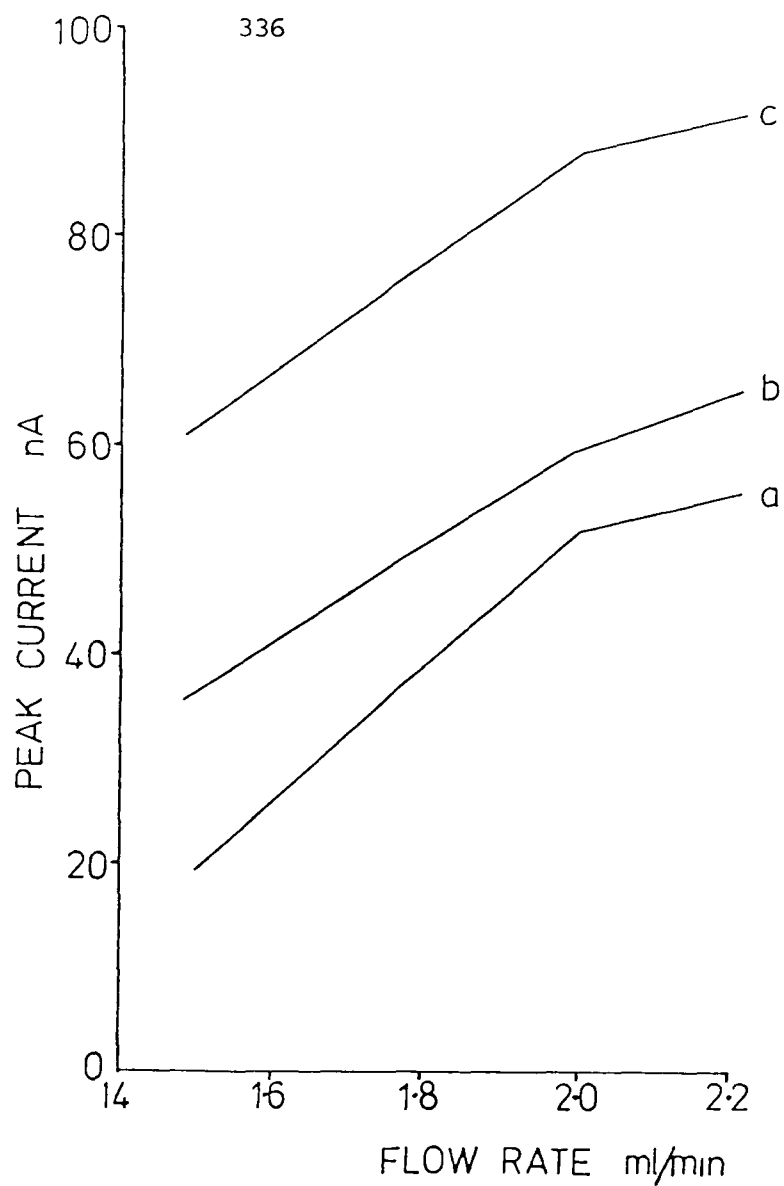


Fig. 5.3. Dependence of peak current on flow-rate for (a) (+)-catechin, (b) sinapic acid and (c) vanillic acid.

Linear increases in peak currents result on increasing the flow-rate up to 2.0 ml/min. Further increases in peak currents result at higher flow-rates but these increases are not as large as those at the lower flow-rates. The fact that the increase was considerably reduced compared with lower flow-rates was initially interpreted in terms of increasing electrode passivation by adsorption of oxidation products on the electrode surface. The circumstances giving rise to this type of behaviour can be explained by considering the overall system. In hydrodynamic voltammetry species are transported to the surface of the working electrode by convection. Subsequently, these species undergo electrochemical change at this electrode surface. Therefore, increasing the mobile phase flow-rate increases convection, so more analyte molecules are transported to the electrode surface. This increase in concentration of analyte molecules at the electrode surface will result in an increased detector response, which is manifested as an increase in peak current in the corresponding chromatogram.

For the phenolic compounds studied, this increase in their concentration at the electrode surface with increasing flow-rates was assumed to increase the amount of adsorption because phenols are known to be adsorbed at

electrode surfaces {20,23}. Consequently, this adsorbed material would reduce the electrode sensitivity. Furthermore, passivation by adsorbed products was thought to be cumulative, as each increase in flow-rate would correspondingly increase the amount of adsorbed material. This was considered to be so because the surface of the working electrode was not cleaned before each incremental change in flow-rate from 1.5 to 2.2 ml/min.

In order to check this hypothesis, the working electrode was polished before each increase in flow-rate. Care was taken not to excessively polish the electrode as this would degrade the surface of the electrode {37}. Increases in peak currents were observed on cleaning the electrode surface. For flow-rates up to 2.0 ml/min this increase was generally small, the average increase in peak current being 4-6%. At the higher flow-rates of 2.1 and 2.2 ml/min the increase in peak currents was 7-9%. These results would seem to indicate that electrode passivation is occurring but that it is not as significant as originally assumed, especially at higher flow-rates. Despite the increase in peak current, on cleaning the working electrode, there is little or no change in the shape of graphs of peak current versus flow-rate. At higher flow-rates (2.1 and 2.2 ml/min) the peak currents do not increase as quickly as those at lower values.

Consequently, the smaller increase in peak currents at flow-rates between 2.0 and 2.2 ml/min is attributable largely to a reduction in the theoretical plate number of the column. Indeed, this explanation would corroborate the results obtained using the UV detector. For both detectors the decrease in  $N$  becomes important at flow-rates greater than 2.0 ml/min. Because the UV detector response is independent of flow-rate, the reduction of  $N$  above 2.0 ml/min immediately causes a reduction in peak heights of eluting compounds. The EC detector response is flow-rate dependent; therefore, increasing the flow-rate increases the resultant peak currents of detected compounds. However, above 2.0 ml/min any increase in peak current is largely negated by a decrease in  $N$ , consequently the peak currents do not increase at the same rate as those at flow-rates below 2.0 ml/min.

Based on these results, it appears that a flow-rate of 2.0 ml/min is the optimum value when the EC and UV detectors are connected in series.

#### 5.3.3.3. Electrochemical Detector Potential

In HPLC analysis most electrochemical detectors are based on constant potential amperometry, i.e., the current is measured as a function of time at a constant

applied potential. This immediately poses the problem of choosing a suitable detector potential. Usually the applied detector potential corresponds to the minimum potential at which the current reaches its limiting current plateau; it is known as the plateau potential ( $E_{\text{plateau}}$ ). By operating at  $E_{\text{plateau}}$  the maximum current response of the analyte is obtained at all times. This is especially important in trace analysis where the current response will be greatly diminished due to lower analyte concentrations.

A number of methods are employed for estimating  $E_{\text{plateau}}$  based on either direct or indirect measurement. Direct measurement of  $E_{\text{plateau}}$  values is made using hydrodynamic voltammetry (HDV). Using HDV the current is measured as a function of the applied detector potential. From the resulting chromatovoltammogram, which is similar in shape to a DC polarogram, the value of  $E_{\text{plateau}}$  can be measured directly. Indirect determination of  $E_{\text{plateau}}$  values is undertaken using techniques such as cyclic voltammetry (CV) or linear sweep voltammetry in a separate cell under quiescent conditions.

In this study, preliminary investigations were undertaken using cyclic voltammetry in quiescent conditions, because the determination of  $E_{\text{plateau}}$  by CV is considerably faster than by HDV. From this work an



arbitrary potential of +0.9V was chosen for the detection of phenolic compounds. However, values of  $E_{\text{plateau}}$  obtained by indirect methods are often not sufficiently accurate when applied to electrochemical detectors operating in hydrodynamic conditions. This is the case because the shape of hydrodynamic voltammograms is dependent on flow-rate, cell geometry and electrode surface properties. Consequently,  $E_{\text{plateau}}$  values determined by HDV will differ from those determined by indirect measurement. For example, in the case of species undergoing oxidation,  $E_{\text{plateau}}$  as determined by HDV is shifted to more positive values than the value obtained with cyclic voltammetry [38]. Because of this fact, further optimisation of the original detector potential of +0.9V was necessary. This investigation was limited to potentials between +0.90 and +1.10V. When the detector potential was increased to +1.20V a significant increase in background current and noise level occurred. This was manifested on the chart recorder as increase in baseline. It required almost one hour before the baseline settled to its original position and hence before any sample could be injected into the system. Further increases in the applied detector potential would presumably cause even larger background currents as the potential limit of the glassy carbon working electrode is approached.

Phenolic Compound	Peak Current (nA)				
	Detector	Potential (V vs. Ag/AgCl)			
	0.90	0.95	1.00	1.05	1.10
Gallic acid	60	62	64	64	64
Protocatechuic acid	40	42	42	42	42
p-Hydroxybenzoic acid	nd	nd	nd	nd	nd
(+)-Catechin	36	46	54	54	54
Vanillic acid	66	80	88	88	86
Caffeic acid	32	32	32	32	32
Syringic acid	92	94	92	92	92
(-)-Epicatechin	84	82	84	88	84
p-Coumaric acid	36	60	110	112	110
Ferulic acid	90	88	90	90	90
Sinapic acid	46	48	49	48	48

Table 5.8. Peak currents of phenolic compounds measured over a range of applied detector potentials. nd - not detected.

The results of the peak currents measured at the different detector potentials are illustrated in Table 5.8. Except for (+)-catechin, vanillic acid, p-coumaric acid and p-hydroxybenzoic acid the increase in detector potential does not alter the response of the phenolic compounds. From the original cyclic voltammetry studies, plateau potentials of +0.89V +0.90V and +0.95V were estimated for (+)-catechin, vanillic acid and p-coumaric acid, respectively. Under hydrodynamic conditions these  $E_{\text{plateau}}$  values are shifted to more positive potentials.

Because of the large number of phenolic compounds it is impossible to measure each compound at its own  $E_{\text{plateau}}$  value as it would necessitate too many measurements for a single sample. Instead, a compromise potential is sought which corresponds to the minimum potential to yield the maximum peak current for all the phenolic compounds. As seen from Table 5.8., this corresponds to a potential of +1.0V. It is not possible to detect p-hydroxybenzoic acid at this potential. An  $E_{\text{plateau}}$  value of +1.20V was estimated from CV measurements for p-hydroxybenzoic acid. Obviously the potential value from HDV measurements would be more positive than this. However, it is not feasible to use such a positive detector potential as it would only increase the background currents and noise levels, and consequently the responses of the

phenolic compounds would be diminished. In general, both background currents and noise levels tend to increase with higher polarisation voltage and are usually greater in eluents based on mixed solvents than those based on purely aqueous solutions. Therefore, in the present mixed solvent system a detector potential of +1.0V is probably the most suitable value if the aforementioned problems are to be avoided.

In conclusion, it is advisable to use a combination of HDV and CV measurement methods when a suitable  $E_{\text{plateau}}$  value is being chosen for a large number of compounds. By using CV for initial measurements an approximate value for  $E_{\text{plateau}}$  can be quickly obtained. This value can then be optimised using HDV. In this way the number of measurements which are made by HDV are minimised.

#### 5.3.3.4. UV Detection Wavelength

In order to establish a suitable detection wavelength for the phenolic compounds, absorption maxima for these compounds were determined using a scanning UV spectrophotometer. A wide range of absorption maxima exist. Cinnamic acid derivatives strongly absorb in the wavelength range from 320 to 360 nm, whilst the remaining

phenolic compounds absorb more strongly at wavelengths between 270 and 290 nm. Given the range of absorption maxima values, it would seem that the most suitable detection wavelength lies between these two ranges. However, a more suitable method would be to have two UV detectors connected in series. If the first detector was operated at 280 nm and the second at 340 nm, then the phenolic compounds could each be detected close to its absorption maximum. Furthermore, this would have the advantage of ensuring the maximum sensitivity for all phenolic compounds. In addition, interferences between benzoic and cinnamic acid derivatives, in particular, caffeic and syringic acids both of whom have similar retention times, could be largely overcome.

Unfortunately, it was only possible to use a fixed wavelength of 254 nm for the detection of the phenolic compounds. Because of this limitation, a comparison of EC and UV detectors is hampered as the UV detector is not being operated at the optimum wavelength to ensure maximum response from the phenolic compounds.

#### 5.3.4. Comparison of UV and EC Detector Characteristics for the Determination of Phenolic Compounds

##### 5.3.4.1. Detection Limit

The detection limit is defined as the concentration of analyte that will produce a signal(S) to noise(N) ratio (S/N) of 2 and is considered to be the minimum concentration that can be detected {14}. One of the primary limitations to the operation of detectors at high sensitivities is the noise associated with the entire HPLC system. The commonest types of noise {14} are short-term noise, long-term noise and drift. Short-term noise is caused by pump pulsations as well as recorder and detector electronics; whereas, long-term noise is produced by temperature and pressure fluctuations. Drift or baseline drift results from either mobile phase or temperature variations.

Some of these potential sources of noise were overcome by the choice of HPLC equipment used in this study. The pump used ensured that pumping pulses were effectively eliminated, thereby reducing the possibility of short-term noise. This is especially important when using electrochemical detectors as they are known to be sensitive to pressure pulses within the detector cell {39}.

The presence of dissolved gases, in particular, dissolved oxygen, has been found to affect not only flow stability but also UV absorption, causing baseline drift and random noise in the response from the UV detector

{40,41}. Therefore, constant helium sparging of the mobile phase solvents, preceded by degassing with an ultrasonic bath, ensured that dissolved gases did not cause any problems. However, occasionally when the mobile phase had not been sufficiently degassed, problems were encountered. On such occasions, gas bubbles formed in the pump, completely stopping the flow of mobile phase through the column and detectors. The easiest and quickest way to remove the gas bubbles causing the obstruction was to re-prime the pump. Besides the problem of bubble formation in the pump, gas bubbles often formed in the EC detector cell on the surface of the working electrode. Such occurrences were indicated by the pen recorder connected to the EC detector going off-scale. Elimination of this obstruction necessitated the removal and cleaning of the working electrode. When refitting the electrode, it was found important that the mobile phase be flowing through the detector cell. In the absence of any mobile phase flow, further bubbles formed on the surface of the working electrode. These arose from the entrapment of air between the surface of the electrode and the surface of residual mobile phase present in the detector cell. No problems were ever encountered with the response from the UV detector when gas bubbles were present in the HPLC system. From this study it would appear that EC detectors are more prone to problems caused by the presence of dissolved gases

in the mobile phase than UV detectors.

From the results in Table 5.9, it is obvious that the best detection limits were achieved with the EC detector. One of the factors which severely limited the detection limit of the UV detector was the considerable up-scale baseline drift observed in chromatograms. This up-scale movement at high detector sensitivities was observed over the entire duration of the gradient. Consequently, the peak heights of the later-eluting compounds, e.g., p-coumaric, ferulic and sinapic acids were difficult to measure because the baseline had almost moved off-scale as these compounds eluted. Surprisingly, very little baseline drift occurred in chromatograms corresponding to the EC detector. This baseline drift is attributable to the continuously changing mobile phase composition inherent in gradient elution chromatography.

A further factor which limited the sensitivity of the UV detector was the presence of noise. This was manifested in chromatograms as a "fuzz" which widened the baseline. Hence, small peaks were enveloped by this "fuzz" making them indiscernible from the baseline. It has been stated that using a fixed-wavelength rather than a variable wavelength detector increases sensitivity because it produces less noise {42}. Given the noise problems encountered with the fixed-wavelength detector in this



Phenolic Compound	Detection Limit (mg/l)	
	UV Detector	EC Detector
Gallic acid	0.20	0.20
Protocatechuic acid	0.20	0.20
p-Hydroxybenzoic acid	-	nd
(+)-Catechin	-	0.05
Vanillic acid	0.08	0.05
Caffeic acid	0.10	0.05
Syringic acid	0.08	0.05
(-)-Epicatechin	0.08	0.05
p-Coumaric acid	0.10	0.05
Ferulic acid	0.10	0.05
Sinapic acid	0.10	0.05

Table 5.9. Comparison of the detection limits of phenolic compounds using UV and EC detectors.

nd - not detected.

study, it would seem inappropriate to use a variable wavelength detector as only higher detection limits could be expected.

Although some noise was present in chromatograms corresponding to the EC detector it did not have the same deleterious effects encountered with the UV detector. The results obtained indicate that the EC detector is less affected than the UV detector by problems of noise and baseline drift. Furthermore, the EC detector response is less affected than the UV detector by gradient elution. Consequently, it may be concluded that the EC detector is more suitable for quantitative determinations of phenolic compounds.

#### 5.3.4.2. Linear Dynamic Range

If a detector is to be used in quantitative analysis, then the response should be linear with concentration. A wide linear dynamic range, typically  $10^4$  -  $10^5$ , is desirable so that samples with a wide range of component concentrations may be measured in a single analysis.

The linear range of each phenolic compound was obtained by plotting the logarithm of the response (peak

height or current) against the logarithm of concentration. Linear UV and EC detector responses over the range 0.1 -  $10^3$  mg/l were obtained for all phenolic compounds except gallic and protocatechuic acid. For these two phenolic compounds, plots were prepared over the range 0.2 -  $10^3$  mg/l because they could not be detected below 0.2 mg/l by either detector. A non-linear response was obtained for both phenolics. This non-linearity is attributable to the pseudo-tailing associated with these two compounds. Because of this non-linear response, neither phenolic could be determined quantitatively.

Ideally, the slopes of the graphs should equal unity, however, the values for those phenolic compounds with linear responses ranged between 0.97 and 1.03.

The linear responses obtained with both detectors indicate their suitability for quantitative determinations of phenolic compounds. Furthermore, the linear dynamic ranges of both detectors are of similar magnitude to values quoted in the literature {43,44}.

#### 5.3.4.3. Precision of Measurements

The precision of the HPLC method employing the UV and the EC detectors in series was investigated by

calculating the coefficient of variation of peak heights of individual phenolic compounds following ten injections of a 1.0 mg/l standard mixture on the column. The coefficient of variation of the UV detector varied from 5.2% for vanillic acid to 9.5% for sinapic acid, whereas that of the EC detector varied from 6.5% for vanillic acid to 9.8% sinapic acid. The coefficient of variation was found to increase for longer eluting compounds, for compounds that are not completely resolved and for those compounds which give rise to tailing effects, i.e., gallic acid and protocatechuic acid. Although the coefficient of variation was found to be slightly better for the UV detector, it should be remembered that the EC detector was connected downstream of the UV detector and was disadvantaged in terms of peak broadening.

#### 5.3.5. Analysis of Beer Samples

In this section the suitability of UV and EC detectors for the detection of phenolic compounds in three Irish-brewed beers is considered.

##### 5.3.5.1. Standardisation

In chromatographic analysis, calibration is usually achieved using either internal or external

standardisation {45}. Quantification using an internal standard requires the addition of a compound that elutes closely to the analyte band, i.e., has a capacity factor ( $k'$ ) within  $\pm 30\%$  of that of the analyte. However, when using external standardisation, the actual compounds of interest are used in the preparation of calibration graphs. Calibration methods based on internal standards are more accurate than external calibration methods because the former method compensates for any variations in the separation conditions.

Unfortunately, it was not possible to use an internal standard calibration as each phenolic compound would require a corresponding internal standard given the differing polarities of the phenolic compounds. Such a situation would cause extreme complications, due to peak overlap, in the resulting chromatograms. In addition, there is the practical problem of trying to find eleven internal standards that are structurally related to the eleven phenolic compounds. Therefore, calibration was restricted to the external standard method.

Calibration graphs of peak height versus concentration were prepared for all phenolic compounds except gallic, protocatechuic and p-hydroxybenzoic acids. For electrochemical detectors it has been suggested that

peak height times the peak width at half-height is a more reliable measure of concentration than peak height, since it takes into account the gradual poisoning of the electrode {46}. Therefore, this method rather than peak height was used for calibration graphs obtained with the EC detector.

#### 5.3.5.2. Extraction of Phenolic Compounds from Standard Solutions and Beer Samples

Preliminary attempts at direct injection of beer samples failed as the chromatograms were too complicated. Furthermore, it took several hours before all compounds in the injected beer sample eluted from the column. Because of these problems, samples were extracted prior to analysis.

Standard solutions containing all eleven phenolic compounds were prepared in 5% (V/V) aqueous ethanol, as this medium approximates beers. The concentration of these standard solutions ranged from 0.1-5.0 mg/l.

Prior to extraction, beer samples and standard solutions were acidified to pH2.0 with 2M HCl, thereby preventing deprotonation of the phenolic acids during extraction. Furthermore, the addition of acid releases any

bound phenolics, ensuring that all acids are present in the free state. Following acidification, samples were twice extracted with iso-octane. The very non-polar nature of iso-octane ensured that only the non-polar constituents were extracted at this stage. The remaining aqueous phase was then extracted four times with ethyl acetate. Less than four extractions resulted in decreased recovery of the phenolics. It was found necessary to centrifuge the ethyl acetate extracts in order to fully separate the aqueous and organic phases. Finally, the ethyl acetate extracts were evaporated under reduced pressure to approximately 2.0 ml and subsequently diluted to 10.0 ml with methanol. Using reduced pressure enabled the sample to be concentrated at room temperature and avoided any possibility of thermal degradation of phenolics.

#### 5.3.5.3. Phenolic Content of Irish-brewed Beers

Three beers were analysed for their phenolic content by HPLC using UV and EC detection (Table 5.10). Slight differences were observed on comparing the results obtained with the two detectors, especially for the later eluting compounds. With ferulic and sinapic acids, the results from the EC detector were slightly lower than those obtained using the UV detector. These differences reflect the difficulties associated with the measurement of peak

Phenolic Compound	Concentration (mg/l)					
	Stout		Ale		Lager	
	UV	EC	UV	EC	UV	EC
<u>Benzoic Acid Derivatives</u>						
Vanillic acid	1.79	1.79	1.42	1.41	2.07	2.08
Syringic Acid	1.16	1.17	0.68	0.68	0.85	0.85
<u>Cinnamic Acid Derivatives</u>						
Caffeic acid	0.29	0.30	0.13	0.13	0.22	0.23
p-Coumaric acid	0.73	0.75	0.92	0.91	0.57	0.57
Ferulic acid	1.35	1.32	1.07	1.05	1.90	1.88
Sinapic acid	0.24	0.20	0.15	0.10	0.20	0.18
<u>Flavanols</u>						
(+)-Catechin	ND	0.28	ND	0.52	ND	0.82
(-)-Epicatechin	0.10	0.11	<0.10	<0.10	0.25	0.25

Table 5.10. Concentration of phenolic compounds determined in three Irish-brewed beers using HPLC with EC and UV detection. Results are expressed as the means of four determinations.

ND - Not determined.



heights in chromatograms obtained with the UV detector, stemming from up-scale movement of the baseline in these chromatograms. Ferulic and sinapic acids are the last of the phenolic compounds to elute (Fig. 5.4a). By the time these compounds elute, the up-scale baseline movement has noticeably increased compared with earlier sections of the chromatogram. In contrast, this up-scale movement is not evident in the chromatogram obtained with the EC detector (Fig. 5.4b). Results were not obtained for gallic, protocatechuic and p-hydroxybenzoic acids, but there were identified as being present in all three beers. For gallic and protocatechuic acids, non-linear responses were obtained on plotting the logarithm of peak height against the logarithm of concentration for standard solutions. This non-linearity was attributed to the pseudo-tailing associated with these two compounds and rendered the UV and EC detector responses unsuitable for quantitative purposes.

The problem of co-elution arising between p-hydroxybenzoic acid and (+)-catechin meant that neither could not be quantified using the UV detector. However, as the applied potential of the EC detector was sufficient for the electrochemical oxidation of (+)-catechin but not p-hydroxybenzoic acid, the former and not the latter compound was quantified.

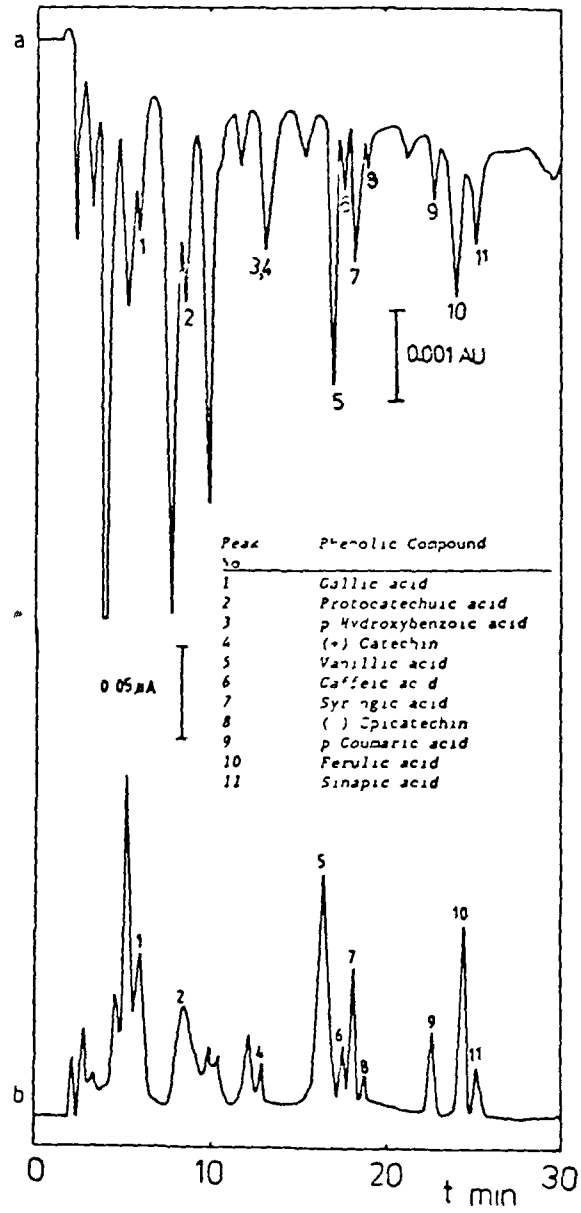


Fig. 5.4. Chromatogram of extract from stout using (a) ultraviolet and (b) electrochemical detection

The results in Table 5.10 are similar to values previously found for Irish-brewed beers {47}. In general, the phenolic content of these beers is low, with only minor differences between the individual beers. The origin of these phenolics is due to the raw materials used, i.e., barley and hops {47}. It has been discovered that the phenolic content in the finished beer is dependent on the amounts extracted during the preparatory stages of the brewing process. However, it has also been noted that some phenolic compounds present in beers may also be formed via the shikimic acid pathway {18}. Sinapic acid is formed from ferulic acid, which results from p-coumaric acid. Therefore, if such a reaction were to occur during the brewing process, the concentration of sinapic and ferulic acids would depend on the initial p-coumaric acid concentration. Consequently, there is a need to establish the exact source of these phenolic compounds.

Typical UV and EC detector responses, for one of the beers, are shown in Figs. 5.4a and 5.4b, respectively. Identification of the individual phenolic compounds was achieved by comparing retention times measured from chromatograms of standard solutions with those of the beer extracts. Chromatograms were obtained in an alternating standard-sample sequence. Such a sequence ensures that the working electrode of the EC detector does not become

fouled. It also takes into account any slight changes in the reference electrode potential and mobile phase composition {19}. Besides the peaks corresponding to the phenolic compounds, some additional peaks were present but were not identified. Most of these additional peaks occurred in the early section of chromatograms. These peaks have been attributed to the presence of oligomeric flavanols {47}. Some extra peaks were also observed in the middle and later sections of chromatograms and are probably due to derivatives of benzoic and cinnamic acids. In general, chromatograms corresponding to the EC detector contained fewer of these peaks in the middle and later sections.

#### 5.4. Conclusions

The conclusion of this study is that EC detection is more suitable than UV detection in HPLC analysis for the determination of phenolic compounds in beer extracts. In particular, EC detection has the advantage of higher sensitivity than UV detection, and also offers greater selectivity, which is very useful when analysing "real" samples as it reduces matrix effects and consequently improves the quantification and identification of analyte peaks. Furthermore, the EC detector was almost insensitive to the changes in mobile phase conditions associated with

gradient elution. Consequently, steady baselines were achieved at high detector sensitivity settings. Unfortunately, severe baseline drift occurred under gradient conditions when the UV detector was operated at high sensitivities. This drift made the measurement of the peak heights of later eluting phenolics particularly difficult.

During the period of this study some fouling of the working electrode by adsorbed phenols or their oxidation products was encountered. This necessitated the removal of the electrode for cleaning purposes. A number of disadvantages are associated with this type of procedure. Manual cleaning can often cause the electrode surface to be seriously damaged. There is also the possibility of the surface becoming contaminated, either during the cleaning process or in handling operations subsequent to the cleaning step. In addition, the procedure of replacing the electrode in the detector cell can cause air bubbles to be trapped in the cell. Elimination of these problems would seem to be possible by using pulsed amperometric detection {48,49}. Application of a triple-step potential waveform would electrochemically clean the surface of the working electrode. It also has the advantage of increasing the signal-to-noise ratio {49}. Hence, application of this detection mode is something

which needs to be more fully explored to ascertain its suitability to the present system.

References

1. R. Julkunen-Tiitto, J. Agric. Food Chem., 33, 213 (1985).
2. D.H. Hahn, J.M. Faubion and L.W. Rooney, Cereal Chem., 60, 255 (1983).
3. K. Wackerbauer, T. Kossa and R. Tressl, European Brewery Convention, Proceedings of the 16th Congress, Amsterdam, 495 (1977).
4. K. Wackerbauer, P. Kramer and J. Siepert, Brauwelt, 122, 618 (1982).
5. D.S. Ryder, J.P. Murray and M. Stewart, Technical Quarterly of the Master Brewers Association of the Americas, 15, 79 (1978).
6. A.R. Goodey and R.S. Tubb, J. Gen. Microbiology, 128, 2516 (1982).
7. I. McMurrough, G.P. Hennigan and M.J. Loughrey, J. Inst. Brew., 89, 15 (1983).
8. I. McMurrough, European Brewery Convention, Proceedings of the 17th Congress, Berlin (West), 321 (1979).
9. R.J. Gardner and J.D. McGuinness, Technical Quarterly of the Master Brewers Association of the Americas, 14, 250 (1977).

10. M. Dadic and J.E.A. Van Gheluwe, *J. Inst. Brew.*, 77, 376 (1971).
11. J.W. Gramshaw, *J. Inst. Brew.*, 79, 258 (1973).
12. E.S. Keith and J.J. Powers, *J. Food. Sci.*, 31, 971 (1966).
13. F.C. Dallas, A.F. Lautenback and D.B. West, *Proc. Am. Soc. Brew. Chem.*, 25, 103 (1967).
14. P.C. White, *Analyst*, 109, 677 (1984).
15. C. Garcia Barroso, R. Cela Torrijos and J.A. Perez-Bustamante, *Chromatographia*, 17, 249 (1983).
16. G. Charalambous, K.J. Bruckner, W.A. Hardwick and A. Linneback, *Technical Quarterly of the Master Brewers Association of the Americas*, 10, 74 (1973).
17. B. Fleet and C.J. Little, *J. Chromatogr. Sci.*, 12, 747 (1974).
18. T.M. Kenyhercz and P.T. Kissinger, *J. Agric. Food Chem.*, 25, 959 (1977).
19. D.A. Roston and P.T. Kissinger, *Anal. Chem.*, 53, 1695 (1981).
20. F.J. Vermillion and I.A. Pearl, *J. Electrochem. Soc.*, 111, 1392 (1964).
21. M. Fleischmann and D. Pletcher, Reactions of Molecules at Electrodes, edited by N.S. Hush (J. Wiley & Sons, New York, 1971), p. 371.
22. R.T. Morrison and R.N. Boyd, Organic Chemistry, Third Edition (Allyn and Bacon Inc., Boston, 1978), pp.



- 361-363.
23. V.D. Parker, Organic Electrochemistry, edited by M.M. Baizer (Marcel Dekker Inc., New York, 1973), pp. 532-540.
  24. R.T. Morrison and R.N. Boyd, Organic Chemistry, Third Edition (Allyn and Bacon Inc., Boston, 1978), p. 396.
  25. I. McMurrough, J. Chromatogr., 218, 683 (1981).
  26. D.G. Swartzfager Anal. Chem., 48, 2189 (1976).
  27. W.A. MacCrehan and R.A. Durst, Anal. Chem., 50, 2108 (1978).
  28. V.V. Berry, J. Chromatogr., 236, 279 (1982).
  29. S.M. McCown, B.E. Morrison and D.L. Southern, Int. Lab., 14, 76 (1984).
  30. S. Caccamese, R. Azzolina and M. Davine, Chromatographia, 12, 545 (1979).
  31. E.J. Conkerton and D.C. Chapital, J. Chromatogr., 281, 326 (1983).
  32. L.R. Snyder and J.J. Kirkland, Introduction to Modern Liquid Chromatography, Second Edition (J. Wiley & Sons Inc., New York, 1979), pp. 791-813.
  33. L.R. Snyder and J.J. Kirkland, Introduction to Modern Liquid Chromatography, Second Edition (J. Wiley & Sons Inc., New York, 1979), pp. 269-322.
  34. R.P.W. Scott and P. Kucera, J. Chromatogr., 142, 213 (1977).
  35. L.R. Snyder and J.J. Kirkland, Introduction to Modern

- Liquid Chromatography, Second Edition (J. Wiley & Sons Inc., New York, 1979), p. 24.
36. L.R. Snyder and J.J. Kirkland, Introduction to Modern Liquid Chromatography, Second Edition (J. Wiley & Sons Inc., New York, 1979), pp. 662-719.
37. D.J. Chesney, J.L. Anderson, E.E. Weisshaar and D.E. Tallman, *Anal. Chem. Acta*, 124, 321 (1981).
38. A.J. Samuel and T.J.N. Webber, Electrochemical Detectors, edited by T.H. Ryan (Plenum Press, New York, 1984), pp. 43-59.
39. D.A. Ventura and J.G. Nikelly, *Anal. Chem.*, 50, 1017 (1978).
40. S.R. Bakalyar, M.P.T. Bradley and R. Honganen, *J. Chromatogr.*, 158, 277 (1978).
41. J.N. Brown, M. Hewins, J.H.M. Van Der Linden and R.J. Lynch, *J. Chromatogr.*, 204, 115 (1981).
42. J.F. Lawrence, *J. Chromatogr.*, 211, 144 (1981).
43. K. Stulik and V. Pacakova, *CRC Crit. Rev. Anal. Chem.*, 14, 297 (1984).
44. L.R. Snyder and J.J. Kirkland, Introduction to Modern Liquid Chromatography, Second Edition (J. Wiley & Sons Inc., New York, 1979), p. 131.
45. D. Dadgar and M.R. Smyth, *Trends Anal. Chem.*, 5, 115 (1986).
46. W.J. Albery, T.W. Beck, W.N. Brooks and M. Fillenz, *J. Electroanal. Chem.*, 125, 205 (1981).

47. I. McMurrrough, G.P. Roche and K.G. Cleary, *J. Inst. Brew.*, 90, 181 (1984).
48. P. Edwards and K.K. Haak, *Int. Lab.*, June, 38 (1983).
49. D.C. Johnson, J.A. Polta, T.Z. Polta, G.G. Neuburger, J. Johnson, A.P.C. Tang, In-Hyeong Yeo and J. Baur, *J. Chem. Soc. Faraday Trans. 1*, 82, 1081 (1986).

List of Publications

1. A Comparison of Electrochemical and Ultraviolet Detection Methods High Performance Liquid Chromatography for the Determination of Phenolic Compounds Commonly Found in Beers.  
  
Part 1. Optimisation of Operating Parameters,  
  
P.J.Hayes, M.R.Smyth and J.McMurrough  
  
to be published in the Analyst, 112(1987).
  
2. A Comparison of Electrochemical and Ultraviolet Detection Methods in High Performance Liquid Chromatography for the Determination of Phenolic Compounds Commonly Found in Beers.  
  
Part 2. Analysis of Beers.  
  
P.J.Hayes, M.R.Smyth and J.McMurrough.  
  
to be published in the Analyst, 112(1987).
  
3. Voltammetric Determination of Inorganic Lead and Dimethyl and Trimethyllead Species in Mixtures  
  
P.J.Hayes and M.R.Smyth  
  
Anal. Proc., 23, 34(1986).
  
4. Determination of Some Environmentally Important Organic Compounds by High Performance Liquid Chromatography with Voltammetric Detection  
  
M.R.Smyth, P.J.Hayes and D.Dadgar  
  
Proc.Int. Conference "Electroanalysis na h'Éireann", Dublin, Ireland, June, 1986, pp. 37-48.